Sunspots: An overview

Sami K. Solanki

Max-Planck-Institut für Aeronomie, 37191 Katlenburg-Lindau, Germany
(e-mail: solanki@linmpi.mpg.de)

Abstract. Sunspots are the most readily visible manifestations of solar magnetic field concentrations and of their interaction with the Sun's plasma. Although sunspots have been extensively studied for almost 400 years and their magnetic nature has been known since 1908, our understanding of a number of their basic properties is still evolving, with the last decades producing considerable advances. In the present review I outline our current empirical knowledge and physical understanding of these fascinating structures. I concentrate on the internal structure of sunspots, in particular their magnetic and thermal properties and on some of their dynamical aspects.

1. Introduction

Sunspots are magnetic structures that appear dark on the solar surface. Each sunspot is characterized by a dark core, the umbra, and a less dark halo, the penumbra. The presence of a penumbra distinguishes sunspots from the usually smaller pores. Images of sunspots made in the g-band around 4305 Å are shown in Fig. 1.1.

Naked eye observations of sunspots are known from different cultures (Bray & Loughhead 1964). In particular, the ancient Chinese have kept detailed although very incomplete records going back over 2000 years (Wittmann & Wu 1987, Yau & Stephenson 1988, Eddy et al. 1989). Nevertheless, it was the rediscovery of sunspots by Galilei, Scheiner and others around 1611, with the help of the then newly invented telescope, that marked the beginning of the systematic study of the Sun in the western world and heralded the dawn of research into the Sun's physical character. Over the ages the prevailing view on the nature of sunspots has undergone major revisions. The discovery of the Wilson effect in 1769 (see Sect. 2.5) even completely changed the prevailing picture of the structure of the entire Sun, at least temporarily. Since the dark umbrae appeared
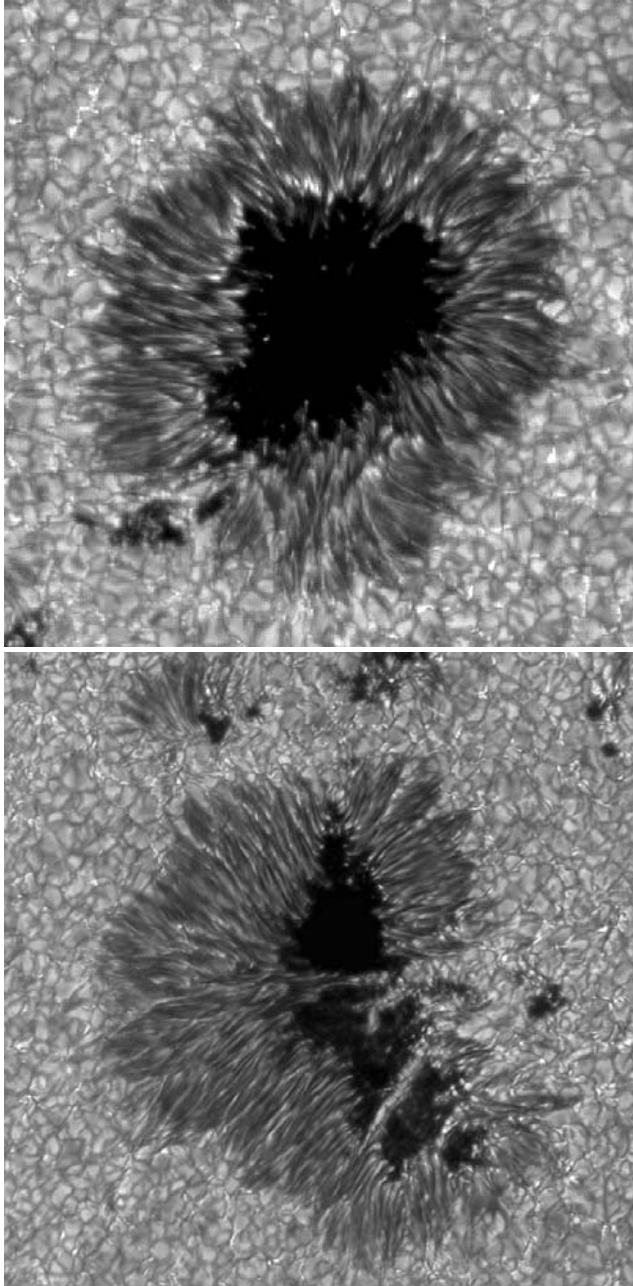
Fig. 1.1. Images recorded in a roughly 10 Å wide band centred on 4306 Å (g-band) of a relatively regular sunspot (*top*) and a more complex sunspot (*bottom*). The central, dark part of the sunspots is the umbra, the radially striated part is the penumbra. The surrounding bright cells with dark boundaries are granular convection cells. The upper sunspot has a maximum diameter of approximately 30000 km, the lower sunspot of roughly 50000 km (upper image courtesy of T. Berger; lower image taken by O. von der Lühe, M. Sailer, T. Rimmele).

to lie deeper than the rest of the solar surface, it was for a time widely believed that the entire solar interior is dark and hence cool, compared to the bright photosphere outside sunspots.

The breakthrough in our understanding of the nature of sunspots came in 1908 when George Ellery Hale first measured a magnetic field in sunspots (Hale 1908b). Since then the magnetic field has become firmly established as the root cause of the sunspot phenomenon.

Overviews of the structure and physics of sunspots are given in the monograph by Bray & Loughhead (1964), in the proceedings edited by Cram & Thomas (1981), Thomas & Weiss (1992a), Schmieder et al. (1997) and Strassmeier (2002), as well as in the review articles by Zwaan (1968, 1981), Moore & Rabin (1985), Schmidt (1991), Soltau (1994), Thomas & Weiss (1992b), Schmidt (2002), Stix (2002) and Sobotka (2003). In addition, specific aspects of sunspots have been reviewed by a host of other authors. References to these are given in the relevant sections of this article. The present article borrows heavily from earlier reviews, specifically those by Solanki (1995, 1997b, 2000a, b, 2002). An introduction to the related, generally smaller sunspot pores, often also simply termed pores, has been given by Keppens (2000).

I take the approach of dividing the discussion of sunspots according to their physical parameters, e.g., magnetic field, velocity, thermal structure, etc. Another possible approach would be to discuss sunspots piecewise according to morphological features, i.e., umbra, penumbra, light bridges, δ-spots etc., or according to the physical processes acting on and within them. Each approach has its advantages and disadvantages. Thus, in the present article, e.g., the magnetic structure of light bridges is discussed in the context of that of the rest of the sunspot, at the cost of making the connection between the magnetic and thermal structure of these features more cumbersome. The advantage is that e.g., the magnetic properties of all parts of a sunspot can be easily compared.

Basically, this article covers similar ground as chapters 4, 5 and 8 of Bray & Loughhead (1964), with the difference that the current article is more up-to-date and the emphasis is placed on aspects presently more in vogue, which reflects the evolution of the field over the past 40 years.

A number of important aspects of sunspots are not or hardly covered here. These include their morphology, oscillations (references to relevant reviews are given in Sect. 7), their spectrum and their relation to starspots (see the volume edited by Strassmeier 2002 for more on this connection).

This review is structured as follows: In Sect. 2 general properties of sunspots are summarized, including location on the Sun, size, lifetime, evolution and Wilson effect. This is followed by a description of our empirical knowledge of the sunspots' magnetic field in Sect. 3. An overview of the physical understanding of the magnetic structure of sunspots is given in Sect. 4. Sections 5 and 6 review the observations and theory of sunspot brightness and temperature. Both observational and theoretical aspects of flows within sunspots are presented in Sect. 7. Finally, I conclude with a list of open questions in Sect. 8.

2. General properties of sunspots

In this section I briefly summarize the basic observed characteristics of sunspots, i.e. their sizes, lifetimes, brightness, evolution, Wilson depression, as well as their magnetic, thermal and velocity structure. The last three quantities are discussed in far greater detail in the following sections.

2.1. Location and evolution

The number of sunspots varies strongly over a solar cycle (Harvey 1992), as was first discovered by Heinrich Schwabe in 1843. There are times at and near solar activity minimum when not a single sunspot is present on the solar disc, while 10 or more sunspots are not uncommon around the maxima of recent solar cycles. Later, systematic daily observations of the solar disc with the specific aim of counting the number of sunspots were started by Rudolf Wolf, who also introduced the sunspot relative number (also called the Zürich number or Wolf number), which is still used as a measure of the coverage of the solar disc by sunspots. Recently, a somewhat more robust variant, the group sunspot number, has been introduced by Hoyt & Schatten (1998).

Sunspots are always located within active regions, which, typically, have a bipolar magnetic structure. The sunspots are thus mainly restricted to the activity belts reaching up to 30° on each side of the solar equator. The latitudes of the sunspots vary with the solar activity cycle. Early in a cycle they appear at high latitudes, with occasional spots lying up to 40° from the equator. In the course of the cycle the new sunspots appear at increasingly lower latitudes, with the last sunspots of a cycle lying close to the equator. This behaviour was first noticed by Carrington (1863) and can be illustrated by a so-called butterfly diagram. Such a diagram is plotted in Fig. 2.1. The fact that sunspots are restricted to low latitudes as well as other observations – such as the somewhat lower latitude of the preceding polarity relative to the following polarity of an active region (Joy's law, Joy 1919, Brunner 1930) – can be reproduced by a model in which sunspots and their host active regions are formed by the emergence of a large magnetic flux tube through the solar surface. It is proposed that near the solar surface this flux tube breaks up into many smaller tubes, the larger of which constitute sunspots (e.g. Zwaan 1978). Sunspots are thus only the most prominent examples of magnetic flux tubes on the Sun. The visible sunspot constitutes the intersection of the solar surface with such a flux tube. The sub-surface footpoints of this flux tube are thought to be anchored in the overshoot layer below the convection zone, where its field strength is an order of magnitude above the equipartition value of approximately 10^4 G (D'Silva & Choudhuri 1993, D'Silva & Howard 1994, Schüssler et al. 1994, Caligari et al. 1995). An initial field strength of roughly 10^5 G is also supported by studies of the stability of this flux tube in the overshoot layer (Moreno Insertis et al. 1992, Moreno Insertis 1992, 1997). A review is given by Schüssler (2002).

Sunspots form the heart of an active region. There is, however, often an asymmetry between the leading and following polarities, with the leading polarity often harbouring the dominant sunspot although in some cases the following polarity may contain an equally massive spot. Sunspots and in particular sunspot groups are classified according

DAILY SUNSPOT AREA AVERAGED OVER INDIVIDUAL SOLAR ROTATIONS
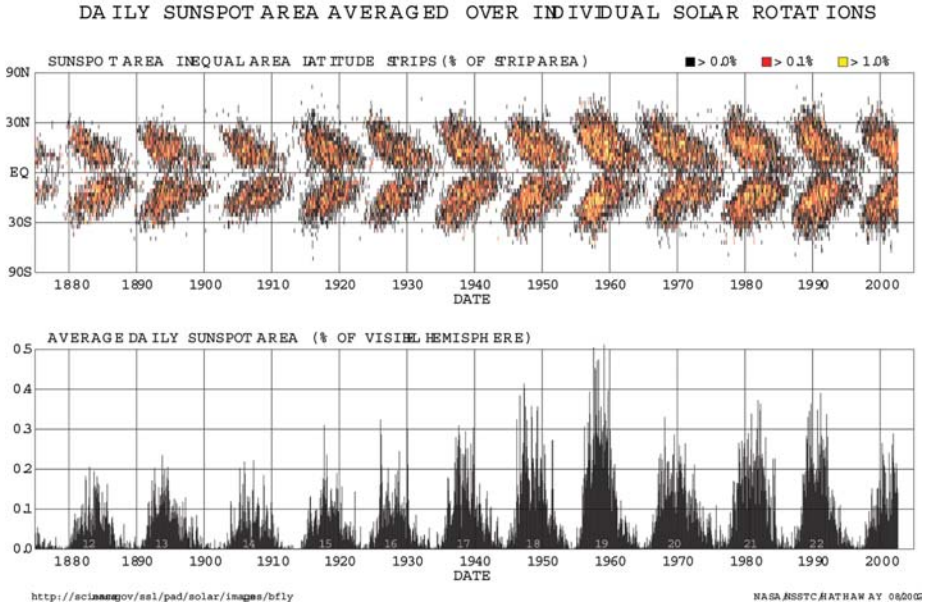
Fig. 2.1. Butterfly diagram (*upper panel*) and record of relative solar surface area covered by sunspots (*lower panel*). *Upper panel*: the vertical axis indicates solar latitude, the horizontal axis time. If a sunspot or a group of sunspots is present within a certain latitude band and a given time interval, then this portion of the diagram is shaded, with the colour of the shading indicating the area covered by the sunspots. (Figure courtesy of D. Hathaway, http://science.nasa.gov/ssl/pad/solar/sunspots.htm).

to their morphology. An introduction to the different classification schemes has been given by McIntosh (2000).

The formation of sunspots is intimately related to the formation of active regions as a whole. The processes observed to occur during the emergence of active regions have been reviewed by Zwaan (1985, 1992), cf. the theses of Brants (1985), Harvey (1993) and Strous (1994). As an increasing amount of magnetic flux emerges, individual pores begin to form. The protopores are associated with redshifted spectral lines (e.g. Leka & Skumanich 1998), so that their formation is compatible with a convective collapse, an instability-driven process invoked to explain the kG fields measured at the solar surface (e.g. Parker 1978, Webb & Roberts 1978, Spruit 1979, Grossmann-Doerth et al. 1998). Alternatively, these downflows may be produced by material draining out of the freshly emerged loop. Later these pores grow and at the same time move towards each other and coalesce, thus forming a larger sunspot (Vrabec 1971a, 1974, McIntosh 1981, Harvey & Harvey 1973, Zwaan 1985). Often small sunspots also merge and form larger sunspots. García de la Rosa (1987a, b) has proposed that a large sunspot retains a memory of its original constituent fragments (outlined by light bridges) and finally breaks up into them again. He argues that this supports the cluster model of sunspots (see Sect. 4). The time scale for the formation of a large sunspot is between a few hours and several days. The coalescence can continue even after fresh flux stops emerging and also after a particular

spot starts decaying, i.e. loosing flux again, so that a sunspot can grow and decay at the same time.

The convergence of magnetic elements and pores to form a sunspot must be driven by some force. One idea is that the coalescence of smaller flux tubes to sunspots is really a recoalescence and that the individual fragments forming the sunspot are all part of a larger flux tube somewhere in the convection zone. Then, like balloons on strings that are held in one hand the fragments will tend to come together if buoyancy is sufficiently dominant (relative to the random convective motions). In contrast to this, Parker (1992) has proposed that attraction between vortices drives the coalescence of individual magnetic fibrils. In his model each flux tube is surrounded by a vortex flow. Such vortices attract each other and he estimated that the inward directed aerodynamic drag exerted by a downdraft vortex is strong enough to overcome the magnetic stresses that tend to keep the fibrils apart. Meyer et al. (1974), cf. Meyer et al. (1977), first pointed out that a strong converging flow (at a depth of $10^3 - 10^4$ km) is required not only to form sunspots, but also to maintain them. Their modelling confirmed that sunspots are located at the centres of convection cells, with an outflow at the surface that is usually termed the moat flow (Sect. 7) and an inflow in the subsurface layers. More recently, Hurlburt & Rucklidge (2000) have published the results of a 2–D model of the flows around a sunspot. They find that sunspots are surrounded by a convection cell such that the updraft lies somewhat beyond the sunspot's periphery. Beyond that there is an outflow (which is interpreted to represent the moat flow) at the surface, while closer to the sunspot and in particular along the magnetopause, there is an inclined inflow, which is mainly a downflow below the sunspot. This collar flow helps to stabilize the spot. The presence of a downflow below a sunspot, that is interpreted as part of a collar, has been confirmed by local helioseismology (Duvall et al. 1996). More recently, subsurface flows qualitatively similar to the proposed collar have been identified (Kosovichev 2002, cf. Sect. 3.2.3). However, no inflow is seen at the surface, in contrast to the simulations. Hurlburt & Rucklidge speculate that radiative effects not included in their simulations might 'hide' the inflow by moving it below the solar surface.

Once the diameter of a pore exceeds roughly 3.5 Mm it usually starts to exhibit penumbral structure, whereby the penumbra can be partial, i.e. not completely surrounding the proto-spot (Bray & Loughhead 1964). An example of a partial penumbra can be seen near the top of the lower frame of Fig. 1.1. Only when pores grow very rapidly do they overshoot this diameter and remain pores in a part of parameter space otherwise populated by sunspots (Zwaan 1992). This situation appears to be unstable and lasts in general less than a day. The penumbra develops very rapidly, with pieces of penumbra (i.e., fully fledged penumbra along a part of the periphery of the pore/proto-spot) being completed within an hour (Bray and Loughhead 1964, Bumba 1965, Bumba & Suda 1984, Leka & Skumanich 1998, cf. Keppens & Martínez Pillet 1996). The penumbra grows in bursts, sector after sector, starting with the edge of the sunspot pointing away from the opposite polarity flux of the active region. Not only is the formation of a sector of the penumbra abrupt, but according to Leka & Skumanich (1998) a newly formed penumbral segment is practically indistinguishable from a more mature one in the range of field strengths, inclination angles and continuum intensities. A penumbral segment also harbours an Evershed flow (see Sect. 7) very soon after its formation. According to Zwaan (1992) the formation of the penumbra is not associated with any dramatic

increase in the flux of the sunspot, while Leka & Skumanich (1998) conclude that the formation of a penumbra does not occur at the expense of umbral flux.

As soon as (or even before) the sunspots are completely formed they begin to decay (McIntosh 1981). Best studied is the decay of sunspot area, dA/dt, and various forms for the decay curve have been proposed. The first such work was due to Cowling (1946), who also investigated the evolution of the peak field strength within the umbra. Later, Bumba (1963a) distinguished between recurrent sunspots, for which he obtained a linear decay law (i.e. a time independent dA/dt), and non-recurrent spots, which he thought decayed exponentially. Later studies have suggested, however, that a linear decay law is more appropriate for over 95% of all sunspots, irrespective of whether they are recurrent or not. Moreno Insertis & Vázquez (1988) and Martínez Pillet et al. (1993) have also tested quadratic decay (i.e. $A(t)$ is a quadratic function of time) and have shown that the data do not allow a distinction to be made between linear and quadratic rates, while Petrovay & Van Driel-Gesztelyi (1997) produce evidence in favour of a quadratic decay rate. Martínez Pillet et al. (1993) distinguish between La Laguna type 2 groups (complex groups) and type 3 (isolated spots). For the former they find an average $dA/dt = -41$ MSH/day, with MSH being a millionth of the solar hemisphere; 1 MSH = $(6.3'')^2$. Isolated spots decay on average at less than half the above rate, $dA/dt = -19$ MSH/day. The median values of the decay rates are 31 and 15 MSH/day, respectively. These authors have also investigated the distribution of decay rates and found it to correspond to a lognormal function. The lognormal decay rate distribution means that in addition to the relatively slowly decaying spots corresponding to the median there is a tail of very rapidly decaying sunspots with dA/dt as high as -200 MSH/day. Although the tail is longer for the complex groups, it is equally prominent for the isolated sunspots, suggesting that the heightened decay is not the result of enhanced flux cancellation expected in some complex active regions (although the generally higher decay rates in complex groups are suggestive of such a behaviour). Sunspots with an irregular shape (Robinson & Boice 1982), more bright structure in the umbra (Zwaan 1968), a larger proper motion (Howard 1992), or a higher latitude (Lustig & Wöhl 1995) suffer from a higher decay rate, as do following spots when classified by their polarity (Royal Greenwich Observers 1925). A lognormal distribution can also be fit to the decay rates of umbrae (Martínez Pillet et al. 1993, cf. Howard 1992), although the mean dA/dt values are much smaller, -3.5 to -7 MSH/day, than for the whole sunspots (note that these smaller values are sufficient to maintain a time independent penumbral-to-umbral area ratio).

Linear and quadratic decay laws have very different consequences for the theory underlying sunspot decay. The consequences of a linear decay law have been explored by Gokhale & Zwaan (1972), Meyer et al. (1974) and Krause & Rüdiger (1975). Such a law implies that flux loss takes place everywhere within the spot, irrespective of the spot's area or the length of its periphery. Thus, Gokhole & Zwaan (1972) assumed a current sheet around the spot and no turbulent diffusion inside it. The decay is driven purely by Ohmic diffusion across the current sheet, but requires the sheet to become increasingly thinner as the spot becomes smaller to achieve a constant decay rate. Meyer et al. (1974) propose small scale eddy motions across the whole surface of the sunspot, which leads to a diffusion of field lines from the whole body of the spot. This mechanism gives $dA(t)/dt \approx -16\eta_T$, where η_T is the turbulent magnetic diffusivity, which is constant in the spot. One problem with the Meyer et al. and Krause & Rüdiger models is that

they have no current sheets around the sunspots, whereas newer observations suggest that such sheets are indeed present (e.g., Solanki & Schmidt 1992).

A contrasting approach is taken by Simon & Leighton (1964) and Schmidt (1968), who propose that sunspots decay by the erosion of the sunspot boundary, which implies that dA/dt should be proportional to the perimeter of the spot: $dA/dt \sim -\sqrt{A(t)}$ (see Meyer et al. 1974, Wilson 1981).

The solution to this differential equation is a parabolic function for $A(t)$, corresponding to the quadratic decay law. A decay mainly along the perimeter of a sunspot is supported by the presence of a moat flow and observations of moving magnetic features (MMFs), small magnetic elements flowing almost radially away from sunspots with approximately the speed of the moat flow. According to Harvey & Harvey (1973) the MMFs carry away sufficient net magnetic flux from the sunspots, 2×10^{20} Mx/day, to explain their decay. However, they compared with the decay rate given by Bumba (1963a), which (for isolated spots) is 4–5 times smaller than more recent estimates. Nonetheless, the rate of decay of a sunspot's magnetic flux deduced from Bumba's measurements (Zwaan 1974b) is within a factor of 2 of that directly measured by Skumanich et al. (1994). These authors find that the total amount of magnetic flux in a simple, relatively symmetric sunspot decreases linearly with time, at a rate of 9×10^{19} Mx/day over a period of 10 days (the initial flux of the spot was 6×10^{21} Mx).

In yet another approach, the evolution of sunspots described as fractal clusters of thin flux tubes has been published by Zelenyi & Milovanov (1992), cf. Zelenyi & Milovanov (1991), Milovanov & Zelenyi (1992). The decay law predicted by their model does not follow the quadratic law favoured by Petrovay & Van Driel-Gesztelyi (1997).

Petrovay & Moreno Insertis (1997) proposed an extension of the erosion model by postulating that the turbulent diffusivity depends strongly on field strength (in the shape of a Fermi function). Their model, which is otherwise similar to that of Meyer et al. (1974) and Krause & Rüdiger (1975), predicts a quadratic decay and in addition the spontaneous formation of a current sheet at the boundary of the sunspot. It also reproduces the Gnevyshev–Waldmeier relation of sunspot lifetimes (see Sect. 2.4). A quadratic decay law has been found to be superior to a linear law on the basis of Debrecen Photoheliographic results (Dezsö et al. 1987, 1997) by Petrovay & Van Driel-Gesztelyi (1997), which favours the erosion models. Petrovay et al. (1999) have extended the model of Petrovay & Moreno Insertis (1997) by introducing plage fields surrounding the sunspot in order to explain the lognormal distribution of decay rates found by Martínez Pillet et al. (1993). The data are qualitatively reproduced if they assume that plage magnetic fluxes follow a Gaussian distribution.

It is currently thought that much of the flux removed from sunspots remains for some time at the solar surface in the form of the smaller magnetic elements (for a review of their properties see, e.g., Solanki 1993). Some older observations when taken at face value suggested that considerable flux disappeared in situ, without visible signs of fragmentation and diffusion (Wallenhorst & Howard 1982, Simon & Wilson 1983, 1985). However, in these investigations the influence of the transition from a cool sunspot atmosphere to a hot magnetic element atmosphere were neglected. Grossmann-Doerth et al. (1987) showed that if the line formation underlying the magnetogram is properly taken into account then the evidence for in situ disappearance of magnetic flux is greatly weakened (cf. Stenflo 1984). Rabin et al. (1984), who also observed large changes of the

flux in an active region, argue for submergence. Wallenhorst & Topka (1982) witness the fragmentation of a sunspot, but also remark that field must also disappear in situ. Wang (1992) and Lites et al. (1995) studied the evolution of the relatively rare δ-spots. The flux in these bipolar sunspots disappears mainly in situ, probably by cancellation across the neutral line. Wang (1992) favoured reconnection followed by submergence, whereby he distinguished between slow reconnection – not associated with magnetic shear and flares – and fast reconnection (with both cases being observed). He did, however, also mention the possibility of the emergence of a U–loop (Spruit et al. 1987). In a modified form, this explanation was favoured by Lites et al. (1995). They argued that the magnetic structure of the δ-spot studied by them was similar to a donut (flux ring or O-loop) and the evolution of the sunspot was consistent with the passage of the rising O-loop through the solar surface. Martínez Pillet (2002) has argued that such a process occurs during the decay phase of normal, single polarity sunspots as well.

2.2. Brightness, magnetic and dynamic structure

Sunspots are usually identified on the basis of their brightness signature. They are distinctly darker than the normal solar photosphere (quiet Sun) and are all composed of an inner, darker part called the umbra (which radiates roughly 20–30% of the wavelength-integrated flux of the quiet Sun) and an outer, less dark part called the penumbra (which radiates 75–85% of the quiet Sun energy flux). Multiple umbrae within a single sunspot are not uncommon (see the lower frame of Fig. 1.1. The presence of a penumbra distinguishes sunspots from pores, which are generally smaller dark features, corresponding to a naked umbra-like structure.

The brightness and thus the temperature of a sunspot is a function of spatial position within the spot. It changes on large scales (umbra and penumbra) and small (bright umbral dots, bright and dark0 penumbral filaments, penumbral grains). The umbra is 1000–1900 K cooler than the quiet Sun, the penumbra is 250–400 K cooler. The temperature is thought to be lowered by the inhibition of convective energy through the magnetic field. Further details are provided in Sects. 5 and 6.

The magnetic field strength in the photosphere is approximately 1000–1500 G averaged over a sunspot, but varies gradually from a value of 1800–3700 G (Livingston 2002) in the darkest part of the umbra to 700–1000 G at the outer edge of the penumbra. The field strength also decreases with height in the atmosphere. At the same time the field fans out very rapidly. The magnetic configuration of a regular sunspot can be approximated to first order by a potential field bounded by a current sheet whereby the magnetic distribution within a regular sunspot is roughly similar to that produced by a vertically oriented magnetic dipole buried below the solar surface. See Sects. 3 and 4 for more information.

A host of dynamic phenomena are seen in sunspots. The best known of these is the Evershed effect, which describes a horizontal outflow in the photospheric layers of penumbrae. In the chromosphere and transition region it reverses into an inflow, and is also seen as a downflow above umbrae. More information may be obtained from Sect. 7. In addition to this primarily steady flow, oscillations are also observed in photospheric and chromospheric layers and in the transition region. They exhibit the typical p-mode periods of 5 minutes and the 3 minutes usual for chromospheric oscillations.
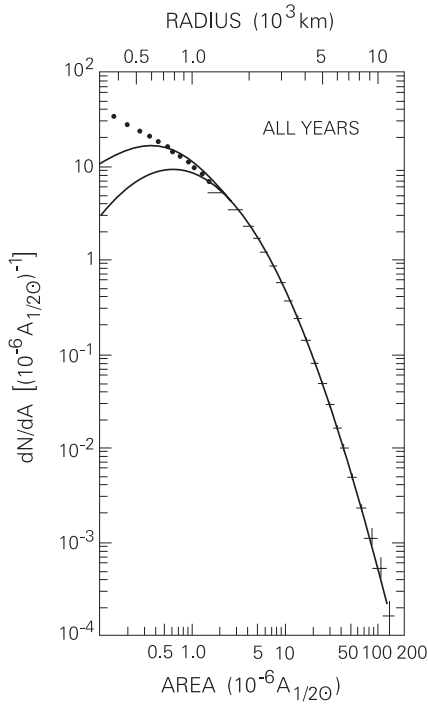
Fig. 2.2. Overall size spectrum for the Mt. Wilson data set of 24615 sunspots (*crosses*). Unreliable smaller sizes are denoted by filled circles. Upper and lower lognormal fits to the crosses have also been sketched (adapted from Bogdan et al. 1988, by permission).

2.3. Sizes

Sunspots exhibit a broad size distribution. Very large sunspots can occasionally reach diameters of 60000 km or more. Particularly large sunspots (or tight groups of smaller ones) are visible to the naked eye under clement conditions (e.g. just before sunset on a hazy day) or when the brightness of the solar disc is reduced with the help of filters. The smallest sunspots are roughly 3500 km in diameter (Bray & Loughhead 1964), making them smaller than the largest pores, whose diameters can be as large as 7 Mm. This fact has been examined theoretically by Rucklidge et al. (1995), cf. Sect. 6.3.

Smaller sunspots are more common than larger ones. Bogdan et al. (1988) conclude from an extensive set of Mt. Wilson white-light images that the size distribution of umbrae is well described by a log-normal function. Binned number densities as well as lognormal fits to the data are plotted in Fig. 2.2. The turnover (maximum of the distribution) occurs below the spatial resolution of the Mt. Wilson data, so that the observed number of sunspots always increases for smaller sunspots (irrespective of the phase or strength of the solar cycle). Since the ratio of umbral to penumbral area does not appear to depend very strongly on the sunspot size (see below), by proxy we expect that such a distribution is also valid for sunspots as a whole.

Typically, the products of a fragmentation process exhibit a lognormal distribution (Kolmogorov 1941). The lognormal distribution of sunspot areas thus implies that the associated magnetic flux tubes are the end products of the fragmentation of a large flux tube (which is thought to be anchored at the bottom of the convection zone and to underly the whole active region; Sect. 2.1).

A number of researchers have published values of $r_A = A_{tot}/A_u$, the ratio of total to umbral area of the sunspot. Thus, Tandberg-Hanssen (1956) found that for sunspots with a total area larger than 150 Mm^2 the umbral area is $17\pm3\%$ of the total, which corresponds to $r_A = 5.9 \pm 1$. Jensen et al. (1955) find $r_A = 5.3$ around the maximum of the sunspot cycle and $r_A = 6.3$ around minimum. Gokhale & Zwaan (1972) obtained $r_A = 5.9 \pm 1$ from the results of earlier investigations. According to Martínez Pillet et al. (1993) a value of $r_A = 4.9 \pm 0.6$ was obtained by Rodríguez Medina (1983), while Osherovich & Garcia (1989) find an even smaller value of 4 ± 1. Steinegger et al. (1990) find roughly 4.6 for large spots, with increasing scatter for small spots, while Brandt et al. (1991) give r_A ranging from 4.1 to 5.2 (for large and small spots, respectively), Antalová (1991) gives $r_A = 5.7$ and Beck & Chapman (1993) obtain $r_A \approx 5.0$. A part of the difference between the results of the various authors probably has to do with the different techniques used by them to measure the umbral and penumbral areas and the sensitivity of these methods to the seeing conditions (Steinegger et al. 1997).

An interesting question is whether r_A depends on other parameters such as sunspot size, age, phase of the solar cycle, etc. There is only a weak and noisy tendency for r_A to decrease with increasing sunspot size (Steinegger et al. 1990, Brandt et al. 1991, Beck & Chapman 1993). A dependence on sunspot age is claimed by Ringnes (1964), but this is not confirmed by Martínez Pillet et al. (1993), although they cannot rule out short term (less than a day) fluctuations and do not sample the late stages of sunspot decay. Most intriguing is the dependence on solar cycle phase. Jensen et al. (1955) and Ringnes (1964) find a dependence in the sense that r_A is smaller at sunspot maximum. Unfortunately, to my knowledge this dependence has not been investigated using newer results. Since it is the only physical parameter of sunspots besides the umbral brightness to depend on the solar cycle, this is an important investigation to carry out.

2.4. Lifetimes

Sunspots live for hours to months. The lifetime increases linearly with maximum size, following the so-called Gnevyshev-Waldmeier rule: $A_0 = WT$, where A_0 is the maximum size of the spot, T its lifetime and $W = 10$ MSH day^{-1} (MSH Micro Solar Hemisphere). This rule was first plotted by Gnevyshev (1938) and formulated by Waldmeier (1955). A more precise value, due to Petrovay & Van Driel-Gesztelyi (1997) is $W=10.89\pm0.18$ MSH day^{-1}. According to this rule most sunspots live for less than a day. Lifetimes on the order of a day, or those longer than approximately a week are often not very certain, due to interruptions of the observations due to nightfall or the passage of the sunspot to behind the solar limb through solar rotation. More on the decay of sunspots, in particular the decay rate can be found in Sect. 2.1.

2.5. The Wilson depression

The Wilson depression refers to the fact that the (visible) radiation from sunspot penumbrae and, in particular, umbrae emerges from a deeper layer than in the quiet photosphere, i.e. it corresponds to a depression of the unit continuum optical depth ($\tau = 1$) layer in the sunspot. The presence of such a depression was deduced by A. Wilson in 1769 on the basis of what is now known as the Wilson effect. As a sunspot approaches the solar limb the penumbra on the side closer to disc centre and often also the width of the umbra (Wilson & Cannon 1968, Wilson & McItosh 1969) decreases by a larger amount than that of the penumbra on the limbward side. An illustration of the Wilson depression and the Wilson effect is given by Bray & Loughhead (1964).

The Wilson effect is difficult to measure quantitatively, since the evolution of the shape of the sunspot interferes with a clean determination of this effect. Nevertheless a number of observers have used such data to obtain estimates of the Wilson depression. Compilations of older observations have been given by Bray & Loughhead (1964) and Gokhale & Zwaan (1972) who also critically combined them. They give values of 400–800 km for the Wilson depression, Z_W, of the umbrae of mature sunspots. Prokakis (1974), however, obtains a larger average depth of 950–1250 km. He also distinguishes between small ($Z_W = 700$–1000 km) and large spots ($Z_W = 1500$–2100 km).

The problem of sunspot evolution during its passage across the solar disc is best resolved statistically, i.e. by employing sufficiently large numbers of sunspots. Then the random effects of evolution cancel out, while the Wilson effect remains. Balthasar & Wöhl (1983) found a clever way to avoid measuring the Wilson effect explicitely while still obtaining an estimate of Z_W from a large number of sunspots. They compared the solar rotation rate determined from sunspots in two different ways: 1. by following sunspots over the solar disc, 2. by determining the interval of time between two successive passages of sunspots across, e.g., the central meridian. The rotation rate derived from the first method depends on the magnitude of the Wilson effect, while the second method is independent of it. From the difference between the two the Wilson depression may be estimated. Balthasar & Wöhl (1983) found values of 500–1000 km. These lie closer to the values quoted by Gokhale & Zwaan (1972) than those given by Prokakis (1974).

Various assumptions enter into the deduction of Z_W from Wilson effect observations. One is that since we see higher layers near the limb than at disc centre, we need to assume that the scale-heights of the optical depth in photosphere, penumbra and umbra are similar. If this is not the case, then Z_W would be a function of μ. Chistyakov (1962), cf. Giovanelli (1982), has, for example, claimed that near the limb the radiation from the penumbra comes from higher layers than from the photosphere. This conclusion is controversial, but it serves to illustrate the importance of the above assumption.

Another parameter influencing the result is the size of umbra and penumbra as a function of height. Usually it is assumed that they appear equally large at all heights. Cannon & Wilson (1968) and Wilson & McIntosh (1969) have argued, however, that the size of the penumbra increases with height, at the cost of the umbral size. They employ this construct to explain why near the limb the discward edge of the umbra is fuzzy, while the limbward edge is sharp. Their conclusion is apparently supported by the observations of Collados et al. (1987) that the umbral size decreases also in the direction parallel to the limb.

Solanki & Montavon (1994), however, pointed out that alternative explanations are possible for these observations. These involve the small-scale structure at the inner edge of the penumbra, which gives rise to a ragged umbral edge in high resolution images. This explanation may be more plausible than that proposed by Cannon & Wilson. Nonetheless it does not as yet allow us to estimate to what extent such ragged edges may falsify the results obtained from Wilson effect measurements.

A depressed $\tau = 1$ level in sunspots has two main causes. Firstly, sunspots are dark and cool compared to the quiet photosphere. The H^- bound-free opacity, however, which provides the dominant contribution to opacity in the visible at photospheric levels, depends very sensitively on temperature. At lower temperatures the opacity is reduced and we see deeper into the Sun. The second reason is the radial force balance. The radial component of the magnetohydrostatic (MHS) force balance equation can be written in cylindrical coordinates as (here P is the gas pressure, r and z the radial and vertical coordinates and B_r and B_z the corresponding components of the magnetic field)

$$\frac{\partial P}{\partial r} = \frac{B_z}{4\pi}\left(\frac{\partial B_r}{\partial z} - \frac{\partial B_z}{\partial r}\right). \tag{2.1}$$

The integration of this equation from a point within the sunspot (r) to the quiet Sun ($r = R_s$) gives

$$P(R_s) - P(r) = \frac{1}{8\pi}B_z^2(r) + \frac{1}{4\pi}\int_r^{R_s} B_z\frac{\partial B_r}{\partial z}\,dr = \frac{1}{8\pi}B_z^2(r) + F_c, \tag{2.2}$$

where F_c symbolizes the radially integrated curvature forces.

In the absence of curvature forces this implies a pure pressure balance, which due to the magnetic pressure indicates a lower gas pressure within the sunspot at a given geometrical height. A lower pressure leads to a lower opacity and a further depression of $\tau = 1$. As Martínez Pillet & Vázquez (1993) first proposed, by employing observed values of B_z and T this equation can also be used to deduce the Wilson depression or conversely to get an estimate of the curvature force, F_c, for a given Z_W. They estimated that for the typical values of Z_W given by Gokhale & Zwaan (1972) the curvature forces play as big a role in the force balance as the gas pressure does.

The unknown value of F_c is the greatest source of uncertainty of the Z_W deduced in this manner. The uncertainties plaguing Wilson effect measurements and their interpretation, however, do not have any influence. It is thus encouraging that the two independent techniques give similar results for $|F_c| \lesssim \frac{B_z^2}{8\pi}$

One major advantage of the force balance method is that it allows the determination of Z_W at every location within a sunspot. Solanki et al. (1993) used this technique to estimate Z_W versus radial distance from the sunspot axis. The result is plotted in Fig. 2.3. According to this analysis the $\tau = 1$ level in the penumbra is approximately 50–100 km deeper than in the photosphere, while in the umbra this level lies approximately 400–500 km deeper (assuming $F_c = 0$). Of course, a variable $F_c(r)$ will cause a change in the shape of the Z_W surface.
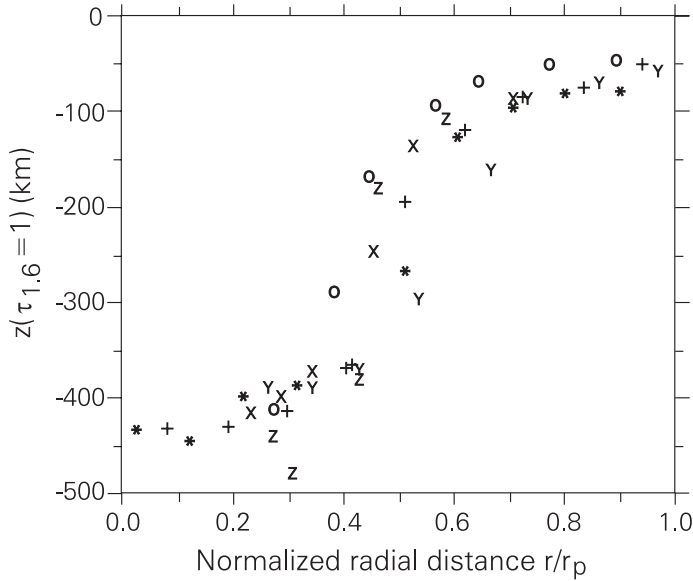
Fig. 2.3. Wilson depression, Z_W, at 1.6 μm vs. r/r_p, the radial distance from the centre of the sunspot normalized to the outer penumbral radius. Each symbol refers to a different cut through the sunspot. The assumption of a potential field inside the boundary current sheet was made when determining Z_W. The symbols represent different slices through the sunspot (see Solanki et al. 1993 for details).

3. Sunspot magnetic field

3.1. Summary of magnetic properties of sunspots

The magnetic field is the central quantity determining the properties of sunspots. It permeates every part of a sunspot and by greatly reducing the convective transport of heat from below is finally responsible for sunspot darkness. Conversely, sunspots were the first astronomical objects recognized to harbour a magnetic field, by Hale (1908a, b). After this discovery Hale continued his observations on Mt. Wilson together with S.B. Nicholson. They found that all observed sunspots exhibit a magnetic field and on the basis of the magnetic field of sunspots also discovered the polarity law of the solar magnetic cycle, often referred to as Hale's law (Hale and Nicholson 1938).

The field strength B is most readily measured through the Zeeman effect in photospheric layers. There it reaches peak values of 2000–3700 G (i.e., 0.2–0.37 T) in parts of the sunspot umbra. The spread in values is intrinsic to the Sun – larger sunspots have higher maximum field strengths. The field strength drops steadily towards the sunspot's periphery, becoming 700–1000 G (0.07–0.1 T) at the edge of the visible sunspot. The strongest field within a sunspot is usually associated with the darkest part of the umbra (dark nucleus) and is generally close to vertical, while at the visible sunspot boundary it is inclined by 70–80° to the vertical. The structure of the magnetic field in a regular sunspot is shown in Fig. 3.1. Plotted are from top to bottom the vertical and radial
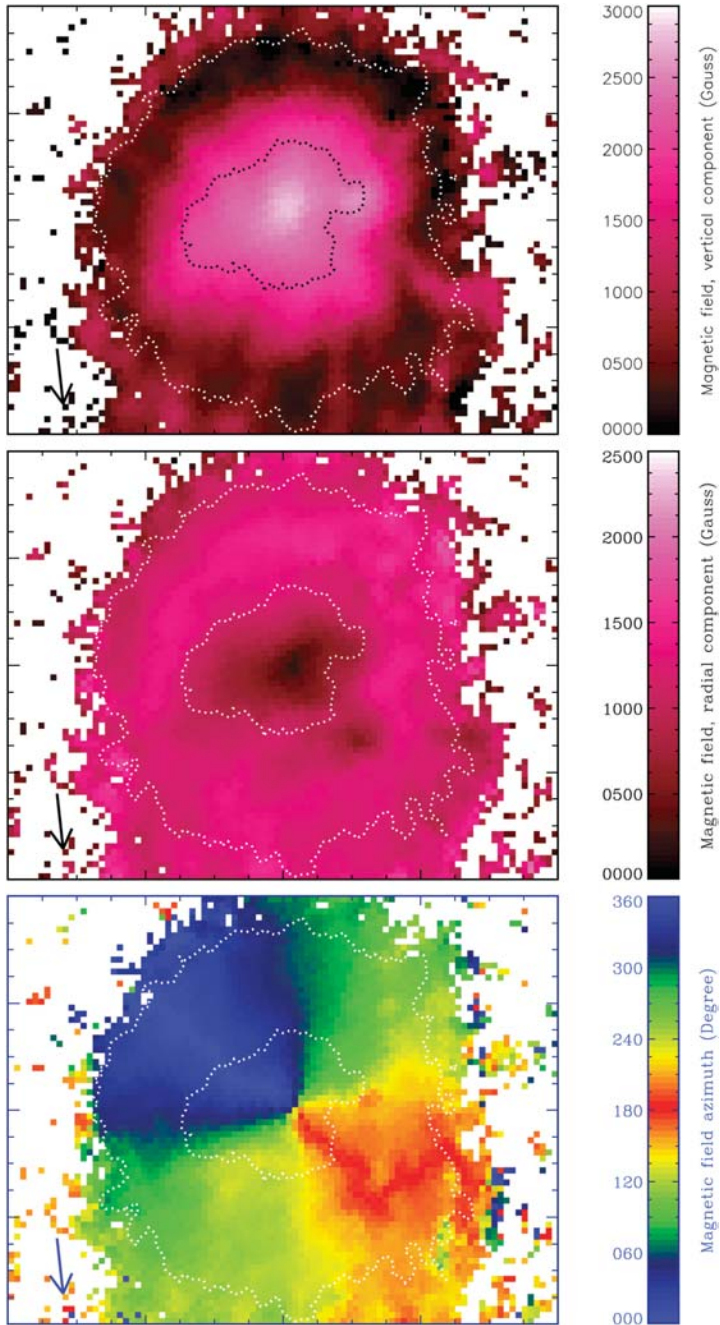
Fig. 3.1. Vertical and radial components of the magnetic vector, as well as the azimuthal direction of the magnetic field in a regular sunspot. The arrow points to disk centre. (Figure kindly provided by S.K. Mathew; see Mathew et al. 2003 for details).
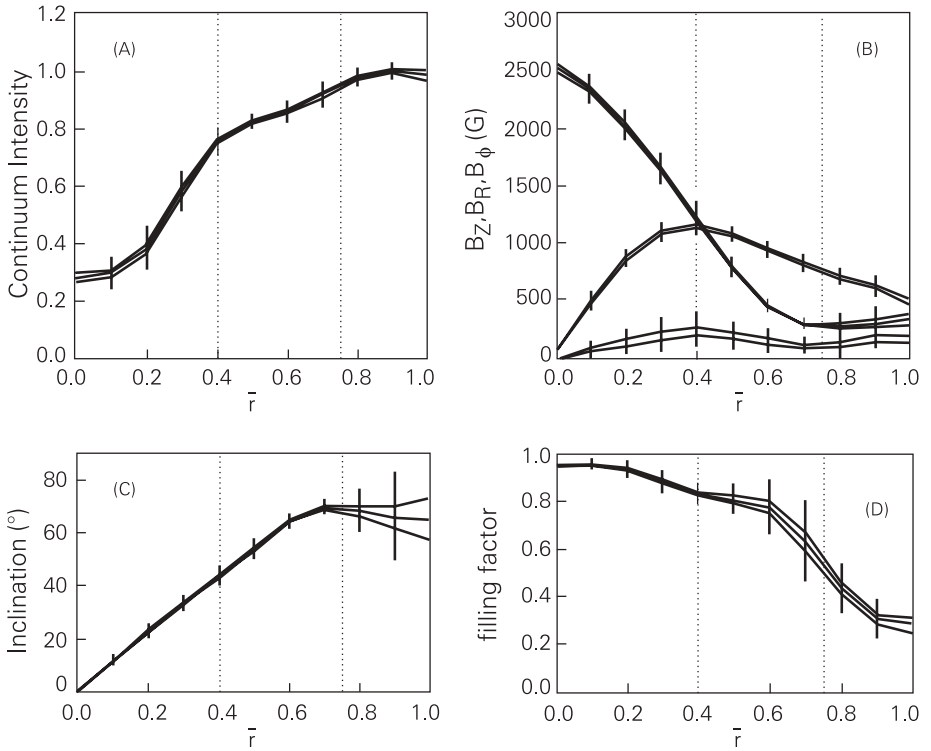
Fig. 3.2. Intensity and magnetic parameters vs. normalized radial distance, $\bar{r}$, from sunspot centre, as determined from 16 observations of sunspots. Vertical dotted lines indicate the umbra-penumbra (*left*) and the penumbra-canopy (*right*) boundaries. Plotted are the continuum intensity in Panel A, vertical (B_z, curve starting at 2500 G), radial (B_r, highest curve for $\bar{r} > 0.6$) and azimuthal (B_ϕ, lowest curve) components of the magnetic field in Panel B, magnetic inclination in Panel C and magnetic filling factor in Panel D. $\bar{r}$ is normalized to the radius at which the canopy could not be seen anymore in the observations (adapted from Keppens and Martínez Pillet 1996, by permission).

components of the field and its azimuthal direction. Azimuthally averaged values of the components of the magnetic vector are plotted in Fig. 3.2.

The observations also indicate that sunspots are bounded by current sheets, i.e., at the solar surface, B falls off rapidly across the sunspot boundary within a radial distance that is small compared to the size of the sunspot. The magnetic field of a sunspot nevertheless continues well beyond its white-light boundary as an almost horizontal canopy with a base in the middle to upper photosphere. The field strength above the height of the canopy base continues to decrease slowly but steadily for increasing distance from the white-light sunspot.

Within the visible outline of the sunspot the field strength decreases with height. In the umbra, at photospheric levels $|\partial B/\partial z| \approx 1$–3 G km^{-1}. When averaged over a height range of 2000 km or more $|\partial B/\partial z|$ is reduced to 0.3–0.6 G km^{-1}.

These observed properties of sunspot magnetic fields support the theoretical concept that visible-light sunspots are the intersection of the solar surface with a large magnetic flux tube emerging from the solar interior into the atmosphere.

At small scales the umbral magnetic field appears to be relatively homogeneous, while the penumbral field is filamented into two radially directed components. These differ by their inclination to the vertical, and possibly also their field strength.

Overviews of the observed magnetic structure of sunspots have been given by Martínez Pillet (1997), Skumanich et al. (1994), Solanki (2002) and may also be found in the volume edited by Thomas & Weiss (1992).

3.2. Large-scale magnetic structure of sunspots

3.2.1. The field strength

Here I discuss only photospheric measurements; the magnetic field measured in the higher layers of the solar atmosphere is the topic of Sect. 3.6. The magnetic field of sunspots has been measured in photospheric layers via the Zeeman splitting of absorption lines in the visible and the infrared. The magnetic field strength is largest near the geometrical centre of regular sunspots, i.e. sunspots with a single umbra that are reasonably circular, and drops monotonically outwards, reaching its smallest values at the outer penumbral edge. Almost all spectral lines show a smooth outward decrease of the field strength. This is in stark contrast to the brightness, which jumps at the boundary between the umbra and penumbra. Hence, the umbral boundary is not evident in the field strength. This simple picture of a relatively smooth magnetic distribution is valid for a spatial resolution of 2–3″ or worse. At higher resolution the fine-scale structure of the field becomes increasingly prominent (see Sect. 3.9). Also, lines that are both strongly B and T sensitive reveal a more complex structure (see end of this section).

Additional evidence that the field strength does not jump at the umbral boundary is provided by the relation between B and continuum intensity, I_c, respectively temperature, T (Kopp & Rabin 1992, Martínez Pillet & Vázquez 1993, Solanki et al. 1993, Balthasar & Schmidt 1994, Stanchfield et al. 1997, Leka 1997, Mathew et al. 2002), which exhibits a discontinuous behaviour there; see Fig. 3.3 and Sect. 5.6.2. This demonstrates that the continuous distribution of the field strength at the boundary is not an artifact caused by smearing due to seeing or by straylight, since the simultaneously measured intensity does indeed show a jump.

There is now a consensus on the approximate general form of the normalized field-strength distribution, $B(r/r_p)/B_0$. Here r is the radial coordinate, r_p is the radius of the outer penumbral boundary and B_0 is the field strength at the centre of the sunspot (i.e. at $r = 0$). The radial dependence of the field strength (in an azimuthally averaged sense) has been measured and reported by, among others, Broxon (1942), Mattig (1953, 1961), Bumba (1960), Treanor (1960), Nishi (1962), Stepanov (1965), Ioshpa & Obridko (1965), Rayrole (1967), Kjeldseth Moe (1968b), Deubner (1969), Beckers & Schröter (1969b), Adam (1969, 1990), Deubner & Göhring (1970), Wittmann (1974), Gurman & House (1981), Kawakami (1983), Deming et al. (1988), Lites & Skumanich (1990), Solanki et al. (1992), McPherson et al. (1992), Hewagama et al. (1993), Balthasar & Schmidt 1993, Keppens & Martínez Pillet (1996), Stanchfield et al. (1997) and West-

a   **b**
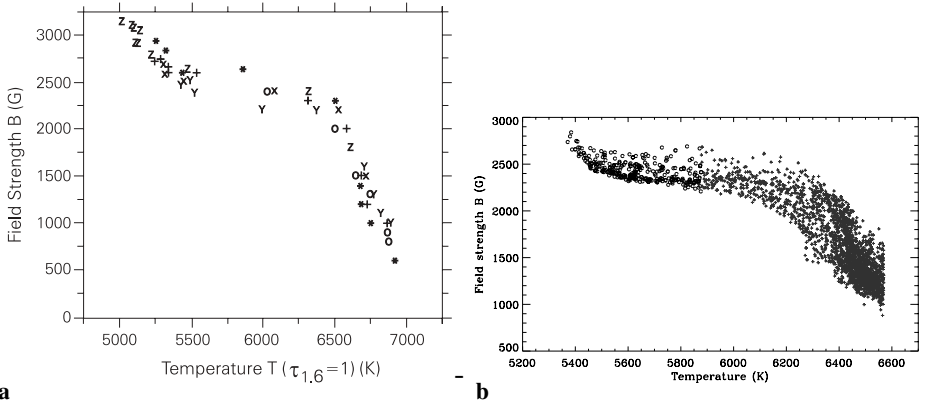
Fig. 3.3a,b. Magnetic field strength, B, vs. temperature at unit continuum optical depth, $T(\tau_{1.6} = 1)$, relationships derived from 1.56 µm lines. **a:** The result for a large sunspot. The different symbols refer to different slices through the sunspot (from Solanki et al. 1993). **b:** The same, but using a larger sample of observations of higher quality, for a smaller sunspot at $\tau_{0.5} = 1$ (from Mathew et al. 2002).

a   **b**
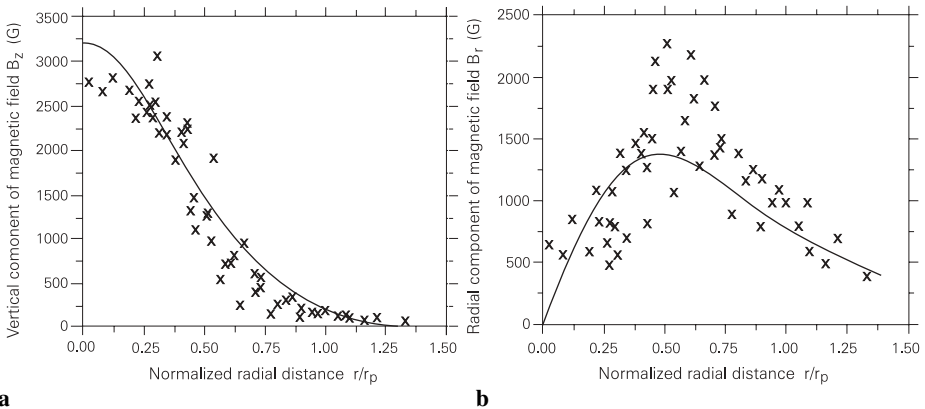
Fig. 3.4. a: $B_z(r/r_p)$ and **b:** $B_r(r/r_p)$. The observed values (based on Stokers I and V profiles at 1.56 µm) are represented by crosses, a fit based on a buried dipole by solid curves. Here B_z is the vertical and B_r the radial component of the magnetic vector, r is the radial coordinate measured from the geometrical centre of the sunspot and r_p is the outer radius of the penumbra. The data are taken from Solanki et al. (1992). Figure kindly provided by U. Walther.

endorp Plaza et al. (2001a). Although all of these investigators find the same qualitative $B(r)$ behaviour, there are nevertheless, considerable quantitative differences.

A set of recent measurements of $B(r/r_p)$ in regular, i.e. almost circular sunspots, are shown in Fig. 3.2. For comparison, the edge of the umbra, r_u/r_p lies at 0.4–0.5. Such regular, isolated sunspots do not appear to show a global azimuthal twist of the field significantly above 20° (e.g. Landi Degl'Innocenti 1979, Lites & Skumanich 1990), cf.

Fig. 3.1, bottom frame. Magnetic dipole fits to such data (e.g., Lites & Skumanich 1990) are reasonable, but not perfect in many cases (see Fig. 3.4).

Early measurements often showed a rapid decrease of B/B_0 toward the sunspot boundary, so that $B(r_p)/B_0 \approx 0.1$ (Broxon 1942, Mattig 1953, 1961, Bumba 1960, Nishi 1962, Deubner 1969). In contrast, Beckers & Schröter (1969b) from high spatial resolution observations concluded that $B(r_p) \approx 1300$ G, corresponding to $B(r_p)/B_0 \approx 0.5$. Rayrole (1967) also found a sizable field strength at $r = r_p$. The measured value of $B(r_p)$ depends significantly on a number of parameters, the most important being seeing ($B(r_p)/B_0$ is lower if seeing is worse), the Zeeman sensitivity of the observed spectral lines ($B(r_p)/B_0$ is less accurate if insensitive lines are used) and the types of diagnostics (the accuracy increases with the number of Stokes parameters employed and depends on the details of the analysis, etc.). The fact that the sunspot magnetic field is weakest and the straylight is strongest at the boundary makes measurements there particularly challenging.

Subsequently deduced values have been found to lie between the extremes mentioned above, with the most reliable coming from infrared observations and data collected with the Advanced Stokes Polarimeter (ASP, Elmore et al. 1992). These give $B(r_p) \approx$ 700–1000 G, which implies $B(r_p)/B_0 \approx 0.2$–0.4 (Lites et al. 1990, Solanki et al. 1992, McPherson et al. 1992, Skumanich 1992, Kopp & Rabin 1992, Hewagama et al. 1993, Balthasar & Schmidt 1993, Skumanich et al. 1994, Keppens & Martínez Pillet 1996). Westendorp Plaza et al. (2001) find that $B(r_p)/B_0$ depends strongly on the height considered, being larger in the upper photosphere than at deeper layers. The fact that B is so large at the white-light boundary of the sunspot suggests that sunspots are bounded by a current sheet (Solanki & Schmidt 1993), although the raggedness of the sunspot boundary in white-light images means that the current sheet is not as smooth as one might picture on the basis of simple flux-tube models. Further evidence for a current sheet surrounding sunspots comes from observations suggesting that (on scales larger than a few arc sec) the field inside sunspots is close to potential, so that the currents bounding the strong field must be mainly located in a relatively thin sheet at the magnetopause (e.g., Lites & Skumanich 1990).

In addition to the systematic differences introduced by the employed observational techniques to the shape of the $B(r/r_p)/B_0$ curve deduced by different investigators, intrinsic differences between sunspots may also contribute. Thus $B(r/r_p)/B_0$ may well depend on other parameters of the sunspot, such as its size, or its regularity. For example, Keppens & Martínez Pillet (1996) find that pores show a considerably larger $B(r_p)/B_0$ [and even a larger unnormalized $B(r_p)$] than the generally larger sunspots.

Another location at which it is difficult to measure accurate properties of the sunspot plasma is near the umbra-penumbra boundary. Particularly on the umbral side of the boundary straylight from the penumbra could falsify local values. The umbral boundary usually corresponds to a field strength of around 1400–2200 G, with the deduced value depending somewhat on the spectral line used (Lites et al. 1990, 1991, Schmidt et al. 1992, Balthasar & Schmidt 1993, Skumanich et al. 1994, Keppens & Martínez Pillet 1996).

Field strength (and inclination) measurements in the umbra are also plagued by problems, the foremost being straylight and increased blending, particularly by molecular lines. This generally led to, on the one hand, inaccuracies in the field strength of the

coolest umbrae (due to blending, cf. Livingston & Wallace 1985 and Berdyugina et al. 2002) and, on the other hand, to a gross underestimate of B of the smallest umbrae (due to straylight). The latter problem was clearly revealed by Brants & Zwaan (1982). They showed that if, as is usual, an Fe I line in the visible is used to measure B in small umbrae (or pores) then the B_0 values keep decreasing with decreasing size of the magnetic feature due mainly to the mixing in of less strongly Zeeman split, or of unsplit profiles from the penumbra and quiet Sun as part of the increasing straylight. If, instead, a Ti I line formed almost exclusively in umbrae is used, then its profile shape is unaffected by straylight and a peak value of at least 2000 G is measured even for the smallest umbrae. Brants & Zwaan (1982) used the Ti I $\lambda 6064.6$ Å (Landé $g = 2$) line, which had originally been proposed by Zwaan & Buurman (1971).

Note, however, that there may also be a solar reason for the larger field strength sampled by the Ti I line. The umbra can be quite inhomogeneous in temperature. Whereas Fe I and II lines obtain larger contributions from the warmer and brighter regions (having smaller field strength according to the almost universal $T–B$ relation, e.g. Fig. 3.3) the Ti I line samples mainly the stronger fields of the cooler regions. The major part of the difference is due to the straylight, however, since for larger spots the 2 lines give rather similar B values, although large umbrae also contain considerable temperature inhomogeneities (see Sect. 5.4.1 and 5.6.2). Additionally, recent observations with lower straylight of small sunspots and pores in Fe I lines (Muglach et al. 1994, Keppens & Martínez Pillet 1996, Sütterlin 1998) confirm the results of Brants & Zwaan (1982). See also the earlier analyses by Steshchenko (1967) and Zwaan (1968).

The maximum field strength within a sunspot (i.e. B_0) thus increases almost linearly with sunspot diameter from $B_0 \approx 2000$ G for the smallest up to 3700 G for the largest (e.g., Ringnes & Jensen 1961, Brants & Zwaan 1982, Kopp & Rabin 1992, Collados et al. 1994, Solanki 1997b, Livingston 2001). Hence B_0 increases by a factor of roughly 2 as the amount of magnetic flux increases by a factor of 30. For the field strength averaged over the sunspot the variation is possibly even smaller, being less than a factor of approximately 1.5. In addition, the average field strength, $\langle B \rangle \approx 1000$–1700 G (or 1200–1700 G if the value deduced for one small sunspot is removed from the list, Solanki & Schmidt 1993) is very similar to the field strength of magnetic elements, or small flux tubes (where, due to the finite spatial resolution of the observations the measured B is always an average over the flux tube cross-section). The averaged B values obtained from recent observations also lie in this range. For example, $\langle B \rangle = 1360$ G, 1270 G and 1370 G for the spots analysed by Lites et al. (1993), Skumanich et al. (1994) and Keppens & Martínez Pillet (1996), respectively. Therefore B averaged over flux tubes remains almost unchanged over 5–6 orders of magnitude of magnetic flux per feature, as pointed out by, e.g., Solanki et al. (1999). For $\langle B_z \rangle$ Skumanich (1999), cf. Leka & Skumanich (1998), obtains roughly 800 G $\pm$ 32 G (considering only the dark part of sunspots). This value is also valid for pores.

One surprising result of recent years has been the discontinuous $B(r)$ relation indicated by infrared Ti I lines at 2.24 μm. This is in contrast to all other diagnostics. These lines are simultaneously very sensitive to magnetic field and temperature, which makes them unique in this respect. They sample mainly the coolest components of the sunspot. So far only a single sunspot has been mapped in these lines. It exhibits a strong field ($B \approx 2700$ G), with comparatively small zenith angle in the umbra which jumps to an

almost horizontal, weak field ($B < 1000$ G) in the penumbra. There is no sign of fields at intermediate strengths or inclinations in these lines (Rüedi et al. 1998a), although a raster in the almost equally Zeeman sensitive, but far less temperature sensitive Fe I line at 1.56 μm displays the usual smooth decrease (Rüedi et al. 1999a).

3.2.2. Magnetic field orientation

The orientation of the magnetic vector has been measured (in some cases only partially) by, e.g., Hale & Nicholson (1938, only Stokes I and V), Bumba (1960), Leroy (1962), Nishi (1962), Stepanov (1965), Kjeldseth Moe (1968b), Rayrole (1968), Adam (1969, 1990), Beckers & Schröter (1969b, only from Stokes I and V), Deubner & Göhring (1970), Wittmann (1974), Gurman & House (1981), West & Hagyard et al. (1983, only of the transverse field component), Kawakami (1983), Lites & Skumanich (1990), Solanki et al. (1992, only from Stokes I and V, but of a fully split line), Hewagama et al. (1993), Lites et al. (1993), Skumanich et al. (1994), Keppens & Martínez Pillet (1996), Stanchfield et al. (1997), Westendorp Plaza et al. (1997b, 2001a), cf. Kálmán (1991), Ye & Jin (1993).

In order to determine the complete orientation all four Stokes parameters need to be measured. When a sunspot located near the centre of the solar disc is observed with Stokes I and V alone basically the zenith angle is determined (although with variable accuracy, depending on γ and the heliocentric angle μ), while measurements of Q and U alone give only the field azimuth. In cases in which only Stokes I and V were used (which includes a number of older observations) often the sunspot was followed over the solar disc and the position of the neutral line was employed as an indicator of the inclination.

Many of the most recent results are based on Stokes vector observations made with the Advanced Stokes Polarimeter (ASP) and on an analysis involving inversions using a Milne-Eddington model. These allow the almost routine determination of vector magnetic fields in sunspots. Nevertheless, some open questions remain which are pointed out later in this section.

The strongest part of a sunspot's magnetic field is in general also the most vertical one. Inclination to the surface normal (i.e. zenith angle, ζ) increases steadily as the field strength decreases. An example of a recent set of $\zeta(r/r_p)$ measurements is plotted in Fig. 3.2. Stanchfield et al. (1997) find an almost linear dependence of ζ on B (cf. Hale & Nicholson 1938, Beckers & Schröter 1969b, Westendorp Plaza et al. 2001a). In the infrared, at 1.56 μm, the functional form seems to be more complex (Solanki et al. 1992). Also, Solanki et al. (1993) find a relatively good correlation between ζ and T, again based on 1.56 μm observations. To what extent the infrared results are influenced by stray light needs to be checked with the help of new observations.

The uncertainty in the $\zeta(r)$ dependence is particularly acute at the sunspot boundary. Early investigations suggested that $\zeta = 90°$ at the boundary, i.e. that the field is horizontal (these include all observations prior to 1970, Wittmann 1974 and Giovanelli 1982). More recently, the evidence for an average inclination of 10–20° to the horizontal (i.e., $\zeta \approx 70$–80°) at the boundary has steadily increased (e.g., Kawakami 1983, Adam 1990, Lites & Skumanich 1990, Solanki et al. 1992, Lites et al. 1993, Title et al. 1993, Hewagama et al. 1993, Skumanich et al. 1994, Shinkawa & Makita 1996, Keppens & Martínez Pillet

1996, Westendorp Plaza et al. 2001a). These last authors also deduce the inclination as a function of height and find ζ to increase with depth in the outer penumbra, with azimuthally averaged values of 65°–85° between $\log \tau = -2.8$ and 0. This broad range of values may explain differences seen between, e.g., visible and IR lines in recent investigations. Skumanich et al. (1994) followed a regular sunspot for close to 10 days. They find that in this period its flux decayed with a decay time of approximately 70 days. Interestingly the inclination to the vertical at the penumbral boundary also decreased with time, starting at around 75° and ending at around 60°, with a "decay time" of roughly 60 days, i.e. comparable with the decay time of the field. This suggests that the inclination to the vertical is a function of sunspot size, not unlike the prediction of the theory of flux tubes. Given the overhelming new evidence against the $\zeta = 90°$ values of older observations, these were therefore probably overestimated due to insufficient correction for stray light, which is particularly acute near $r/r_p = 1$ (cf. Stenflo 1985, who pointed out that too large ζ values are deduced if the magnetic field strength is underestimated).

An azimuthally averaged zenith angle $\lesssim 70°$ at the penumbral edge, as deduced from careful recent observations in the visible, is difficult to reconcile with the evidence for a low-lying, almost horizontal magnetic canopy just outside the penumbra (see next section). The problem is enhanced by the finding of Westendorp Plaza et al. (1997a, 2001a) that a part of the field lying horizontally in the penumbra (and thus contributing to a larger ζ) disappears into the solar interior and does not contribute to the canopy. Solanki et al. (1992) and Keppens & Martínez Pillet (1996) argue that the too small measured values of the zenith angle are caused by the contribution from signals arising from small magnetic elements around sunspots, e.g., the so called moving magnetic features (Harvey & Harvey 1973, Harvey et al. 1975, Ryutova et al. 1998; see Sect. 7.3.5) into those from the sunspot. If this is correct then infrared observations at 1.56 μm have an advantage, since, due to their large Zeeman sensitivity (Solanki et al. 1992), they can distinguish between the two magnetic components, although right at the sunspot boundary there may still be intermixing due to the similar field strengths. One problem with this interpretation is that on average there is a nearly equal amount of flux in both polarities in moving magnetic features and it is not *a priori* clear whether on average a more vertical field will be seen due to their presence. Other possible explanations should therefore also be studied, such as the fact that visible spectral lines are more sensitive to fields associated with brighter material which have smaller ζ (this could be tested by determining ζ using the 2.2 μm Ti I lines, which sample the cooler material), or the unknown differential influence of stray light from the canopy on Stokes Q, U and V. Note that Solanki et al. (1996a) considered the opposite problem, namely the influence of sunspot canopies on the inclination angle of plage fields and found that errors of 5–10° were introduced in this manner. Interestingly they found that inclination obtained with 1.56 μm lines were more reliable than with visible lines. This is also expected to be true for the inclination of the sunspot field.

The generally more horizontal fields in the outer penumbra seen by infrared lines is probably at least partly also due to the fact that they sample on average somewhat cooler material and lower heights than visible lines. The cooler material is associated with more horizontal fields (Rüedi et al. 1998a), but see the discussion in Sect. 3.9.3.

Furthermore, the field in lower layers of the outer penumbra is more horizontal according to Westendorp Plaza (2001a).

Early vector-magnetograph observations often suggested that the magnetic field of regular sunspots is significantly twisted (Hagyard et al. 1977). Landi Degl'Innocenti (1979) showed, however, that these ubiquitous twists or spirals were an artifact produced by neglecting magnetooptical effects (cf. West & Hagyard 1983, Landolfi & Landi Degl'Innocenti 1982, Landolfi et al. 1984, Balasubramaniam & Petry 1995). Once such effects are included in the analysis the magnetic fields of regular sunspots become almost radial (see Fig. 3.1). A small residual twist of up to 10–15° still persists, however, according to Lites & Skumanich (1990), Skumanich et al. (1994), Keppens & Martínez Pillet (1996) and Westendorp Plaza et al. (1997b; 2001a). On one particular day Gurman & House (1981) even found a twist of 35° for a single sunspot. On the previous day, however, the same sunspot showed no significant twist. In the absence of other such observations, this single measurement of a strongly evolving twist must be treated with caution.

A residual twist is not entirely surprising considering the fact that in Hα the super-penumbra is seen to be strongly twisted. This twist increases with increasing distance from the sunspot. Near solar disc centre there appears to be a reasonable coincidence rate (50–70%) between the direction of the *transverse* component of the field determined from photospheric transverse magnetograms and Hα fibrils (Tsap 1965, Kálmán 1979, Makita et al. 1985, Kawakami et al. 1989). However, the coincidence rate decreases rapidly towards the limb (20% near the limb). Kawakami et al. (1989) successfully model this effect on the basis of the different heights sampled by Hα and the magnetogram. These results suggest that the residual twist of the sunspot magnetic field is consistent with the twisted Hα fibrils seen in the superpenumbra around symmetric sunspots. Note, however, that the 180° ambiguity in the azimuth (defined in the plane perpendicular to the LOS) also implies an even less reliable determination of the direction of the transverse component of the field as one goes closer to the limb. Kálmán (1991) investigated the alignment of the transverse field with photospheric penumbral fibrils. He also noticed a strong decrease of the alignment when going from disc centre to the limb. He quantitatively reproduced this using a model which incorporates horizontal penumbral fibrils, while the field is inclined by up to 50° to the horizontal in the penumbra. Finally, the orientation of the Hα fibrils near disc centre is found to correlate with the orientation of moving magnetic features (MMFs, Yurchyshyn et al. 2001; Zhang et al. 2002; see Sect. 7.3.5).

3.2.3. Subsurface magnetic structure

The magnetic structure of a sunspot below the solar surface is not directly observable, but can in principle be deduced from the change in the properties of p-modes in and around sunspots.

Observations by Braun et al. (1987, 1988, 1992), Bogdan et al. (1993), Braun (1995), Lindsey & Braun (1999) and others of the change in amplitude and phase of p-mode waves passing through sunspots provide evidence of subsurface absorption and scattering of incoming waves by the magnetic and thermal inhomogeneity constituting the sunspot and carries information on the subsurface structure of the sunspot. The theory

of the interaction of p-modes with complex magnetic structures (such as sunspots, if the fibril model of their subsurface field is correct, see Sect. 4.3) is not yet complete, but numerous simplified approaches have been taken (see Bogdan & Braun 1995, Bogdan 2000, Bogdan et al. 2002 for reviews).

One attempt to distinguish between different models of the subsurface structure of sunspots has been made by Chen et al. (1997) on the basis of data from the Taiwan Oscillation Network (TON; Chou et al. 1995). They interpret the results of inversions in terms of the sunspot cross-section as a function of depth with the help of two simple models, one in which the flux tube underlying the sunspot is cylindrical, the other in which it is funnel shaped. The two models give somewhat different signatures, but unfortunately both of these lie within the error bars of the data. Chen et al. (1997) do find, however, that a spot with a field having depth independent plasma β is not compatible with the acoustic images of the solar interior in a sunspot region made by Chang et al. (1997). These suggest that the horizontal size of the p-mode absorption region does not change significantly down to a depth of 30 Mm. Such a constant cross-sectional area is consistent with Parker's fibril model of the subsurface field of sunspots (Sect. 4.3).

The subsurface flow crossing a sunspot deduced by Zhao et al. (2001) has also been argued to support the fibril model. Such a flow can weave its way between individual fibrils, but cannot cross a monolithic flux tube (see Kosovichev 2002 for a review). Evidence has also been found for a collar flow, with a converging vortex flow in the top 4 Mm below the solar surface which turns into a downflow and finally an outflow at greater depth (Kosovichev 2002). Note, however that in the top few hundred km below the surface an outflow is found (Gizon et al. 2000), which is compatible with the Evershed effect and the moat flow (Sect. 7). Finally, the fact that wave speed disturbances are not seen any more at depths greater than 12–20 Mm below sunspots has been interpreted by Jensen et al. (2001) to indicate that B^2 does not increase so rapidly with depth as the gas pressure, in agreement with the conclusion drawn by Chen et al. (1997).

3.3. Magnetic canopy

In the solar atmosphere the magnetic field continues beyond the white-light boundary of sunspots. It forms an almost horizontal canopy with a base in the middle or upper photosphere, i.e. the field is limited to the upper part of the photosphere and higher atmospheric layers; it overlies relatively field-free gas. The lower boundary of the magnetized layer in the superpenumbra is called the canopy base. The magnetic canopy is a natural result of the expansion with height of the magnetic flux tube underlying the sunspot. Recall that the visible sunspot is just a cross-section through this flux tube. In this picture the canopy base corresponds to the current sheet surrounding the sunspot.

Most older observations showed no consistent signs of the continuation of the sunspot's magnetic field beyond its boundary. This had mainly to do with the fact that the measurements were not particularly sensitive and were often limited to the longitudinal component of the magnetic field, whereas the field is almost horizontal, i.e. perpendicular to the line-of-sight at disc centre.

A number of observers have explicitly argued that the magnetic field stops abruptly (e.g., Beckers & Schröter 1969b, Wiehr et al. 1986, Wiehr & Balthasar 1989) or relatively abruptly (Zhang 1996) at the sunspot boundary. However, they usually base their con-

clusions to a large extent or even exclusively on the splitting or broadening of Stokes I, which is insufficiently sensitive to detect canopy fields of the type surrounding sunspots. Note also that the gas pressure above the canopy base is lower than at the same height in the quiet Sun (due to force balance across the canopy base). This implies that spectral lines obtain less contribution from the magnetized material above the canopy than naively expected. This may also contribute to the non-detection of canopies in some cases.

The signature of sunspot canopies was first noticed by W. Livingston in magnetograms taken in lines formed in the upper photosphere and lower chromosphere, which show large diffuse patches of field filling the limbward and discward superpenumbrae of sunspots located near the solar limb. These observations were interpreted by Giovanelli (1980) in terms of canopies with base heights in the upper photosphere covering large areas around sunspots. His analysis was refined by Jones & Giovanelli (1982) and applied to additional observations of sunspots and their surroundings by Giovanelli & Jones (1983). They deduced canopy base heights below 400 km in the superpenumbra (the height being measured relative to the $\tau = 1$ level in the quiet photosphere).

More recently, canopies have been regularly detected using different types of observations. These include infrared Stokes observations in Zeeman sensitive lines at $12\,\mu$m (Bruls et al. 1995, on the basis of the observations of Hewagama et al. 1993, cf. Deming et al. 1988), at $1.56\,\mu$m (Solanki et al. 1992, 1994, 1999, cf. Finsterle 1995) and most recently at $2.2\,\mu$m (Rüedi et al. 1998a). The derived canopy base heights generally lie below 400 km. The comparison of sensitive observations taken in a photospheric (Si I 10827 Å) and a chromospheric line (He I 10830 Å) reveal the difference in smoothness of the field at the two heights and indicate the presence of a canopy in the sense that the chromospheric line indicates more flux in the vicinity of the sunspot than the photospheric line (Rüedi et al. 1995a). Similarly, the comparison of chromospheric magnetograms (in Hβ) and photospheric vector magnetograms (Zhang 1994) suggested that the chromospheric field extends into the superpenumbra, where it is almost horizontal, another confirmation of sunspot canopies. Zhang (1994) also argues that the field in the canopy follows the Hβ fibrils and is strongest in the fibrils. Given the difficult interpretation of the Balmer lines confirmation of this last result using other spectral lines would be welcome. The parts of the canopy close to the sunspot have also been detected as homogeneous horizontal fields in observations of the full Stokes vector (e.g., Lites et al. 1993, Adams et al. 1994, Skumanich et al. 1994, Keppens & Martínez Pillet 1996). Finally, inversions indicating a rapid increase of the field strength with height in the superpenumbra have been interpreted as showing the presence of a canopy by Westendorp Plaza et al. (2001a). Note, however, that the field is also found to be more vertical with height there. The interpretation of this last result is less obvious, unless the observations are contaminated by polarized stray light from the penumbra. Note that all these newer techniques also allow canopies to be detected when the sunspot is close to disc centre and they all give roughly consistent results.

The Zeeman sensitivity of infrared observations provides them with the capability to determine the intrinsic field strength in the canopy. $B(r/r_p > 1)$ is found to decrease continuously without any visible break at the white-light boundary of the sunspot (Solanki et al. 1992). The base height of the canopy increases relatively rapidly close to the sunspot, consistent with an average inclination of $10°$ of the field lines to the
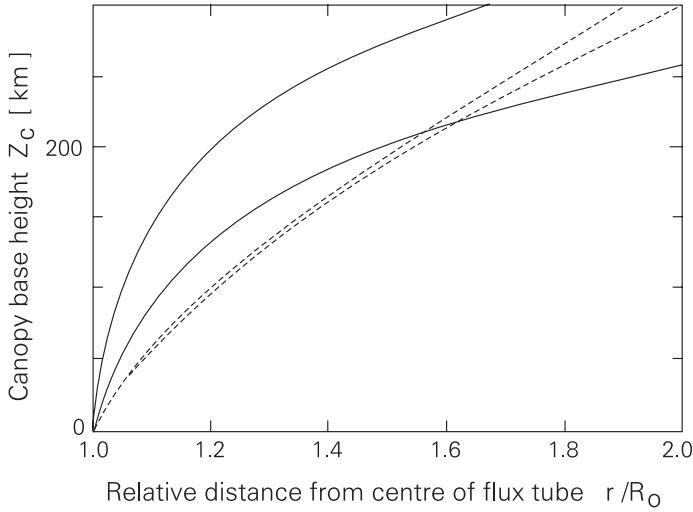
Fig. 3.5. Canopy base height, Z_c, vs. distance from the centre of the flux tube normalized to its radius. The solid curves encompass the range of canopy base heights of sunspots, the dashed curves for slender flux tubes (from Solanki et al. 1999).

horizontal at $r = r_p$ (but not with 20° unless the field lines are strongly bent there). However, this rise soon slows, so that the canopy can be followed out to almost twice the sunspot radius using purely photospheric lines.

Recently Solanki et al. (1999) have demonstrated that if the pressure balance is taken into account properly the canopy base height is lowered by 100–150 km relative to the results of Solanki et al. (1992, 1994). Then the base height increases with r/r_p in a way consistent with the thin flux tube approximation, although sunspots definitely do not satisfy the conditions under which the thin-tube approximation is expected to be valid (namely that the width of the flux tube is smaller than the pressure scale height). The expansion of sunspots in the photosphere (i.e. the canopy base height) compared with that of thin tubes in plotted in Fig. 3.5. Hence, in some ways the largest and the smallest flux tubes behave in a surprisingly similar manner.

Evidence is now emerging that the magnetic canopy is intimately connected with Moving Magnetic Features (MMFs, e.g. Harvey & Harvey 1973, Shine & Title 2001). Recent studies of bipolar MMFs (Yurchyshyn et al. 2001, Zhang et al. 2002) have indicated that their orientation follows that of the superpenumbral fibrils, i.e. of the field in the magnetic canopy, with the bipoles being directed such that the leading MMF of the pair has the polarity of the sunspot. This has been interpreted by Zhang et al. (2002) to indicate a U-loop produced by a dip in the canopy. The visible MMFs are located where the 2 arms of this loop intersect the solar surface.

3.4. Return flux and depth of the penumbra

Spruit (1981b) has argued that the general inclination of the field inside the penumbra is compatible with the emergence of a considerable amount of flux there. An analysis based

on the premise that the sunspot magnetic field is potential inside the bounding current sheet allows more quantitative estimates to be made. Thus Schmidt (1991) and Solanki & Schmidt (1993) find that approximately 1–1.5 times as much magnetic flux emerges in the penumbra as in the umbra. The penumbra is thus deep, in contrast to the model of a shallow penumbra in which the magnetopause (current sheet bounding the flux tube forming the sunspot) lies along the solar surface in the penumbra and no magnetic flux emerges there. The assumption of a potential field underlying this analysis is reasonable (e.g., Lites & Skumanich 1990), although it is not exactly fulfilled by sunspots (e.g., Jahn 1989, Leka 1997).

The presence of a canopy implies that at least some of the magnetic flux emerging in the sunspot penumbra does not return to the solar interior in the immediate surroundings of the sunspot. X-ray images overlaid on white-light images further suggest that a considerable fraction of the penumbral flux probably returns to the solar interior far from the sunspot (Sams et al. 1992). Solanki & Schmidt (1993) and Lites et al. (1993) came to the conclusion that little flux re-enters the solar interior beyond the sunspot boundary in the vicinity of the sunspot, i.e. that there is relatively little so-called "return flux", whose presence was predicted by Osherovich (1982).

Inversions of data gathered by the Advanced Stokes Polarimeter (ASP) have meanwhile revealed the presence of return flux at some locations along the boundary of the sunspot (Westendorp Plaza et al. 1997a, 2001a). These locations are cospatial with downflows which are interpreted as a part of the Evershed flow draining down into the solar interior again. The 1-D inversions in conjunction with earlier investigations suggest that higher-lying field lines and the associated flowing gas pass on into the canopy, while at least some of the lower lying, almost horizontal field lines return to the solar interior at the sunspot boundary. Since at the sunspot's periphery return flux and the associated downflows are only seen at some localized positions the amount of return flux is probably a minor fraction of that emerging through the penumbra. Nevertheless, due to the strong stratification of the mass with height, a large fraction of the mass carried by the Evershed effect may submerge there. The localized downflows at the outer penumbral edge have been confirmed by Schlichenmaier & Schmidt (1999) on the basis of direct wavelength shift measurements of the C I 5380 Å line, which is formed deep in the photosphere. More recently, Del Toro Iniesta et al. (2001) report return flux in the interior of the penumbra. How significant the amount of return flux within the penumbra is cannot be judged on the basis of the 2 profiles that they discussed. A certain amount of return flux, associated with downflows could solve a problem associated with getting the thermal flux needed to heat the penumbra to the solar surface (Solanki et al. 2002).

3.5. Magnetic filling factor

In order to explain phenomena such as umbral dots some theorists (e.g., Choudhuri 1986) have proposed the intrusion from below of field-free material into umbrae. In addition, prior to the discovery of the downflows at the outer penumbral edge the presence of field-free material in penumbrae could resolve the mass-flux problem of the Evershed effect in a straightforward manner (if the Evershed flow were restricted to field-free channels). It is therefore worthwhile to look for field-free gas at different locations in sunspots.

In order to answer the question of whether and how much field-free material is present in sunspots at the level of line formation either the field-free intrusions need to be resolved or the magnetic filling factor needs to be determined. Only in light bridges is there direct evidence for the presence of narrow lanes of field-free material in sunspots (Lites et al. 1990, 1991; cf. Leka 1997, Sect. 3.9.2). Elsewhere the filling factor is the only source of relevant information. Obtaining the filling factor is not straightforward, since straylight from the much brighter field-free photosphere is generally not completely suppressed and can be distinguished from the signature of field-free gas inside the sunspot only with difficulty. Hence, in general only upper limits on the relative area coverage by field-free material inside sunspots can be given. Using the 12.32 μm emission line Hewagama et al. (1993) set an upper limit of only 5% in the outer, warmer part of the umbra and the inner penumbra. In the outer penumbra this limit rises to 10–20% due to the increasing amount of stray light.

Similarly, from visible-light ASP observations Lites et al. (1993), Skumanich et al. (1994) and Keppens & Martínez Pillet (1996) obtain an upper limit of 5% in the central penumbra and 3–4% in the central part of the umbra for a total of 4 sunspots. Near the umbral boundary the upper limit lies around 15% and also grows rapidly close to the outer penumbral boundary. The azimuthally averaged filling factor deduced by Keppens & Martínez Pillet (1996) is plotted in Panel D of Fig. 3.2.

One caveat to keep in mind when considering these observations is that the Fe I 6302 Å line observed by the ASP is formed in mid-photospheric layers, and the Mg I 12.32 μm line is formed in the upper photosphere. The magnetic energy begins to dominate over that of the gas at these heights, but does not do so in the lower photosphere (cf. Solanki et al. 1993). If field-free patches exist then it is far more likely that these are located in the lower photosphere. Indeed, Degenhardt & Lites (1993a, b) showed that a field-free intrusion of the type expected for umbral dots should only reach into the lower photosphere. Hence it would be visible in the Fe I 1.56 μm line, but not, e.g., in Fe I 6302 Å formed 100–150 km higher and certainly not in the 12.32 μm line. So far the only published investigation of the filling factor in sunspots using the 1.56 μm line has been carried out by Solanki et al. (1992) and it gives an upper limit of 5% in the central penumbra. However, only individual cuts through the sunspot in Stokes I and V were considered and it is important to obtain and analyse extensive measurements of the full Stokes vector of this line.

Hence, combining the results of all investigations we can conclude that less than 5% of the material in the photospheric layers of sunspots is unmagnetized, with the exception of the outer part of the penumbra, where the upper limit is much weaker. However, further investigations at 1.56 μm are needed.

3.6. Magnetic field in the upper atmosphere

In addition to the large number of observations in the lower and central photospheric layers the sunspot magnetic field has been recorded and in some cases mapped at greater heights as well. These investigations include observations of the upper photospheric layers in the 12 μm line (Deming et al. 1988, 1991, Hewagama et al. 1993), the lower chromospheric layers observed in Na I D (Metcalf et al. 1995, Eibe et al. 2002) or the

Mg I b lines (Livingston, [1] Lites et al. 1988, Murphy 1990), the middle chromosphere probed with the Ca II K line (Martínez Pillet et al. 1990, although only for a few spatial points) and the Hα and Hβ lines (e.g., Abdussamatov 1971a, b, Wang & Shi 1992, Dara et al. 1993, 1995, Li et al. 1994, Zhang 1996), the upper chromosphere studied with He I 10830 Å (Harvey & Hall 1971, Rüedi et al. 1995a, 1996, Penn & Kuhn 1995), the transition zone probed by the C IV line near 1550 Å (e.g. Tandberg-Hanssen et al. 1981, Henze et al. 1982, Hagyard et al. 1983, Henze 1991) and, finally, the lower corona investigated using radio observations (Ginzburg & Zheleznyakov 1961, Gelfreikh & Lubyshev 1979, Alissandrakis et al. 1980, Schmahl et al. 1982, Akhmedov et al. 1982, 1983, Kundu & Alissandrakis 1984, Alissandrakis & Kundu 1984, Krüger et al. 1986, Gary & Hurford 1987, Akhmedov et al. 1986, White et al. 1991, Brosius et al. 1992, Lee et al. 1993a, b, 1997, Gary et al. 1993, Schmelz et al. 1994, Abramov-Maksimov et al. 1996; see White & Kundu 1997, Alissandrakis 1997, White 2002 for introductory reviews).

Basically, the observations suggest that the maximum field strength at the centre of regular sunspots decreases with height, but still has values of 1000–1800 G in the upper chromospheric to lower coronal layers. The magnetic field is in general more homogeneous in the upper atmosphere (Harvey & Hall 1971, Rüedi et al. 1995a). It can be followed over a larger distance in the upper atmosphere and decreases more slowly with distance from the sunspot axis.

Particularly intriguing are the observations of White et al. (1991), who find a field of strength 1800 G in the lower corona above a large and rather regular sunspot. This large field strength is localized to a region far smaller than the sunspot and is offset from both the umbra and the strongest photospheric magnetogram signal by approximately $10''$. Such a magnetic distribution implies a strong concentration of the field, which would only be possible by strong currents. Note that other investigators also found evidence for almost equally strong fields (1300–1700 G) in the upper chromosphere and low corona (e.g., Henze et al. 1982, Akhmedov et al. 1986, Gary & Hurford 1987, Gary et al. 1993, Lee et al. 1993a, Rüedi et al. 1995a, Lee et al. 1997). Evidence for a stronger concentration of the field in the low corona (Lee et al. 1993b) than expected from a simple buried dipole extrapolation of the photospheric field has also been found by Lee et al. (1993a) and Vourlidas et al. (1997). The latter authors discovered that an analytical solution to the MHS equation found by Low (1980), which has a Gaussian radial dependence of B_z and remains relatively confined with height, reproduces the observations far better than a buried dipole field. They suggest that the magnetic peak seen in coronal layers comes mainly from the umbra. Not all coronal measurements give such high field strengths, however. For example, Gary et al. (1993) find that at the highest observable coronal level (sampled at 3 GHz, the lowest frequency at which gyro-resonance radiation stands out clearly from free-free radiation) the field strength at the centres of sunspots is only approximately 360 G. They estimate that this field strength is reached at heights greater than 6000 km above the base of the corona.

From the centre-to-limb variation of radio observations Alissandrakis & Kundu (1984) reconstructed the angle of inclination of the field of a large sunspot, finding that the field has an inclination of 40° at the outer penumbral boundary at coronal heights. A force-free model better reproduces their observations than an inclined buried dipole,

---

[1] Livingston's observations have been described by Giovanelli (1980).

due to the presence of an azimuthal component of the field found under the assumption of a homogeneous electron temperature (plane parallel atmosphere). Without this assumption an azimuthal component of the field is not needed.

The surprising and physically difficult to interpret result found by Wang & Shi (1992), Dara et al. (1993, 1995) and Li et al. (1994) that in chromospheric layers the polarity above sunspot umbrae is opposite to that in the photosphere finds its most natural and straightforward explanation in the core reversal of Hβ, the line employed by these authors, in the presence of low-level flaring as shown by Sánchez Almeida (1997). This reversal is sufficiently weak not to show up in filtergrams taken in the inner wings of the line, but sufficiently strong to reverse Stokes V there. Hence there is currently no reason to expect a reversal in polarity with height.

3.7. Vertical gradient of the magnetic field

Knowledge of the magnetic field at different heights allows the average vertical gradient of the field strength between these heights to be determined (and to be compared with the predictions of models).

The values of the obtained vertical gradient depend on both the horizontal position in the sunspot and the height range over which they are measured (i.e., the formation heights of the 2 diagnostics used). One also needs to distinguish between gradients of the actual field strength, i.e. $|\partial B/\partial z|$ and the gradient of the line-of-sight component of the field strength averaged over the resolution element, i.e. $|\partial \langle B \cos \gamma \rangle/\partial z|$. The former is obtained when comparing, e.g., the Zeeman splitting of two completely split lines, the latter requires only the measurement of Stokes I and V of two lines formed at different heights.

Consider first measurements comparing lines formed at different heights in the photosphere, i.e. those determining $|\partial B/\partial z|$ over a small height range.

Early work (Dubov 1965, Kusnezov 1968, Ikhsanov 1968, Beckers & Schröter 1969b, Wiehr 1969, Rayrole & Semel 1970, Guseynov 1970, cf. Bray & Loughhead 1964) has been summarized by Schröter (1971). According to him $|\partial B/\partial z|$ values are 0.5–1 G km^{-1} at the sunspot centre, 0.2–0.3 G km^{-1} at the umbra-penumbra boundary and 0.05–0.2 G km^{-1} within the penumbra. He also lists the many uncertainties besetting the measurement of vertical gradients. They stem from imprecisely known formation heights of lines, differential influence of scattered light on the lines used, etc. To a certain extent the same uncertainties still plague current observations.

More recently, larger values of $|\partial B/\partial z|$ have been obtained in both umbrae and penumbrae from purely photospheric lines. Balthasar & Schmidt (1993) obtained 2.5–3 G km^{-1} in the outer umbra and the inner penumbra. Although they do not specifically point this out, their Fig. 6 suggests a decrease of the vertical gradient of the field to roughly half this value in the outer part of the penumbra. Schmidt & Balthasar (1994) confirmed the high value in the umbra (and in an umbral dot), while Pahlke & Wiehr (1990) obtained a slightly lower value of 2 G km^{-1}. Bruls et al. (1995) analyzed the data of Hewagama et al. (1993) and obtained $|\partial B/\partial z|$ values of 2–3 G km^{-1} in the inner penumbra, which drops to around 1 G km^{-1} in the outer penumbra. The result of Eibe et al. (2002) that $|\partial B \cos \gamma/\partial z| = 10^{-3} \, B \cos \gamma$ (G km^{-1}) is in good agreement with the dependence found by Bruls et al. (1995). Obridko & Teplitskaya (1978) observed a

large scatter in gradients (0.3–10 G km^{-1}) suggestive of significant uncertainties in their results. Finally, $|\langle dB/dz \rangle| \approx 1.5 - 2$ G km^{-1} is deduced in the umbra by Westendorp Plaza et al. (2001a), although from their Fig. 9 a value below 1 G km^{-1} also appears reasonable. Uniquely among the more recent investigations these authors find that the field strength increases with height in the outer penumbra, where they find $|d\langle B \rangle/d\tau|$ to be much larger than in the umbra (their Fig. 9). Using their Fig. 9 and 100 km per decade of log τ_{5000} we obtain a positive gradient of 2.5 G km^{-1} from their data (but see Martínez Pillet, 2000, for an interpretation involving unresolved horizontal flux tubes that does not require B to increase with height in order to reproduce the observations).

When diagnostics formed at sufficiently different heights are compared (i.e. usually a photospheric line with either a chromospheric or transition region line, or a coronal diagnostic) then considerably smaller vertical gradients are obtained. A comparison of chromospheric with photospheric data by Abdussamatov (1971a, b) gave $|\partial B/\partial z|$ values of 0.5–0.8 G km^{-1}. He also noted that $|\partial \langle B \cos \gamma \rangle /\partial z|$ decreases with increasing field strength, which does not agree with newer findings, however (see below). Radio data originating at around 2×10^6 K give a vertical gradient of 0.25 G km^{-1} (Akhmedov et al. 1982). From a comparison of the upper chromospheric He I 10830 Å line to a photospheric line Rüedi et al. (1995a) find $|\partial \langle B \cos \gamma \rangle /\partial z| = 0.4$–0.5 G km^{-1} in the umbra, which drops to 0.1–0.3 G km^{-1} in the outer penumbra. Penn & Kuhn (1995) parameterize the gradient as $\partial B/\partial z \approx -10^{-4} B$ G km^{-1}, which gives approximately 0.25 G km^{-1} for a typical umbral field strength of 2500 G and 0.1 G km^{-1} near the outer penumbral edge. This dependence of $|\partial B/\partial z|$ on B or position in the sunspot is just another expression of the fact that the field is much more homogeneous in the upper atmosphere than in the photosphere, since the larger photospheric umbral field strength decreases more rapidly with height than the weaker field in the penumbra. Note that both Abdussamatov (1971b) and Penn & Kuhn (1995) actually determined $|\partial \langle B \cos \gamma \rangle /\partial z|$ rather than $|\partial B/\partial z|$, although they may not explicitly say so. An upper limit of 0.15 G km^{-1} on $|dB/dz|$ in the corona has been set by Gary et al. (1993) on the basis of the fact that the gyroresonance radiation is optically thick (the quantity $B/\nabla B$ enters linearly into the expression for optical depth, Dulk 1985). From the centre-to-limb variation of radio emission from a regular sunspot (including its occultation by the solar limb) Lee et al. (1993b) obtain $\partial B/\partial z \approx 0.2$ G km^{-1}.

Henze et al. (1982) found maximum gradients of 0.4–0.6 G km^{-1} by comparing the longitudinal field strength obtained from the C IV 1548 Å line with photospheric magnetograms. Hagyard et al. (1983) analyzed the same data more extensively. They compared the directly derived field-strength gradient with that obtained by extrapolating the photospheric field or by applying the div **B** $= 0$ condition to the photospheric transverse field. The two latter methods give over a factor of two smaller gradients than the direct measurement (assuming that C IV is formed at the canonical 2000 km above $\tau_{5000} = 1$). To reconcile this Hagyard et al. (1983) propose that the C IV emission comes from 4000–6000 km above the photosphere.

Hofmann & Rendtel (1989) applied the constraint of div **B** $= 0$ to photospheric vector magnetograms and obtained a maximum $|\partial B/\partial z|$ of 0.32 in the umbra, consistent with the value deduced by Hagyard et al. (1983) and Liu et al. (1996) using the same technique. Eibe et al. (2002) obtain equally low gradients ($|\partial B \cos \gamma /\partial z| \approx 10^{-4} B \cos \gamma$) from a potential field extrapolation starting from the photosphere. They discuss possible

causes of the order of magnitude discrepancy between gradients obtained from photospheric lines formed at different heights and by other methods. The presence of hidden return flux is one proposal. Another possibility is that the height scale assumed for line formation in sunspots is not correct.

Solanki et al. (1993) use observations of the Wilson depression and force balance arguments to limit $|\partial B/\partial z|$ to less than approximately $2\,\mathrm{G\,km^{-1}}$ at the umbral boundary. They also constrained $-0.006°/\mathrm{km} \le \partial\zeta/\partial z \lesssim 0.04°/\mathrm{km}$ (where ζ is considered in a spatially averaged sense, averaged over 2–3″).

Note that the highly unconventional vertical profiles of B found by Abramov-Maksimov et al. (1996) by combining Zeeman splittings of various spectral lines in the visible with radio measurements need to be treated with caution: The fact that they find peak field strengths above 6000 G suggests that there are serious problems with their analysis.

The sum of all observations suggests that the field strength drops rapidly with height in the photosphere and more slowly at greater heights. The decrease of $|\partial B/\partial z|$ with height above the umbra was already noted by Wittmann (1974), who determined the gradient at different heights by measuring the field strength using 4 spectral lines at different limb distances. He found that the gradient varies from $3\,\mathrm{G\,km^{-1}}$ in the low photosphere to $0.6\,\mathrm{G\,km^{-1}}$ in the low chromosphere. Collados et al. (1994) employed inversions to derive $B(z)$ in the umbral core of 2 sunspots. The qualitative height dependence is similar to that found by Wittmann (1974) and agrees also with the expectations of a flux-tube model, although they obtain considerable quantitative differences between large and small sunspots. No satisfactory solution has been found as yet for the unexpectedly small vertical gradients obtained by applying the div $\mathbf{B} = 0$ condition.

Almost all the observations also indicate a decrease of $|\partial B/\partial z|$ from the centre of the sunspot toward its periphery (or from stronger to weaker field). The only observers explicitly claiming the opposite are Abdussamatov (1971b), only by a small amount, from $0.6\,\mathrm{G\,km^{-1}}$ to $0.8\,\mathrm{G\,km^{-1}}$, and Westendorp Plaza et al. (2001a).

The inversions of Westendorp Plaza et al. (2001a, b) actually return field strengths increasing with height by several hundred G over the line-formation height range in the outer penumbra ($r/r_p > 0.7$). However, as demonstrated by Martínez Pillet (2000), the application of an inversion based on a plane-parallel model to a multicomponent atmosphere including horizontal flux tubes embedded in an inclined field (as proposed by Solanki & Montavon 1993) can return such gradients, even if the field strength does not actually increase with height.

The measured umbral gradients are in reasonable but by no means perfect agreement with simple theoretical predictions of $|\partial B/\partial z| = 0.5$–$1\,\mathrm{G\,km^{-1}}$ at the flux-tube axis (Yun 1972). Theory also predicts both a decrease of the magnetic gradient with height and with increasing distance from the centre of a symmetric sunspot whose magnetic configuration is not too far from that of a potential field bounded by a current sheet.

3.8. Electric currents

When discussing electric currents in sunspots we need to distinguish between large-scale currents and small-scale ones. The latter are associated with small-scale magnetic intromogeneities such as the fluted or "uncombed" magnetic field in the penumbra (see

Sect. 3.9.3). Here we concentrate on the large-scale currents and refer to Title et al. (1993) for an estimate of the currents (j_x, j_y, j_z) associated with the small-scale structure of the field in the penumbra. We also need to distinguish between simple, regular sunspots, which usually possess small currents, and more complex sunspots containing (partial) light bridges, multiple umbrae, or even both magnetic polarities (δ spots, defined by Kunzel 1960, cf. Zirin & Liggett 1987).

The currents at the photospheric level in regular sunspots have been estimated by, e.g., Hofmann et al. (1988), Lites & Skumanich (1990) and Lites et al. (1993). Hofmann et al. (1988) deduce a relatively complex vertical current system in a magnetically simple sunspot. They interpret this as a sign of the subsurface cluster structure of the sunspot. Lites & Skumanich (1990) assume the azimuthal field to be the main source of currents in their sunspots (since a buried dipole provides a good fit to B_z and B_r) and find that the azimuthally averaged current density (with a maximum of 6–7 mA m^{-2}) peaks in the umbra and drops steadily outwards. However, the maximum azimuthal field is reached in the penumbra, suggesting that the largest forces act there.

Particularly large horizontal magnetic gradients and thus vertical currents are present in light bridges and at their edges, as well as in δ spots. Thus, for partial light bridges Rüedi et al. (1995b) derived 160 mA m^{-2}, which is over 20 times larger than the maximum value obtained by Lites & Skumanich (1990) in a large symmetric sunspot. In the 15 light bridges that Leka (1997) studied the largest horizontal gradients (1 G km^{-1}) correspond to 80 mA m^{-2}, which is also an order of magnitude larger than for normal sunspots. The current densities in light bridges are only exceeded in δ-spots. Many of these have similar j_z as the strongest found in light bridges (Leka 1995, Skumanich & Semel 1996), but at least in one case (Zirin & Wang 1993a) a δ-spot possessed a maximum current density of 500 mA m^{-2}. Not surprisingly, δ-spots are associated with enhanced flaring activity. Lee et al. (1997), from a study of a complex δ-spot with multiple umbrae, found a comparatively small j_z of 7 mA m^{-2} (probably an average — this is not stated in the paper) which, however agrees well with the force-free α parameter giving the best correspondence to radio multi-frequency observations.

In the upper atmosphere evidence for electric currents is found by comparing maps of the measured and the predicted magnetic field, whereby the prediction is based on the measured photospheric field. From such a comparison White et al. (1991) concluded that considerable currents are present in the low corona of a sunspot. Other active regions (Alissandrakis et al. 1980, Lee et al. 1997) and regular sunspots (Lee et al. 1993a, b) also provide evidence for sizable currents in the corona, i.e. strongly non-potential fields.

On the other hand, Schmelz et al. (1994) found that field strengths deduced from microwave observations in parts of an active region are well reproduced by potential field extrapolations from the photosphere.

3.9. Fine-scale structure of the magnetic field

The fine-scale structure visible in white-light images of sunspots is predominantly due to umbral dots and light bridges and to penumbral or superpenumbral filaments and grains. As far as the magnetic field is concerned the main known inhomogeneities are concentrated in the penumbra.

3.9.1. Umbral dots

Various investigators have searched for the signature of umbral dots in the magnetic field. Whereas older observations showed a huge scatter in deduced field strength values, there has been convergence towards a rough consensus in recent years. The lowest value was obtained by Beckers & Schröter (1968, 1969a). They claimed that the field strength in the dots is roughly 10% of B in the surrounding umbral background and that the field has opposite polarity in the dot relative to the rest of the umbra due to a weak reversed polarity signal in the core of Stokes V (cf. Severny 1959, Mogilevsky et al. 1968). Wittmann (1971), however, argued that Beckers & Schröter (1968) misinterpreted magnetooptical effects as the umbral dot contribution (cf. Beckers 1969). Faraday rotation indeed produces a weak inversion in the core of Stokes V for atmospheric parameters typical of umbrae. Also, no other observer has found evidence of a reversed magnetic polarity in umbral dots. Higher field strengths than Beckers & Schröter were found by Obridko (1968a) and Kneer (1973), who obtained 50% of the umbral field strength in umbral dots, while Buurman (1973) measured a value close to 90%.

The investigations carried out in the 1980s and 90s have favoured the results of Buurman; see, e.g., Adjabshirzadeh & Koutchmy (1983), Pahlke & Wiehr (1990) and Balthasar & Schmidt (1994). Thus, Schmidt & Balthasar (1994) find a 10–20% lower field strength in a central umbral dot and a 5–10% lower B in a peripheral dot. The two types of umbral dots are distinguished by their location in the umbra, as suggested by their names. A small field-strength reduction in umbral dots (reduced by 7%, as obtained from the Fe I 6302.5 Å line) was also found by Tritschler & Schmidt (1997) and by Socas Navarro (2002) from Stokes profile inversions (10% reduced field strength at all heights). Finally, Zwaan et al. (1985), Lites & Scharmer (1989), Lites et al. (1991) and Tritschler & Schmidt (1997; from the blended Fe I 8468.5 Å line) find no evidence of a significantly weaker field in umbral dots. Since these investigators only considered Stokes I of a single line, the accuracy of the derived field strengths may not be sufficiently high to signal any inconsistency between their results and those of, e.g., Schmidt & Balthasar (1994).

Schmidt & Balthasar point out that the 5–20% reduction in field strength found by some investigators in umbral dots may just be an apparent decrease due to the fact that B decreases with height and the observed radiation is emitted from higher layers in hot and bright regions (due to the temperature dependence of the continuum opacity). Both Pahlke and Wiehr (1990) and Schmidt & Balthasar (1994) found that the vertical magnetic gradient within the umbral dots is the same as in the surroundings and amounts to 2–$3\,\mathrm{G\,km^{-1}}$ in the mid photosphere. A difference in temperature (such as that between umbral background and dot) can also lead to a difference in formation height of spectral lines. The magnitude of this formation height change depends on the spectral line and may possibly explain some of the remaining discrepancies between the results obtained by different groups. However, further model calculations are needed to quantify this effect.

The fact that no significant decrease in B is seen above umbral dots does not necessarily mean that the Parker (1979c) and Choudhuri (1986) model of their production (Sect. 6.2) is wrong since, as Degenhardt & Lites (1993b) pointed out, only lines formed very deep in the atmosphere are expected to see the decrease in B in the dots predicted by these models. The observations of Wiehr & Degenhardt (1993) support this interpre-

tation. They obtain a 20% lower field strength in peripheral umbral dots in the lower photosphere (measured in Fe I 6843 Å), but no reduction in Ca I 6103 Å which samples higher layers of the umbral photosphere. High resolution observations at 1.56 µm are needed to finally resolve this question.

3.9.2. Light bridges

Light bridges are lanes of relatively bright material dividing an umbra into two parts (or, equivalently, separating two umbrae of like polarity; see lower frame of Fig. 1.1). In contrast to the smaller and less obvious umbral dots, light bridges definitely have a significantly lower field strength than the neighbouring umbral material in photospheric layers (e.g., Beckers & Schröter 1969b, Abdussamatov 1971a, Lites et al. 1990, 1991, Rüedi et al. 1995b, Leka 1997). Thus Rüedi et al. (1995b) observe a decrease of 1400 G within 1–2″ at the boundary of a narrow partial light bridge, or penumbral protrusion. The most thorough study is that of Leka (1997), who investigated 15 light bridges in 11 sunspots and found all of them to have a reduced field strength relative to the umbra, with the reduction ranging from 200 to 1500 G.

From observations with high spatial resolution, Lites et al. (1991) even conclude that at a scale of 0.5″ there is an intrusion of field-free material in the light bridge. Also, Leka (1997) obtains magnetic filling factors significantly below unity in light bridges. Assuming that the amount of straylight from the quiet sun is the same as in the neighbouring umbra she concludes that up to 20% of the material in light bridges is field free.

At the same time the field in the light bridge is also more inclined, with ζ being between 5° and 30° larger than in the nearby umbra (Beckers & Schröter 1969b, Lites et al. 1991, Wiehr & Degenhardt 1993, Rüedi et al. 1995b, Leka 1997).

Note that a reduced filling factor is no proof of field-free material. For example, a mixture of magnetic polarities or a distribution of magnetic orientations also seemingly lowers the filling factor due to the cancellation of Stokes profiles, even if the whole atmosphere is filled with field. Another possibility is that in places at which large horizontal gradients in the intensity and temperature are present the ASP inversion program (used by Leka) needs larger amounts of stray light to compensate for its inability to calculate mixtures of parameter values. Recall that the ASP inversions deliver lower α values at the inner edge of the penumbra (Sect. 3.5), a similar situation to light bridges (with strong brightness gradients). These possibilities must be kept in mind when postulating the presence of field-free material in light bridges based on filling factors.

At chromospheric heights light bridges are inconspicuous in the magnetic field (Abdussamatov 1971a) or even show enhanced $B \cos \gamma$ values (Rüedi et al. 1995a), so that the vertical field-strength gradient in light bridges must be considerably smaller than in umbrae. The data of these authors is compatible with a complete absence of a vertical gradient of the field in the light bridges observed by them. However, as Rüedi et al. (1995a) point out a differential change of magnetic inclination with height could also influence these results.

After considering all the data on physical conditions in light bridges Leka (1997) proposes that light bridges are intrusions of field-free material from below, over which

the field expands in a canopy-like fashion. This would explain the smaller B there in photospheric layers.

The rarer light-bridge-like structures in δ-spots that separate umbrae with opposite polarities have partly rather different properties. The field therein is also more horizontal (Zirin & Wang 1993a, Lites et al. 1995), but it is aligned almost parallel to the neutral line or brightness ridge, i.e. it does not directly connect the two umbrae of opposite polarity. Remarkably however, the transverse field is strong, exhibiting line splittings corresponding to field strengths up to or even over 4000 G (Tanaka 1991, Zirin & Wang 1993b). Such high field strengths are not otherwise seen in sunspots and field strengths close to these values are only found in the darkest parts of the umbrae of large sunspots. ASP data, however, show no particularly enhanced B at the neutral line (Lites et al. 1995), but unlike normal light bridges the brightness ridges in δ-spots exhibit an enhanced magnetic filling factor (and a filament in the chromosphere). A physical interpretation of this observation is difficult, since already the neighbouring umbrae are expected to have a true magnetic filling factor of close to unity. Hence the magnetic structure of light bridges in δ-spots must still be considered to be unclear.

3.9.3. Fluted magnetic field in the penumbra

The azimuthal inhomogeneity of the penumbral magnetic field on small scales, in particular of its zenith angle, is now well established. Beckers & Schröter (1969b) first presented evidence for different inclinations of the magnetic vector in bright and dark filaments with (more horizontal, stronger fields in dark filaments). Additional (weak) hints were found by Lites et al. (1990) from Stokes I observations and Kálmán (1991). Much stronger evidence came from the work of Degenhardt & Wiehr (1991) and final, incontrovertible evidence was provided by Schmidt et al. (1992) and Title et al. (1992, 1993). These authors found that the magnetic field is fluted or "uncombed" on small scales, in the sense that when travelling on a circle around the centre of the umbra of a regular sunspot the zenith angle of the field fluctuates by 10–40° on an arc sec and sub-arc sec scale (see Fig. 3.6). This basic result is confirmed by Lites et al. (1993), Hofmann et al. (1993, 1994), Rimmele (1995a), Stanchfield et al. (1997), Westendorp Plaza et al. (1997b) and Wiehr (2000), while evidence supporting it is provided by Solanki & Montavon (1993) and Martínez Pillet (2000); cf. Keller et al. (1992).

Less clear than the mere presence of fluctuations in the zenith angle ζ of the magnetic vector is the correlation of the zenith angle with brightness at a fixed distance from the centre of the sunspot. All three possibilities, namely positive, negative and no significant correlation have been proposed in the literature (see Skumanich et al. 1994 for a critical review):

– Schmidt et al. (1992), Hofmann et al. (1994, although with correlation coefficient $\lesssim 0.5$), Rimmele (1995a), Wiehr (2000) and Westendorp Plaza et al. (2001a) propose that ζ is larger in dark structures, i.e. that the field is more horizontal there.
– Lites et al. (1993), propose that in the inner penumbra ζ is larger in bright structures.
– Little correlation between inclination and brightness is seen by Lites et al. (1993) in the outer penumbra (they do find a weak correlation in the sense that ζ is larger in dark structures), by Title et al. (1993, the generally positive correlation coefficient is
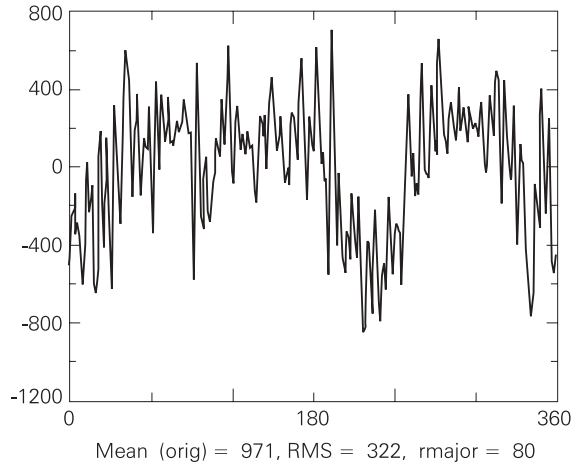
Fig. 3.6. Magnetogram signal (ordinate in G) on an ellipse laid through the mid-penumbra of a relatively regular sunspot. The mean value, first Fourier component and white noise have been removed to more clearly show the small-scale structure. The abscissa shows the azimuth angle. Zero degrees is in the direction of disk centre (adapted from Title et al. 1993, by permission).

in most cases less than 0.2, however) and by Stanchfield et al. (1997, again, absolute value of correlation coefficient less than 0.2).

Although they find that ζ does not correlate with brightness, Title et al. (1993) do find a significant correlation with the velocity. The Evershed flow appears to be concentrated in the horizontal magnetic filaments (cf. Sect. 7.3).

In the inner penumbra Lites et al. (1993) see spines of field with small ζ well correlated with dark material protruding from the umbra into the penumbra (such structures have also been called umbral extensions). The measurement of the full Stokes vector also allowed Lites et al. (1993) to deduce that the field of the spines expands somewhat in the azimuthal direction.

Another point that has been heavily debated is whether the field strength in the penumbra is azimuthally inhomogeneous. On the spatial scale of the I_c fluctuations little evidence for significant fluctuations of $B \cos \gamma$ is found by Mattig & Mehltretter (1968), probably due to the relatively low spatial resolution of their observations (since Title et al. 1993 do see such fluctuations clearly, and interpret them as fluctuations in γ). Similarly, Stellmacher & Wiehr (1981), Lites et al. (1990), Schmidt et al. (1992), Title et al. (1993) and Rimmele (1995a) see no strong fluctuations in B.[2] The upper limit on such fluctuations depends on the sensitivity of the employed technique. The spatial resolution of the observations may also play a role, since small-scale fluctuations can remain undetected if the spatial resolution is low.

A number of authors, however, are in favour of field strength fluctuations. Thus, Beckers & Schröter (1969b) came to the qualitative conclusion that the field is stronger in dark filaments. Harvey (1971) and Abdussamatov (1976) found higher B values

---

[2] Lites et al. (1990) do find a single example of a significant localized excursion of the field strength of 400 G, i.e. one that is significantly larger than their uncertainty of 100–200 G.

in dark penumbral fibrils than in their bright counterparts (by 100–400 G according to Mamadazimov and Abdussamatov). Wiehr & Stellmacher (1989) detected a small fluctuation with a weak correlation between B and continuum brightness. The spatial scale of the variations in the lines (of both Evershed effect and Zeeman splitting) appears to be larger than of I_c. Hofmann et al. (1994) also see some fluctuations in field strength, but no clear global correlation with brightness. They do observe local trends, however, which point to a higher B in bright features in the inner penumbra and to the opposite dependence in the outer penumbra. Wiehr (2000) provides evidence for a roughly 10% increase in B in dark filaments. He proposes that the good correlation between B and I_c results from the fact that he observes a deeply formed line at high spatial resolution. Westendorp Plaza et al. (2001a), however, argue for the opposite dependence, namely that stronger fields are associated with warmer gas.

Interestingly, the Ti I 2.2 μm lines, which sample the cool parts of the penumbra with great Zeeman sensitivity, show low field strengths, below 500 G at some locations (Rüedi et al. 1998a). Fe I 1.56 μm observations of the same sunspot indicate stronger fields (Rüedi et al. 1999). Since the lines at 1.56 μm sample higher temperatures, this suggests that in the penumbra hotter gas harbours stronger fields (whereas the converse is true in the umbra). This appears to contradict the results of Beckers & Schröter (1969b), Harvey (1971) and Abdussamatov (1976). Note, however, that Ti I 2.2 μm lines sample regions that are cool in the layers in which they are formed, whereas a correlation with brightness means a correlation with the layer at which the continuum is formed. In theory it is therefore possible to reconcile these different observations, even if the proposed explanation involves strong temperature gradients and may appear somewhat artificial. The 2.2 μm Ti I results do agree, however, with the findings of Westendorp Plaza et al. (2001a), who also compare B and T at the same layer.

Finally, the σ-components of the 12.32 μm lines are found to be broader than the π-component by Deming et al. (1988), suggestive of a field-strength distribution with a FWHM of 470 G in the penumbra (see Hewagama et al. 1993 for more evidence). This conclusion has, however, been questioned by Bruls et al. (1995), who point out that a combination of reasonable large-scale horizontal and vertical gradients, associated with the overall expansion of the sunspot's field with height, can explain the observed excess σ-component broadening. Further observations at this wavelength would be of great value.

Other researchers have concentrated on uncovering possible connections between ζ and B fluctuations. Degenhardt & Wiehr (1991) found (from Stokes V only) that the more vertical filaments have a 200 G higher field strength. ASP data also suggest that the more vertical fields (the so called "spines" of field) in the penumbra are somewhat stronger: $\Delta B \approx 100\,\mathrm{G}$ (rms) for an rms value of $\Delta \zeta$ of 10° (Lites et al. 1993, Stanchfield et al. 1997, Westendorp Plaza et al. 1997b, 2001a). The anti correlation is in general quite weak, with a correlation coefficient below 0.5, although Westendorp Plaza et al. (2001a) find 0.7 at the log $\tau = -1.5$ level. In the lowest layers of the penumbral boundary, however, the opposite correlation is seen. The rms ζ variations ($\lesssim 10°$) seen by these authors are considerably lower than those found by Title et al. (1993), however. None of these data were obtained at the spatial resolution of the observations analyzed by Title et al. (1993) and therefore miss fluctuations at the smallest scales. This appears particularly true for the ASP. The "spines of field" mainly seen by this instrument may be larger structures

than many of the features analyzed by Title et al. (1993). If this is indeed the case, then the two types of features may well have different properties.

Conversely, however, Martínez Pillet (1997) has argued that the measurement of only I and V, and in particular the use of magnetographic data (instead of spectroscopic) does not allow ζ fluctuations to be distinguished clearly from B fluctuations. He contends that inspite of the fact that Schmidt et al. (1992) and Title et al. (1993) do not see any field-strength fluctuations these may well be present in the sunspots, together with ζ fluctuations. Hence, both types of data have somewhat complementary advantages and disadvantages. How the results from both are best combined to give a more complete and rounded view is not yet clear.

A final word on azimuthal fluctuations of the field strength: the presence of significant brightness and hence temperature contrast between filaments in the penumbra implies that the continuum formation level and also line formation levels are different in bright and dark filaments, due to the temperature sensitivity of the opacity. Thus, due to the vertical field strength gradient (Sect. 3.7) one would expect to find a difference in the *observed* field strength in bright and dark filaments, even if at a fixed geometrical height the field strength and pressure were exactly equal in both filaments.

An alternative diagnostic of unresolved fine structure of the magnetic field in sunspot penumbrae is provided by broad-band circular polarization (BBCP). BBCP was observed by Illing et al. (1974a, b, 1975), Kemp & Henson (1983), Henson & Kemp (1984), Makita & Ohki (1986), etc., and has been shown to be due to the blue-red asymmetry of Stokes V profiles of atomic spectral lines by Makita (1986) and Sánchez Almeida & Lites (1992), although extremely asymmetric V profiles produced by some molecular transitions (those lying in the Paschen-Back regime at kG field strengths) also contribute to a smaller extent (Illing 1981). The BBCP produced by atomic lines is related to the well-known cross-over effect seen around magnetic neutral lines (Kjeldseth Moe 1968a, Grigorjev & Katz 1972, 1975, Golovko 1974, Mickey 1985a, b, Skumanich & Lites 1991, Sánchez Almeida & Lites 1992 and Schlichenmaier & Collados 2002). There the Stokes V profiles lose their nearly antisymmetric, two-lobed appearance, to be replaced by profiles that can have three or even more lobes, and that may be nearly symmetric with respect to the central wavelength.[3]

The blue-red Stokes V asymmetry can be reproduced most easily by co-spatial line-of-sight gradients of the magnetic vector and the line-of-sight velocity (Illing et al. 1975, Auer & Heasley 1978). Sánchez Almeida & Lites (1992) showed that the observations can be reproduced by postulating sufficiently large vertical gradients in these quantities, in particular the velocity and the inclination angle of the field. However, as Solanki & Montavon (1993) point out, global gradients of the magnitude required would lead to magnetic curvature forces strong enough to destroy the sunspot. They demonstrated that the observations could be reproduced just as well by two magnetic components that differ in inclination, with an Evershed type flow in them. However, there must be a horizontal boundary between the two components. Hence the two differently inclined magnetic components in the penumbra found by, e.g., Title et al. (1993) or Lites et al. (1993) cannot be simply vertical sheets of magnetic flux. The penumbral fine-scale field is better described by (more or less) horizontal flux tubes embedded in an inclined field, as sketched in Fig. 3.7.

[3] The cross-over effect was first described by Babcock (1951) in the spectra of Ap stars.
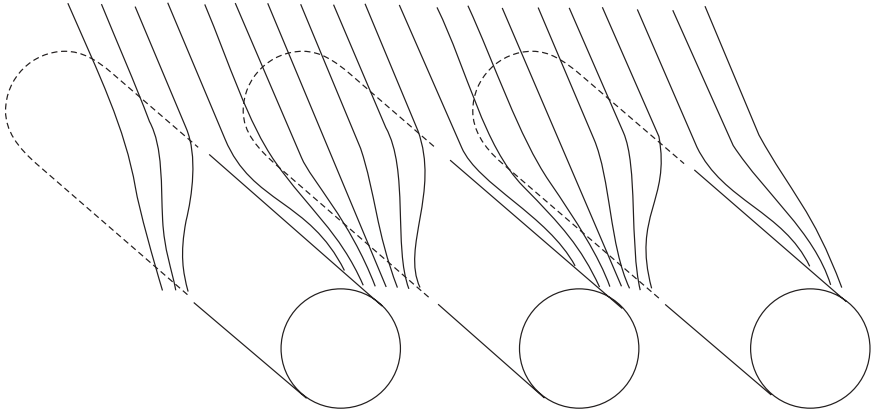
Fig. 3.7. Sketch of the local fine-scale structure of the magnetic field in sunspot penumbrae. The field is composed of two components, a flux-tube component, represented by the horizontal cylinders, and a more inclined magnetic field, indicated by the field lines threading their way between the flux tubes at an angle.

This picture has been taken up and developed by Martínez Pillet (2000) and Schlichenmaier & Collados (2002). The latter authors propose a mixture of cool horizontal and hot inclined flux tubes embedded in an inclined background field. With this model, which is a simplification of the simulation results of Schlichenmaier et al. (1998a, b), they are also able to reproduce such subtleties as the change in sign of the Stokes V asymmetry of Fe I 1.5648 μm along a radial cut through the penumbra.

Another development has come form Sánchez Almeida et al. (1996), who argue that the magnetic flux tubes composing the penumbra are exceedingly thin in diameter (far thinner than the photon mean-free-path). Sánchez Almeida (1998) has argued that the large measured broad-band circular polarization and the small horizontal RMS fluctuations can only be reconciled if the field is structured at a very small scale, of 1–15 km, which is well below the photon mean-free-path (cf. Sánchez Almeida 2001). Martínez Pillet (2000) has, however, shown that flux tubes with a diameter of roughly 200 km can indeed reproduce these observations simultaneously as well as a few additional ones (cf. Sánchez Almeida 2001, Martínez Pillet 2001). An inversion of 1.56 μm Stokes profiles including a possible horizontal flux tube by Borrero et al. (in preparation) has also returned a broad flux tube with a width of roughly 200 km. Similarly, Müller et al. (2002) can reproduce the different observed spatial dependence of the net circular polarization of a spectral line in the visible (Fe I 6302 Å, Westendorp Plaza et al. 2001a) and the IR (Fe I 15648 Å, Schlichenmaier & Collados 2002) based on the theoretical flux tube models of Schlichenmaier et al. (1998a, b). Furthermore, Sütterlin (2001) provides evidence that at least the brightness structure in the penumbra has to a large part been resolved. Hence the true size of the magnetic fine structure in the penumbra is still open, so that in Fig. 3.7 the cross-section of the plotted flux tube is as yet uncertain (as was already pointed out by Solanki & Montavon 1993), but the evidence tends to favour broader tubes.

3.10. Evolution of sunspot magnetic fields

Relatively little work has been done on the evolution of the sunspot magnetic field. For example, the evolution of sunspots is studied mainly on the basis of white light images, of which sufficiently large data sets exist for this purpose. Consequently, the evolution of sunspot areas (Sect. 2.1) is known far better than that of the magnetic flux and field strength. Cowling (1946) suggested that the (maximum) field strength of sunspots remains unchanged once it has reached its maximum value, whereas Bumba (1963b) found that the field strength decreases by $12\,\mathrm{G\,day}^{-1}$ during the decay phase of sunspots (i.e. while a sunspot's area is decreasing). The time dependence of the large-scale sunspot magnetic field has been investigated by Skumanich et al. (1994), who followed a sunspot for 10 days and found that its flux decreases by $9 \times 10^{19}\,\mathrm{Mx\,day}^{-1}$. They also discovered that the zenith angle at the penumbral boundary decreased from around $75°$ to $60°$ in the course of the 10 days. This agrees with the predictions of thin-tube theory that smaller flux tubes expand less rapidly (cf. Solanki et al. 1999).

On the 3 and 5 min timescale, oscillations in the field strength, or more generally the magnetogram signal strength, have been found by, e.g., Mogilevskij et al. (1973), Gurman & House (1981), Efremov & Parfimenko (1996), Horn et al. (1997), Rüedi et al. (1998b), Norton & Ulrich (2000), Kupke et al. (2000), Bellot Rubio et al. (2000), Norton et al. (2001) and Khomenko et al. (2002a, b), while Lites et al. (1998) only obtain an upper limit of 4 G rms of the amplitude. The signal is never very strong (although clearly above 3σ in at least some of the observations) and can be seriously affected by instrumental effects, so that the results of the earlier investigations need to be treated with caution. The newer observations show high power in usually small, inhomogeneously distributed patches, often near the umbral boundary (Rüedi et al. 1998b, Balthasar 1999a, b). Balthasar (1999a, b) does not find a periodic signature and looks for a stochastic excitation mechanism. The reality of the measured field strength fluctuations has been doubted on different grounds. These include the non-simultaneous measurement of wavelengths by the Michelson Doppler Imager (Settele et al. 2002); fluctuations induced by irregular seeing (Landgraf 1997); or the influence on the line formation by an acoustic wave in the presence of a vertical field gradient (Rüedi et al. 1999a). A review has been given by Staude (2002).

Lites et al. (1998) find a persistent inward motion of small-scale features with a speed of approximately $0.4\,\mathrm{km\,s}^{-1}$ in the umbra and inner penumbra. These features are visible in magnetic field strength and inclination, as well as in the line-of-sight velocity signal and continuum brightness. Since the small-scale features in the various physical quantities do not appear to correspond to each other, the interpretation of these features in field strength, inclination and velocity is not clear, although the brightness features probably correspond to the inward moving peripheral umbral dots and penumbral grains (Muller 1973b, 1992, Kitai 1986, Sobotka et al. 1993, 1997a).

Lites et al. (1993) found that the magnetic fine-scale structure of the umbra and the penumbra remains remarkably constant over a period of 30 minutes. Using time series recorded by the Michelson Doppler Interferometer (MDI), Solanki & Rüedi (2003) deduced that the mean lifetime of penumbral magnetic fine structure is well over an hour. They also found that this lifetime is longer than that of the brightness pattern. These results are restricted to the larger elements of penumbral fine structure due to

MDI's pixel size of 0.6″, but have the advantage of being based on data that do not suffer from variable seeing.

4. Models of the sunspot magnetic field

4.1. Introduction to the theoretical description of sunspots

Models of sunspots are of very diverse types and aim to either reproduce observed properties of sunspots, or to understand the physical processes occurring in them. Besides empirically derived models (discussed in Sects. 3 and 5) we need to distinguish between four classes of theoretical models. Firstly, there are numerical experiments, usually idealized simulations of some physical process, such as magnetoconvection, thought to act in the magnetic feature. The second class is composed of static descriptions of symmetric flux tubes that aim to reproduce the global observed properties of sunspots at the cost of some physical realism. The third class is composed of (simplified) descriptions of dynamic phenomena in (or around) sunspots. Finally, full-fledged simulations make up the fourth class. These include time-dependence, compressibility, partial ionization, radiative transfer, 2- or, ideally, 3-dimensionality, a fine spatial and temporal grid and a sufficiently large computional domain.

Unfortunately, the large size of sunspots and the small-scale structure dominating many of the dynamic processes within them conspire to make the fourth class of models beyond current reach, at least for the sunspot as a whole. The large spectrum of timescales relevant to the problem make it even more intractible. Such simulations do exist for small-scale magnetic features (magnetic elements), however (e.g., Steiner et al. 1997, 1998, Gadun et al. 2001, Cattaneo 1999, Emonet & Cattaneo 2001, Stein & Nordlund 2002, Vögler et al. 2002) and it is basically insufficient computing power which keeps complete sunspots from being similarly described.

Hence, most models deal with some aspect of sunspots in detail, while neglecting or simplifying other aspects. Most numerous among the physical models are those describing the magnetic structure of a sunspot on the basis of an axially symmetric vertical flux tube in (often only approximate) magnetohydrostatic equilibrium. Models that aim to describe the processes giving rise to a sunspot's thermal structure (generally simulations of magnetoconvection) differ in that they often accept a simpler description of the magnetic structure.

Finally, a physical description of the dynamics in and around sunspots has also been the subject of considerable effort, whereby one must distinguish between models of the Evershed effect and those of sunspot oscillations. The theoretical studies of these different aspects, although related (as pointed out by Alfvén 1943, Dicke 1970, Maltby 1977, etc., for the magnetic and the thermal structure), are nevertheless distributed over several sections of this review, following the observational results related to each parameter.

Since the thermal and magnetic structure of sunspots is known in considerable detail from observations, rather tight constraints can be set on physical models. One obvious difference between actual and modelled sunspots is that whereas the former are generally irregular (see Fig. 1.1), the latter almost always possess axial symmetry. However, relatively regular sunspots do exist and can be used to test whether the models reproduce the observed radial dependence of the field strength, field direction, brightness,

Wilson depression, etc. Although models in many cases provide reasonable descriptions of sunspots and can reproduce many observations, they provide far fewer ab initio explanations. There is as yet no complete explanation for such basic questions as to why sunspots have penumbrae, or why umbrae carry 20% and penumbrae 80% of the heat flux density of the quiet Sun.

In the present section I concentrate on the magnetic field. Further details, and in particular further references, about models of the magnetic structure of sunspots are to be found in the following reviews: Moreno Insertis (1986), Thomas & Weiss (1992b), Jahn (1992, 1997), Deinzer (1994), Schlichenmaier (2002) and Solanki (2002), cf. Schüssler (1986).

4.2. Introduction to models of the magnetic structure of sunspots

Sunspots are thought to be the cross-sections at the solar surface of large, nearly vertically oriented magnetic flux tubes (Cowling 1934). Hence the large-scale magnetic structure of sunspots is generally represented by axially symmetric flux tubes. Most models of the magnetic structure are calculated in the magnetohydrostatic approximation, i.e. they neglect evolutionary aspects, convective motions, the Evershed effect, and the influence of waves and oscillations (but see Wilson 1981 for a review of early models including evolution). For the overall structure of the magnetic field this is a satisfactory approximation since large mature sunspots evolve on time scales far longer than the time taken by disturbances travelling at the Alfvén or sound speed to cross them (the Alfvén transit time is on the order of an hour). Further arguments in favour of a static description of sunspots are given by Jahn (1997). Dynamic phenomena are important, however, for shaping the small-scale magnetic (and thermal) structure, which is particularly prominent in penumbrae (penumbral fibrils and grains), but is also seen in umbrae (umbral dots). Most models of the whole sunspot neglect the fine-scale structure in the interest of tractability.

The sunspot magnetic field is confined horizontally by a combination of the excess gas pressure in the field-free surroundings of the sunspot and magnetic curvature forces. In contrast to small magnetic flux tubes the latter cannot be neglected, making the modelling of the sunspot magnetic field far more challenging, notwithstanding the result of Solanki et al. (1999) suggesting that at least in some aspects sunspots are well described as thin tubes. The magnetohydrostatic equilibrium is described by the force balance equation and one of Maxwell's equations:

$$\frac{1}{4\pi} \, \mathrm{curl} \, \mathbf{B} \times \mathbf{B} = \nabla p - \rho \mathbf{g} \, , \tag{4.1}$$

$$\mathrm{div} \, \mathbf{B} = 0 \, , \tag{4.2}$$

where $\mathbf{B}$ is the magnetic vector, p is the gas pressure, ρ denotes the density and $\mathbf{g}$ gravitational acceleration. Hydrostatic equilibrium along field lines is already implicit in the force balance equation. Usually significant additional assumptions are made, since the computation of the magnetic configuration without further assumptions requires the simultaneous and consistent solution for the magnetic and thermodynamic structures, which in turn makes it necessary to solve an energy equation in addition to the above

equations (e.g. Alfvén 1943, Cowling 1957, Dicke 1970, Maltby 1977). Most such "comprehensive" solutions that have been attempted are not general (e.g. Deinzer 1965, Yun 1970) since the magnetic structure is often partially prescribed and the thermodynamics are greatly simplified, although recently significant progress has been made on both accounts. Unless the energy equation is solved together with the force-balance equation either the magnetic field, the temperature or the gas pressure must be specified. An equation of state also needs to be postulated. The assumption of an ideal gas is generally adequate. The simplifications here mainly concern the ionization and chemical equilibrium.

Types of magnetic solutions that have been investigated include similarity solutions, return-flux models, force-free models, current-sheet models and models with arbitrary, but prescribed smooth horizontal pressure distributions. Before considering these particular solutions, however, we need to distinguish between two basic configurations.

4.3. Monolith vs. cluster model

One basic assumption underlying all attempts to quantitatively model the global magnetic structure of sunspots is the assumption that the sunspot is monolithic below the solar surface (e.g., Cowling 1957), i.e., that it can be represented by a single flux tube. Since these layers are not directly accessible to observations, this assumption cannot be rigorously tested, although the techniques of local helioseismology can set some constraints on the subsurface magnetic field (Sect. 3.2.3).

Parker (1979a, b, c) proposed that just below the surface the magnetic field of a sunspot breaks up into many small flux tubes due to the fluting or interchange instability (Parker 1975b, Piddington 1975). Through this instability, the magnetic energy of the system is lowered by the fragmentation of a large flux tube (with strong magnetic curvature terms) into many small ones (with small curvature terms). In this picture, a sunspot can be described by a monolithic tube above the surface, but only by a crowd of small flux tubes (spaghetti) below the surface, as illustrated in Fig. 4.1b. This model is often referred to as the spaghetti or jellyfish model. It turns out that magnetic buoyancy can save sunspots ($\phi > 10^{20}$ Mx) from going unstable to fluting in the layers close to the solar surface (Meyer et al. 1977, Bünte et al. 1993). In deeper layers, however, the interchange instability may still act. The depth at which the instability occurs and subsurface 'spaghetti' are produced depends on the total magnetic flux emerging in the sunspot and on details of the magnetic structure. In spite of this uncertainty a cluster model of sunspots has the advantage that it can readily explain the relatively high thermal flux seen in the umbra, as well as umbral dots in a natural manner (the latter as field-free intrusions into the sunspot, Parker 1979c, Choudhuri 1986; see Sect. 4.9). The complex magnetic structure in the penumbra, in which fibrils of field pointing in different directions are interlaced, suggests that the magnetic field is indeed concentrated into many small flux tubes. Further arguments for the cluster model have been presented by Choudhuri (1992). The patchy distribution of power of oscillations of the Zeeman signal in sunspots also suggests an inhomogeneous magnetic field in the subphotospheric layers (e.g. Rüedi et al. 1998b, Staude 1999, Balthasar 1999a). Finally, investigations of the subsurface structure of sunspots favour a cluster model (Chen et al. 1997, Zhao et al. 2001; see Sect. 3.2.3).
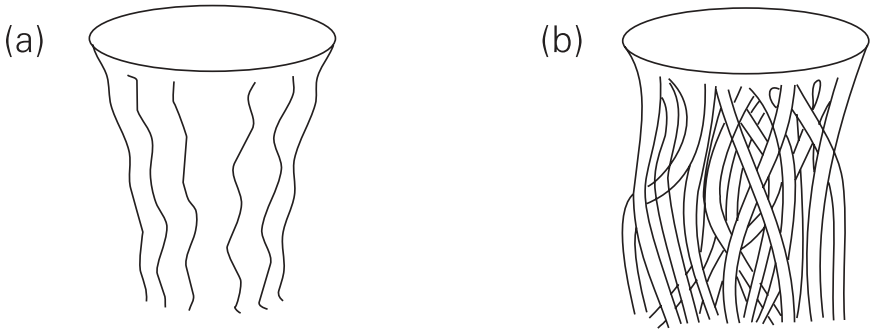
Fig. 4.1. Sketch of the monolith **a** and cluster **b** models of the subsurface structure of sunspot magnetic fields (adapted from Thomas & Weiss 1992b).

One argument against the cluster model comes from Spruit (1981a), who considered the very simple cluster of a collection of buried magnetic monopoles held together at great depth. He pointed out that the potential field in the observable layers produced by such a cluster has a maximum strength (achieved at the geometrical centre) that increases too strongly with the number of monopoles. It increases much more rapidly with the size of the "sunspot" than shown by the observations (e.g. Brants & Zwaan 1982, Kopp & Rabin 1992). To what extent a flux-tube cluster is described by a group of magnetic monopoles still needs to be worked out, however.

Various arguments have been presented why the cluster is not expected to be too loosely constructed (as in Fig. 4 of Thomas & Weiss 1992b). One is that the observed radial dependence of the field is not too different from a buried dipole (Fig. 3.4), which is prototypical of a monolithic flux tube (cf. Skumanich 1992). Further arguments for a relatively tight clustering are given by Thomas & Weiss (1992b).

Let us now turn to specific, quantitative descriptions of sunspot magnetic fields.

4.4. Self-similar models

In such models the radial dependence of **B** at a given, constant geometrical height is prescribed and is imposed to be the same at all heights, except for a scaling to take into account the expansion of the field with height. Hence the name similarity or self-similar models. These models are sometimes also called Schlüter–Temesváry models after Schlüter & Temesváry (1958), who first introduced them to describe sunspot magnetic fields. This prescription allows the vertical and radial magnetic coordinates to be separated,

$$B_z = f(r/R(z)) \, B_0(z), \tag{4.3}$$

$$B_r = -\frac{r}{2} \, f(r/R(z)) \, \frac{\mathrm{d}B_0}{\mathrm{d}z}(z) \,. \tag{4.4}$$

Hence only an ordinary differential equation for $B_0(z)$, the field strength along the flux-tube axis, needs be solved. $f(r/R)$ is called the shape function. In most applications a Gaussian shape function has been chosen.

Due to their early success in reproducing the observed field distributions and their simplicity, such models have attracted considerable attention. Examples of self-similar models have been constructed by, amongst others, Schlüter & Temesváry (1958), Chitre (1963), Deinzer (1965), Jakimiec (1965), Yun (1970, 1971b), Landman & Finn (1979), Low (1980), Skumanich & Osherovich (1981), Osherovich (1979, 1980), Murphy (1990), Solv'ev (1997) and Moon et al. (1998). Some of these models include a description of the energy balance (e.g., Chitre 1963, Deinzer 1965, Yun 1970, Solv'ev 1997, Moon et al. 1998), for others the pressure difference between the axis and the field-free surroundings of the sunspot was prescribed at all heights (e.g., by taking it from empirical models in the observable layers). The model of Yun (1971b) includes the possibility of adding an azimuthal twist to the field.

Self-similar models, although straightforward to construct, may be too restrictive to describe sunspots accurately. For example, classical similarity models have great difficulty reproducing the observed continuum structure of sunspots composed of a central umbra surrounded by a penumbra (Jakimiec & Zabża 1966, Landman & Finn 1979, Murphy 1990). These models usually produce a bright ring that is often located near the umbra-penumbra boundary, contrary to observations. This anomaly, which may be an artifact of the particular choice of the shape function (see the tests by Murphy 1990), has so far only been removed by ad hoc changes in the thermodynamic structure (Landman & Finn 1979, Murphy 1990).

A more basic limitation of self-similar models has been discussed, in the context of smaller flux tubes, by Pneuman et al. (1986) and Steiner et al. (1986). The magnetic field of sunspots, like that of small flux tubes, expands nearly exponentially with height. If, e.g., the field is nearly potential or force-free inside a boundary current sheet (which is expected to be the case above the photosphere), then the rapidity of this expansion influences the radial distribution of the field. The more strongly the field expands the more strongly the field strength decreases towards the edge of the flux tube at a given geometrical height. Since the rate of expansion itself increases significantly from the solar interior to its outer atmosphere the correct description of the magnetic field near the solar surface does not automatically imply that the field is correctly described also below the surface or higher in the atmosphere. This criticism is supported by the results of more sophisticated models (such as those of Jahn 1989), which give a magnetic structure that is not self-similar.

Nevertheless, Moon et al. (1998) have found more realistic self-similar solutions. They include the observed horizontal variation of the Wilson depression (taken from Solanki et al. 1993) when determining the shape function $f(r/R)$ from the observed radial dependence of the magnetic field. Note that the latter is only known along a level of constant optical depth, which differs from a fixed height by the Wilson depression. These models reproduce a fair number of observations, although Moon et al. did not show the predicted continuum structure, which is a sensitive test of the shape function.

4.5. Return-flux models

Osherovich (1982) extended self-similar models to include field lines in the outer part of the sunspot that return to the solar surface just outside the visible sunspot (return flux). In this model the emerging return flux is said to constitute the penumbra. Since observations suggest that approximately half of the magnetic flux of a sunspot emerges in the penumbra this provides an estimate of the amount of return flux that is present according to this model. Such models have been elaborated, extended and studied in detail by Flå et al. (1982), Osherovich & Flå (1983), Osherovich & Lawrence (1983), Osherovich & Garcia (1989), Murphy (1990) and Liu & Song (1996). In the form it has been propagated so far, however, this model finds little support from observations, since the amount of opposite polarity flux seen in the immediate surroundings of sunspots is small (e.g. Solanki et al. 1992, Solanki & Schmidt 1993, Lites et al. 1993), although probably not negligible within the sunspot penumbra itself (Westendorp Plaza et al. 1997a, Schlichenmaier & Schmidt 1999). The observed return flux appears to be related to the horizontal field strands carrying the Evershed flow and is only seen in the lowest observable layers at some locations at the periphery of the sunspot. The dominant fraction of the magnetic flux emerging in the penumbra continues in and above the magnetic canopy which surrounds every sunspot (a layer of almost horizontal field overlying a field-free layer; see Sect. 3.3).

For realistic parameters the predicted continuum intensity of return flux models is not much closer to the observations than for the standard self-similar models. Nevertheless, by reducing the Wilson depression to the unrealistically low value of 250 km Murphy (1990) was able to obtain a qualitative agreement with observations at disk centre. However, near the limb unrealistic bright rings again appeared at the umbra-penumbra boundary, as in most Schlüter-Temesváry models. Another approach was taken by Liu & Song (1996). They modified the shape function $f(r/R)$ to a more complex form than the usually used Gaussian. This improves the correspondence of the predicted magnetic structure to the observations (although the model still predicts, by definition, a horizontal field at the outer penumbral boundary, which is too flat as compared with the observations; Sect. 3.2.2). The temperature profile looks reasonable, but unfortunately the intensity profile is not calculated.

4.6. Force-free and potential field models

The magnetic field is called force free when the terms describing the influence of the gas (and the gravity), i.e. the terms on the right-hand-side of the force balance equation in Sect. 4.2, can be neglected. In that case the force balance reduces to

$$\nabla \times \mathbf{B} = \alpha \mathbf{B} \qquad (4.5)$$

(Lüst & Schlüter 1954, Chandrasekhar & Kendall 1957). In general, α is a scalar function of the spatial coordinates and is constant along field lines (as can be seen by taking the divergence of the above equation). Solutions are particularly simple if $\alpha = $ constant everywhere. Then $\nabla \mathbf{B} = 0$ is automatically satisfied. A further simplification, a potential field, is obtained when α vanishes. Force free and potential fields are uncoupled from the

rest of the atmospheric parameters. Hence it is sufficient to know the field at the boundary of the computational domain in order to compute it in the whole volume. Conversely, this decoupling implies that force-free models can, by definition, not reproduce the thermodynamic properties of sunspots. They are also unable to describe the relatively sharp boundary between the sunspot and the surrounding almost field-free gas (at least without additionally introducing a current sheet, see below).

The magnetic field inside sunspots certainly comes close to being force free in chromospheric and coronal layers due to the small gas pressure and density there. If small-scale structure is neglected then even a potential field can provide a reasonable description in these layers for a regular sunspot (but see Sect. 3.8). In the photosphere this assumption is less secure since the plasma β, defined as $\beta = 8\pi p/B^2$, is actually larger than unity in large parts of a sunspot at photospheric layers (Solanki et al. 1993).

Nevertheless, various models based on the assumption of a force-free or potential sunspot magnetic field have been constructed. Potential field models can be easily derived by taking well-known solutions of Laplace's equations (e.g., using dipole or Bessel function potentials). Purely potential-field models predict no natural boundary of the sunspots. They are therefore generally artificially bounded by a current sheet, termed the magnetopause. At the magnetopause the pressure difference Δp and its derivative need to be matched to the external atmosphere. This approach has been taken by Simon & Weiss (1970), Spruit (1976), Meyer et al. (1977), Simon et al. (1983) and Schmidt & Wegmann (1983). These models have difficulty reproducing the observed magnetic field distribution in sunspots, although they appear to provide a reasonable description of the magnetic field of pores. The comparison with observations suggests the need for body currents in sunspots, in particular under the penumbra (see also Sect. 4.8). Since pores are like naked umbrae, they may harbour only very small body currents.

The first force-free model was a constant α solution due to Schatzmann (1965). It approximately reproduces early observations of the radial dependence of the magnetic field strength, indicating that the constant α approximation is adequate for the visible layers of simple sunspots (Martens et al. 1996).

This model was used by Martens et al. (1996) as the solution representing the large-scale structure of a sunspot's magnetic field. To it they added further terms describing the flutedness, i.e. the small-scale structure, of the penumbra (see Sect. 4.9). A more self-consistent approach (but one that is still based on force-free fields) to describing the uncombed penumbral field has been taken by Neukirch & Martens (1998). The main prediction of these models is the height evolution of the fluted field. Whereas in the approach taken by Martens et al. (1996) the small-scale inhomogeneity is smoothed out exponentially with height, it decreases more slowly, with roughly $1/z^2$, in the model of Neukirch & Martens (1998), although the exact dependence is determined by the details of the solution. Obviously, only high-resolution polarimetric observations of the penumbral field in the upper atmosphere can distinguish between the models. The fact that Rüedi et al. (1995a) find evidence for 'uncombed' fields in the upper chromosphere above a sunspot penumbra seems to support the model of Neukirch & Martens (1998). These models additionally need to reproduce observations of broad-band circular polarisation, since such observations contain information on the vertical structure of uncombed fields that cannot be obtained from high-resolution filtergrams alone (e.g., Illing et al. 1974a, b, Sánchez Almeida & Lites 1992, Solanki & Montavon 1993, Martínez Pillet

2000). Note that a rather different description of the uncombed field in terms of small flux tubes embedded in the general field of the sunspot also exists (see Sect. 4.9).

Another phenomenon that has been modelled using force-free fields is the super-penumbra of sunspots, which according to Hα images often has a vortical structure (e.g., Richardson 1941). Nakagawa et al. (1971) and Nakagawa & Raadu (1972) obtained force-free spirals of a desired twist around a sunspot by prescribing the corresponding α. The superpenumbra seen in Hα is a chromospheric phenomenon, so that the magnetic pressure dominates over gas pressure. Hence the validity of the force-free assumption depends mainly on whether the force exerted by the inverse Evershed effect can be neglected. Peter (1996) considered the case when this assumption cannot be made. He took an MHD approach with the Coriolis force now playing an important role (due to the inverse Evershed effect). With even a simple model of this type he was able to reproduce the observations fairly well. The interaction of solar rotation, Evershed flow and the magnetic field leads to a situation similar to that encountered when modelling the solar wind, with a critical point where the Alfvén and flow speeds are the same (e.g., Weber & Davis 1967). The curvature and the direction of the twist – clockwise or counterclockwise – of the resulting spiral depends on the parameters of the field and the flow.

4.7. Models without current sheets

A set of models that solve for the magnetic field on the basis of the full MHD equilibrium but without a current sheet was calculated by Pizzo (1986) — cf. Pizzo (1987). The pressure is specified throughout the numerical box, but not simply as a function of spatial position. Rather, it partly depends on the distribution of the field lines themselves (hydrostatic equilibrium acts along each field line). The formalism underlying these computations was originally developed by Low (1975). Pizzo (1986) tried different pressure distributions, including ones derived observationally. This procedure was necessitated by the fact that no energy equation was solved in parallel with the force balance.

Such models are more sophisticated than self-similar or return-flux models and consequently also have the potential of coming closer to describing the observations adequately. For example, Pizzo (1986) found a choice of the pressure distribution that gives a good qualitative description of the brightness distribution in sunspots. This approach is well suited to a combined solution of the force balance and energy equations, since, instead of being arbitrarily prescribed, the pressure distribution may also be obtained via the temperature from the energy equation. One problem that such models face is the lack of a clear sunspot magnetic boundary, whose presence is suggested by various observations (e.g., Beckers & Schröter 1969b, Solanki & Schmidt 1993).

4.8. Current-sheet models

The simplest consistent current sheet model is composed of a flux tube in whose interior the magnetic field is potential, i.e. current free, so that all the current is concentrated in a sheet at the boundary of the flux tube, termed the magnetopause. The main difficulty then

facing the modeller is the determination of the horizontal position of the magnetopause as a function of height in the presence of arbitrary stratifications in the flux tube and in its surroundings. Approximate solutions have been found and applied to sunspots and pores by Simon & Weiss 1970) and Simon et al. (1983). Wegmann (1981) proposed the first general solution to the free boundary problem and Schmidt & Wegmann (1983) were the first to apply this technique to sunspots.

There are, however, indications that a potential-field model bounded by a current-sheet at the magnetopause is too simple to describe sunspots. In particular, it is inadequate to describe the presence of the penumbra. Hence Jahn (1989) extended the Schmidt & Wegmann (1983) model to include body currents in addition to a current sheet at the boundary. The body currents are restricted to the outer part of the sunspot (corresponding approximately to the penumbra) and chosen such that the surface field matches the observations of Beckers & Schröter (1969). It turns out that the field deviates somewhat from potentiality, but this deviation is not very large anywhere (except at the boundary, of course). It is nevertheless important for reproducing the observations. Although only a single boundary current sheet fails to reproduce the observations satisfactorily (Jahn 1989), combined sheet and body current models provide relatively good fits to the observations of the global magnetic structure of regular sunspots. The resulting magnetic field is not self-similar. The magnetic structure at and below the solar surface resulting for Jahn's model HP is plotted in Fig. 4.2. HP stands for 'Half Potential', since below a certain depth all currents are confined to the magnetopause. Body currents are present only between the two nearly vertical dotted lines in Fig. 4.2. The solid arrows indicate the direction of the computed field, while the dotted arrows have been taken from the observations of Beckers & Schröter (1969b). There is some discrepancy between the model and the data in the outer penumbra, with the dashed arrows being more horizontal. More recent observations, however indicate a less horizontal field in the outer penumbra than found by Beckers & Schröter (Sect. 3.2.2), so that the agreement between model and observations is actually better than suggested by Fig. 4.2.

Jahn & Schmidt (1994), cf. Jahn (1992), considered a model very similar to that of Jahn (1989), but they replaced the body currents in Jahn's (1989) model by a current sheet located between the umbra and penumbra (in addition to the current sheet at the magnetopause). This structure allows for sharp thermal boundaries between umbra, penumbra and quiet Sun by specifying different mixing length parameters in each of these three domains and (partially) inhibiting the transport of heat across the magnetic boundaries. Between the current sheets the field is potential. This simplification of the magnetic structure relative to the models of Jahn (1989) is dictated by the aim of Jahn & Schmidt (1994) of obtaining a realistic thermal structure of the sunspot with distinctly different umbral and penumbral thermal transport mechanisms. These models are marred somewhat by the jump in the field strength at the boundary between the umbra and the penumbra, which is not present in the earlier models of Jahn (1989).

Further current-sheet models of sunspots have been constructed by Pizzo and by Solov'ev. Pizzo (1990) used multigrid techniques to calculate the magnetic structure of a sunspot bounded by a current sheet. His main interest lay in the demonstration of the technique and not in constructing a realistic sunspot model. Solov'ev (1997) has extended the self-similar sunspot models by introducing a current sheet at the sunspot boundary.
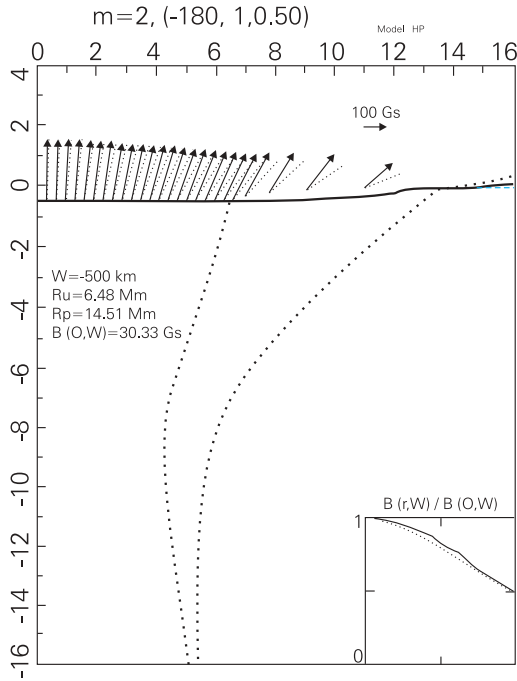
Fig. 4.2. Cutaway through the flux tube model HP ('Half Potential') of Jahn (1989). Dots represent the magnetopause and the inner edge of the penumbral current system, the horizontal continuous line the photospheric level $\tau = 2/3$. Continuous arrows at the surface give the distribution of the magnetic field in model HP, the dotted arrows the observations of Beckers & Schröter (1969b). The length of the arrows indicates the field strength (also plotted relative to $B(r = 0)$ in the inset at the bottom right of the figure), their inclination the inclination of the field lines. The geometrical scale of the model is given in mM. Also printed in the figure are the values of the Wilson depression W, the umbral and penumbral radii, Ru and Rp, and the surface field strength at the spot axis, $B(0, W)$ (adapted from Jahn 1989).

Finally 2-D simulations of flux tubes with different amounts of magnetic flux, concentrated by the influence of convection in their surroundings (Hurlburt & Rucklidge 2000), indicate that a current sheet is automatically produced, with the current sheet becoming narrower as the magnetic Reynolds number R_m is increased. The resulting field strength averaged over the flux tube cross-section is roughly independent of the total flux in the tube, in good agreement with the observational results of Solanki & Schmidt (1993) and Solanki et al. (1999). Unlike the observations, however, the maximum of the field strength is not reached at the flux tube axis, but rather near its boundary (where also the minimum plasma β is achieved in the models). This suggests that additional mechanisms besides concentration by convective cells are responsible for the formation of at least the larger solar flux tubes.

One interesting numerical experiment reported by Hurlburt & Rucklidge (2000) is the effect of increasing the magnetic Reynolds number R_m from 60 to 1000. It leads to more compact flux tubes with stronger fields. Since the field strength achieved at

R_m=1000 already agrees well with solar values a substantial further increase in R_m is not expected to lead to a corresponding increase in averaged field strength, although more subtle effects are likely to occur.

4.9. Uncombed fields and umbral dots

On a small azimuthal scale horizontal and inclined field lines are observed to alternate in the penumbra. Basically three ideas have been proposed to explain the origin of these so-called uncombed fields. The first two of these ideas consider the small-scale magnetic structure to be dynamic and its complexity to result from an instability. A recent proposal invokes downward pumping of magnetic flux by granular convection to produce the uncombed magnetic structure.

Spruit (1981b), Schmidt (1991) and Jahn (1992) propose that the complex magnetic fine structure of the penumbra is due to the convective exchange of flux tubes. One possible scenario for interchange convection is the following: A flux tube near the magnetopause below the (deep) penumbra is heated by the field-free convective gas with which it comes into contact. The heated tube is buoyant and rises (if the gas below the penumbra is superadiabatically stratified). At the surface it radiates away its excess energy, loses its buoyancy, becomes more horizontal and finally sinks again.

The first part of this scenario has been confirmed and quantified by 2-D numerical simulations (Schlichenmaier 1997, Schlichenmaier et al. 1998a, b). An illustration is given in Fig. 4.3. A thin flux tube lying at the magnetopause (i.e. the outer boundary of the penumbra) heats up, becomes buoyant and begins to rise (the background penumbral field and gas, stratified superadiabatically, was taken from the model of Jahn & Schmidt 1994). The part of the flux tube near the outer boundary of the penumbra reaches the surface first. Below the surface the tube rises almost adiabatically, but above the surface radiative losses make it denser and reduce the buoyancy. Also, the background stratification above the surface is no longer superadiabatic. Consequently, the parts of the flux tube above the surface come to rest, staying horizontal, while the surrounding field remains strongly inclined with respect to the surface. With time parts of the flux tube closer to the umbra emerge into the solar atmosphere and lengthen the horizontal portion of the flux tube. The horizontal flux tube remains in equilibrium, since, e.g., the negative buoyancy is balanced by the upward accelaration due to the expansion with height of the background field.

The part of the flux tube passing through the solar surface (i.e. the portion of the horizontal flux tube closest to the umbra) is filled with hot gas and appears bright, the other parts of the flux tube lying above the solar surface have had time to cool down and appear dark. Hence an observational signature of the formation of a horizontal flux tube is the movement of a bright point towards the umbra. Such moving bright points (called penumbral grains) have indeed been observed (see Sect. 5.3.2, Muller 1992, Sobotka et al. 1999). This model also predicts an outward gas flow along the horizontal flux tube, which is similar to that giving rise to the Evershed effect (Sect. 7).

The loss of buoyancy and return to the original more vertical state of the flux tube is, however, not produced by the simulations. If they are correct, then the amount of magnetic flux carried by horizontal fields in the penumbra should increase with time, possibly until some critical concentration of horizontal flux tubes has been reached. On the other

hand, the simulations may be missing some physical ingredient necessary for the second phase of interchange convection. The need for a more realistic treatment of the radiative losses through a proper radiative transfer has been recognized (see Schlichenmaier et al. 1999). Predictions of this model are compatible with the observed variations across the penumbra of the Stokes V asymmetry of Fe I 15648 Å (Schlichenmaier & Collados 2002, Müller et al. 2002, cf. Schlichenmaier et al. 2002).

Recently, the improved treatment of artificial viscosities by Schlichenmaier (2002) has led to results that are more dynamic than before. An instability develops in the horizontal part of the flux tube (cf. Holzwarth & Schüssler 2003), which produces kinks in the flux tube. These kinks travel outward and can give rise to field lines pointing into the solar interior in the outer penumbra, as observed by Westendorp Plaza (1997a). Outside the sunspot these travelling kinks may be related to moving magnetic features.

The second proposal for the origin of uncombed penumbral fields comes from Wentzel (1992). He starts with an inclined field and produces a horizontal field component by invoking a density inversion with height in the atmospheric layers. To create the density inversion he postulates a spatially localized impulsive upflow in the inclined magnetic component. In the almost vertical field of the umbra he expects such an upflow to be visible as an umbral dot. Note, however, that umbral dots do not show marked upflows (Lites et al. 1991, Schmidt & Balthasar 1994), but see Degenhardt & Lites (1993a, b), who pointed out that such an upflow may be present, yet remain undetected in most spectral lines. In the penumbra, at a larger inclination of the field to the vertical, the flow, which fills a small flux tube up to a certain height, now causes dense material to overlie less dense material. A Rayleigh-Taylor instability develops which, according to Wentzel (1992), causes the filled flux tube to fall and become horizontal. Further, he expects the surplus material, which flowed up into the inclined flux tube, to now flow outwards along the horizontal tube. An interesting feature of his proposal is a kink in the horizontal flux tube at the boundary of the umbra. As pointed out by Solanki & Montavon (1994), this feature provides one possible explanation of the observations of Wilson & Cannon (1968) and Wilson & McIntosh (1969) that the discward boundary of the umbra appears more diffuse than the limbward boundary. A detailed numerical treatment of the collapse of a flux tube would be of great value to test this scenario, since the influence of curvature forces and the force acting on the flux tube due to the vertical gradient of the "background field" of the penumbra have not yet been considered in detail. These may well quench any instability from developing beyond the initial stage.

The third and most recent proposal comes from Thomas et al. (2002a, b). They address the question as to why a part of the magnetic field submerges below the solar surface again within or near the penumbra. They argue that convective pumping of magnetic flux by the rapid downflows in intergranular lanes keeps the field submerged beyond the penumbral boundary. Convective or turbulent pumping was introduced to explain the concentration of the magnetic field near the base of the convection zone (Nordlund et al. 1992, Brandenburg et al. 1996, Tobias et al. 1998, 2001, Dorch & Nordlund 2001), where the solar dynamo is thought to be located.

Thomas et al. (2002a, b) propose that initially, as a pore grows and its magnetopause becomes increasingly horizontal, convectively driven instabilities lead to an initial filamentation (Rucklidge et al. 1995, Schlichenmaier et al. 1998a, b). The resultant fluting at the boundary brings some of the outermost field lines down to the surface, where they
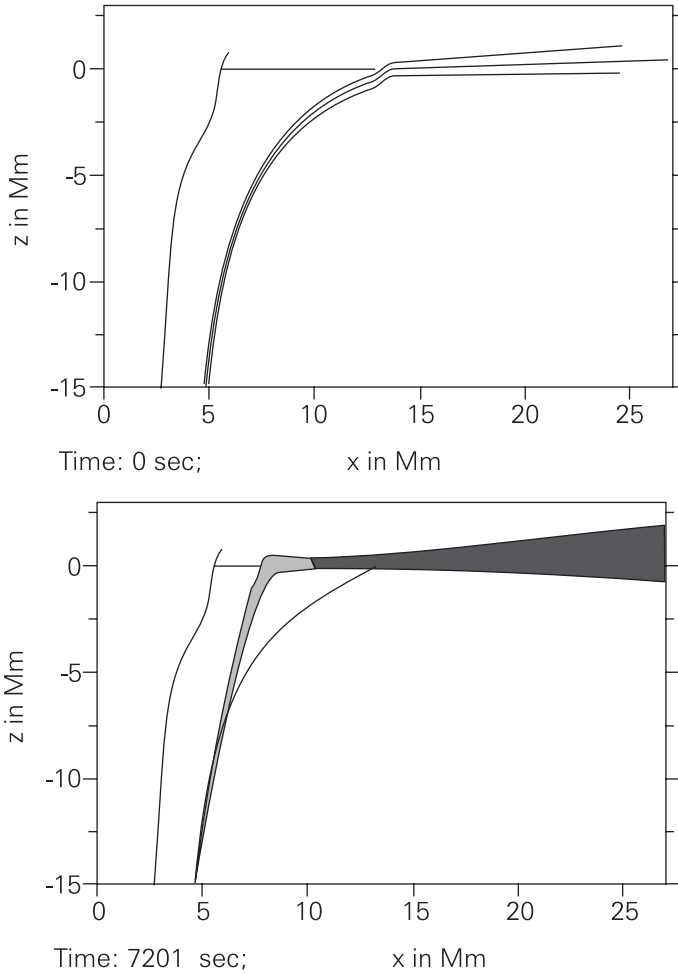
Fig. 4.3. Vertical cut through a model penumbra. Vertical axis: height *z*, horizontal axis: radial distance *x* from the center of the sunspot (lying to the left). Indicated are the solar surface (horizontal line near $z = 0$), the magnetopause between penumbra and quiet sun and the current sheet between umbra and penumbra. Shown is (*top*) a flux tube, at its initial location at the magnetopause and (*bottom*) its final position when it lies partially horizontally at the solar surface within the penumbra (adapted from Schlichenmaier 1997, by permission).

can be grabbed and pumped downwards by granular convection. This process introduces a hysteresis into the evolution of a sunspot's penumbra. As a sunspot decays, the pumping keeps most of these field lines submerged, thus explaining the existence of sunspots (with penumbrae) that contain less magnetic flux than the largest pores.

The mechanisms described by Schlichenmaier et al. (1998a, b), Schlichenmaier (2002) and by Thomas et al. (2002a, b) are not necessarily exclusive of each other and can occur in tandem.

In addition to these models of the processes leading to the formation of uncombed fields are models that aim only to describe the magnetic structure in a static sense (Martens et al. 1996, Neukirch & Martens 1998). These models have been discussed already in Sect. 4.6. One advantage of flux-tube models relative to models eschewing a smooth distribution of fields (e.g., the force-free models) is that the large gradients of magnetic field and velocity across the sharp flux tube boundary can easily explain the production of the broad-band circular polarization observed in sunspot penumbrae (see Sect. 7.3.3). On the other hand, the force-free models more naturally explain the presence of a fluted field also in higher atmospheric layers, whose presence is supported by the crossover effect observed in the He I 10830 Å line (Rüedi et al. 1995a).

Theoretical concepts underlying umbral dots in general consider them to be associated with some form of magnetoconvection (disregarding older concepts like the one due to Roberts 1976, who proposed them to be locations where Alfvén wave cooling is inefficient). In models of a monolithic umbra the bright umbral dots are related to hot upflows. Simulations leading to the production of pulsating bright structures at the top of a monolithic magnetic structure (with vertical field) have been presented by Weiss et al. (1990) and Hurlburt et al. (1996). The 'umbral dots' produced by these simulations are associated with upflows and a weaker magnetic field, so that the observational signature of umbral dots in a monolithic umbra is not expected to be very different from that in an umbra composed of many small flux tubes (see below). The proposal of Wentzel (1992) belongs to this group, although his model does not require the sunspot to be monolithic below the surface.

In the spaghetti model umbral dots are thought to be the protrusion of field-free material from below the surface into the penumbra (Parker 1979c, Choudhuri 1986, 1992). In this model intrusions of field-free, convectively unstable gas are present between the numerous thin flux tubes (the 'spaghetti') below the umbra. If sufficient pressure builds up in this gas it rises, pushing the field lines aside. In some cases the gas can burst through the solar surface, becoming visible as an umbral dot. A sketch of the situation is given in Fig. 4.4. According to Choudhuri (1986) the system acts like a magnetic valve.
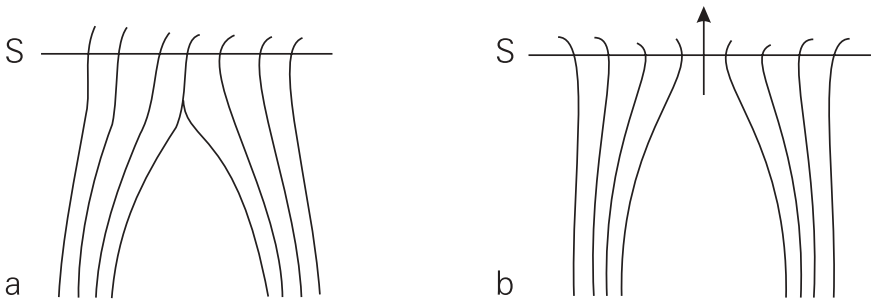
Fig. 4.4a,b. Sketch of the model of Parker (1979a) and Choudhuri (1986) for the production of an umbral dot in a spaghetti model of a sunspot. Shown is field-free fluid surrounded by magnetized fluid with magnetic pressure dropping above the surface (horizontal line marked S). **a:** A convective upflow has started in the field-free fluid, whose apex has not yet reached the surface S. **b:** A flow path has been established (adapted from Choudhuri 1986, by permission).

Once sufficient gas has moved above the surface through the open valve the pressure from above increases again so that the valve should close. Many of the details of this model still need to be worked out. The main consequence for the magnetic field of these models, in particular that of Choudhuri (1986), is that at the continuum-forming layers there is a localized region of no field. However, only 100-200 km above that level the field is practically homogeneous again (Degenhardt & Lites 1993a, b). Thus, in order to test this model using polarimetric measurements, lines formed very deep in the atmosphere need to be observed. Choudhuri (1986) has proposed that the same mechanism acting in the penumbra gives rise to penumbral grains.

5. Brightness and thermal structure of sunspots

5.1. Introduction

A knowledge of sunspot brightness and thermal structure is important for a variety of reasons. For example, sunspot (spectral) brightness is an important parameter entering into studies of solar total and spectral irradiance. It is also needed for accurate line profile calculations, which in turn underly empirical studies of sunspot dynamics and magnetism. Also, the measured brightness and thermal stratification can constrain theoretical models of energy transport mechanisms. Questions that may be addressed by comparing empirical with theoretically predicted thermal stratifications concern the factor by which convective energy transport is inhibited in umbrae and penumbrae as a function of height, the layers at which mechanical (e.g., wave) energy transport and deposition become important, mechanical heating rates in sunspots compared to other solar magnetic features, etc.

Previous reviews bearing on the subject matter of this chapter have been written by Bray & Loughhead (1964), Schröter (1971), García de la Rosa (1987a), Muller (1987, 1992), Solanki (1990, 1997b), Maltby (1992a, b, 1994) and Sobotka (1997). Parts of this chapter draw heavily on the review by Solanki (1997b).

The umbra and penumbra are generally observed and always (empirically) modelled separately, with umbrae grabbing the lion's share of the effort. This chapter is structured accordingly, with most of the space devoted to umbrae. I start, however, with a discussion of observations of the brightness of sunspots as a whole.

5.2. Brightness of sunspots: Global observations

An accurate knowledge of the brightness of sunspots as a whole is needed for a quantitative modelling of variations of total and spectral solar irradiance. Early researchers employed total sunspot contrasts, $\alpha = 1 - I_s/I_{qs}$, of approximately 0.32 (Foukal 1981, Hudson et al. 1982, see also the measurements discussed by Bray 1981), where I_s is the wavelength-integrated sunspot intensity (or more precisely the radiance) and I_{qs} is the same for the quiet Sun. More recently, Beck & Chapman (1993), Chapman et al. (1994) and Brandt et al. (1994), cf. Steinegger et al. (1990), find this quantity to depend on sunspot area, A_s. Thus Chapman et al. (1994) obtained $\alpha = 0.276 + 3.22 \times 10^{-5} A_s$, while Brandt et al. (1994) found $\alpha = 0.2231 + 0.0244 \log(A_s)$. It should be noted that

the measurements are carried out in a given wavelength band and are then extrapolated to cover the whole spectrum, assuming an atmosphere in radiative equilibrium, which is a reasonable assumption (see Sect. 5.5.2). Usually, the spectral details are neglected (cf. Lean 1991), although Solanki & Unruh (1998) and Unruh et al. (1999, 2000) have carried out detailed calculations of the sunspot spectrum averaged over umbra and penumbra at a resolution of 2–3 Å using opacity distribution functions (Kurucz 1991, 1992, 1993).

Separate measurements of umbral and penumbral contrast are discussed by e.g., Makita & Morimoto (1960), Zwaan (1968), Maltby & Mykland (1969), Maltby (1970, 1972), Wöhl et al. (1970) and Bray (1981). For the umbra the estimates vary between $\alpha_{\mathrm{umb}} = 0.5$ and 0.8, for the penumbra $\alpha_{\mathrm{pen}} = 0.15$–$0.25$. These estimates suffer from the same uncertainties as α for the whole sunspot. They correspond to effective temperatures of the umbra of 3900–4800 K and of the penumbra of 5400–5500 K. Separate detailed spectra for umbrae and penumbrae have also recently been calculated. Such spectra are plotted, together with a similarly calculated spectrum of the quiet Sun, in Fig. 5.1. For simplicity two radiative equilibrium atmospheres computed by R.L. Kurucz (at $T_{\mathrm{eff}} = 5500$ K and $T_{\mathrm{eff}} = 4500$ K) are used to describe the penumbra and umbra. In particular for the umbra this effective temperature is just one of a range of possible values observed in different sunspots. For most purposes radiative equilibrium is an adequate approximation, as long as one is only interested in the photosphere. A particularly interesting approach for the future has been that taken by Fontenla et al. (1999), who calculate such spectra with unprecedented accuracy by including the detailed NLTE equilibrium of the atomic species when calculating the stronger spectral lines. This is important in the Far Ultra-Violet (FUV) and Extreme Ultra-Violet (EUV) parts of the spectrum, where much of the radiation is chromospheric in origin.

One quantity that is important in this context is the ratio of umbral to penumbral area of a sunspot. Due to the large difference in radiance between these two parts of a sunspot (the contrast to photospheric radiance differs by a factor of 3–4), even a weak trend in this ratio can lead to a significant trend in the contrast of the spot. As discussed in Sect. 2.3 the $A_{\mathrm{u}}/A_{\mathrm{p}}$ ratio depends only weakly on other parameters, but Beck & Chapman (1993) found that the global contrast of sunspots, α, does depend significantly on the umbral to penumbral area ratio, $A_{\mathrm{u}}/A_{\mathrm{p}}$ (regression coefficient ≈ 0.6):

$$\alpha = 0.22 + 0.34 \frac{A_{\mathrm{u}}}{A_{\mathrm{p}}} \;. \tag{5.1}$$

The correlation of $A_{\mathrm{u}}/A_{\mathrm{p}}$ with A_{s} (the sunspot area) is weaker (coefficient ≈ 0.4).

The umbral contrast exhibits almost no Centre-to-Limb-Variation (CLV; Maltby et al. 1986) and the same is predicted by the empirical penumbral models for the penumbral contrast (since their temperature stratification is consistent with radiative equilibrium; see Sect. 5.9). However, since the penumbra partly hides the umbra near the limb due to the Wilson effect (as can be deduced from the results of Collados et al. 1987) we expect the contrast of sunspots as a whole to decrease somewhat towards the solar limb.

An interesting phenomenon first seen in photographic images by Waldmeier (1939), cf. Das and Ramanathan (1953), Maltby (1960), Bray and Loughhead (1964), is the presence of bright rings, with a contrast of 2–3 % at a wavelength around 4000 Å, surroundings sunspots. Later photoelectric measurements give lower contrasts of 0.1–0.3% (Fowler et al. 1983, Rast et al. 1999) or 0.5–1% in both the blue, 4094 Å, and the
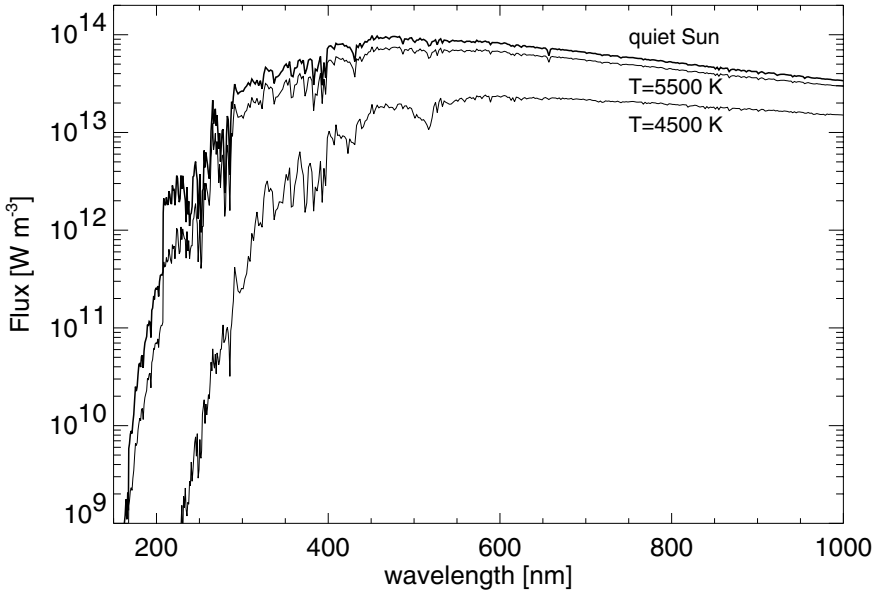
Fig. 5.1. Flux spectra resulting from radiative equilibrium models approximately describing the quiet Sun, $T_{eff} = 5780$ K, a sunspot penumbra ($T_{eff} = 5500$ K) and a typical umbra ($T_{eff} = 4500$ K). Figure kindly provided by Y.C. Unruh.

red, 6071 Å, parts of the spectrum according to Rast et al. (2001). These rings are distinct from photospheric faculae since their contrast relative to the quiet Sun decreases towards the limb (Waldmeier 1939). This result can also be deduced from direct comparisons with polarimetric observations (Rast et al. 1999, 2001). Rast et al. (2001) estimate that the excess flux radiated in these bright rings corresponds to only 10% of the flux blocked by the sunspot and thus is quite inadequate to balance the latter (Sweet 1955), in agreement with the predictions of Spruit (1977, 1982a, b).

Recently, local helioseismology has been providing new insight into the subsurface structure of sunspots (Duvall et al. 1993, D'Silva & Duvall 1995, Kosovichev et al. 2000, Jensen et al. 2001, Zhao et al. 2001), in particular using time-distance helioseismology (Duvall et al. 1993). One problem with the interpretation of such data is that it is not straightforward to distinguish between thermal and magnetic origins of wave speed perturbations. A relatively clear result is that the wave speed perturbations below sunspots are quite strong, ranging from 0.3 to 1 km s^{-1}, and are limited in depth to within 20 Mm (Jensen et al. 2001, Kosovichev et al. 2000). This implies that sunspots are, thermally, a near-surface phenomenon. Interestingly, if the wave speed perturbations are interpreted entirely in terms of temperature perturbations, then the gas below sunspots is cool relative to its surroundings down to only 4–5 Mm. At deeper layers it is hotter (higher sound speed) than the surroundings (Kosovichev et al. 2000), with the higher sound speed extending at least 60 Mm below the solar surface (Kosovichev 2002). At a depth of 4 Mm the temperature variations correspond to roughly 2800 K (i.e. 10% of the ambient temperature), compared to a contrast of 9000 K at the level of the Wilson depression
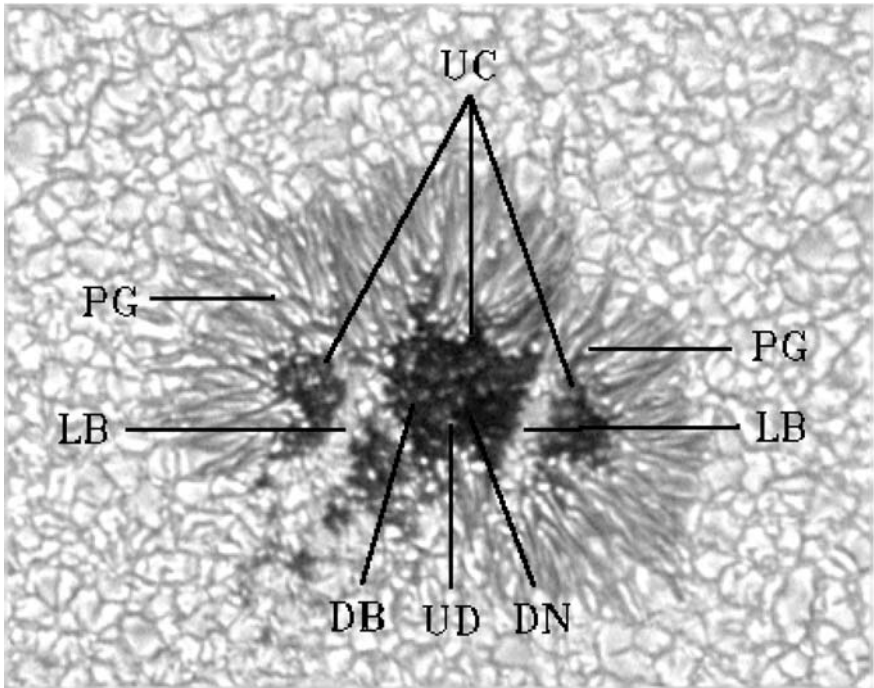
Fig. 5.2. Illustration of sunspot fine structure. The following elements contributing to sunspot fine structure are marked (see also the text). UC: umbral core, PG: penumbral grain, LB: light bridge, UD: umbral dot, DN: dark nucleus. Contrast has been enhanced in order to reveal fine structure better (from Sobotka 1997 by permission).

(such a high temperature difference can be achieved at a fixed height of, say, 500 km below the surface of the quiet Sun, corresponding to the Wilson depression, since the temperature increases very rapidly with depth just below the solar surface). Note that the temperature variations deduced from theoretical estimates (Meyer et al. 1974) decrease even more rapidly with depth.

5.3. Sunspot fine structure

When observed at a spatial resolution better than approximately $1''$, sunspots reveal a rich fine-structure in brightness. It is particularly evident in the penumbra, but also the umbra, which appears rather bland on most images, harbours many small-scale brightness inhomogeneities if the exposure and contrast of the image are chosen accordingly.

An overview of the fine structure within sunspot umbrae can be gained from Fig. 5.2 (see Sobotka 1997). The various small-scale features are identified on that image using the following abbreviations (clockwise from the top):

UC :   umbral cores = individual umbrae separated by light bridges
PG :   penumbral grains = bright, dot-like or elongated features located primarily in the
       inner penumbra

LB : light bridges = lanes of bright material separating two umbrae, or two umbral cores

DN : dark nucleus = the darkest, almost structureless part(s) of an umbra

UD : umbral dot = bright dot-like feature inside an umbra

DB : diffuse background = the darker part of the umbra between the umbral dots

In addition to these features the elongated bright and dark penumbral fibrils which constitute most of the penumbra are clearly visible in Fig. 5.2. The terminology is not completely standardized. E.g., what Sobotka calls dark nuclei have also been termed umbral cores or voids (Livingston 1991), while what he (perhaps somewhat misleadingly) calls umbral cores are often referred to as individual umbrae or sub-umbrae.

With the exception of the elusive umbral dots, the other fine-scale structure had been identified already in the 19th century, primarily by Secchi (1872), but many can also be seen in a beautiful drawing made by Langley (and published by, e.g., Flammarion 1880) or the pioneering photographs of Chevalier (1907, 1914, 1919), cf. Bray & Loughhead (1964). As far as the fine-scale structure of sunspot brightness is concerned, therefore, progress over the past century, with the exception of the (re-)discovery of umbral dots by Danielson (1964), — but see also Chevalier (1916), Thiessen (1950), Bray & Loughhead (1959), Loughhead & Bray (1960) — has been made mainly in fleshing out the properties of the features (brightness, sizes, lifetimes, evolution), in uncovering their connection with other physical parameters (velocity, magnetic field) and in finding adequate theoretical descriptions for them.

Reviews of the fine-scale brightness structure of sunspots have been given by Bray & Loughhead (1964), García de la Rosa (1987a), Muller (1987, 1992) and Sobotka (1997), where further details and references can be found. The relationship between sunspot thermal and magnetic fine structure is discussed in Sect. 3.9.

5.3.1. Umbral fine structure

The dominant fine-scale brightness structure in umbrae is caused by umbral dots, point-like bright features embedded in the umbral background. Umbral dots cover 3–10% of the umbral area and contribute 10–20% of the total brightness of the umbra (Sobotka et al. 1993). Some umbrae appear to be entirely free of dots, however, showing instead a fibril-like structure reminiscent of penumbrae (Livingston 1991). The number density (or filling factor) of umbral dots increases with the brightness of the umbral background. In particular, the darkest cores of the umbrae (the 'dark nuclei' in Fig. 5.2) exhibit almost no visible, fine-scale brightness structure (Livingston 1991, see Loughhead et al. 1979 for a different view). These dark nuclei cover 10–20% of the total umbral area and have $I_c \approx 0.05$–$0.3 I_{c,phot}$ (where I_c is the continuum intensity at 5400 Å and $I_{c,phot}$ is the same quantity for the quiet photosphere). Their average size is approximately $1.5''$ according to Sobotka.

Due to their size near and quite possibly below the spatial resolution of the best current observations, the true brightness of umbral dots is not easy to determine. Direct observations of the contrast give values that depend on the spatial resolution. Colour temperatures of bright umbral dots, obtained from blue and red images (which unfortunately were not recorded simultaneously) gave brightnesses close to the photospheric value (Beckers & Schröter 1968, Kneer 1973, Koutchmy & Adjabshirzadeh 1981). Since

the radiation in the two colours needed for temperature determination in general arises from somewhat different heights, it is assumed that the temperature gradient in dots and the umbral background are the same and that dot sizes are independent of height (see the discussion in Tritschler & Schmidt 2002a). Evidence that this assumption is not fulfilled has been presented by Wiehr (1994): the contrast of umbral dots relative to the umbral background decreases with height z, so that they either become smaller with z, or have steeper $T(z)$. Socas Navarro (2002) has shown that umbral dots possess a steeper temperature gradient and that they (the dots) are significantly hotter than their surroundings only in the lower photosphere. Any errors in the colour temperature, induced by this assumption should be systematically the same for all such investigations (see also Foukal et al. 1981 and Foukal & Duvall 1985 for similar investigations related to faculae). According to Sobotka (1997) some of the problems associated with the earlier investigations, namely non-simultaneous images and restriction to bright umbral dots, have been removed by more recent investigators. Using such improved observations he found that the intensities cover a wide range, often being lower than I_{phot}. The problem with two-colour photometry mentioned above remained, however. More recently Sütterlin & Wiehr (1998) combined speckle reconstruction and 3 colour photometry, which overcomes some of the major disadvantages of 2-colour photometry. They find that the umbral dots are 900–1300 K hotter than the umbral background, i.e. still some hundred degrees cooler than the quiet photosphere. Pahlke & Wiehr (1990), cf. Pahlke (1988), also deduced umbral dot brightnesses close to photospheric (temperatures within 500 K, but not higher than photospheric) based on the Stokes V profiles of lines of different excitation potential. Note, however, that although their technique reduces the influence of stray light, it cannot remove it; see Sect. 5.4. Finally, Tritschler & Schmidt (2002b) conclude that umbral dots are on average 700 K hotter than the umbral minimum, with a scatter of over 1000 K, and $\sim$ 750 K colder than the mean photosphere. The brightest umbral dots are still found to be fainter than the quiet photosphere.

Grossmann-Doerth et al. (1986) distinguished between brighter 'peripheral' umbral dots and darker 'central' umbral dots, based on their location. Such a distinction is supported by Ewell (1992), but on the basis of umbral dot proper motions, with peripheral dots moving inwards and central dots being stationary (cf. Kitai 1986, Molowny Horas 1994, Sobotka et al. 1995, 1997b, Tritschler & Schmidt 1997). Ewell (1992) deduced considerably lower than photospheric dot brightnesses, a result supported by Obridko & Staude (1988) and Sobotka (1988). The separation into two types of dots introduced by Grossmann-Doerth et al. (1986), cf. Tritschler & Schmidt (2002a), was extended by Sobotka et al. (1993) to a continuous relation between the brightness of umbral dots, I_{ud}, and that of the background, I_{bg}, valid in an average sense: $I_{\mathrm{ud}} \approx 3I_{\mathrm{bg}}$ (cf. Sobotka et al. 1991). This result is based on the comparison of the observed contrast (of 1.5 I_{bg}) with 2-component, semi-empirical model calculations qualitatively confirmed by Denker (1998), although he finds a lower contrast (1.3 I_{bg}) of the dots relative to the local background directly from the observations. Finally, Adjabshirzadeh & Koutchmy (1980), Sobotka et al. (1997b) and Rimmele (1997) have found evidence that the umbral dot brightness fluctuates with time.

If some umbral dots are indeed spatially unresolved, then only upper limits on their size can be given. Nevertheless, various techniques have been employed in an attempt to obtain more accurate estimates. Thus Harvey & Breckinridge (1973) set an upper

limit of 180 km on the size of the smallest umbral dots. Assuming them to have photo-spheric brightness, Koutchmy & Adjabshirzadeh (1981) concluded by using the observed brightness and size that they have diameters of 0.11–0.28″ (80–200 km). Similarly, by comparing the colour with the brightness temperature Aballe Villero (1992) deduced diameters of 0.15–0.6″ (110–440 km). Likewise, Grossmann-Doerth et al. (1986) obtained 0.4–0.9″ (290–650 km), Lites et al. (1991) found 0.17–0.39″ (120–280 km) from images deconvolved from the estimated point spread function (PSF) of the telescope. Sobotka et al. (1993) obtained 0.25–0.41″ (180–300 km), Rimmele (1997) 0.3″–0.8″ and Denker (1998) 0.3″–0.55″ (220–400 km) from speckle images, while Sobotka et al. (1997a) and Tritschler & Schmidt (2002b) found the number of umbral dots to increase with decreasing size, right down to the spatial resolution, suggesting that the majority is indeed unresolved. This raises the interesting question how much of the intensity of the umbral background is actually due to unresolved umbral dots, and to which extent are variations in the brightness of this background due to changes in the number density of these umbral dots. The view that most umbral dots are unresolved is contradicted by Denker (1998), who concludes from his symmetric size distribution that the smallest dots have been resolved.

The density of umbral dots is largest in bright areas of the umbra (Sobotka et al. 1993), where also the large umbral dots tend to be located (Sobotka et al. 1997a).

Umbral dots live less long than their host umbrae. Estimates of mean lifetimes range from 15 min (Ewell 1992), over 25-30 min (Danielson 1964, Beckers & Schröter 1968, Adjabshirzadeh & Koutchmy 1980) and 40 min (Kitai 1986) to 60 min (Kusoffsky & Lundstedt 1986). There is a large distribution of lifetimes according to Sobotka et al. (1997a), with 2/3 of the dots having lifetimes shorter than 10 min, although exceptional cases live longer than 2 hours (cf. Kusoffsky & Lundstedt 1986, Ewell 1992).

5.3.2. Penumbral fine structure

The most prominent structures in the penumbra are the radial filaments or fibrils; followed by the more point-like bright penumbral grains. The filaments are often separated into bright and dark, allowing a simple (probably too simple) 2-component description of the penumbra. The bright filaments are approximately 0.3–0.6″ broad and 0.5–2″ long or longer, depending partly on the location in the penumbra (Danielson 1961a, Muller 1973a, Tönjes & Wöhl 1982, Sobotka et al. 1999). Denker (1998) finds wider filaments, on average 0.7″. It is likely that some of them are narrower than these values, since a number of authors find power right down to the resolution limit (e.g. Harvey & Breck-inridge 1973: 0.28″; Stachnik et al. 1983: 0.11″; Denker et al. 1995: 0.23″; Sánchez Almeida & Bonet 1998: 0.28″). Very high resolution is achieved with speckle recon-structions by Stachnik et al. (1983), who argue that the narrowest penumbral filaments are only 0.11″ wide (cf. Stachnik et al. 1977). Similarly, the widths of the narrowest penumbral filaments are near the diffraction limit according to Danielson (1961a), Krat et al. (1972), Moore (1981a) and Bonet et al. (1982), who cannot rule out that a number of them lie below the resolution limit, as has been argued by Sánchez Almeida (1998). The dominant spatial power is not at such fine scales according to Harvey (1985), however, since the finest interferometric fringes he detects in sunspots from 2-entrance-aperture interferometry are at 0.2″, well above his resolution limit. Also, a recent speckle re-

construction by Sütterlin (2001) using data from the Dutch Open Telescope (DOT) has revealed the power in the penumbra to drop more rapidly than the modulation transfer function (i.e. the Fourier transform of the point spread function). The conclusion that most penumbral filaments have indeed been resolved is supported by Scharmer et al. (2002), who obtain a width of 150–180 km (i.e. 0.2–0.25″), in good agreement with Harvey's early results. Scharmer et al. (2002) do find evidence for unresolved structure in their images. They report the discovery of dark thread-line cores of bright penumbral filaments best seen where the latter protrude into the umbra.

Penumbral filaments live between 10 min and 4 hours. At least for the broader filaments (diameters $\geq$ 1000 km) the lifetime exceeds 2h (Bray & Loughhead 1958, Balthasar et al. 1996, Solanki and Rüedi 2003). Danielson (1961a), Muller (1973a), Tönjes & Wöhl (1982), Sobotka et al. (1999) and Sobotka & Sütterlin (2001) determine lifetimes of penumbral grains, obtaining values ranging from roughly 20 min to well over an hour.

The continuum observations of Muller (1973b) indicate $I_c \approx 0.3$–$0.7I_{phot}$ (on average 0.65I_{phot}) and a filling factor of 0.6 for the dark component and $I_c \approx 0.7$–$1.0I_{phot}$ (average 0.95I_{phot}) with a filling factor of 0.4 for the bright. These observations were criticised by Grossmann-Doerth & Schmidt (1981). Their analysis suggested that the actual distribution of brightness in a penumbra is single peaked. Collados et al. (1987) argue that both points of view are justified. A single peaked distribution can also be produced by the sum of two distinct brightness components, if each component exhibits a sufficiently wide distribution of brightness. This interpretation is supported by Denker (1998) and Tritschler & Schmidt (2002b). Sütterlin & Wiehr (1998) find typical spatial fluctuations of 700K in the penumbra, based on speckle reconstructions of images obtained in three colours. Their dark fibrils have $T \approx 5650$K (colour temperature), corresponding to a contrast of 0.64 to the quiet sun, in good agreement with Muller (1973b) and Collados et al. (1987). Their bright grains are actually 100K *hotter* than the quiet sun. This need not contradict earlier measurements, since the grains considered by Sütterlin & Wiehr (1998) are brighter than even the bright fibrils. Denker (1998) obtains on average 0.86 I_{phot} for his bright fibrils, in agreement with earlier observations, but finds for the dark filaments an average brightness of 0.73 I_{phot} (at 550 nm) which is comparatively high. Finally, Sobotka et al. (1999) find $I_{pg} \approx 0.84$–$1.10 I_{phot}$, where I_{pg} is the intensity of a penumbral grain.

In any case, bright and dark only has local significance, since bright features in one part of a penumbra may well be darker than the dark structures in another part (Grossmann-Doerth & Schmidt 1981, Wiehr et al. 1984, Muller 1992). On the best images, the dark parts of the penumbra appear multiply connected, in a topologically similar manner to intergranular lanes, while the bright fibrils appear more isolated. Their morphological structure differs from granulation in the sense that the bright fibrils often appear to have a bright dot at their inner, umbral end (these bright dots are usually referred to as penumbral grains). More than one fibril, often placed in a V-shape, can start from a single penumbral grain. Muller (1973a, b) has argued that at high resolution the bright penumbral filaments are chains of elongated penumbral grains, each being comet-shaped.

The penumbral grains are seen to move radially in the penumbra. Regarding the direction and speed of the motion, as with so many other aspects of sunspot fine structure,

divergent views have been expressed. Schröter (1962) found an *outward* motion of 1–2 km s^{-1}, while Muller (1973a, 1976), Tönjes & Wöhl (1982), Shine et al. (1987) and Sobotka et al. (1995) found an *inward* motion of 0.3–1 km s^{-1}. A number of recent studies reconcile these opposite results. Thus, Wang & Zirin (1992), Denker (1998), Sobotka et al. (1999) and Sobotka & Sütterlin (2001) find both *inward* motion (concentrated in the inner 60%-70% of the penumbral area) at 0.3–0.5 km s^{-1} and an *outward* motion at 0.5–0.7 km s^{-1} (in the outer penumbra). If local correlation tracking is used then both dark and bright features are seen to follow this pattern of motion (Wang & Zirin 1992, Sobotka et al. 1999). It is at present unclear to what extent these motions of brightness structures are associated with mass motions. For example, flow velocities are always directed outward in the penumbra, suggesting that at least the inward moving penumbral grains are not tracing a gas flow.

Lifetimes of penumbral grains were found by Muller (1973a) to vary between 40 min, for grains born near the edges of the penumbra, and 3–4 h, for grains near the centre of the penumbra. The longer lifetime near the centre of the penumbra may result from the fact that these grains have to move further before they leave the penumbra. A large range of lifetimes, between 1 and 3 h, was also obtained by Tönjes & Wöhl (1982). Finally, Sobotka et al. (1999) distinguish between inward moving (mean lifetime 40 min) and outward moving (25 min) penumbral grains. The comparatively small lifetimes obtained by them suggest that the large maximum lifetimes found by the earlier authors are reached by only very few penumbral grains.

Small scale features are also prominent in filtergrams referring to chromospheric heights, although somewhat larger scales tend to dominate. Also, these structures often appear outside the white-light sunspot, in the superpenumbra. This is a region in which, e.g. in Hα line-core images, prominent bright and dark fibrils are seen extending out from the sunspot. These superpenumbral fibrils have a length of roughly 10^4 km and a width of less than 2000 km, often even close to the spatial resolution limit of 200–300 km. The individual Hα fibrils live for less than 20 min and are associated with material inflow (inverse Evershed effect; Moore & Rabin 1985, Bray & Loughhead 1964). Whether the dark chromospheric superpenumbral fibrils seen in Hα are in any way related to the "cool" canopy fields suggested by Ti I 2.2 μm lines (Rüedi et al. 1998) remains to be seen. Note that the structure registered in the core of a strong (photospheric) line correlates poorly with the structure seen in continuum radiation (Wiehr & Stellmacher 1989), suggesting that it is different physical features producing the structure seen at different heights.

5.4. *Need for multi-component models*

As discussed in Sect. 5.3 a sunspot contains considerable unresolved fine structure. The closest one comes to a single-component situation is in the dark umbral nuclei, which are thought to be spatially resolved. However, their low intensity means that stray light from the much brighter surroundings can significantly influence the observations. If a part of the stray light comes from the penumbra then it is also likely to affect the polarized Stokes parameters:

$$I_{\mathrm{obs}} = \alpha I_{\mathrm{u}} + (1-\alpha)I_{\mathrm{s}} , \tag{5.2}$$

$$P_{\text{obs}} = \alpha_{\text{p}} P_{\text{u}} + (1 - \alpha_{\text{p}}) P_{\text{s}} \, , \tag{5.3}$$

where I_{u} is the intensity profile arising from the umbra, I_{s} is the intensity of the stray light, α is the "magnetic" filling factor (i.e. the fraction of the surface area within the resolution element covered by umbral magnetic field, or rather the fraction of the radiation from the observed umbra) and $P = Q, U$, or V represents the 2 linearly and the circularly polarized Stokes parameters. Here $\alpha_{\text{p}} \geq \alpha$, where α_{p} is the "filling factor" derived from the polarized radiation. It can be larger than α because a part of the stray light may be unpolarized.

Methods for countering stray light are discussed by, e.g., Rossbach & Schröter (1970), David & Elste (1962), Zwaan (1965), Brahde (1972), Mykland (1973), Köppen (1975) and Martínez Pillet (1992).

Finally, in the penumbra and the brighter parts of the umbra at least 3 components are present, a bright component denoted in the following by subscript b (bright filaments in the penumbra, dots in the umbra), a dark component denoted by a subscript d (dark filaments and the umbral background, respectively) and the stray light. In the simplest case we can therefore write

$$I_{\text{obs}} = \alpha_{\text{b}} I_{\text{b}} + \alpha_{\text{d}} I_{\text{d}} + (1 - \alpha_{\text{b}} - \alpha_{\text{d}}) I_{\text{s}} \, , \tag{5.4}$$

$$P_{\text{obs}} = \alpha_{\text{b,p}} P_{\text{b}} + \alpha_{\text{d,p}} P_{\text{d}} + (1 - \alpha_{\text{b,p}} - \alpha_{\text{d,p}}) P_{\text{s}} \, . \tag{5.5}$$

Again, $\alpha_{\text{b,p}} \geq \alpha_{\text{b}}$ and $\alpha_{\text{d,p}} \geq \alpha_{\text{d}}$. Clearly, a good stray-light correction is central to the correct modelling of sunspot thermal structure. Although the polarized Stokes parameters are less affected by stray light than the intensity, the situation is nevertheless more complicated than in plages. There the polarized Stokes profiles are — to first order — sensitive only to the magnetic flux tubes.

In reality the situation, at least in the penumbra, is far more complex than outlined here and a simple multi-component model probably does not do it justice. For example, the fact that penumbral fine structure does not correlate well when comparing images refering to different heights (Wiehr & Stellmacher 1989) casts doubts on the concept of independent components. Similarly, the uncombed magnetic structure of the penumbra suggests that also the thermal structure may be more strongly interlocked than a model composed of independent components suggests. For purposes of empirical modelling, however, it is often adequate to retain this simplified concept.

5.5. Single component empirical umbral models

Umbrae have been empirically modelled as either one- or two-component structures (the stray-light fraction of the total radiation is in general not counted as a separate component). The total number of empirical umbral models, in particular of 1-component models, is large, although not all models are independent of each other; many have grown out of older models by way of minor or major changes. In the present section I discuss single-component models. The 2-component models are the subject of Sect. 5.8.

Since sunspot umbrae are not homogeneous, single-component models can only describe a part of the umbra (or an average over it). Usually such models are meant to describe the dark umbral background, or the dark nuclei (according to the nomenclature of Sobotka 1997), which are thought to be relatively homogeneous.

In addition to the assumption of homogeneity another important assumption underlying almost all single-component models is universality, i.e. the assumption that a single model is valid for all umbrae, or at least the dark background of all umbrae. This assumption has been advocated by Albregtsen & Maltby (1981a), who contend that the brightness of the dark nucleii of large umbrae (with diameters $d_u \gtrsim 10''$) is independent of size or other umbral parameters and depends only on the phase of the solar cycle. This assumption is scrutinized in Sect. 5.7.

We need to distinguish between models restricted to the photospheric layers of umbrae and those including the chromosphere or even the transition zone. Purely photospheric models are therefore discussed separately.

5.5.1. Models of the umbral photosphere

Models of the umbral photosphere are based on LTE radiative transfer calculations and observations of continuum contrast, weak spectral lines, or in some cases the wings of strong spectral lines. Both the centre-to-limb variation (CLV) and the wavelength dependence of the continuum intensity (I_c) or continuum contrast ($\phi_u = I_{c,u}/I_{c,\text{phot}}$) have been used, although the wavelength dependence provides information only on a rather limited height interval unless a very large wavelength range is considered. Note that I_c is often obtained from relatively broad-band measurements and may be significantly affected by line blanketing.

Early models were generally based on the CLV of continuum contrast and belonged to either the class of rarified (Michard 1953, Van t'Weer 1963, Fricke & Elsässer 1965, Zwaan 1965) or the non-rarified models (Mattig 1958, Jakimiec 1965, Zwaan 1965). Near the $\tau = 1$ level the gas pressure in rarified models is generally reduced by some factor (2–10) below that given by hydrostatic equilibrium. The $\tau_c = 1$ level lies 2000–3000 km deeper inside sunspots than in the quiet sun according to these models and it is not obvious how they can be reconciled with Wilson-effect measurements, which reveal Wilson depressions of 400–800 km (e.g., Gokhale & Zwaan 1972). Rarified models are also expected to be unrealistically bright near the solar limb (Jensen & Maltby 1965). Such models were introduced in order to reproduce the observations current at that time. A rarefaction was required mainly due to the neglect of the contribution of line opacity to the total opacity. The non-rarified models usually build on the assumption of hydrostatic equilibrium. At least in the photospheric layers such models are expected to be far more realistic (cf. Mattig 1974). Early umbral models are reviewed in detail by Bray & Loughhead (1964).

Models since the end of the 1960s have been constructed by Hénoux (1969), who derived the temperature stratification from continuum measurements and the Na I D line wings and checked it using equivalent widths of medium-strong lines (cf. Hénoux 1968); by Wittmann & Schröter (1969), from the CLV of I_c at different wavelengths between 4680 Å and 7900 Å; Mattig (1969), who chose a simple linear $T(\tau)$ to reproduce the CLV of his I_c observations; Stellmacher & Wiehr (1970), who modified Hénoux's model to reproduce $I_c(\lambda)$ and line observations made by the authors; Dicke (1970), from the temperature vs. field strength relation derived from observations by Von Klüber (1947) under the assumption that the field is truly cylindrical below the solar surface (this model covers the low photosphere only); Yun (1971a), based on the

CLV of I_c for different $\lambda \lesssim 1.6$ μm and on the wings of Na I D; Webber (1971), from molecular lines of MgH and TiO; Kneer (1972), from the profiles of three Fe I lines and continuum (this model turns out to be very similar to that of Stellmacher & Wiehr 1970); Kjeldseth-Moe & Maltby (1974b), based on I_c observations (this model explains differences between measured I_c values of different sunspots by temperature fluctuations in the upper photosphere); Zwaan (1974a, 1975), constructed to reproduce the wavelength dependence of I_c taken from different sources, Stellmacher & Wiehr (1975), based on the Na I D line wings, Fe I 5434 Å, 2 infrared C I lines and $I_c(\lambda)$; Kollatschny et al. (1980), from the wings of Ca II 8542 Å and other strong lines, as well as $I_c(\lambda)$; Boyer (1980), a model derived from the equivalent widths of 147 TiO lines, which is similar in $T(\tau)$ to the Stellmacher & Wiehr (1975) model; and Van Ballegoijen (1984), a model of the deep layers of sunspot umbrae based on a spectrum covering the wavelength range $1.1 < \lambda < 2.3\mu$m, obtained by a Fourier Transform Spectrometer (FTS).

5.5.2. Chromospheric models

Such models are based on either strong spectral lines in the visible or on lines in the UV. The radiative transfer is always carried out in NLTE. Since the calculation of upper atmospheric lines usually also requires a knowledge of the photospheric thermal structure almost all chromospheric models include a photospheric part. In many cases this is simply taken from one of the photospheric models listed in Sect. 5.5.1. This section also covers models of the umbral transition zone and corona (cf. Sect. 5.6).

Early observations (Hale 1892) showed that the Ca II H and K lines have emission cores, suggesting that sunspots also possess chromospheres (see Linsky & Avrett 1970 for a review). First exploratory models of sunspot umbral chromospheres were constructed by Baranovsky (1974a, b; cf. Staude 1981) and later by Kneer & Mattig (1978), based on general properties of the Ca II H, K and IR lines, and by Teplitskaya et al. (1978), by inverting Ca II H and K line profiles.

This early work set off a spate of modelling, which resulted in a model based on Ca II H, K and 2 IR triplet lines, Hα and Na I D (Yun et al. 1981, Beebe et al. 1982), an umbral chromospheric and transition zone model deduced from the cores of Ca II H and K, Mg II h and k, H I Lyα and β and C IV observations made with the OSO-8 satellite (Lites & Skumanich 1981, 1982, cf. Gurman 1984), a model due to Staude (1981), which agrees closely with the Stellmacher & Wiehr (1975) model in the photosphere, the Teplitskaya et al. (1978) model in the chromosphere and reproduces data obtained by the HRTS instrument and OSO-8 (see Staude et al. 1983, 1984), a model of the transition zone above an umbra that relies on HRTS spectra of FUV lines of various ions formed mainly in the temperature range 2×10^4–2×10^5 (Nicolas et al. 1981), and an investigation of the coronal temperature structure above umbrae by Foukal (1981).

In their chromospheric layers the various models can differ significantly. For example, Staude (1981) finds an almost steady increase of the temperature throughout the chromosphere, while Lites & Skumanich (1981, 1982) deduce a flat chromospheric temperature plateau. All models show, however, an increased height of the umbral temperature minimum relative to the quiet sun, needed to explain, e.g., the narrow Ca II H and K emission peaks in umbrae.

The efforts of a number of modellers have been synthesized into models by Avrett (1981) and Staude et al. (1983). Avrett's "Sunspot sunspot model" of the umbral photosphere, chromosphere and transition zone combines the low photospheric model of Albregtsen & Maltby (1981b) with the upper photospheric and chromospheric parts of the Lites & Skumanich (1981, 1982) model and the transition region model of Nicolas et al. (1981). Staude et al. (1983), cf. Staude (1981), produced a comprehensive umbral model covering the full height range from the photosphere to the corona. It is based on a large set of observations (radio, optical, EUV, X-ray), but takes its photospheric structure largely from Stellmacher & Wiehr (1975), while its lower chromospheric stratification is similar to that of Teplitskaya et al. (1978).

Since the mid 1980s the largest effort in single component umbral modelling has been invested into testing and improving the model of Avrett (1981). First Maltby et al. (1986) improved Avrett's model in the deep layers using photometric data obtained at Oslo. Their set of 3 models (each for a different phase of the solar cycle, see Sect. 5.7.3) has become something of an industrial standard.

Lites et al. (1987) compared the observed Stokes V profile shape of the Mg I intercombination line at 4572 Å with the synthetic profile resulting from the Maltby et al. (1986) atmosphere (for the atomic model of Altrock and Canfield 1974). Since the synthetic profiles show a strong inversion in the Stokes V core whereas the observations do not, they concluded that the chromospheric temperature rise must begin at a considerably greater height than in the Maltby et al. model. The conclusion of Lites et al. (1987) has been criticised by Mauas et al. (1988), who argued that the true transition probability of the Mg I intercombination line is significantly smaller than the value employed by Lites et al. (1987). Briand & Solanki (1995) obtained good fits to quiet-sun profiles of this line with $\log(gf)$ values close to those of Mauas et al. (1988), indicating that the criticism may be well-founded.

Caccin et al. (1993) constructed a modified version of one of the Maltby et al. (1986) models with a steeper temperature gradient in the photosphere, resulting in a minimum temperature of 2500 K. Their modification is based on fits to Na I D and K I 7699 Å profiles. The Caccin et al. (1993) model was in turn slightly modified by Severino et al. (1994), who raised the minimum temperature to 2900 K, without otherwise significantly changing the model. The temperature in the middle and upper photosphere of the Maltby et al. (1986) model is constrained mainly by the CO first overtone lines at 2.35 μm. These were used to fix the minimum temperature at 3400 K, giving a very flat temperature stratification through most of the photosphere. Support for the steeper photospheric temperature gradient in umbrae comes from Ayres (1996), who constructed a modified LTE version of the Maltby et al. (1986) model (i.e. a version without a chromosphere) that reproduces fundamental band CO lines at 4.67 μm. Since these lines are stronger than the first overtone lines at 2.3 μm they are more sensitive to upper photospheric temperatures. In the photospheric layers his model turns out to be much closer to that of Caccin et al. (1993) and Severino et al. (1994) than the original Maltby et al. (1986) model. The only recent model that agrees well with that of Maltby et al. (1986) in the upper photosphere is that of Collados et al. (1994), which, however, is not well constrained in these layers by the data it is based on (B. Ruiz Cobo, private communication).

Severino et al. (1994) point out the good agreement between the photospheric temperature stratification of their model and a non-grey radiative equilibrium model. The Maltby et al. (1986) umbral photosphere, on the other hand, corresponds more closely to a grey radiative equilibrium atmosphere.

It thus appears that at least in photospheric layers the energetics of sunspot umbrae are determined by radiation. The fraction of the total energy flux transported by radiation is fairly large in all observable layers of umbrae (greater than 70% for $\log \tau < 1$). In contrast, this fraction drops rapidly with depth in the quiet photosphere (e.g., Maltby et al. 1986, Maltby 1992a, Collados et al. 1994). This implies that energy transport by convection, although definitely present in one form or another (as pointed out already by Zwaan 1974a, 1975), plays a much smaller role in sunspot umbrae than in the quiet Sun and stresses the need to properly incorporate radiation into simulations of magnetoconvection aimed at understanding the umbra.

One diagnostic that future models should also consider is submillimeter brightness. In such radiation, formed in LTE and arising from the low to mid chromosphere, sunspot umbrae appear darker than the photosphere (but with a positive temperature gradient), while penumbrae may in some cases be brighter (Lindsey and Kopp 1995). Umbral oscillations seen in microwaves by Shibasaki (2001) have been proposed by him as another diagnostic of the temperature minimum region. The most likely value of T_{min} he finds is 4100 K, which is much hotter than other determinations and suggests the need either for data with higher spatial resolution that isolate the umbra, or for improvements to the diagnostic.

5.6. The transition region and corona above sunspots

The space above visible-light sunspots is not particularly bright in coronal XUV (Tousey et al. 1973) or in X-ray radiation (Vaiana et al. 1976) coming from the corona (e.g. Pallavicini et al. 1979, Kingston et al. 1982, Walker et al. 1988, Golub et al. 1990, 1994; Sams et al. 1992, Harmon et al. 1993, Nindos et al. 2000) and is comparable in brightness to network boundaries in the FUV (Cheng et al. 1976). This is particularly true for umbrae, thus suggesting that the relationship between spatially averaged magnetic field strength and solar activity (as manifested by upper atmosphere brightness) seen for weaker fields (e.g. Schrijver et al. 1989) does not hold for large concentrations of the field. At transition region temperatures the picture is quite complex (see below). The observations also suggest that the coronal temperature above sunspots is lower than in their surroundings (Alissandrakis & Kundu 1982, Siarkowski et al. 1989, Fang et al. 1997, Nindos et al. 2000). The highest temperatures observed in sunspots are larger than in the quiet Sun, but lower than the average value in the active region harbouring them.

The transition region and corona above sunspots has been studied both at short (EUV and X-ray) as well as long (cm radio) wavelengths. Here I first consider the radio observations and the results obtained from them. Sunspots (and the associated active regions) are strong sources of radio waves. Covington (1947) first discovered a relationship between sunspots and 10.7-cm radio flux using a solar eclipse to overcome the lack of spatial resolution. Indeed 10.7-cm radio flux has turned out to be an excellent proxy of sunspot number.

Zhelethyakov (1962) and Kakinuma & Swarup (1962), among others, proposed that thermal gyroresonance emission is an important component of the observed radio signal. By taking some model input for the magnetic field structure (e.g. buried dipole, potential or force-free field extrapolated from the photosphere), and the electron temperature and density (whose height distribution is usually calculated assuming constant conductive flux and hydrostatic equilibrium throughout the transition region) it is possible to predict the spectrum and appearance of radio emission above sunspots (e.g. Zlotnik 1968, Gel'freikh & Lubyshev 1979, Alissandrakis et al. 1980, Strong et al. 1984, Krüger et al. 1985, Alissandrakis & Kundu 1984, Brosius & Holman 1989, Bogod et al. 1992, Lang et al. 1993). Typical predictions are listed below: the radio sources associated with the sunspots are compact, having sizes similar to those of the underlying sunspots. The brightness temperature spectrum has a negative slope (at high frequencies; due to the assumption of temperature increasing with height). The radio emission is expected to be circularly polarized in the sense of the extraordinary or x-mode. For a circularly symmetric sunspot the peak of the net polarized emission comes from a ring, when viewed directly from above, or else a crescent.

These predictions have been confirmed by many authors. Thus the ring or crescent shape of the polarized emission feature has been observed by Lang & Willson (1982), Alissandrakis & Kundu (1982) and Chiuderi-Drago et al. (1982), as well as many subsequent authors. Observed brightness spectra were shown to agree well with the theoretical expectations by, e.g., Gary & Hurford (1987, 1994) and Lee et al. (1993b).

In some sunspots the core of the emission ring emits radiation polarized according to the ordinary or o-mode. This result can be explained in terms of a temperature inhomogeneity (Kundu & Alissandrakis 1984, Vourlidas et al. 1996, 1997).

Let us now turn to properties of the sunspot transition region deduced from EUV observations. The spatial distribution of gas at a given (coronal, but in particular transition-region) temperature above a sunspot can be quite inhomogeneous, e.g. Brynildsen (1998a, b, 1999a). The most striking such transition-region features are sunspot plumes, localized regions which on average are roughly an order of magnitude brighter than the active region as a whole. The term 'sunspot plume' was first introduced by Foukal et al. (1974) based on Skylab data. Noyes et al. (1985) proposed that sunspot plumes are parts of larger active-region loops where the temperature is considerably lower than in the main part of the active region. In radiation from the lower or cooler transition region ($T \lesssim 10^5$ K) sunspot plumes are very rare (Kingston et al. 1982), whereas in somewhat hotter gas the majority of sunspots are found to harbour plumes (Maltby et al. 1998 – 5 out of 9 studied sunspots – Brynildsen et al. 1999a – 15 out of 17 sunspots – and Brynildsen et al. 2001a – 33 out of 40 sunspots). The fraction of sunspots exhibiting plumes depends not only on the analyzed spectral line (see Maltby et al. 1999), but also on the exact criterion employed to identify them. In particular, far more sunspots are found to harbour plumes if bright regions lying solely above the penumbra are also allowed (e.g. Brynildsen et al. 2001a, 1999a), than if a criterion requiring some of the bright material to lie above the umbra is employed (Maltby et al. 1998, Brynildsen et al. 1998c).

Brynildsen et al. (1999a) also found that the plumes are most prominent in the temperature range $\log T = 5.2$–5.6. In most cases the plume is not restricted to the visible outline of the sunspot, which, given the expansion of the sunspot magnetic field

with height and the fact that the sunspot field forms coronal loops is not surprising. Since the transition region and coronal line emission is due to the collisional excitation from the lower energy level followed by the radiative de-excitation of the upper level, the line emission is proportional to n_e^2, where n_e is the number density of electrons. The distribution in brightness over a sunspot indicates up to 2 orders of magnitude variation in n_e over a sunspot at upper transition region temperatures. At coronal temperatures this variation is often smaller (Brynildsen et al. 1999a).

If the peak intensity above a sunspot is considered, however, then the variation of n_e from one sunspot to the next is larger at coronal temperatures (Brynildsen et al. 1999a). Larger plumes are generally also brighter (Brynildsen et al. 2001a), but this is not necessarily the case for plumes associated with larger sunspots. EUV emission above sunspots is variable (Foukal 1976, Fredrik & Maltby 1998; Brynildsen 1999a, 2001a), with both a rapidly – minutes timescale – and a slowly — day timescale – varying component, but observations from the Solar and Heliospheric Observatory (SOHO) indicate that plumes tend to remain intact for days, in contrast to the earlier Skylab results.

Plumes are more common above sunspots lying further from the neutral line (Brynildsen et al. 2001a) suggesting that a simple magnetic geometry aids the formation of a plume. Brynildsen et al. (2001a) propose that sunspot plumes are the product of siphon flows along loops, whose other footpoints end in faculae or the network (with smaller field strength). Hence the flow is a necessary prerequisit for the presence of the plume (cf. Nicolas et al. 1982, Doyle et al. 1985).

An unexpected recent result has been the discovery of blinkers, i.e. localized brightenings lasting some tens of minutes in mid-transition region lines (Harrison 1997, Harrison et al. 1999, Brković et al. 2000, Bewsher et al. 2002) above the umbra and penumbra of a regular, unipolar sunspot (Parnell et al. 2002). The sunspot blinkers do not appear to be significantly different from blinkers found elsewhere on the Sun, suggesting a common mechanism. Since they were observed in a unipolar sunspot the latter authors rule out any mechanism involving local reconnection.

5.7. Dependence of the umbral temperature on other parameters

5.7.1. Dependence on sunspot size

The question whether the umbral brightness and temperature depends on umbral size or not touches on a basic assumption underlying almost all single component models, namely that it is possible to describe all umbrae (or at least those above a certain size) by a single thermal model. This question also has a bearing on heat blocking by sunspots. An excellent review of the relevant work up to the end of the 1980s has been given by Maltby (1992a).

Early observations suggested that large sunspots are darker than small sunspots (continuum observations prior to 1963 are listed and discussed by Bray & Loughhead 1964). Such observations were often insufficiently corrected for stray light produced in the earth's atmosphere (seeing) and in the instrument (scattered light). Zwaan (1965) first pointed out that the amount of stray light affecting the umbra increases rapidly with decreasing umbral size. Observations made since then have usually been corrected
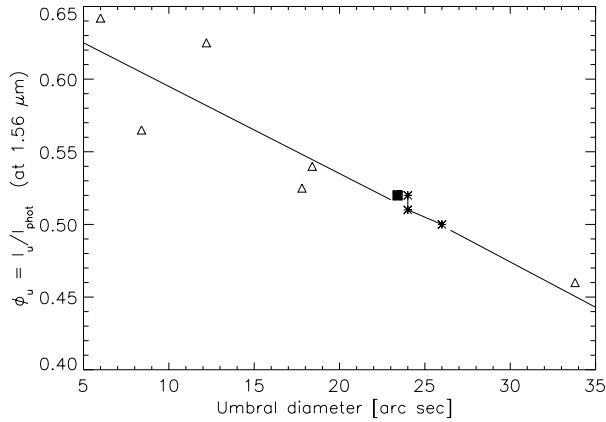
Fig. 5.3. Umbral normalized continuum intensity $\phi_{\mathrm{u}} = I_{\mathrm{u}}/I_{\mathrm{phot}}$ at $1.56\,\mu$m plotted vs. umbral diameter. Here I_{u} is umbral intensity and I_{phot} the corresponding photospheric value. Plotted are the lowest stray light corrected ϕ_{u} values of 8 umbrae. The 6 umbrae represented by triangles were observed by Kopp & Rabin (1992), the umbra represented by the filled square was analyzed by Solanki et al. (1992). The 3 stars denote a single umbra observed on 3 different days by Rüedi et al. (1995b). The straight line indicates the trend.

for stray light with much greater care. For sunspots with umbral diameters greater than 8–$10''$ subsequent observations did not reveal any significant dependence of umbral core brightness on sunspot size (e.g., Zwaan 1965, Rossbach & Schröter 1970, Albregtsen & Maltby 1981a).

More recently, however, evidence against this result has been mounting. Stellmacher & Wiehr (1988) found that 2 small spots with $d_{\mathrm{u}} = 7''$ have T_{eff} values 600 K higher than model M4 of a large sunspot umbral nucleus (Kollatschny et al. 1980). They take stray light into account in their modelling of lines that have virtually opposite temperature sensitivity. Kopp & Rabin (1992) present observations that show a clear relationship between the umbral brightness at $1.56\,\mu$m and sunspot size after correction for stray light (note that their correction is much larger for small sunspots than for large ones, in agreement with the expectations). All their observations were obtained on the same day, but the umbral contrast $\phi_{\mathrm{u}} = I_{\mathrm{u}}/I_{\mathrm{phot}}$ shows a dispersion as large as over the whole solar cycle according to Albregtsen & Maltby (1978). In Fig. 5.3 the Kopp & Rabin results (triangles) are shown together with measurements of the minimum brightness at $1.56\,\mu$m of 2 sunspots (filled square and stars) made by Solanki et al. (1992) and Rüedi et al. (1995b), by the latter on 3 different days. The linear dependence on sunspot umbral diameter is evident.

Martínez Pillet & Vázquez (1993) confirm this result for 7 sunspots observed within 2 weeks of each other in 1989 at similar $\mu = \cos\theta$ values (θ is the heliocentric angle). They correct carefully for stray light (Martínez Pillet 1992). Collados et al. (1994) have inverted spectra from the darkest parts of 3 sunspots of this sample, two large spots and a smaller one. The 2 larger spots (umbral diameters d_{u} of $22''$) gave similar results, $T(\tau = 1) = 3940$ K, while for the small spot they obtained $T(\tau = 1) = 5030$ K. The stray-light problem in the small spot was reduced by fitting only Stokes V (note,

however, that Stokes V may still be contaminated by polarized stray light from the penumbra). Their conclusions are supported by Steinegger et al. (1996) and Tritschler & Schmidt (2002a), who obtain a similar spectral trend for the contrast (obtained by the latter authors after a phase diversity reconstruction) of a small sunspot, but a much smaller absolute value of the contrast than previous observes of larger sunspots. Further indirect support comes from the study of Sütterlin (1998) of pores, which in some senses can be considered to be small naked umbrae and which exhibit higher temperatures than larger sunspot umbrae.

An independent line of evidence for a dependence of T on d_u comes from the nearly universal relationship between B and T, with T being lower when B is larger (see Sect. 5.7.2). Since the maximum field strength B_{max} of sunspots scales with their size (Brants & Zwaan 1982, Kopp & Rabin 1992) this relationship implies that larger spots should also be darker.

Finally, Sobotka et al. (1993) derive from high spatial resolution observations a relation (with considerable scatter) between radius and brightness of umbral nuclei. It is, however, unclear how these results relate to a dependence of the (minimum) relative umbral brightness $\phi_u = I_u/I_{phot}$ vs. d_u, plotted in Fig. 5.3 since the umbral nuclei are considerably smaller than the host umbrae. It does nevertheless suggest that even the relatively homogeneous umbral nuclei cannot be described by a single universal atmosphere.

5.7.2. Dependence on magnetic field strength

Alfvén (1943) first predicted a relationship between the vertical component of the magnetic field, B_z, or alternatively the field strength, B, and temperature, T, at a given geometrical height. This relationship has later been extensively investigated, both theoretically and observationally. Much of the observational work prior to 1992 has been reviewed in the introduction to their paper by Martínez Pillet & Vázquez (1993).

Investigators have either considered the relationship between the maximum field strength B_{max} of a sunspot and the associated minimum temperature (respectively continuum brightness), or the B vs. T relationship at different locations within a single sunspot. I first review investigations of the former type.

Cowling (1957) considered the theoretical aspects of this relationship. Deinzer (1965) compared the observations of Stumpff (1961) via a relation given by Houtgast & van Sluiter (1948), with the predictions of his self-similar sunspot model (cf. Schlüter & Temesvary 1958), which includes a mixing length formalism to describe energy transport. The model qualitatively reproduced the data. Dicke (1970) provided an alternative formulation of the theoretical prediction and used the data of Von Klüber (1947) to test it. Maltby (1977) published a clear derivation of the relationship. He also compared the well calibrated and stray-light corrected intensity measurements of Ekmann & Maltby (1974) and Ekmann (1974) with routine field strength measurements made at Rome observatory (which are uncorrected for stray light). Unsurprisingly he found only a small variation of T, but a large variation of B_{max} from spot to spot. Chou (1987) presented a B_{max} vs. $\phi_u(\lambda = 6100\,\text{Å})$ relationship for stable spots, as well as showing that growing sunspots depart from this relationship. His stable spot relationship falls between those of Deinzer (1965) and Dicke (1970), but must be treated with caution since some of

his measurements are obviously systematically incorrect (e.g., he claims $B_{\mathrm{max}} \approx 600$ G and $\phi_{\mathrm{u}} \approx 0.6$ for sunspots having $d_{\mathrm{u}} \approx 6\text{–}10''$. This B_{max} is much too low and the ϕ_{u} probably too large).

Also, Kotov & Koutchmy (1994) claim a correlation (which is not very well visible in their plots) between I_c and B based on observations from 1974 made at various limb distances that are uncorrected for stray light.

Careful and thorough studies of this type, although limited to small sunspot samples, have been made by Kopp & Rabin (1992) and Martínez Pillet & Vázquez (1990, 1993), the former at 1.56 μm, the latter around 6300 Å. Their results show a clear relationship, as illustrated for the infrared data in Fig. 5.4a, in which data from the same spots is plotted as in Fig. 5.3. Livingston (2002) extended the study of Kopp & Rabin to a much larger sample of sunspots, covering a larger range of brightness and field strength. His result is plotted in Fig. 5.4b. Although the scatter is larger than in Fig. 5.4a this figure indicates that $B \sim 1/I_{\mathrm{u}}$ rather than the linear relationship suggested by Fig. 5.4a. Since the brighter umbrae are in general also smaller and stray light has not been corrected for, we probably cannot rule out that the non-linearity in the relation shown in Fig. 5.4b is (partly?) produced by the influence of stray light. Steinegger et al. (1996) also found a correlation between a sunspot's bolometric contrast and its peak field strength.

The first to investigate the T vs. B relationship for different locations within a single sunspot was Von Klüber (1947), who published figures of B and I_c along slices through sunspots. He did not, however, explicitly plot I_c vs. B. Abdussamatov (1971b, cf. 1973) did plot this relation for a sunspot pair. Although both his intensity and magnetic-field measurements are affected by stray light, his results for the preceding spot look similar to the best current observations and show the separate signatures of the umbra and the penumbra, including the relatively sharp transition in brightness between the two.

Gurman & House (1981) carry out a Milne-Eddington inversion of Fe I 6302.5 Å to determine the magnetic parameters at a large number of locations in 4 sunspots. They find a linear relationship between B and I_c for all their data sets. Although they correct for stray light, their relationship remains linear all the way from $I_c \approx 0.3$ to 1.0 and from $B = 1800$ G to 0 G. In the absence of stray light and with a correctly measured B one would expect to see a break in the relationship at the umbral boundary. Lites et al. (1991) similarly conclude from their high spatial resolution observations (of Stokes I only) that, on scales larger than those of umbral dots, B is inversely correlated with continuum intensity. Martínez Pillet & Vázquez (1990, 1993) and Del Toro Iniesta et al. (1991) have also presented such relationships. Martínez Pillet & Vázquez observed at many locations in 8 sunspots and carried out a thorough stray-light analysis. They found a nearly linear relationship between B^2 and T throughout the umbra and into the penumbra. Again no break is seen at the umbral boundary. Note that the scatter in B^2 vs. T between different sunspots is not significantly larger than the scatter between individual positions in one spot. A linear trend of B^2 vs. T is also presented by Lites et al. (1993). In their case only the umbra of a small, symmetric sunspot is considered. Westendorp Plaza et al. (2001a) show that the slope of the B vs. T relationship changes with depth in the photosphere, being steeper at intermediate layer ($\log \tau_c = -1.5$) than at higher and deeper layers.

Using infrared data Kopp & Rabin (1992) and Solanki et al. (1993) also find, like the rest of the investigators, that the brightness of the umbra is clearly a function of location,
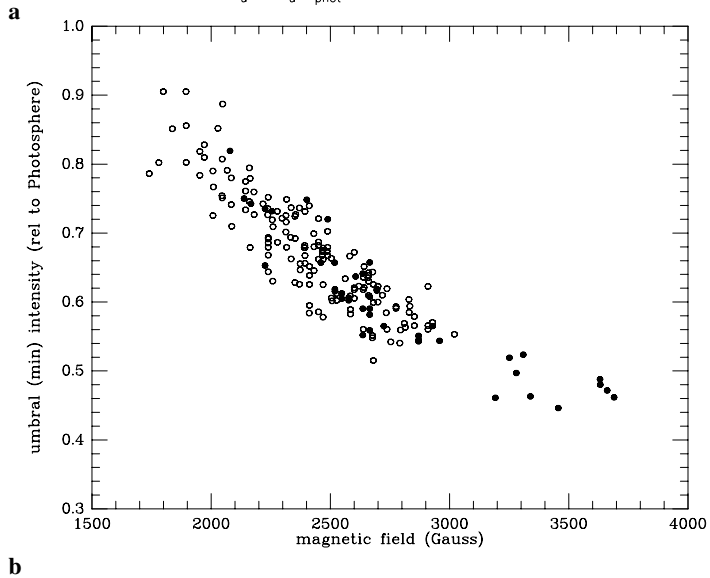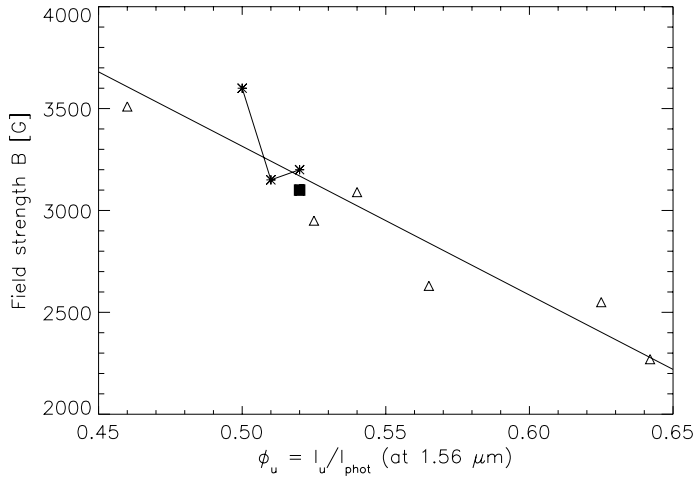
Fig. 5.4. a: Umbral normalized continuum intensity ϕ_u vs. umbral field strength B. Plotted is the minimum value of ϕ_u and the maximum value of B of each of the sunspots represented in Fig. 5.3 (same symbols). **b**: B vs. ϕ_u. Each sunspot is represented by a filled circle (sunspots measured in 1990–1991) or an open circle (2000–2001). Figure from Livingston (2002) by permission.

with the darkest part usually coinciding with the strongest magnetic field (which is particularly well determined using infrared data). This position need not coincide with the centre of the sunspot, but may lie quite close to the edge of the umbra (Solanki et al. 1993); this also suggests that the brightness variation is not due to stray light. In addition, the strengths of various spectral lines were also monitored. Since different spectral lines exhibit very different correlations with I_c, stray light can be ruled out as the source of these intensity and field strength variations.

In summary, the umbral temperature is a function of position within the umbra, in agreement with results obtained from high spatial resolution images (Sect. 5.3.1). Furthermore, the minimum umbral temperature varies from one sunspot to another, and closely follows the maximum field strength. Both quantities are roughly linear functions of sunspot size.

The first unambiguous sign of a change in the B–T relationship across the umbral boundary was provided by Kopp & Rabin (1992). They obtained one linear relationship between B and T in the umbra, but another (steeper) linear relationship in the penumbra. The break at the umbral boundary is even more clearly visible in the data of Solanki et al. (1993), Balthasar & Schmidt (1993) and Stanchfield et al. (1997). According to their high-resolution observations the B in the penumbra changes by nearly a factor of 2, while T remains almost constant. Hence, unlike the umbra, the penumbra appears to be almost free of large-scale radial variations of T. There are, of course, considerable small-scale variations (visible as penumbral filaments) and also large-scale azimuthal variations; see Sect. 5.3.2. The evolution with height of the break at the umbral boundary and of the B–T relationship in the penumbra has been studied by Westendorp Plaza et al. (2001a).

Further measurements related to the work reviewed here (e.g. plots of B and I_c slices) have been published by Lites & Scharmer (1989), Lites & Skumanich (1990), Lites et al. (1991), Balthasar & Schmidt (1994) and Hofmann et al. (1994).

Let me now outline how the T vs. B relationship may be used to estimate the Wilson depression and the curvature forces within a sunspot. By integrating the radial component of the MHD force-balance equation (over the radial coordinate r) one obtains

$$P_0(z) - P(r, z) = \frac{1}{8\pi} \left(B_z^2(r, z) + F_c(r, z) \right), \qquad (5.6)$$

where P_0 is the gas pressure outside the sunspot, P the gas pressure in the sunspot, B_z the vertical component of the magnetic field and F_c an integral describing the magnetic curvature forces. Equation (5.6) is valid for a given geometrical height z. B_z is directly observed at some optical depth τ corresponding to an unknown z, $P(r, \tau)$ is a more or less unique function of the temperature stratification in the sunspot (in hydrostatic equilibrium), while $P_0(z)$ is known from standard atmosphere and convection zone models describing the quiet Sun. With this information it is possible, in a first step, to determine the Wilson depression $Z_W(r)$ (Martínez Pillet & Vázquez 1990, 1993) and its variation across the sunspot (Solanki et al. 1993) if one assumes that $F_c = 0$. Basically, one searches for the depth in the quiet sun at which P_0 equals the combined measured magnetic and gas pressure inside the sunspot. This depth is approximately the Wilson depression. In a following step one can compare the $Z_W(r)$ derived in this manner with other measurements of this quantity and therefrom set limits on the curvature forces and magnetic gradients in the sunspot. Two results of such an analysis are: Curvature forces are of a similar magnitude as forces driven by the gas pressure gradient, and at $\tau_c = 1$ (where τ_c is the continuum optical depth) the gas pressure in a sunspot is always larger than the magnetic pressure (i.e. plasma $\beta > 1$).

The sensitivity of the T vs. B relationship to magnetic curvature forces is illustrated by Rüedi et al. (1995b), who analysed it on 3 different days for the same (relatively young) sunspot and found evidence for a relaxation process. This is visible in Fig. 5.3 in

which this sunspot is marked by the three stars. The symbol lying furthest from the solid line represents the observations of the first day, when the sunspot also showed extreme magnetic gradients around a partial lightbridge ($dB/dz \approx 1400$ G/arc s), corresponding to currents almost as large as the largest seen in a flaring δ-spot (Zirin & Wang 1993a). On the other days no such large gradients are seen and the T vs. B relationship of this spot also looks more similar to that of other mature sunspots.

5.7.3. Dependence on the solar cycle

One of the most surprising discoveries related to sunspots has been the dependence found by Albregtsen & Maltby (1978), of the umbral core brightness of large sunspots ($d_u > 8''$) on the phase of the solar cycle, cf. Albregtsen & Maltby (1981a). Sunspots present early in the cycle are the darkest, while sunspots appearing later in the cycle have increasingly brighter umbrae, until the spots belonging to the next cycle appear (which again have dark umbrae). According to Albregtsen et al. (1984) the solar cycle variation is approximately of the same magnitude as the difference in brightness between sunspots at high and low latitudes (5–35°). Since the average latitude of sunspots changes over the solar cycle it is conceivable that the solar cycle dependence is mainly a latitude dependence. Albregtsen et al. (1984) have therefore corrected for this effect and found that the cycle dependence holds also when ϕ_u is extrapolated to $\mu = 1$. Also, Maltby (1992a) has pointed out that the scatter of the ϕ_u vs. latitude relationship is larger than of ϕ_u vs. solar cycle phase. Unfortunately, no other group of investigators has to my knowledge made a similar study as yet. Confirmation of these intriguing results appears particularly important in the light of the recently found dependence of sunspot brightness on size.

   Two explanations have been put forward. Schüssler (1980) proposed that the umbral brightness may be influenced by the age of the sub-photospheric flux tube (formed and wound up at the bottom of the convection zone over the solar cycle). Yoshimura (1983), on the other hand, suggests that it is rather the depth in the convection zone at which the flux tube is formed which is responsible for the umbral temperature. He proposes that this depth varies over the solar cycle.

5.7.4. Dependence on limb distance (CLV)

The CLV of umbral brightness or contrast is one of the most commonly used observables for the modelling of the sunspot thermal stratification. However, various observers have found contrasting results. Thus the measurements of Wittmann & Schröter (1969) suggest that I_c of the umbra increases towards the limb, so that the umbral contrast decreases (cf. Rödberg 1966; Schatten 1993). More recently the measurements of Albregtsen & Maltby (1981a) have shown no net change in umbral contrast with μ, while Albregtsen et al. (1984) find that although I_c in the umbra decreases towards the limb, the contrast does the same. New measurements of this type are obviously needed, preferably from space, as pointed out by Albregtsen & Maltby (1981c).

5.7.5. Dependence on age or evolution

Little work has been specifically directed at this question. In the only relevant paper known to me, Sobotka (1988), from 2-component models of umbrae, finds no dependence of the brightness of either his bright or dark component or of their filling factors on evolutionary phase of his sample of 11 spots. Possibly a much larger sample is needed to uncover a dependence, if one exists.

5.8. Umbral 2-component models

The temperature is a function of position within the umbra. This follows both from low-resolution (see, e.g., Sect. 5.7.2) and high-resolution observations, which often show umbral dots in addition to a varying background (see Sect. 5.3.1). Although some umbrae appear to be free of dots and reveal only filaments (Livingston 1991) the majority are thought to be composed of bright umbral dots and a dark umbral background.

Hence the obvious next step in umbral modelling is the construction of 2-component models (Sect. 5.4). The advantage of this simple scheme is that by varying the filling factors of the two components it is possible to produce a whole range of brightness. One weakness of 2-component models arises from the fact that umbral dots are often not spatially resolved and there is an ongoing debate regarding their true temperature and field strength (or the height variation of these quantities). Since the temperature of the hot component cannot be determined with certainty, the filling factor is equally uncertain (the measured intensities cannot distinguish between the two parameters). Due to the unknown $B(z)$ of umbral dots, it is not clear how the filling factor varies with height. Also unknown is whether hot features in the upper atmosphere are at all related to hot features in the lower photosphere. In addition, the work of Sobotka et al. (1993) regarding the variation in brightness from one dark nucleus in an umbra to the next, undermines the assumptions on which the 2-component model is based, namely that only the mixture of the 2 components varies from spot to spot, while the properties of each of the components remains universal (cf. Stellmacher & Wiehr 1985).

Early 2-component models of the umbra have been constructed by Makita (1963) and Obridko (1968b). More recent 2-component models are due to Adjabshirzadeh & Koutchmy (1983), Staude et al. (1983, 1984), Obridko (1985), Obridko & Staude (1988), Pahlke & Wiehr (1988), Sobotka (1988) and Sobotka et al. (1993). The models of Staude et al. (1983, 1984) possess two components in the higher layers only. In the photosphere and chromosphere they are single component models.

The most comprehensive 2-component model is the "working model" of Obridko & Staude (1988). They propose that different mixtures of cool and hot gas describe the observed umbral dark nucleus and the umbral dots. In the umbral dark nucleus the hot and bright component must occupy a volume fraction of $\beta = 5$–10% in order to reproduce the observations of Albregtsen & Maltby (1981a), while in the dots $\beta = 50\%$ in order to reproduce the high-resolution observations of Wiehr & Stellmacher (1985). The filling factor of the secondary component varies with height according to horizontal pressure balance assuming a weak secondary-component field at the $\tau_c = 1$ level and a height-independent field of 3000 G in the umbral nucleus. The basic philosophy behind this choice is that the thermal structure follows field lines.

In conclusion, 2 or more component models are important and some good models of this type have been constructed. Nevertheless, a basic uncertainty remains and there is a strong need at the moment for observations that allow the properties of umbral dots to be determined, not just in continuum-forming layers, but at all heights in the atmosphere.

5.9. Penumbral models

The most striking feature of the penumbra are the fibrils. It is therefore not surprising that studies of penumbral brightness have concentrated on the fine structure, i.e. the effort has focussed on the horizontal variation of the temperature rather than on its vertical stratification (see Sect. 5.3.2). Consequently, empirical penumbral models are rare.

The first penumbral model was that of Kjeldseth-Moe & Maltby (1969). It is a single-component scaled quiet-sun model (with $\delta\theta = 0.055$, where $\theta = 5040/T$) that can reproduce weak spectral lines and observations of penumbral continuum intensity (normalized to the quiet sun value) $\phi_{\mathrm{pen}}(\lambda) = I_{\mathrm{pen}}(\lambda)/I_{\mathrm{phot}}(\lambda)$. It is only meant to be a model of the lower photospheric layers of the penumbra.

Models that include not just the photosphere, but also the chromosphere have been published by Yun et al. (1984) and Ding & Fang (1989). These models are based on observations of strong spectral lines (Ca II H and K, two of the Ca II IR triplet lines and the Na I D doublet in the case of Yun et al. and Ca II H and K, the Ca II IR triplet, Hα and Hβ in the case of Ding & Fang). Most of the effort has gone into modelling the chromospheric layers. In particular, the authors have not taken into account weak lines or continuum observerations to reliably fix photospheric temperature and hence both models are too cool in the photosphere. A promising way of producing a better penumbral model is to consistently combine the chromospheric part of such a model (that of Ding & Fang 1989 appears less arbitrary) with a photospheric penumbral model, such as that of Kjeldseth-Moe & Maltby (1969).

Judging from white-light images of penumbrae a 2-component penumbral model seems obvious, although, given the complexity of the penumbral brightness distribution (Sect. 5.3.2), it may be too simplistic. A 2-component model has indeed been constructed by Kjeldseth-Moe & Maltby (1974a), with one component describing the bright filaments and the other the dark. It is a straightforward extension of the Kjeldseth-Moe & Maltby (1969) model to 2 components, being partly based on the same data. The weighted sum of the ϕ_{pen} of both components is compared with the observed, low-spatial-resolution data of Maltby (1972). The temperature stratification of both components is scaled down from the photosphere, with the continuum brightness of each component being required to correspond with the high resolution observations of Muller (1973b).

As a next step in complexity, Del Toro Iniesta et al. (1994) have inverted 801 profiles of the Fe I 5576.1 Å line to derive the temperature stratification at each spatial location. The profiles were constructed by scanning a narrow-band filter through the line. The scatter of the temperature of all the models around the mean temperature stratification varies between 200 and 500 K at different heights, with the scatter being smallest in the low and mid photosphere, i.e. in the layers best constrained by the observations.

Del Toro Iniesta et al. (1994) have also constructed average temperature stratifications at different distances from the umbra. The temperature generally increases somewhat as the distance to the umbra increases (which may well be the result of stray light). This

is in contrast to the findings of Westendorp Plaza et al. (2001a) from inversions of full Stokes vectors of Fe I 6301.5 Å and 6302.5 Å that the azimuthally averaged temperature in the inner penumbra is slightly higher than in the outer penumbra. Del Toro Iniesta et al. (1994) have also created a model of the average penumbral temperature stratification by combining the $T(\tau)$ of 411 of their models. This average is very similar to the hotter of the Kjeldseth-Moe & Maltby models. This is also partly true of the mean model obtained by Westendorp Plaza et al. (2001a) and in particular Rouppe van der Voort (2002a). That the Kjeldseth-Moe & Maltby models may be slightly too cool is also supported by the contrast measurements of Tritschler & Schmidt (2002a). Interestingly the standard deviation of the individual Del Toro Iniesta et al. models is smaller than the difference between the 2 Kjeldseth-Moe & Maltby (1974a) components, suggesting that the spatial resolution of the observations underlying the Del Toro Iniesta et al. (1994) models was lower than of Muller's (1973b) observations.

Rouppe van der Voort (2002a) constructed 3 models to represent cool, hot and intermediate structures in the penumbra. The temperature contrast between the hot and cold models in approximately 300 K, and thus somewhat smaller than between the 2 Kjeldseth-Moe & Maltby (1974a) models. Rouppe van der Voort (2002a) also discusses the difference in temperaute stratification between the disc- and limbside penumbra, with the former being slightly hotter. He proposes that the brightness structure is inclined relative to the horizontal (inclined downwards towards the sunspot boundary) to explain this difference.

5.10. Conclusion

Observations of sunspot brightness and spectra at high or low spatial resolution are numerous and quite a number of these have found their way into the various models of sunspot temperature. These in turn have evolved to the point that a single umbral model (or a pair of them in the case of 2-component models) can now reproduce a large variety of observations. In the penumbra the situation is less satisfactory. Currently no model exists which gives a good representation of both the photospheric and the chromospheric layers. Inversions of large data sets and detailed numerical simulations whose output can be directly compared with observations may well be the direction in which this field will move in the future.

6. Models of sunspot brightness and thermal structure

6.1. Sunspot darkness

Biermann (1941) first proposed that the reduced brightness of sunspots is due to the inhibition of convective motions by the magnetic field (see Gough & Tayler 1966 and Knölker & Schüssler 1988 for the modification caused by the magnetic field to Schwarzschild's criterion for the onset of convection, cf. Chandrasekhar 1952, 1961). Since convection dominates energy transport below the observable layers, a quenching of convection turns a sunspot into an obstacle for the heat flowing outward through the convection zone. This leads to a diversion of energy away from the sunspot, which reduces the energy

flux through the spot and produces a darkening. Almost all of the diverted energy flux is distributed and stored throughout the convection zone and released only over a timescale of 10^5 years, the time-scale of the thermal adjustment of the convection zone, which is much longer than the lifetime of a sunspot (Spruit 1982a, b, Foukal et al. 1983, cf. Spruit 1977, 1991, 2000). In addition to a high thermal conductivity, the convection zone also possesses a large heat capacity, which means that its temperature is raised only by an imperceptible amount by the redistribution of the blocked flux. Consequently, sunspots lead to an instantaneous darkening followed by a semi-permanent, but exceedingly small brightening of the Sun (10^{-10} of the total luminosity for an average sized sunspot). Due to the high lateral thermal conductivity of the gas in the convection zone, most of the diverted heat flux is distributed throughout the convection zone, so that no significant bright ring is expected around a sunspot (Spruit 1977, 1982a, b, Clark 1979, Foukal et al. 1983, Nye et al. 1988 cf. Eschrich & Krause 1977) as had been feared by Parker (1974) on the basis of a simple steady-state model of a shallow sunspot (but note the contrasting results of Fox et al. 1991). The theory is confirmed by observations, since only a small fraction, a few percent, of the total diverted flux does not travel far, but reappears within a few sunspot radii as a weak bright ring (Waldmeier 1939, Miller 1960, Fowler et al. 1983, Rast et al. 1999, 2001).

In the layers below the solar surface convection is much more efficient in transporting energy than radiation. Consequently, a complete quenching of convection would reduce the heat flux so effectively that the question to ask then would not be why umbrae and penumbrae are so dark, but rather why they are still so bright, in particular the penumbrae. Cowling (1953, cf. 1957) first pointed out that the inhibition of convection below sunspots is probably only partial. See Sects. 6.2 and 6.3 for a discussion of attempts to address this problem. Cowling (1953) also provided a nice overview of early theories for explaining sunspot darkness.

Another proposal for explaining the darkness of sunspots is the deviation of the heat-flux vector from the vertical due to the influence of the sunspot's magnetic field on the convection (Hoyle 1949). Hoyle pointed out that it is mainly the motions across the field lines which are suppressed, so that the heat flux is channelled by the field. Its expansion with height leads to a dilution of the thermal flux. This effect has been tested quantitatively by Chitre (1963), Deinzer (1965) and Chitre & Shaviv (1967). All find that this effect on its own does not explain the observed umbral flux, but for contradictory reasons. Whereas Deinzer (1965) concludes that channelling alone is too small to explain the darkness of umbrae, Chitre (1963) and Chitre & Shaviv (1967) find that the umbra turns out to be too dark due to this effect. According to current thinking the latter authors overestimated the magnitude of this effect. It is now thought to enhance the effect of the suppression of convection and is included in recent models, such as that of Jahn & Schmidt (1994).

Finally, Parker (1974, 1975a) proposed that the heat flux is not diverted away from sunspots at all, but rather that umbrae are actively cooled by the conversion of thermal energy into Alfvén waves (cf. Roberts 1976, who discusses overstable Alfvén waves, and the earlier papers by Danielson 1965, Zwaan 1965, Musman 1967 and Savage 1969). This mechanism now seems unlikely, since the expected flux of Alfvén waves is not observed. For example, the non-thermal widths of photospheric and coronal spectral lines above the umbra are too small (Beckers 1976, Beckers & Schneeberger 1977). Also, Cowling

(1976) has argued on theoretical grounds against this mechanism, pointing out that it is extremely difficult to make the excitation of waves so efficient as to carry off 80% of the energy flux. Further counter-arguments are presented by Thomas & Weiss (1992b).

6.2. Umbral brightness

Basically two approaches have been taken to solve the problem of excessively cool umbrae resulting when convection is suppressed completely by the magnetic field (sub-surface radiative energy transport alone cannot explain umbral brightness). The first has been to form the sunspot out of a cluster of small flux tubes that merge just below the continuum-forming layers, as initially proposed by Parker (spaghetti or jelly fish model, see Sect. 4.3). Due to the tapered shape of each small flux tube, increasingly more field-free gas is present between them at increasing depth. Consequently, below the sunspot convection can penetrate relatively unhindered until close to the surface. In addition, for a sunspot composed of n small flux tubes the surface area of the side walls of the flux tubes, over which the convective gas can radiate into the magnetized gas, is $\sqrt{n}$-times larger than for a simple monolithic sunspot. A larger side-wall surface compared to the horizontal cross-sectional area leads to a more efficient heating of the tubes even if the radiation enters the tube below the continuum-forming layer (isolated small-scale tubes can have a bright bottom relative to the quiet sun, e.g. Knölker et al. 1988). This theory, like many other aspects of the cluster model, has not been worked out in detail. Besides making the magnetized gas hotter, subsurface field-free material can also directly lead to a brightening of the sunspot. Such material penetrating to above the solar surface along hot columns that are not resolved by current observations (cf. Parker 1979c, Choudhuri 1986, 1992) could also provide (a part or all of) the missing radiative flux. Even if the individual small flux tubes were to carry no heat flux, then a 20% area coverage by field-free columns would suffice to produce the observed flux (but possibly not the observed spectrum). The columns would have to be very thin and numerous, however, since all parts of an umbra exhibit a minimum brightness. The presence of unresolved field-free intrusions can in principle be observed using polarized line profiles, but as Degenhardt & Lites (1993a, b) have shown, only spectral lines formed very deep in the atmosphere have a chance of detecting them, since the magnetic field expands very rapidly with height to fill the field-free space. One advantage of this model is that it provides an explanation of bright umbral dots embedded in the dark umbral background. They may be considered to be intrusions of field-free material from below the solar surface into the photosphere (Parker 1979c, Choudhuri 1986, 1992). Possibly the observed umbral dots only represent the large-scale end of a distribution of such intrusions having different sizes.

The second proposal incorporates convective transport within a monolithic sunspot. Magnetoconvection is a vast subject in itself, of which the surface is barely scratched here. I refer the reader to reviews devoted specifically to this topic for more details (e.g. Proctor et al. 1982, Hughes & Proctor 1988, Weiss 1991, 1997, 2002, Proctor 1992). Simulations of magnetoconvection are generally restricted to an initially homogeneous magnetic field in an idealized geometry and to simplified physics (e.g., neglecting radiation). Furthermore, such simulations often relate to plasma parameters far removed from those present in real sunspots. The newer ones are nevertheless much more realistic than the

initial linearized, incompressible calculations of Chandrasekhar (1961). From a fully compressible calculation in an externally imposed vertical magnetic field Weiss et al. (1990) confirmed the results of linearized theory that the character of the convection below a sunspot umbra depends strongly on the parameter $\zeta = \eta/\kappa$, where η is the magnetic diffusivity and $\kappa = k/c_p\rho$ is the thermal diffusivity. Here ρ is the gas density, c_p the specific heat, and k the thermal diffusion coefficient. They find that if $\zeta < 1$ then the convection is oscillatory, whereas if $\zeta > 1$ then the convection is overturning. At the solar surface $\zeta \approx 10^{-3} \ll 1$, but increases rapidly with depth, eventually becoming larger than unity (Meyer et al. 1974, Cowling 1976, Weiss et al. 1990). Therefore, the current picture for a monolithic spot is that oscillatory convection dominates in the 2000 km immediately below the surface, while the far more efficient overturning convection takes over in the deeper layers (depths of 2000–20000 km).

The two forms of convection are coupled through non-linear interactions, so that hot convective plumes form which penetrate right up to the upper boundary of the simulation of Weiss et al. (1990). This coupled form of magnetoconvection is more efficient than purely oscillatory convection (an example of which is shown in Fig. 6.1) and conceivably could transport enough energy to explain the brightness of umbrae even in a monolithic sunspot, although further studies are needed to settle this point. In this picture the umbral dots are interpreted as the tops of the convection cells (e.g. Knobloch & Weiss 1984). Blanchflower et al. (1998) find robust signs of flux separation if the field strength is not too large and the aspect ratio of the computational domain is sufficiently big (cf. Tao et al. 1998). This may be a natural way of producing spaghetti below the solar surface, where the plasma β is big. They also propose that the dark nuclei of umbrae result from a form of flux separation, leading to isolated regions with enhanced field strength. Finally, they compare the results of their simulation with light bridges, proposing that these are locations of chaotic oscillatory convection.

Hurlburt & Toomre (1988) considered non-linear compressible magnetoconvection in 2-D with an imposed magnetic field and investigated mainly the influence of changing the Chandrasekhar number, Q, which is proportional to the square of the imposed magnetic field. Most of their simulations are of greater relevance for non-spot magnetic fields, but at larger Q ($\approx 10^3$) they recover oscillatory convection in which the magnetic field remains comparatively homogeneous and basically sways back and forth in response to the oscillation.

This work has been extended to three dimensions by Matthews (1994), Matthews et al. (1995) and Weiss et al. (1996), cf. Rucklidge et al. (2000). In these simulations the density increases exponentially with depth and ζ is set proportional to $1/\rho$, so that ζ can be below unity near the top of the box and above unity at the bottom. The latter authors also considered the influence of varying the magnetic field strength, or Chandrasekhar number Q. At sufficiently large Q convection is completely suppressed. As Q is reduced, first weak, steady convection is excited, with isolated columns of rising gas and a continuous network of sinking fluid. When Q is lowered even further, an oscillatory bifurcation sets in, with alternate plumes waxing and waning in antiphase. At still smaller Q the convection becomes more vigorous and chaotic, with the convective pattern changing rapidly. (A similar behaviour is also produced if the Reynolds number is increased, although in a Boussinesq simulation, Emonet & Cattaneo 2001). The smallest Q values considered by Weiss et al. (1996) may be more appropriate for
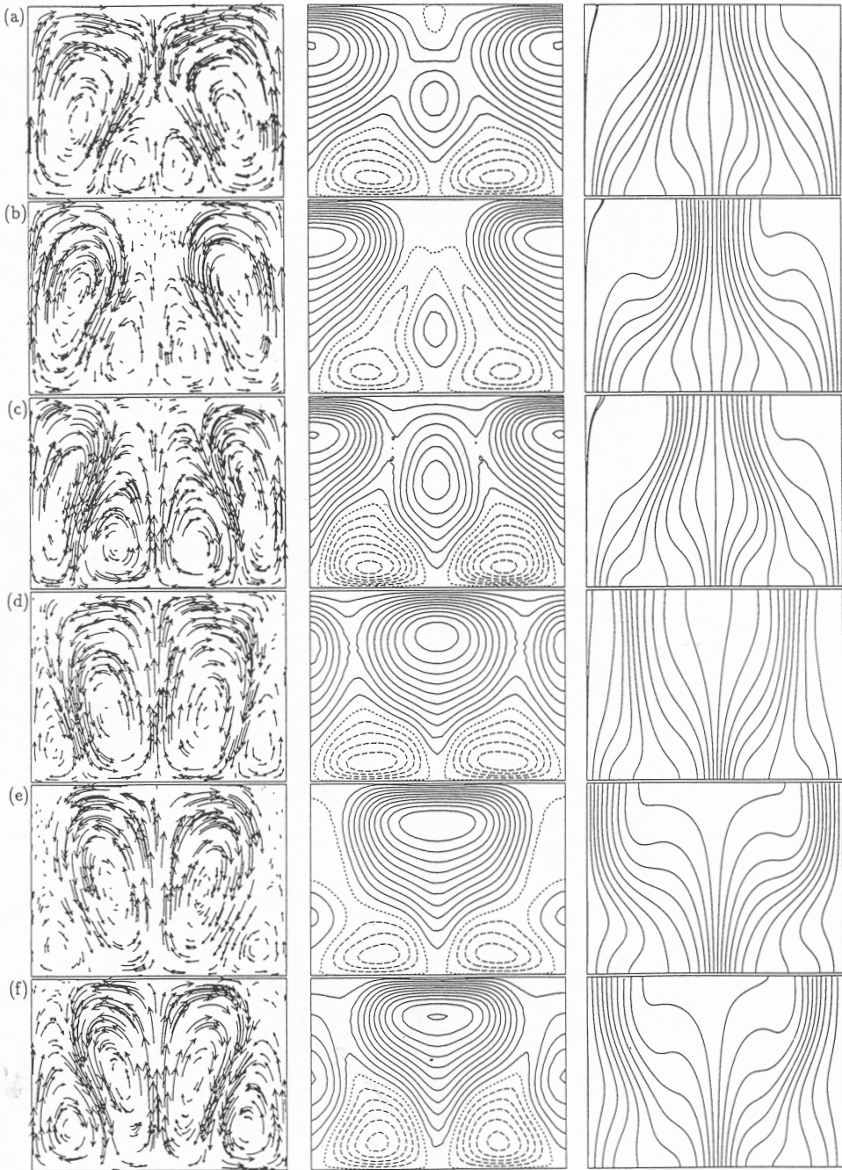
Fig. 6.1a–f. Oscillatory convection produced in a 2-D simulation with $\zeta = 1.2$ and $R = 100000$, where R is the Rayleigh number, a measure of the superadiabatic gradient. Plotted are from left to right streaklines (outlining the flow), contours of the temperature fluctuations ΔT and magnetic field lines. Time runs from top to bottom and the figure covers half an oscillation period (from Weiss et al. 1990, by permission).
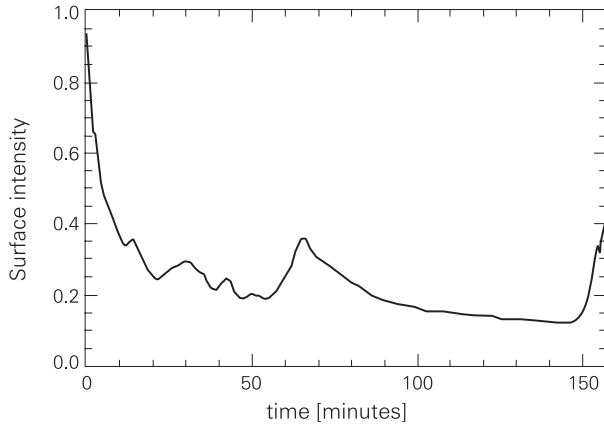
Fig. 6.2. Surface intensity vs. time resulting from 3-D simulations of magnetoconvection under situations appropriate for the umbra (adapted from Nordlund & Stein 1990, by permission).

the situation in solar plages rather than in sunspot umbrae. In all cases the convection introduces an inhomogeneity into the magnetic field. At the top of the box the field becomes concentrated in the downflowing network, while at the bottom there is a strong concentration below the upflowing plumes (see Fig. 6.1).

Nordlund & Stein (1990) carried out a 3-D, fully compressible calculation of a box including the solar surface near its top. They treated radiative transfer consistently. First granular convection is allowed to develop. Then a strong, homogeneous, vertical field is added. The field immediately begins to inhibit the convection and the surface intensity falls rapidly with time, until it becomes as low as 10% of the original granular (i.e. quiet-sun) intensity, as shown in Fig. 6.2. [4] At this point the temperature gradient of the atmosphere becomes so large that a short episode of convection is started, which raises the emergent intensity for a brief period of time. After this the intensity again gradually drops until another convective episode is triggered. The convection in these simulations is overturning. They indicate that episodic convection can produce and maintain the correct umbral temperature in a monolithic model of the umbra, in a time averaged sense. The significant brightening due to the episodes of enhanced convection should be observable, however. They are not seen, suggesting that episodic convection of the form found by Nordlund & Stein (1990) is not the solution chosen by nature for sunspot umbrae.

In most "comprehensive" models of sunspots, i.e., models in which the force balance and energy equations are consistently solved throughout the whole sunspot, the convective transport is treated by applying the mixing length formalism and the radiative transport by the diffusion approximation. The efficiency of the convective energy transport is varied by adapting the mixing length parameter $\lambda = l/H$, where l is the mixing length and H is the pressure scale height (e.g. Chitre 1963, Deinzer 1965, Chitre & Shaviv 1967, Yun 1970, Jahn 1989). Often even this parameterized approach is further

[4] Throughout this review I loosely use intensity instead of the more rigorously correct term 'radiance')

simplified. For example, when combining the similarity assumption of the magnetic field with an energy equation, the thermal structure needs to be determined only along the axis of the symmetric sunspot and outside the sunspot. The horizontal variation of the temperature is fixed by the prescribed magnetic shape function. Hence the 3-D problem of energy transport in a sunspot is first reduced to a 2-D problem in an axially symmetric flux tube and in many cases further reduced to a 1-D problem.

Jahn & Schmidt (1994) simultaneously solved both the force balance and energy equations employing an iterative scheme. The energy equation included radiative energy transport (in the diffusion approximation) and convective transport (in the mixing length approximation). The umbra and penumbra were treated separately, in that each had its own mixing length parameter λ, which was depth dependent. In addition, the volume below the umbra was assumed to be thermally isolated in the horizontal direction, so that the heat flux below the umbra was required to be independent of depth. It turns out that in order to ensure a constant heat flux λ must increase rapidly with depth, being approximately 0.15 near the surface and reaching 0.7–0.8 at greater depths. For comparison $\lambda = 1$ was used to model the quiet sun by the same authors. A larger λ implies more efficient convection, so that the above result says that convection plays an increasingly important role relative to radiation with increasing depth below the umbra. This confirms the local convective stability analysis applied to sunspots by Meyer et al. (1974) and is also consistent with the prediction of Weiss et al. (1990) that ζ goes from $\ll 1$ to > 1 with increasing depth. The small mixing length near the surface also agrees with the fact that the empirically derived temperature stratification at and just below the surface is close to radiative equilibrium (Maltby et al. 1986).

6.3. Penumbral brightness

The situation in the penumbra is rather different from that in the umbra. The thermal flux through the penumbra is almost 4 times larger than in the umbra and around 3/4 that in the quiet sun. Also, the field is far less vertical and less strong in the penumbra, although no significant change in the magnetic field structure (at a scale of a few arc s) is seen at the umbral boundary. In white light the penumbra exhibits a prominent, radially elongated filamentary structure, so that there is a rapid azimuthal variation of brightness. On a larger spatial scale, however, there is a relative absence of a radial or azimuthal temperature gradient. These last two observed properties were explained relatively well by field-aligned horizontal convective rolls (Danielson 1961b). This model can transport energy efficiently to the surface, but requires the magnetic field in the penumbra to be mainly horizontal, a condition that is fulfilled by a thin penumbra. Convective modes in the presence of an imposed homogeneous horizontal field have also been studied with great insight by Moreno Insertis & Spruit (1989) and by Tagore & Murali (1994).

The idea that the penumbra is thin, i.e. that the field lines lie roughly parallel to the solar surface and that the magnetopause is located just below the surface everywhere in the penumbra, is driven by the need to get a sufficient *energy* flux through the penumbra (Schmidt et al. 1986). Observations, however, suggest that over 50% of the *magnetic* flux of the sunspot emerges in the penumbra (e.g., Schmidt 1991, Solanki & Schmidt 1993) and field lines are considerably inclined to the horizontal there (by between 15 and 50°; Keppens & Martínez Pillet 1996), signifying that the penumbra is thick or deep

(i.e., the magnetopause lies many scale heights below the solar surface under most of the penumbra). Danielson's convective rolls therefore are not the solution to the penumbral heating problem. Similarly, the proposal of Schmidt et al. (1986) for thermal transport in a thin penumbra has lost some of its relevance.

The heating of a thick penumbra requires some form of magnetoconvective energy transport. Relevant simulations have been carried out in 2-D by Hurlburt et al. (1996) and Hurlburt & Matthews (1998) in three dimensions (cf. Weiss 1997). They consider magnetoconvection in the presence of an inclined, initially prescribed magnetic field. The main difference to the vertical (or horizontal) field case is that all solutions travel, although the direction or speed of travel depends sensitively on the parameters of the simulation. The main flow at the top of the box is always in the direction of the tilt of the magnetic field, however, and was proposed to represent the Evershed flow. The travelling bright features associated with the convection cells have been tentatively identified with penumbral grains by Hurlburt et al. (1996). Clearly, these simulations have some attractive features and similar simulations under conditions corresponding more closely to those in sunspots are needed.

As in the case of the umbra, convection under the penumbra is often described by the mixing length formalism. Again, the mixing length must be reduced compared to the quiet sun in order to reproduce the observations, but on the whole remains larger than in the umbra. For example, Jahn & Schmidt (1994) find $\lambda \approx 0.7$ below the penumbra. However, the comparison with the umbra is not quite straightforward in their model, since the authors allow radiation to leak in from the quiet sun across the magnetopause, whereas the subsurface volume enclosed by the umbral field lines is thermally insulated. According to their model most of the radiative flux emerging through the penumbra enters into the sunspot through the magnetopause. This feature is driven by the idea that most of the heat flux is transported from the magnetopause to the surface layers of the penumbra by interchange convection, as proposed originally by Spruit (1981b) and Schmidt (1991), cf. Jahn & Schmidt (1994). Interchange convection is an inherently 3-D process in which whole flux tubes rise and fall in the convectively unstable stratification below the penumbra. Each of these flux tubes must be much thinner than the penumbra, of course, and its width is thought to correspond to the scale of observed fluting of the penumbral field. Below the solar surface each such flux tube undergoes little heat exchange with its surroundings, so that it rises basically adiabatically. Hence, the gas trapped between the field lines of a rising flux tube has the (high) heat content of the gas at the magnetopause. On the other hand, the heat content in a falling flux tube is similar to that at the surface.

Rucklidge et al. (1995) followed up on this idea and explained the difference between sunspots and pores by suggesting that significant energy flows across the magnetopause only when it is inclined by more than a critical angle to the vertical. Depending on whether this condition is achieved or not, a sunspot with a relatively bright penumbra (if the energy flows in from the sides) or a pore without a penumbra is formed. One type of feature can switch to another rather abruptly in their model and a hysteresis can occur at the pore-sunspot transition (namely that sunspots exist with smaller flux and area than the largest pores). One observation Rucklidge et al. (1995) tried to explain is that in a plot of the radius vs. magnetic flux, sunspots and pores do not lie on the same curve, due to significant differences in their magnetic structure caused by the absence of a penumbra in

pores. Skumanich (1999) finds that this is true only if the magnetic flux visible also just outside the actual dark pores and sunspots is considered. The flux passing through the dark features falls on a single curve for both pores and sunspots (cf. Leka & Skumanich 1998). Martínez Pillet (1997) has argued that at least pores are surrounded by significant flux associated with them, which does not appear dark. Possibly it is this additional flux which serves to form the penumbra when the pore transforms into a sunspot. As noted by Leka and Skumanich (1998) this transition is rapid and does not happen at the cost of 'umbral' flux.

The simulations of Schlichenmaier et al. (1998a, b) numerically confirm part of the interchange convection scenario. A flux tube lying along the magnetopause does indeed rise to the surface once it is heated sufficiently. It also brings hot gas to the surface, which then radiates away a part of its thermal energy. This model reproduces the presence of inward moving bright penumbral grains (and possibly outward moving bright grains; see Schlichenmaier 2002) and partly also bright and dark filaments. Unless the footpoints of some of the horizontal flux tubes remain in the outer penumbra for a considerable time, according to this model there is more bright material in the inner penumbra (i.e. near the umbra), which is not supported by most observations. Note, however, that Westendorp Plaza et al. (2001a) do deduce a temperature decreasing with distance from the umbra. Also, the exact visibility of bright and dark filaments will need to be treated using proper radiative transfer before it can be quantitatively compared with observations. A first step to improve the computation of the radiative cooling of the gas flowing along a horizontal flux tube has been taken by Schlichenmaier et al. (1999).

In contrast to the interchange convection scenario, however, the simulated flux tube does not sink back down again once it has cooled. This may be due to the simplifying assumptions underlying the simulations. For example, a more realistic treatment of the radiative transfer may lead to a more efficient cooling and allow the flux tube to sink below the surface again (see Schlichenmaier et al. 1999 for first such calculations). Possibly, however, the flux tubes do in reality continue to lie horizontally for a much longer time than required by the interchange convection scenario. Schlichenmaier & Solanki (2003) show that the long lifetimes of magnetic features in the penumbra (see Sect. 3.10) are not compatible with the energy necessary to heat the penumbra coming from interchange convection as originally proposed (unless the energy is transported mainly in thin flux tubes that cannot be resolved by the observations considered by Solanki & Rüedi 2003).

The simulations of Schlichenmaier et al. (1998a, b) do provide an alternative source of energy transport in the penumbra. They reveal that even after a flux tube has emerged and a part of it has been lying horizontally above the surface for some time, hot material keeps flowing up through its footpoint in the inner part of the penumbra and replenishes material that is flowing horizontally outwards along the tube. This horizontal outflow, which exhibits many of the properties of the Evershed flow, is driven by the excess of gas pressure at the inner footpoint, which is partly built up during the rise of the flux tube and is partly due to the higher temperature of the gas at the inner foot point. The material emerging from the solar interior then flows towards the outer boundary of the sunspot, radiating away its excess heat on the way.

The heat flux transported by the Evershed flow turns out to be insufficient, to explain the excess brightness of the penumbra relative to the umbra for the geometry of the flux

tube considered by Schlichenmaier et al. (1998a, b); i.e. a single horizontal flux tube crossing much of the penumbra. The problem is that the material flowing through the cross-section of a less than 200 km wide flux tube must provide the radiative flux along the whole length of the tube, i.e. across the whole width of the penumbra. Schlichemaier & Solanki (2003) show that, under reasonable assumptions, sufficient energy can be provided to the penumbra by a hot upflow only if the horizontal part of the flux tubes is very limited in extent, i.e. flux tubes form short arches in the penumbra. Hence no single horizontal flux tube spans the width of the penumbra.

Of course, the convective heat transport in the penumbra does not need to take the form of the interchange of flux tubes. The idealized simulations of Hurlburt et al. (1996) lead to travelling waves with the direction of their propagation depending to a certain extent on the imposed geometry (see Hurlburt & Rucklidge 2000). Both the strength and inclination of the field is affected by the waves. These waves (oscillatory convection) may in principle transport the energy needed to heat the penumbra. However, they may run into the same problems as other mechanisms if they lead to visible changes of the magnetic structure. Such changes are not observed, however (e.g. Lites et al. 1993, Solanki & Rüedi 2003), although the magnetic field changes may have escaped detection if they are restricted to sufficiently small spatial scales.

In summary, although a number of proposals have been made to transport the energy necessary to maintain the temperature and radiative output of the penumbra, they all face some problems. Long time-series of Stokes-vector measurements at very high and constant spatial resolution will be necessary to finally distinguish between the different proposals.

7. Dynamic structure

7.1. Introduction

A broad variety of phenomena contribute to the dynamics of sunspots as a whole as well as the dynamics present within them. Some examples are listed in Sect. 7.2. Observations of dynamics related to sunspots have been reviewed by, among others, Moore (1981a), Moore & Rabin (1985), Zwaan (1987, 1992), Foukal (1987), Stenflo (1989, 1994), Martin (1990), Schüssler (1990, 1992), Solanki (1990, 1993, 1995, 1997a), Spruit et al. (1992), Lites (1992), Muller (1992), Thomas & Weiss (1992a), Title et al. (1992) and Schmidt (2002), while overviews of aspects of the theory have been provided by Bogdan (1992, 2000), Bogdan et al. (2002), Chitre (1992), Staude et al. (1987), Staude (1999), Thomas (1981, 1985, 1996), Roberts & Ulmschneider (1997), Roberts (1986, 1992). In the following sections I concentrate on the Evershed effect and related phenomena. For a discussion of oscillations within sunspots I refer to the excellent reviews by Lites (1992), Thomas & Weiss (1992a), Staude (1991, 1994, 1999), Bogdan (1994, 1999, 2000) and Bogdan et al. (2002), cf. Chitre (1992). Sects. 7.2 and 7.3 closely follow Solanki (1997a), although they have been heavily updated and extended.

7.2. Overview of dynamic phenomena connected with sunspots

In this section I list the main dynamic phenomena found in sunspots, with a brief description and selected references.

1. *Solar rotation*: Sunspots rotate at a different rate than the non-magnetic plasma (Ternulo et al. 1981, Gilman & Howard 1985, Schröter 1985, Balthasar et al. 1986, Brajsa et al. 2002, Khutsishvili et al. 2002). This difference has, with some theoretical input, been used to gain information on the rotation law at the anchoring depth of the flux tube forming the sunspot. The rotation rate of sunspots decreases with their age (Tuominen 1962, Nesme-Ribes et al. 1993, Pulkkinen & Tuominen 1998, Hiremath 2002) which may mean, e.g., that the anchoring depth changes with time, or that the emerging flux rope forming the active region is asymmetric near its apex and relaxes to a more symmetric shape after emergence.

2. *Meridional motions:* Sunspots can be used to trace large-scale equatorward or poleward flows (e.g. Kambry et al. 1991; Javaraiah 1999), which have been proposed as drivers of solar differential rotation.

3. *Motions of individual sunspots*: Peculiar motions of sunspots, i.e. local deviations from the rotation law, are observed as part of the evolution of active regions (e.g. Leka et al. 1994, Bumba et al. 1996). For example, preceding and following spots move away from each other (Gilman & Howard 1985) and at different speeds from the neutral line (Van Driel & Petrovay 1990). These motions give information on the shape and the dynamics of the large flux tube underlying the spots and emerging through the solar surface in the form of an Ω loop (Petrovay et al. 1990, Moreno Insertis et al. 1994).

4. *"Shearing" motions of sunspots relative to each other, or flux emergence within sunspots*: Such motions and processes can lead to energy build-up in the overlying magnetic arcade and its subsequent release through e.g., magnetic reconnection that becomes visible as a flare (e.g., Hagyard et al. 1984, Kurokawa 1991, Van Driel-Geszetlyi et al. 1994, Wang 1994).

5. *Moat flow*: Small magnetic features, so-called moving magnetic features (MMF), and granules are seen to stream away from a sunspot at speeds up to 1 km s^{-1} (Sheeley 1969, Harvey & Harvey 1973, Brickhouse & LaBonte 1988, Wang & Zirin 1992, Yurchyshyn et al. 2001). See Sects. 7.3.5 and 7.5.

6. *Evershed effect*: An outward directed flow is observed in the photospheric layers of penumbrae and an inward directed flow in the chromospheric layers (see Sect. 7.3). Downflows at some locations at the outer edge of the penumbra and up- and downflows at its inner edge have also been observed (e.g., Westendorp Plaza et al. 1997a, Schlichenmaier & Schmidt 1999).

7. *Proper motion of penumbral grains*: An inward motion at a rate of roughly 0.4 km s^{-1} of bright (penumbral grains) and possibly dark features in the inner penumbra is observed, often accompanied by the outward motion of brighter structures in the outer penumbra (Schröter 1962, Muller 1973, 1976, Tönjes & Wöhl 1982, Kitai 1986, Zirin & Wang 1989, Wang & Zirin 1992, Molowny-Horas 1994, Denker 1998, Lites et al. 1998, Sobotka et al. 1999). To what extent these proper motions of brightness structures are related to the Evershed flow is unclear.

8. *Transition-region downflows*: Strong downflows are detected in transition-region spectral lines, mainly above sunspot umbrae. These downflows, which can reach supersonic speeds, are probably related to the chromospheric inverse Evershed effect (Alissandrakis et al. 1988, Dere et al. 1990, Kjeldseth-Moe et al. 1993, Brynildsen et al. 1998c).

9. *Oscillations*: These are observed both in the umbra and the penumbra, with a 5 min period in photospheric layers and a 3 min period in chromospheric layers and in the transition region, although the shorter period is seen mainly in the umbra (Brynildsen et al. 1999b, Maltby et al. 1999, 2000, see Staude 1999 for a review).

10. *Running penumbral waves*: Time series in the Hα line of the chromospheric layers reveal waves travelling out from the umbra through the penumbra (Giovanelli 1972, 1974, Zirin & Stein 1972, Maltby 1975b, Christopoulou et al. 1999, 2000, 2001, Tsiropoula et al. 2000; cf. Sengottuval & Somasundaram 2001 – note, however, that the observed running penumbral waves hardly follow the surface to the field-free atmosphere as the latter authors assume).

11. *Absorption of p-modes by sunspots*: The energy flux carried by *p*-modes towards a sunspot is considerably larger than the energy flux carried away from the sunspot. This absorption (and scattering of waves) can be used to obtain information on the subsurface structure of sunspots (Braun et al. 1987, 1988, 1992, Bogdan et al. 1993, cf. Bogdan 1992). The likely cause is mode conversion, as proposed by Spruit & Bogdan (1992), cf. Cally et al. (1994), Zhang (1997), Barnes & Cally (2000).

12. *Downflows below sunspots and collar flows*: Helioseismic (tomographic) measurements by Duvall et al. (1996) and Kosovichev (1996) have led to the discovery of a large-scale downflow below (growing) sunspots (but see Bogdan et al. 1998). Such a downflow had been proposed by Parker (1992) on theoretical grounds. Recent inversions suggest a more complex velocity pattern below sunspots, with inflows at depths of 1.5–3 Mm feeding the downflows, which turn into outflows at a depth of 5–9 Mm, so that this flow pattern is reminscent of a collar flow (Zhao et al. 2001, Kosovichev 2002).

13. *Flows in δ-spots*: A supersonic siphon flow has been observed across the neutral line of a δ-spot (Martínez Pillet et al. 1994). In another δ-spot Lites et al. (2002) find converging flows towards the polarity inversion line, which they interpret to follow an interleaved magnetic structure and to flow into the solar interior again.

14. *Flows in umbrae of young sunspots*: (upflow in preceding spot, downflow in following spots). Such flows are interpreted as part of the counter rotating flow along a rising magnetic flux loop and are thought to be driven by the Coriolis force (Sigwarth et al. 1998).

15. *Flows in umbral dots*: A small upward velocity of 30–50 m s^{-1} and 200 m s^{-1} has been reported in umbral dots relative to the umbral background by Rimmele (1997) and Socas Navarro (2002), respectively (cf. Beckers & Schröter 1969b; Kneer 1973), in agreement with predictions by Parker (1979c) and Degenhardt & Lites (1993a, b).

16. *Rotation of sunspots around their axis*: Sunspots observed in white light have been seen to rotate by up to 180°, leading also to a rotation and sometimes an eruption of the coronal loops fanning out from the sunspot (Brown et al. 2002).

17. *Umbral flashes*: Sudden brightenings of the cores of some chromospheric spectral lines, followed by a slower decay to their normal state (Beckers & Tallant 1969, Wittmann 1969, Thomas et al. 1984, Kneer et al. 1984, Alissandrakis et al. 1992, Lites 1992). They have been empirically modelled by Socas-Navarro et al. (2000), who give two scenarios of how the underlying oscillation may produce a flash.

18. *Convection in light bridges*: Photospheric light bridges, i.e. light bridges exhibiting structure reminiscent of granules have been found to harbour significant vertical velocities (Rüedi et al. 1995, Rimmele 1997), whose correlation with the intensity suggests a convective origin (Rimmele 1997).

7.3. The Evershed effect: observations

7.3.1. The Evershed and the inverse Evershed effects

The dominant signature of photospheric dynamics in sunspots is the Evershed effect, named after its discoverer, J. Evershed. It is composed of a blueshift and (usually) a blueward asymmetry (i.e. an enhanced blue wing) of photospheric spectral lines in the discward part of the penumbra and a corresponding redshift and redward asymmetry in the limbward part of the penumbra (e.g. Evershed 1909, St. John 1913, Servajean 1961, Holmes 1961, 1963, Maltby 1964, Schröter 1965a, b; Bhatnagar 1967, Stellmacher & Wiehr 1971, 1980; Lamb 1975, Wiehr et al. 1984, Küveler & Wiehr 1985, Ichimoto 1987, 1988a; Alissandrakis et al. 1988, Dere et al. 1990, Wiehr & Stellmacher 1989, Arena et al. 1990, Adam & Petford 1991, Shine et al. 1994, Rimmele 1994, 1995a, b; Wiehr 1995, 1996, Balthasar et al. 1996, Schlichenmaier & Schmidt 2000, Schmidt & Schlichenmaier 2000, Westendorp Plaza et al. 2001b, Rouppe van der Voort 2002a). The magnitude of the line shift generally increases from the inner edge of the penumbra to its outer edge, as does the line asymmetry. A map of the Evershed effect is shown in Fig. 7.1.
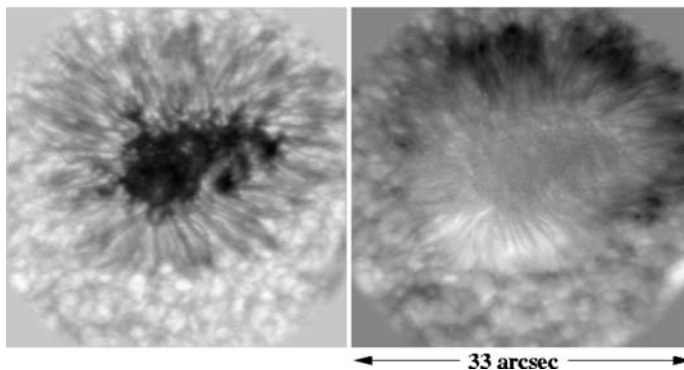
Fig. 7.1. Contrast enhanced continuum image (*left*) and Evershed effect, i.e. Doppler shift map produced in the line wing of Fe I 557.6 nm (*right*) of a regular sunspot. Blueshifts are bright, redshifts dark. The observed sunspot was located at $\mu = 0.9$. Disk centre is located towards the bottom left of the images. (Observations at the German Vaccum Tower Telescope, Tenerife, with the 2D spectrometer TESOS; figure kindly provided by R. Schlichenmaier).

The Evershed effect is height dependent. In the photosphere the line shifts decrease rapidly with height of line formation (e.g. St John 1913, Maltby 1964, Börner & Kneer 1992, Rouppe van der Voort 2002). Above the temperature minimum the line shifts change sign, with the discward part of the penumbra now showing redshifts. This so-called inverse Evershed effect has been observed by, e.g., St. John (1913), Beckers (1962), Haugen (1967, 1969), Maltby (1975), Bones & Maltby (1978), Alissandrakis et al. (1988), Dere et al. (1990), Börner & Kneer (1992), Tsiropoula (2000).

The simplest interpretation of the Evershed effect is an outflow from the umbra in the photosphere with a velocity of a few km s^{-1} (neglecting unresolved fine-structure of the flow) and an inflow with a larger velocity in the chromosphere. Nevertheless, the mass flux producing the inverse Evershed effect is only a few percent of that in the photospheric flow (due to the orders of magnitude lower gas density in the chromosphere).

7.3.2. Inclination to the horizontal

In the photosphere the flow is nearly horizontal in most of the penumbra, with inclination values of $\lesssim 5 - 10°$ (e.g., Maltby 1964, Lamb 1975, Abdussamatov 1980, Dialetis et al. 1985, Alissandrakis et al. 1988, Dere et al. 1990, Adam & Petford 1991, Börner & Kneer 1992, Johannesson 1993, Shine et al. 1994, Schlichenmaier & Schmidt 2000), but see Arena et al. (1990) for more strongly upward inclined flows and, e.g., Rimmele (1995b), Westendorp Plaza et al. (1997), Schlichenmaier & Schmidt (2000), Schmidt & Schlichemaier (2000) for evidence of downflows, particularly in the outer penumbra. These are also found to be relatively horizontal, however. The magnetic field observed at a spatial resolution of a few arc sec, however, is inclined by up to 50° to the horizontal in the penumbra (Kawakami 1983, Lites & Skumanich 1990, Solanki et al. 1992, Hewagama et al. 1993, Lites et al. 1993, etc.). Since the field lines are frozen into the plasma this situation is at first sight unexpected. This problem was recognized by Lamb (1975), Abdussamatov (1980) and Adam & Petford (1991), who reconstructed both the magnetic and velocity vectors of sunspots. The following scenarios to explain both observations simultaneously have been proposed:

1. The gas flows in field-free channels embedded in the otherwise magnetic penumbra. In this manner the flow and the magnetic field would not interfere with each other. The observations show, however, that it is indeed the magnetized gas which is flowing (Solanki et al. 1992, 1994), ruling out this hypothesis.
2. The component of the flow perpendicular to the field-lines drags these along with it (proposed, e.g., by Lamb 1975, Arena et al. 1990, Adam & Petford 1991). Since sunspots do not 'explode', i.e. expand rapidly with time, this scenario appears un-likely. Setting an upper limit of 3″ per day on the expansion of sunspots we obtain an upper limit of 30 m s^{-1} on the cross-field flow component, roughly an order of magnitude smaller than the values deduced by Lamb (1975) and Adam & Petford (1991).
3. The Evershed effect is not caused by a material flow at all, but is rather produced by waves through the temperature-velocity correlation (Maltby & Erikson 1967, Erikson & Maltby 1968, Bünte et al. 1993). An extended analysis shows, however, that the wave hypothesis is inconsistent with the observations (Bünte & Solanki 1995).

4. The penumbral magnetic field is inhomogeneous on a small scale, with a horizontal component parallel to the flow and an inclined component. In this picture the Evershed flow is restricted to the horizontal component, as proposed by, e.g., Abdussamatov (1980) and Title et al. (1993), cf. Degenhardt & Wiehr (1991). High-resolution observations, measurements of broad-band circular polarization, infrared spectropolarimetric observations and inversions of Stokes profiles support a complex magnetic structure of this type (Degenhardt & Wiehr 1991, Schmidt et al. 1992, Title et al. 1993, Solanki & Montavon 1993, Hofmann et al. 1994, Rüedi et al. 1998a, 1999b, Martínez Pillet 2000, Westendorp Plaza et al. 2001a, b; see Sect. 3.9.3). In particular, Westendorp Plaza et al. (2001b) find a strong correlation between Evershed velocity and magnetic inclination, at least for the limb-side penumbra.

Even slight deviations of the velocity vector from the horizontal are important for understanding the nature of the Evershed effect and the basic structure of the sunspot magnetic field. E.g., if the flow is inclined downward near the outer penumbral edge it is suggestive of material and by proxy magnetic field lines returning into the solar interior at the sunspot boundary (since the flow is expected to follow the field lines). The measurement of such small deviations requires care, since small false vertical velocities can easily be introduced by, e.g., errors in the zero-level of the velocity, which is typically uncertain by 200–300 m s^{-1} or more (Shine et al. 1994). The zero level is fixed by assuming that either the quiet Sun or the umbra is at rest, i.e. shows unshifted spectral lines. Its uncertainty is due to the granular blue-shift of spectral lines outside sunspots and due to scattered light from the inner penumbra and the photosphere into the umbra. In the absence of such scattered light the umbra is expected to show no time-averaged shift (Beckers 1977). Thus the uncertain zero-level may (partly) explain the difference between the results of Rimmele (1995b), who finds evidence for a downflow of 400–600 m s^{-1} in the outer penumbra (and an upflow of 200–300 m s^{-1} in the inner penumbra), and Shine et al. (1994), who deduce a small upflow (200–400 m s^{-1}) near the outer penumbral edge. The results of Schlichenmaier & Schmidt (2000) and Schmidt & Schlichenmaier (2000) quantitatively support the conclusions drawn by Rimmele (1995b); they find upflows of 300–500 m s^{-1} in the inner penumbra and downflows of 150–300 m s^{-1} in the outer penumbra. Finally, Johannesson (1993) observes localized $< 0\rlap{.}''4$ upflows in bright penumbral grains. These upflows are in good agreement with the predictions of Schlichenmaier et al. (1998b).

The observations of Rimmele (1995b), are suggestive of a flow along a shallow Ω-loop; those of Schlichenmaier & Schmidt (2000) and Schmidt & Schlichenmaier (2000) indicate multiple such loops over the penumbral radius. Just how tricky it is to accurately determine the vertical component of the velocity is illustrated by the following estimate. This result is based, in the case of Rimmele's analysis, on the assumption that all line-of-sight velocities are vertical, which in turn derives from the location of the sunspot, which was very close to disc centre. As it turns out, the spot was not exactly at disc centre, however. Rimmele reports that the sunspot moved from $\mu = \cos \vartheta = 0.999$ to 0.985 during the two hours over which he observed it. The average μ of his observations, $\langle \mu \rangle \approx 0.992$, corresponds to $\langle \theta \rangle = 7.3°$. Horizontal velocities (v_H, e.g. due to the Evershed flow) can thus contribute to the line-of-sight velocity, v_{LOS}, although reduced by a factor $\sin \langle \theta \rangle \approx 0.13$. For a typical $v_H \approx 2$–3 km s^{-1} this gives $v_{LOS} = 300$–400 m s^{-1}, which is of the magnitude corresponding to his observations. Note that the blue-

and red-shifts do not form complete, symmetric rings around the otherwise symmetric sunspot, but rather appear to be concentrated on opposite sides of the spot, as expected for the normal, horizontal Evershed effect. However, this does not rule out that a part of the redshift he finds is indeed due to downflows, under the condition that the angle of the flow to the horizontal is small (cf. discussion of the results of Westendorp Plaza et al. 2001b, below).

Rimmele's observations do, however, provide a robust result that is independent of the exact location of the sunspot. The blue-shift is located closer to the umbra than the red-shift. Consequently, the flow appears to follow a convex path (as seen from Earth), with the exact angles to the solar surface suffering from some uncertainty, however. At first sight the larger magnitude of the redshift (than the blueshift) suggests that the flow does indeed curve downwards at the outer penumbral edge. The conflicting observations of Shine et al. (1994) and the earlier conclusion reached by Ichimoto (1987, 1988a) and Rimmele (1995a) that the Evershed flow is concentrated into elevated filaments near the outer penumbral edge speak against a downflow at the outer penumbral edge, unless it occurs in layers which these investigations did not sample. That the latter interpretation is probably (also) correct follows from the fact that using lines formed in the deep photosphere Schlichenmaier & Schmidt (2000) and Schmidt & Schlichenmaier (2000) qualitatively reproduced the results of Rimmele (1959b). Similarly, Rouppe van der Voort (2002a) argues on the basis of observations of a group of spectral lines that the flow is concentrated at heights below roughly 200 km. The conclusion of Schlichenmaier & Collados (2002) that the number of flux tubes carrying upflows decreases when going from the inner to the outer penumbra is consistent with this 'convexity' of the Evershed flow and may well be the underlying cause for the observational signal seen by Rimmele (1995b).

Even the convexity of the Evershed flow-lines is not unchallenged. For example, Stellmacher & Wiehr (1971) claim that the velocity-neutral line in a sunspot lies on the discward side of the umbra. This appears to be supported by the majority of the observations of Pevtsov (1992). If this result is correct then it implies that at least in the inner penumbra the flow lines are concave (which would be consistent with the fallen flux-tube model of Wentzel 1992). Note, however, that these measurements depend critically on the rather uncertain velocity zero-level (cf., e.g., Arena et al. 1990), and need to be redone with particular care regarding this parameter.

A resolution of the inconsistency between the different measurements may partly rest in the inhomogeneous, localized and complex nature of such flows. Thus Westendorp Plaza et al. (1997a, 2001b) found substantial downflows at the outer edge of the penumbra from the inversion of Stokes profiles (LOS velocities >3 km s^{-1}) while Del Toro Iniesta et al. (2001) infer downflows at or above the sound speed in the deepest photospheric layer of the central penumbra (they consider only 2 spatial locations). However, the downflows found by Westendorp Plaza et al. (1997a) are restricted to certain locations along the penumbral edge (and sometimes to points outside the penumbra) and to the deepest atmospheric layers sampled by these observations. At the same time Westendorp Plaza et al. (1997a, 2001b) also found evidence for an outflow in mid photospheric layers, which is not associated with a downflow. Thus their results reproduce the features of the observations of both, e.g., Rimmele (1995b) and Ichimoto (1987, 1988a). The reality of the downflow in the lower layers of the photosphere has been confirmed by

Schlichenmaier & Schmidt (1999), with the help of the C I 5380 Å line, which is among the lines formed deepest in the visible solar spectrum (Stürenburg & Holweger 1990) and by recent 1.56 μm observations (Mathew et al. 2003). In addition, Schlichenmaier & Schmidt (1999) also found isolated upflows near the inner penumbral edge correlated with bright features. The most surprising result of their work is, however, the discovery of isolated cool downflows near the *inner* edge of the penumbra. How these relate to the rest of the Evershed observations, or fit into a model of the Evershed effect is unclear. The combination of strong downflow velocities and the high density at the formation height of C I 5380 Å implies a large downflowing mass flux, much larger than that transported by the inverse Evershed flow, hence ruling out these downflows as the footpoints of the inverse Evershed effect. To what extent effects like instrumental cross-talk from Stokes *V* to *I* can influence their results remains to be studied (A. Gandorfer, private communication). Assuming that the flow locally follows the field lines, Westendorp Plaza et al. (2001b) find an upflow near the inner edge of the penumbra in addition to the downflow near the outer edge, both restricted to the lower photosphere. Significantly, the upflow is seen mainly in the centre-side penumbra, the downflow in the limb-side penumbra, suggesting that the field-lines carrying these flows are inclined by not much more than 16° to the horizontal (corresponding to μ=0.963). The upflowing and downflowing mass balances each other according to these authors. This is in agreement with the findings of Solanki et al. (1994, 1999) that less than half of the mass flowing horizontally in the penumbra continues out into the canopy.

The most commonly used method to determine all three Evershed velocity components, radial, vertical and azimuthal, is to measure Doppler shifts over a complete regular sunspot and to assume that the velocity structure is axially symmetric (Haugen 1969). Unfortunately, any departure from axial symmetry in the true velocity induces errors in the deduced velocity structure. Thus the (normally small) vertical and azimuthal velocities derived in this manner in the photospheric layers of sunspots (Lamb 1975, Adam & Petford 1991) need to be treated with at least a modicum of caution, although the larger radial velocities are probably relatively reliable. Chromospheric vertical velocities obtained with this technique (by, e.g., Alissandrakis et al. 1988, Dere et al. 1990), being considerably larger, might also have a larger relative accuracy than their photospheric counterparts. By applying a variant of this technique to both the LOS velocity and magnetic fields Klvaňa et al. (1998) deduced that in the photosphere the velocity vector is much more horizontal than the magnetic vector. An alternative approach has been proposed by Krivtsov et al. (1998). They reconstruct the velocity by assuming that it is mainly horizontal and that the horizontal component follows the horizontal projection of the magnetic field-line direction, while the vertical component is derived from mass conservation. Using this approach they find upflows in the inner penumbra and downflows in the outer penumbra, which is not surprising, in view of the fact that in Stokes *I* the flow is seen to begin and end within the penumbra. Their approach does have the advantage of providing an estimate of the full velocity vector without having to assume any symmetry in the sunspot shape. Tsiropoula (2000) deduced a convex flow structure for the inverse Evershed flow based on preassumed angles.

In conclusion, the balance of the evidence is in favour of convex flow- and field-lines, but it is unclear which fraction of the mass of the flowing material returns into the

Sun within the penumbra or at the outer sunspot boundary and which fraction continues moving in the superpenumbral canopy.

7.3.3. Horizontal structuring and vertical gradient of the Evershed effect

If the Evershed effect is indeed restricted to filaments with horizontal field, then, just like the magnetic field, it must be highly structured on a small scale. A number of authors (e.g. Schröter 1965b, Beckers 1968, Beckers & Schröter 1969, Harvey 1971, Stellmacher & Wiehr 1971, 1980, Moore 1981a, Wiehr et al. 1984, Title et al. 1993, Shine et al. 1994, Wiehr 1995, Rimmele 1995a, Westendorp Plaza et al. 2001a, b, Rouppe van der Voort 2002a) find a correlation of the Evershed effect with the dark penumbral filaments, or argue for such a correlation based on indirect observational evidence.

On the other hand, some authors have not found any significant spatial correlation between flow velocity and brightness (e.g., Wiehr & Stellmacher 1989, Lites et al. 1990 and to a certain extent Hirzberger & Kneer 2001). Observations which may reconcile the contradictory results have been presented by Degenhardt & Wiehr (1994), Wiehr & Degenhardt (1994) and Rimmele (1995a). They find a good anticorrelation between velocity and brightness as long as they compare these quantities in similar levels of the atmosphere. The correlation disappears if two sufficiently different levels are compared. For example, the velocity measured in the cores of stronger lines does not correlate well with continuum intensity, but does with the brightness spatial fluctuations seen in the line core. This result is in agreement with measurements which show that line core intensity also correlates poorly with continuum intensity (Wiehr & Stellmacher 1989). Partly, this loss of correlation is due to the fact that the size of both brightness and velocity structures in the penumbra increases with height (Degenhardt & Wiehr 1994). An alternative or complementary explanation for the contradictory results obtained by different groups has been suggested by Wiehr & Degenhardt (1992; 1994). They maintain that a good correlation of the Evershed effect with continuum intensity minima is only achieved if the spatial resolution is better than $0\overset{''}{.}5$. Finally, Schmidt & Schlichenmaier (2000), besides finding a slightly larger flow velocity in dark features of the outer penumbra compared with the bright ones, argue that the flow tends to be directed upwards in bright features relative to the flow direction in the dark filaments, throughout the penumbra.

Further support for a concentration of the Evershed flow in cool and hence dark channels comes from spectropolarimetry of the Ti I lines at 2.2 μm. These lines, which are much stronger in cool features, reveal a strong (4 km s^{-1}) outflow even at a spatial resolution of only 2–3$''$ (Rüedi et al. 1998a, 1999b). This value is compatible with the slower speeds obtained from observations in the visible only if the flow is concentrated in the cool channels preferentially sampled by the Ti I lines.

Additional evidence for the inhomogeneity of the flow is provided by profiles of strong spectral lines exhibiting a kink or in extreme cases a well developed second line component (Bumba 1960, Holmes 1961, Schröter 1965a, Wiehr 1995), which is usually interpreted in terms of two spatially separated velocity components producing a complex line profile (e.g., Stellmacher & Wiehr 1971). Such complex line profiles are extreme cases of asymmetric profiles.

The line asymmetry is another diagnostic having a bearing on the spatial inhomogeneity of the Evershed effect. In principle it is possible to explain such an asymmetry

with either a vertical velocity gradient, or a horizontal distribution of velocities. There is evidence for both types of velocity structuring. The directly observed vertical velocity gradient (from core shifts of lines formed at different heights) appears to be too small to account for all the asymmetry observed in stronger lines formed over a broad range of heights (e.g., Stellmacher & Wiehr 1971, 1980, cf. Balthasar et al. 1997), and certainly cannot reproduce observed spectral lines showing two distinct velocity components (e.g., Wiehr 1995). Nevertheless, a number of authors have argued that the vertical gradient of the velocity is the main source of the asymmetry (Servajean 1961, Brekke & Maltby 1963, Maltby 1964, Makita & Kawakami 1986, Ichimoto 1987, 1988a, b).

Based on the automated least-squares fitting (or inversion) of line profiles, Del Toro Iniesta et al. (1994) derive horizontal fluctuations and vertical gradients of the Evershed velocity along different slices through a sunspot penumbra, and find that both the velocity and its large vertical gradient fluctuate along a slice. Their result favours the role of the vertical gradient in producing the line asymmetry. It is, however, based on the inversion of a single spectral line, so that they probably cannot properly distinguish between vertical gradients and sub-resolution horizontal fluctuations. The inversion approach has been applied to more suitable data, allowing for a more flexible model, by Westendorp Plaza et al. (2001b). They obtain a very strong vertical gradient of the velocity in the penumbra, with peaks of 2.5–3 km s^{-1} at $\log \tau_c = 0$, which drops to below 0.5 km s^{-1} at $\log \tau_c = -1.5$ when considering azimuthal averages over sectors of $120°$.

Undoubted is the importance of a vertical velocity gradient for the production of the broad-band circular polarization observed in penumbrae (Illing et al. 1975, Sánchez Almeida & Lites 1992, Solanki & Montavon 1993, Sánchez Almeida et al. 1996, Sánchez Almeida 1998, Martínez Pillet 2000). The sense of the velocity gradient is not determined by these observations, however. Only the relative sign of the gradient of the LOS velocity and the magnetic vector enters into the production of net circular polarization over a spectral line. In particular, a model such as that proposed by Solanki & Montavon (1993) and slightly modified by Martínez Pillet (2000), with a horizontal flux tube embedded in an inclined field, reproduces these and numerous other observations even if the net change in magnetic inclination and velocity with height is small or even zero. However, as first noticed by Solanki & Montavon (1993) and stressed by Martínez Pillet (2000), the observations are only reproduced if a flow is present along both horizontal flux tubes and the inclined field. Slightly different magnetic and flow geometries may overcome this shortcoming (Müller et al. 2002). These authors and Schlichenmaier et al. (2002) furthermore show that the uncombed field model also reproduces the non-symmetric net-circular-polarization distribution obtained in maps of sunspots.

The importance of the model geometry has been demonstrated by Degenhardt (1993). He showed that the observed line shifts *and* asymmetries can be reproduced, contrary to conventional wisdom, by a velocity that *increases* with height, if the filling factor of the flowing material decreases rapidly with height (since the line shifts reflect the product of velocity and its filling factor).

7.3.4. The upper atmosphere

The inverse Evershed effect observed in the chromosphere has a significant vertical component. According to the reconstructions of Dialetis et al. (1985), Alissandrakis et

al. (1988) and Dere et al. (1990) the flow is almost horizontal in the superpenumbra, but becomes increasingly vertical towards the umbra. At disc centre downflows – called 'coronal rain' – can be seen in Hα above umbrae. EUV spectra have allowed such downflows to be followed into the hotter transition zone (e.g. Foukal 1976, 1978; Bruner et al. 1976, Brueckner et al. 1978, Nicolas et al 1982). Abdussamatov (1971b) and Lites (1980), however, see no such downflows, and Neupert et al. (1992, 1994) actually see an upflow in the coronal Mg IX 368 Å line, but not in the also recorded lines of Ne II, Fe XV and Fe XVI. Finally, Kjeldseth-Moe et al. (1988), Brynildsen et al. (1999a, 2001a) find both down- and upflows within a sunspot.

According to Nicolas et al. (1982) sub- and supersonic downflows can be present within the same umbra. Brynildsen et al. (1999a, 2001a) observe elongated downflow channels extending to outside the spot, reminiscent of flows along inclined flux tubes. The observed velocity structure changes with temperature. At relatively low temperatures (6000 – 10 000 K, probed by EUV lines of neutral atoms) only subsonic velocities are seen. With increasing temperature the maximum of these subsonic downflow velocities increases, from less than 5 km s^{-1} observed in O I 1355.50 Å to approximately 40 km s^{-1} in O V 1371.29 Å (log τ = 5.4). The spatial distribution of the flows also changes strongly with temperature (Brynildsen et al. 1999a). For example, the flow patterns visible in O III and O V correlate with each other only marginally (note, however, that the correlation coefficient of 0.4 is artificially reduced by noise in the data). However, the difference is even larger to the corona, with O V and Mg IX correlating at a level of less than 0.1 (Brynildsen et al. 1999a; cf. Brynildsen et al. 1998c). Obviously the transition region flows are not fed by the coronal gas above the sunspot. At even higher, truly coronal temperatures, probed by spectral lines like Fe XII 1349.40 Å, no downflow greater than approximately 10 km s^{-1} is observed.

In general, brighter areas within a sunspot transition region tend to be associated with downflows. Within sunspot plumes, parts of the sunspot transition region that are nearly an order of magnitude brighter than the active region on average (see Sect. 5.6), the gas almost exclusively flows downward. The downflow speed of this gas also increases with temperature, reaching a peak of 15–40 km s^{-1} at log τ = 5.5 K, before dropping to below 10 km s^{-1} at log τ = 6 K (Brynildsen et al. 1998c, 1999a, 2001a). The flow within the plumes remains practically unchanged for hours.

Brynildsen et al. (2001a) find evidence for a horizontal inflow of gas at transition region temperatures to feed the downflow in sunspot plumes, but no significant upflows to feed these horizontal flows. These may either lie far from the sunspot, or may be in the form of cooler gas and thus not be visible in transition-region line radiation. At high spatial resolution, separate line components with shifts corresponding to supersonic velocities often become visible above umbrae over the whole transition region temperature range (Kjeldseth-Moe et al. 1988, 1993). This is in addition to the subsonic downflows. These supersonic flows are extremely small-scale and there is evidence for multiple velocity components within a single pixel as small as $1'' \times 1''$ (Brynildsen et al. 2001b). From a careful analysis of HRTS data and simple physical arguments Laming (1994) even concludes that the umbral downflow is fragmented at a scale of less than 50 km. The inverse Evershed effect at transition-region temperatures is hence highly inhomogeneous and possibly strongly filamented, in agreement with photospheric (Sect. 7.3.3) and chromospheric observations (Maltby 1975). From Hα Dopplergrams, Maltby finds that

the chromospheric inflow is concentrated into channels with apparent average widths and lengths of $1\overset{''}{.}6$ and $14''$, respectively, but with a very large scatter in these values. He argues for a loop-like structure of these channels, with the outer, upflowing part lying in the superpenumbra, well outside the penumbra. There is also strong evidence for a vertical structuring (or more precisely, structuring along the field lines). Based on the fact that the slow component takes part in the normal umbral oscillations while the rapidly flowing component does not, Brynildsen et al. (2001b) propose that the fast and slow components occupy different heights along the line-of-sight, with the slower component occurring deeper. Also, the absence of supersonic flows at chromospheric temperatures implies the presence of shocks at higher temperatures, or greater heights. Note, however, that the chromospheric inverse Evershed effect (i.e. not just the downflow) may exhibit almost sonic velocities just outside the photospheric sunspot (Beckers 1962), implying that the total velocity in these layers is largest at this location.

The velocity of the inverse Evershed flow can possess a significant azimuthal component, which increases with distance from the sunspot (e.g., Maltby 1975a, Dere et al. 1990). Such a twist is also seen in the superpenumbral Hα fibrils themselves (e.g., Hale 1908a, 1930, Richardson 1941, Dere et al. 1990) and sometimes in extrapolations of photospheric magnetic fields into the chromosphere (e.g., Schmieder et al. 1989). It has recently been explained in terms of cyclonic motions in the presence of a magnetic field (Peter 1996, cf. Sect. 4.6).

7.3.5. The Evershed effect outside the penumbra, the moat flow and moving magnetic features

There has been considerable controversy about the presence or not of the photospheric Evershed effect beyond the outer boundary of the penumbra. Some investigators have presented convincing observations that the Evershed effect ends abruptly at the sunspot boundary (Brekke & Maltby 1963, Wiehr et al. 1986, Wiehr & Balthasar 1989, Wiehr & Degenhardt 1992, Title et al. 1992, 1993; Wiehr 1996, Hirzberger & Kneer 2001, cf. Fig. 5 of Johannesson 1993), while others have argued equally convincingly that it continues well beyond the visible boundary of the sunspot (Sheeley 1972, Küveler & Wiehr 1985, Dialetis et al. 1985, Alissandrakis et al. 1988, Dere et al. 1990, Börner & Kneer 1992, Rimmele 1994, 1995b). Solanki et al. (1994) reconciled both schools by showing that although the Evershed effect does continue outside the sunspot boundary, it does so only above the base of the magnetic canopy (i.e. in the upper half of the photosphere). The results of previous attempts to observe the photospheric Evershed effect outside the visible sunspot thus depend strongly on the type of spectral line employed to measure it and the exact technique used to determine the line shift and/or asymmetry.

Wiehr (1996) argues, however, against a continuation of the Evershed effect, even above the canopy base, on the grounds of the disappearance of the Stokes I shift of lines of different strength just outside the penumbral boundary. Now, Stokes I profiles may have quite different formation heights in the presence of magnetic canopies than in the quiet sun (due to the gas pressure reduction caused by the field). This and other problems makes such observations less than ideal for the detection of flows in the canopy. Needed are new Stokes V, Q and U observations, as well as radiative transfer calculations to

study the influence of the change in the atmosphere at the transition from the penumbra to the quiet sun on the line profiles.

Even if the flow continues into the superpenumbral canopy the mass flux there is smaller than in the penumbra, as was first pointed out by Solanki et al. (1994). The most recent estimate suggests that at the most 50% of the material flowing through the penumbra continues into the canopy (Solanki et al. 1999). The remainder probably returns to the solar interior at the sunspot's outer boundary, in the downflows seen there by various observers (Sect. 7.3.2).

Sunspots are often surrounded by a moat or moat cell, an annular zone with an outflow of 0.5–1 km s^{-1} surrounding the periphery of a sunspot. This is roughly twice the outflow speed in supergranules and shows no systematic variation with any sunspot property. Moats are typically 10–20 Mm wide, i.e. the size of a typical supergranule when they surround small sunspots. For larger sunspots the moat radius is roughly twice the sunspot radius (Brickhouse & LaBonte 1988). Moat cells possess many similarities with supergranule cells, but live longer (they often exhibit little change for several days). Indeed, it takes around a day for a moat to develop (Pardon et al. 1979). They have been studied by Sheeley (1969, 1972), Harvey & Harvey (1973), Vrabec (1974), November et al. (1986), Brickhouse & La Bonte (1988), Molowny-Horas (1994), Balthasar et al. (1996) and Rimmele (1997). In addition to these observations based either on the tracking of brightness features (granules) or on Doppler shifts, helioseismic measurements have also been providing evidence. Thus Lindsey et al. (1996) and Sun et al. (1997) obtained an outflow whose velocity first increases and then decreases with increasing depth. The averaged absolute values are small compared with the measurements at the surface, being 40–80 m s^{-1} according to Sun et al. (1987). Recently Gizon et al. (2000) have employed the f-mode, which samples roughly the top 2 Mm of the convection zone to probe sunspots and their surroundings. They find an outflow extending well beyond the sunspot boundary (up to 30 Mm) which reaches a peak of 1 km s^{-1} just outside the penumbra. This flow is consistent with the moat flow, but its speed is smaller than the Evershed flow in the penumbra, suggesting that the Evershed effect is shallow compared with the depth of 2000 km sampled by the f-mode (see Duvall & Gizon 2000 for more details on the method).

Moats are free of stationary magnetic fields, except the sunspot canopy and may also exist around large pores. They harbour the moving magnetic features (MMFs), so called because they traverse the moat starting at the sunspot and move outwards parallel to the $H\alpha$ fibrils at speeds up to 2 km s^{-1} (Sheeley 1969, Harvey & Harvey 1973, Ryutova et al. 1998). MMFs tend to come in pairs of mixed polarity and appear to carry net flux away from the sunspot at approximately the rate at which it decays (10^{19} Mx/h, while the total flux carried by the MMFs amounts to ($|\phi_+| + |\phi_-|) \approx 3 \times 10^{19} - 10^{20}$ Mx/h). The MMFs are first seen right at the edge of a sunspot. For MMFs clearly identified as bipolar, the opposite polarity with respect to the sunspot is closer to it (Yurchyshyn et al. 2001, Zhang et al. 2002) in contrast to the earlier results of Lee (1992) based on fewer examples. Interestingly, bipolar MMFs are not visible in the upper chromospheric layers (Penn & Kuhn 1995) although the photospheric MMFs are also visible in radiation sampling the lower chromosphere (Harvey & Harvey 1973). A summary of the properties of MMFs has been given by Shine & Title (2001), who also distinguish between 3 types of MMFs, with type I MMFs being bipolar, type II MMFs being slowly moving single

polarity features and type III MMFs being unipolar features moving rapidly from the sunspot (and having opposite polarity to the sunspot).

7.3.6. The Evershed effect as a non-stationary phenomenon

Recent observations have provided evidence that the Evershed flow is not entirely stationary. Time series of Dopplergrams recorded by Shine et al. (1994) show an average outward directed velocity of 3–4 km s^{-1} which, however, exhibits peak-to-peak modulations of 1 km s^{-1}. This modulation has an irregular, but repetitive behaviour, with a typical interval between peaks of roughly 10 minutes. Rimmele (1994) also finds the Evershed effect to be composed of velocity packets that repeat irregularly on a time scale of 15 minutes and that propagate with speeds of 2–5.5 km s^{-1}. Earlier evidence for a time-dependent outflow in penumbrae had been found by Schröter (1967), who studied the outward motion of bright structures (which may or may not be associated with the Evershed effect, see Sect. 5.3.2), and Maltby (1975), who analyzed the inverse Evershed effect observed in Hα and deduced that the flow channels have a half-life of roughly 5 minutes. The most direct and convincing evidence for a significant time dependence of the Evershed effect has been presented by Rouppe van der Voort (2002b) on the basis of high resolution spectra.

   There is to my knowledge no evidence that the Evershed effect evolves in the course of the evolution of a sunspot. Leka & Skumanich (1998) observed the development of a pore into a sunspot, in particular the formation of a penumbra. They find that the penumbra not only forms rapidly as compared to the flux increase of the whole pore/spot, but that it also exhibits the Evershed effect right from the beginning (i.e. within the 10–15 min interval between two scans in their data). This observation confirms the belief that the Evershed effect is a fundamental property of the penumbra, which is present all the time that a penumbra is present.

7.4. Theory of the Evershed effect

Line shifts can be produced either by net mass flows or by oscillatory mass motions, such as waves. Currently theories are favoured that consider the observed line shifts to be produced by more or less steady motions. For the sake of completeness, however, wave models are also briefly discussed in the following.

7.4.1. Siphon flow models

The first serious contender for a physical driving mechanism was the siphon effect (Meyer & Schmidt 1968). These authors considered a flux tube forming a loop whose footpoints (i.e. intersections with the solar surface) have different field strengths. If the field strength $B_1(z = 0)$ of footpoint 1 at a fiducial height $z = 0$ is less than the field strength of the other footpoint, i.e. $B_1(z = 0) < B_2(z = 0)$, then the second footpoint also possesses an excess magnetic pressure. Due to horizontal pressure balance $p_1(z = 0) > p_2(z = 0)$ must be satisfied. In this situation, once a flow is started along the loop it will be sustained by the imbalance in the gas pressure. Meyer & Schmidt (1968) proposed that the first footpoint is located within the penumbra, with the second being in the umbra of another

spot, or in a concentration of field outside the sunspot. They also discussed the physics of the flow, including the transition from a subsonic to a supersonic flow at the apex of the tube and its deceleration by a shock near the downflow footpoint. Finally, they pointed out that their model could easily explain an inverse Evershed flow if the field lines carrying it ended in the umbra. Since such field lines are expected to lie higher than those emerging in the outer penumbra, the reversed flow is expected to be seen in spectral lines formed higher than those exhibiting the outward flow.

Spruit (1981b) updated the qualitative results of this model in the light of improved measurements of the field strength in and outside sunspots. Thus, the field strength in the outer penumbra (700–1200 G) is lower then that in magnetic elements (1500–1700 G at around the same height). A loop connecting these two regions would thus fulfil the requirements of the siphon flow model. A loop starting in the inner penumbra ($B_1 \approx 1800$–$2200\,\mathrm{G}$), on the other hand, would then transport a flow with reversed sign, consistent with the inverse Evershed effect. The proposal of Meyer & Schmidt (1968), made well before the uniformly high intrinsic field strengths of magnetic elements had been established, turns out to be valid also in the light of these observations. Note that field lines ending in the umbra should also harbour the inverse Evershed effect, but since these field lines are rather vertical (inclinations to vertical $\lesssim 40°$) the flow along them should be visible mainly as a downflow in transition-region or chromospheric lines. Thus the downflows observed in EUV lines above the umbra may be manifestations of such siphon flows. The large difference in velocity between chromospheric subsonic velocities and transition region supersonic velocities (see Sect. 7.3.4) is suggestive of the shock deceleration of supersonic downflows proposed by Meyer & Schmidt (1968). The detection of only low velocities in coronal lines can be reconciled with this model if the flowing gas never heats up beyond transition region temperatures, either due to cooling (e.g. through approximately adiabatic expansion) or because it flows too fast to be heated sufficiently, since it may not allow the usual heating mechanisms enough time to act.

One shortcoming of the calculations of Meyer & Schmidt (1968) is that they did not consider the effect of the flow on the shape of the flux tube, i.e. they only dealt with rigid tubes. In reality, however, the flux tube supporting the Evershed flow is influenced by the supersonic gas flow and the external magnetic field it is embedded in. Siphon flows along isolated tubes at increasing levels of sophistication were studied in a series of papers by Thomas (1988), Montesinos & Thomas (1997, 1993) and Thomas & Montesinos (1990, 1991), as well as by Degenhardt (1989, 1991). In the most advanced of these models both the flow and the equilibrium structure of the tube are treated self-consistently, the shocks are treated through jump conditions (derived earlier by Herbold et al. 1985 and Ferriz Mas & Moreno Insertis 1987) and radiative exchange with the surroundings is taken into account in an approximate manner.

Siphon flow models have no particular problem explaining that the Evershed effect starts along with the formation of the penumbra (Leka & Skumanich 1998), since it does not necessarily need much time to build up the pressure differences between different parts of the penumbra. However, siphon flows in isolated flux tubes face the problem that the loops produced by the models are short compared to the typical width of the penumbra, in particular when the loop-tops are required to remain in the photosphere. This problem can be alleviated to a certain extent either by embedding the loop in an

ambient field (Thomas & Montesinos 1993) or by lowering its field strength to a few hundred Gauss in the upflow footpoint (Degenhardt 1991). Even in these cases the longest tubes constructed by these researchers are roughly 3000 km long, which is considerably less than the width of a large penumbra. It is also possible that the Evershed flow simply takes place along short loops, but that many such loops, lying at different radial distances in the penumbra, are present. Thus field lines and gas emerge and submerge again at practically all radial distances in the penumbra. Evidence for such submergence has been found by del Toro Iniesta et al. (2001).

Another problem was created for the siphon flow mechanism by the discovery of downflows near the outer edge of the penumbra (e.g., Westendorp Plaza et al. 1997a, Schlichenmaier & Schmidt 2000, Schmidt & Schlichenmaier 2000) along which the majority of the flowing material must return to the solar interior. These observations imply that both footpoints of the loop supporting the siphon flow lie within the penumbra. Now, the field strength decreases by over 1000 G between the inner and outer edges of the penumbra, so that one would expect the flow to be directed towards the umbra from pressure balance arguments. Montesinos & Thomas (1997) have argued that differences in height at which the field is measured inside and outside the penumbra (or possibly in the inner and outer parts of the penumbra) can make the observed field strength in the downflow footpoint appear lower, although at equal geometrical height the relative field strengths are ordered exactly the other way round. However, the effect was demonstrated only for a background field that is horizontally constant, whereas all reasonable MHD descriptions of a sunspot field require its strength to decrease when moving radially outwards at a fixed height (see Sects. 3.2.1 and 4).

One possibility of getting round this problem within the constraints of the thin-tube approximation is through a localized enhancement in the magnetic field at the down-flowing footpoint of the magnetic arch. Montesino & Thomas have argued that the field strength there is enhanced by the downflow itself through the convective collapse mechanism known to act in isolated magnetic elements (Parker 1978, Spruit 1979, Solanki et al. 1996b, Grossmann-Doerth et al. 1998). The discovery of downflows in isolated magnetic features close to the sunspot by Börner & Kneer (1992), which indicates that at least a part of the Evershed flow returns to the solar interior just outside the penumbra, could lend support to this interpretation.

The field lines returning within the penumbra could also support a downflow, even if B there is smaller than at the upflowing footpoint, if the field has a geometry as proposed by Zhang et al. (2002), see Sect. 7.5.2. According to this proposal the submerged field emerges again after a relatively short distance and continues along the magnetic canopy before finally submerging in the form of an intense magnetic element. The siphon flow is finally driven by the difference between the gas pressure in this (magnetic element) footpoint and in the inner penumbral footpoint.

7.4.2. Buoyant and fallen flux tubes

One shortcoming of the studies of the siphon flow mentioned so far is that they presuppose the penumbral field to have a fluted structure, in particular they assume the presence of horizontal flux tubes without attempting to give a physical reason (Thomas et al. 2002a, b do propose a physical mechanism for producing horizontal fields in the penumbra

which can be combined with the siphon flow mechanism). Here I discuss two proposals that model the Evershed flow in connection with the formation of the fluted structure of the penumbral field. In contrast to the siphon-flow model, which is stationary, these models are dynamic.

The first of these was put forward by Wentzel (1992), who started with a locally homogeneous inclined field. By producing a density inversion in the atmospheric layers of a thin inclined flux tube of penumbral field he causes the flux tube to fall and become horizontal over most of the penumbra, while leaving a hump in the inner penumbra. The excess gas in the fallen flux tube is then drained, producing a horizontal outflow. A more detailed discussion of the model can be found in Sect. 4.9.

The resulting Evershed flow follows a concave path, which agrees with the results of Stellmacher & Wiehr (1971) and Pevtsov (1992). These are themselves not free of uncertainties, however (Sect. 7.3.2). On the other hand the predictions of the model conflict with the results of Rimmele (1995b), Schlichenmaier & Schmidt (2000) and Schmidt & Schlichenmaier (2000). Of particular interest is the downflow predicted by Wentzel's model near the inner penumbral edge, since it is a possible source of the strong, localized downflows seen there by Schlichenmaier & Schmidt (1999). One strength of Wentzel's model is that it naturally, if only qualitatively explains the presence of a ragged border between the umbra and penumbra (Solanki et al. 1994), as well as the presence of umbral filaments, as observed by Livingston (1991). It also proposes that the original mechanism for umbral dots and penumbral filaments are the same, an upwelling of hot material. Also, according to Wentzel's model the Evershed flow is episodic, since the gas only flows until the hump near the inner footpoint of the fallen tube has emptied. An estimate of the time scale depends on the adopted flow speeds and the reservoir of gas in the hump, but lies typically in the range of 1-5 minutes, in rough agreement with the observations (see Sect. 7.3.6). The variability in the velocity is also associated with an equally variable magnetic field, which is not observed, however (Lites et al. 1993, Solanki et al. 2002). Given this problem and the convex shape of the flow, Wentzel's model may require some improvements before providing a viable description of the Evershed effect.

A major alternative to fallen flux tubes is the buoyant flux tube model described in Sect. 4.9. In this model the flux tubes do not fall to the solar surface out of the atmosphere, but rather rise buoyantly from the solar interior. Unlike the fallen flux tube scenario this idea has been worked out and simulated in detail by Schlichenmaier et al. (1998a, b).

In this model the part of the thin penumbral flux tube, which ends up lying horizontally at the surface, starts below the surface at the outer magnetopause of the sunspot. It reaches the surface due to buoyancy and carries hot gas with it (see Sect. 4.9). The excess pressure due to the high temperature of the gas at the up-stream footpoint of this tube (with the footpoint being defined as its intersection with the solar surface) accelerates the gas outward along the horizontal part of the flux tube. The flow starts as hot gas in the inner penumbra and cools rapidly during its passage toward the outer penumbral boundary. The hot gas is not expected to be well visible, however, since it is optically thick (due to the strong temperature dependence of the H^- opacity), so that at these locations the $\tau = 1$ level lies above the horizontal flux tube. At some distance from this footpoint, as the gas cools, the $\tau = 1$ level falls below the top of the flux tube, revealing the now cool outflowing gas. The model can thus reproduce a number of features of the observed

penumbra. Also, only relatively cool gas is seen to flow outward, although it is unclear as yet how the gas can cool down to temperatures below those of the ambient penumbra, as observations suggest. Effects caused by differences between the optical depth scales across the horizontal flux tubes and in the ambient medium may play an important role. For example, one sees somewhat less deep in horizontal flux tubes (higher density, lower field strength) than in the surroundings. Due to the vertical temperature gradient gas in higher layers is cooler, thus mimicking the observed effect.

The fact that the C I 5380 Å line, whose strength increases rapidly with temperature (at temperatures typical of the photosphere), exhibits upflows in the inner penumbra (Schlichenmaier & Schmidt 2000), but the Fe I lines near 6302 Å do not (Westendorp Plaza et al. 1997a), could reflect high temperatures associated with these upflows, as predicted by this model. On the other hand, such upflows may be of extremely small scale ($< 0\rlap{.}''4$, Johannesson 1993) and may have escaped detection by Westendorp Plaza et al. (1997a) for that reason. This model also predicts the inward motion of bright points (corresponding to the upflow footpoint), which agrees with the observed inward motion of penumbral grains in the inner penumbra (Sect. 5.3.2). The outward motion of penumbral grains in the outer penumbra (e.g. Wang & Zirin 1992, Denker 1998, Sobotka et al. 1999) is, according to this model, caused by an instability that kinks the horizontal flux tube into a sea serpent (Schlichenmaier 2002). According to this model the Evershed effect is intimately related to the presence of a fluted field in the penumbra and also to hot material from the solar interior entering the penumbra. Since the presence of fluted field is turning out to be a basic characteristic of the penumbra this model also appears to be compatible with the observation of the Evershed effect in a newly formed penumbra (Leka & Skumanich 1998). Finally, a simplified version of this model has qualitatively reproduced the distribution of the Stoker V asymmetry of Fe I 15648 Å over a sunspot penumbra (Schlichenmaier & Collados 2002), again strengthening the case for this model.

Inspite of these successes the buoyant flux tube model faces a similar problem as the siphon flow model described in Sect. 7.4.1. The employed thin flux tube approximation requires balance of total pressure at a given height. Due to the excess thermal pressure at the upflowing footpoint, the field strength at the downflowing footpoint needs to be larger. For a horizontal flux tube having both its footpoints within the penumbra the inner footpoint would thus harbour the weaker field. This potential conflict with observations can be defused by the arguments given in the last 2 paragraphs of Sect. 7.4.1.

7.4.3. Wave models

Acoustic waves were proposed as the source of the Evershed effect by Erikson & Maltby (1967) and Maltby & Erikson (1967). Their idea was that a wave leads not only to an oscillatory behaviour of the wavelength of a spectral line, but via its pressure oscillations also to periodic changes in the line strength. When averaged over a wave period the phases at which the line is strengthened dominate, so that the average line profile has a net wavelength shift with a sign corresponding to that present at these phases. Observations may average over a wave period either temporally, if they integrate for a sufficient time, or spatially, if the wavelength of the wave is short or if neighbouring wave trains are randomly out of phase.

This model was extended by Bünte et al. (1993) to overcome various problems encountered by the originally proposed acoustic wave by incorporating the influence of magneto-acoustic-gravity-surface waves (whose MHD theory has been worked out by Miles & Roberts 1992, Miles et al. 1992). These waves are proposed to run along the magnetic inhomogeneities of the penumbra (between the different components of the fluted magnetic field). In these waves temperature, pressure and horizontal velocity perturbations are correlated in a way which reproduces the wavelength shifts of individual spectral lines. Since the velocity amplitude of these waves is a strong function of height they also reproduce the correct line asymmetry (Bünte et al. 1993).

A more detailed analysis of the influence of waves on the profiles of multiple spectral lines with different properties gave a less positive picture (Bünte & Solanki 1995). Nearly adiabatic waves with large temperature fluctuations affect line profiles with different temperature sensitivies in different ways (e.g., lines with different excitation potentials), so that these waves cannot systematically reproduce the spectral signature of the Evershed effect, as observed by Ichimoto (1987). A nearly isothermal wave, on the other hand, influences lines with different excitation potentials in a similar manner. However, in this case the ionisation balance plays an important role in determining the net line shift. Hence lines of different ions do not behave in the same way. Thus Fe II lines are predicted to exhibit an oppositely directed shift to Fe I. The observations of Stellmacher & Wiehr (1980) do not confirm such a difference.

These problems are not specific to the particular wave modes studied by Bünte & Solanki (1995) and apply equally to other compressible waves. Waves of this type are thus ruled out as the primary source of the Evershed effect.

7.4.4. Magnetoconvection as the source of the Evershed effect

Hurlburt et al. (1996) presented 2-dimensional simulations of compressible magnetoconvection in the presence of a uniform, externally imposed, inclined magnetic field. They find that all their solutions travel horizontally. This leads to a relatively slowly travelling pattern which can move in either direction, toward the umbra or away from it, depending on the details of the convection cells. The speed of the pattern increases with the inclination of the field. At the same time an outward material flow is found near the top of the simulation (outward being in the direction of the field inclination). The authors interpret this as the Evershed outflow. Converting to solar parameters they obtain a speed of 1 km s^{-1} for this flow.

Hurburt et al. (2000) have extended this work to 3-dimensions. They distinguish between cases with different inclinations of the magnetic field. As in the 3-D case they obtain travelling cells, with the cell pattern moving against the inclined field, i.e. towards the umbra. They interpret this as penumbral grains. As the imposed inclination of the field increases so does the elongation of the cells, so that they look somewhat more like penumbral grains. At the same time the flow field of these cells becomes more asymmetric, with the velocity in the direction of the tilt increasing, while decreasing in the opposite direction. This results is a net outward velocity, which is again interpreted as the Evershed flow.

Such simulations thus provide a simultaneous explanation of penumbral grains and Evershed effect, at least at the qualitative level.

7.5. *Models describing the moat and moving magnetic features*

7.5.1. Models of the moat flow

Meyer et al. (1979) considered the motion of flux tubes within prescribed supergranular cells. They found that the motion of the flux tube depends, among other things, on the amount of magnetic flux it caries. Tubes with larger flux have a tendency to end up near the center of the supergranule, while the smaller tubes move toward the boundary. The authors speculate that even if the back-reaction of the field is considered the final picture will not change very much. Hence the supergranule harbouring the sunspot is the moat cell according to their model. Galloway & Proctor (1983) solved the kinematic problem for a hexagonal convection cell with an imposed vertical magnetic field and obtained concentrations of magnetic flux both at the boundary and the center of the convection cell. This led Schmidt et al. (1985) to revisit the work of Meyer et al. (1979). They criticize the earlier work: "studying two-dimensional behaviour is inherently unsatisfactory, like watching Miss Universe on a flat television screen" and propose a 3-D model.

They obtain the same basic result as Meyer et al. (1979). The results of these kinematic calculations do need to be treated with caution since they all assume closed convective cells and the strong horizontal inflows at the bottom boundary of the computational domain is partly responsible for the concentration of field around cell centre.

A different approach was taken by Nye et al. (1988). They considered sunspots as rudimentary combinations of vertically oriented rectangles blocking the flow of heat. This blocked heat drives a convection reminiscent of a moat: The excess heat around the blockage causes the gas to flow away near the surface layers (this is the opposite behaviour to that found around small flux tubes which produce an increase in surface area and cause heat to flow towards them, producing cells with inflows at the solar surface – Deinzer et al. (1984a, b). In the linear calculations of Nye et al. (1988) the basic properties of the moat appear reasonable for the anelastic approximation (e.g. reasonable velocity amplitude). In the compressible case a too small moat cell is produced. In both cases the predicted size of the cell does not scale with the size of the (large) sunspot, in contrast to what is observed (Brickhouse & LaBonte 1988).

Fox et al. (1991) extended such calculations to the non-linear case, but are mainly concerned with the heat flux and possible bright rings around sunspots. They do not analyse the moat flow in detail.

Hurlburt & Rucklidge (2000), cf. Hurlburt et al. (2000), also obtain a moat around their 2-D spots. However, such a cell is only found further away from their model flux tubes (which span a range of fluxes corresponding to pores and sunspots). Closer in, an oppositely directed "collar flow" is present, which is not observed. Hurlburt & Rucklidge (2000) speculate that such a collar flow is present below the penumbra, where it cannot be directly observed and helps to stabilize the sunspot. Local helioseismology indeed produces evidence for a subsurface inflow towards the spot (e.g. Kosovichev et al. 2002) but lying underneath the moat's outflow. The near-surface outflow has been recovered using the f-mode (Gizon et al. 2000).

7.5.2. Models of Moving Magnetic Features

So far no fully physically consistent description of MMFs exists and most models are to a greater or lesser extent empirical. Of the three types of MMFs in the classification introduced by Shine & Title (2001), i.e. bipolar MMFs and unipolar MMFs with the same or the opposite polarity as the sunspot, almost all models only apply to the MMF pairs of mutually opposite polarity, which are by far the most common types of MMFs. The first such model was proposed by Harvey & Harvey (1973). According to them a flux tube breaks away from the parent sunspot close to the photospheric level and is swept away from it by the moat flow. The intersections of this flux tube with the solar surface are seen as the MMFs. This explains nicely that the amount of net flux carried away by MMFs is similar to the amount of flux lost by the sunspot. In order to make the unsigned total flux, $|\phi_+| + |\phi_-|$ up to an order of magnitude larger they propose that the detached flux tube has the shape of a sea serpent. In their model this is produced by a combination of buoyancy and the hypothesis that the field is twisted (i.e. kinked) below the surface. In this manner they can also reproduce the fact that MMFs tend to form bipoles. Variants of this basic model have been proposed by Wilson (1973) and Spruit et al. (1987), with horizontal magnetic flux tubes forming sea serpents and being dragged away from the sunspot. In the variant published by Wilson (1973) a thin flux tube is detached from the main flux tube forming the sunspot well below the solar surface while (at least initially) staying attached at photospheric heights. The detached part of the tube floats turbulently to the surface, developing twists and kinks which are seen as MMFs once it reaches the solar surface. In this case too, a structure similar to a sea serpant can be formed.

Meyer et al. (1974) suggested that small-scale convection within the sunspot allows flux to diffuse out into the surrounding flow which then carries the field (organized in flux tubes that have broken away from the sunspot) across the moat. Meyer et al. (1979) simulated this effect. Their computations give an upper limit of roughly 2×10^{18} Mx for MMFs. Larger features (more magnetic flux) are too buoyant and do not move away from the sunspot rapidly.

An alternative scenario was proposed by Wilson (1986). He argued that the energy density of granular motion is far below that of kG flux tubes and hence is insufficient to form the kinks required by the mechanism of Harvey & Harvey (1973). In his model the interaction of the sunspot magnetic field with convection leads to the formation of small O-loops that are then carried away from the sunspot by the moat flow. Wilson's mechanism is in turn criticized by Ryutova et al. (1998) as requiring a special velocity field and failing to reproduce MMFs that propagate faster than the general moat flow. Ryutova et al. (1998) counter Wilson's criticism of the Harvey & Harvey mechanism by proposing that the kinks in the flux tube are due to kink waves, in particular solitary kink waves, produced by shear instabilities developing along the subsurface flux tubes, which in their model harbours a rapid flow (subsurface Evershed flow outside the visible sunspot). MMF pairs according to this model are parts of Ω loops. A mechanism to keep a horizontal flux tube stably located just below the solar surface, namely turbulent magnetic flux pumping by granular convection, has been proposed by Thomas et al. (2002a, b; see Sect. 4.9). Although the predicted orientation of polarities of MMF pairs agrees with that stated by Shine & Title (2001), it disagrees with the results of the recent

studies by Yurchyshyn et al. (2001) and Zhang et al. (2002). Thomas et al. (2002b) also provide qualitative descriptions of the other types of MMFs.

Finally, Zhang et al. (2002) propose that pairs of MMFs are produced by downward kinks in the magnetic canopy of sunspots (U-loops). In this case the inner polarity is opposite to that of the sunspot and the MMF pair is oriented along the superpenumbral magnetic field, hence along Hα filaments. This agrees well with the observations of Yurchyshyn et al. (2001), Zhang et al. (2002). The absence of a signature in the upper chromospheric layers is quite naturally produced in this model. The predictions of this model are also in good agreement with the vector measurements of Bernasconi et al. (2002) of bipolar features near a forming sunspot.

The question, what produces such a kink in the canopy of course arises. The simulations of Schlichenmaier (2002) display the development of such a kink, probably due to an instability in a flux tube carrying a flow (see, e.g. Holzwarth & Schüssler 2002). Another proposal is outlined below. A part of the Evershed flow continues out of the penumbra into the canopy. According to Shine et al. (1994), Rimmele (1994) and Rouppe van der Voort (2002b) this flow is not completely steady, but rather bursty (see Sect. 7.3.6). Hence, from time to time a particularly large blob of material flows along the flux tube. Such a massive blob is pulled downward by gravity. Within the penumbra the upwardly expanding magnetic field, along with magnetic buoyancy keeps the horizontal flux tube from developing a kink at the location of the blob. Outside the penumbra, the missing support from the surrounding field may allow such a kink to develop, and the flux tube to be locally pulled below the solar surface. This corresponds to the formation of a bipolar MMF, which, although it may originally be faster than the moat flow (as is sometimes observed), soon settles down to a speed similar to that of the moat flow. Possibly, convective flux pumping (Thomas et al. 2002b) is responsible for keeping the downward kink submerged and prolonging the life of a MMF pair.

8. Conclusion: Some open questions

Sunspots have proved to be a source of fascination and physical insight for almost four centuries. The pace of research, instead of slowing down, as may quite reasonably be expected for such a mature subject, has continued unchecked and shows no sign of abating in the near future. In spite of the vast amount of knowledge gathered on sunspots and the improvements in their theoretical description, of some aspects of which this paper has tried to provide an overview, a number of fundamental questions and many more of a less fundamental nature remain unanswered. A selection of such questions is listed below. For some of them partial answers may already have been found.

- What is the subsurface structure of sunspots: are they monolithic or do they break up into a spaghetti of smaller flux tubes? How tightly clustered are such small flux tubes?
- Why do sunspots have penumbrae? What causes their rapid formation?
- What determines the intrinsic brightness of umbrae and penumbrae, in spite of the strong magnetic field which inhibits convection? Does interchange convection provide sufficient energy to the penumbra or is an additional mechanism needed?
- What is the nature of umbral dots?

- What is the true small-scale (magnetic) structure of penumbrae? How small are the smallest brightness and magnetic structures?
- Is there field-free material in sunspots?
- What drives the flow which produces the Evershed effect?
- What happens to the Evershed flow and the associated field lines at the outer penumbral boundary, after they pass through the solar surface into the solar interior?
- Does the Evershed flow follow a single loop across the penumbra or many small loops?
- How are the umbral oscillations seen in different atmospheric layers related to each other and to the running penumbral waves?
- What is the origin and nature of moving magnetic features? How do they interact with the sunspot canopy? Are they related to the field lines diving back under the solar surface at the penumbral boundary?
- How do sunspots decay? Do moving magnetic features really carry off all the lost flux?
- Why do sunspots have the observed size and lifetime distributions? What places an upper limit on sunspot size?
- How come more active stars possess seemingly larger spots?
- Are larger umbrae really darker and if so why?
- Do the relative areas covered by umbrae and penumbrae depend on sunspot size or on other parameters (such as the phase of the solar cycle)?
- Is the umbral temperature really a function of solar cycle phase? What causes such a dependence?
- How does the small-scale "uncombed" structure of the photospheric penumbral magnetic field propagate to higher layers?
- What drives the supersonic downflows seen in the transition region above umbrae?
- What is the nature of sunspot plumes?
- Why are umbrae far less bright than the surrounding plage in extreme ultraviolet radiation? Why are penumbrae brighter?
- How is the umbral chromosphere heated?
- What determines the solar rotation rate traced by sunspots and its evolution over the solar cycle?
- How common are siphon flows across the neutral lines of δ-spots?
- Why are leading polarity spots in an active region often larger than following polarity spots?
- How common is magnetic reconnection in sunspots and their canopies? For example, is the complex penumbral magnetic field stable, or subject to constant reconnection?
- What are the dynamics of the gas during the formation of sunspots?
- What happens to the energy absorbed by sunspots from p-mode oscillations?
- What are the subsurface dynamics of the flux tube which will become a sunspot? How strongly and at what level does it split into small flux tubes?
- Which fraction of the heat flux blocked by sunspots is stored in the convection zone and which fraction is immediately radiated elsewhere on the solar surface?
- How do sunspots differ from their counterparts on more active stars?
- How large is the Wilson depression at different points in a sunspot?

– Why is the averaged field strength and its height variation in the photosphere so similar for all flux tubes, from magnetic elements to sunspots?

The resolution of some of these questions awaits observations with higher spatial resolution, others require improved local helioseismic observations, while advances in theory and modelling are also expected to help answer many open questions. At the same time I expect that improved observations will reveal new and unexpected features that give rise to additional questions and will thus keep the field flourishing for a long time to come.

References

Aballe Villero M.A., 1992, Thesis, University La Laguna

Abdussamatov H.I., 1970, *Astron Zh.*, **47**, 82

Abdussamatov H.I., 1971a, in *Solar Magnetic Fields*, R.F. Howard (Ed.), Reidel, Dordrecht, *IAU Symp.* **43**, 231

Abdussamatov, H.I., 1971b, *Solar Phys.* **16**, 384

Abdussamatov H.I., 1973, *Bull. Astron. Inst. Czech* **24**, 118

Abdussamatov H.I., 1976, *Solar Phys.* **48**, 117

Abdussamatov H.I., 1980, *Solar Phys.* **65**, 197

Abramov–Maksimov V.E., Vyalshin G.F., Gelfreikh G.B., Shatilov V.I., 1996, *Solar Phys.* **164**, 333

Adam M.G., 1967, *Monthly Notices Royal Astron. Soc.* **136**, 71

Adam M.G., 1969, *Monthly Notices Royal Astron. Soc.* **145**, 1

Adam M.G., 1990, *Solar Phys.* **125**, 37

Adam M.G., Petford A.D., 1991, *Solar Phys.* **135**, 319

Adams M., Solanki S.K., Hagyard M.J., Moore R.L., 1993, *Solar Phys.* **148**, 201

Adjabshirzadeh A., Koutchmy S., 1980, *Astron. Astrophys.* **89**, 88

Adjabshirzadeh A., Koutchmy S., 1983, *Astron. Astrophys.* **122**, 1

Akhmedov Sh.B., Gelfreikh G.B., Bogod V.M., Korzhavin A.N., 1982, *Solar Phys.* **79**, 41

Akhmedov Sh.B., Gelfreikh G.B., Fürstenberg F., Hildebrandt J., Krüger A., 1983, *Solar Phys.* **88**, 103.

Akhmedov Sh.B., Borovik V.N., Gelfreikh G.B., et al. 1986, *Astrophys. J.* **301**, 460

Albregtsen F., Maltby P., 1978, *Nature* **274**, 41

Albregtsen F., Maltby P., 1981a, *Solar Phys.* **71**, 269

Albregtsen F., Maltby P., 1981b, in *Physics of Sunspots*, L.E. Cram, J.H. Thomas (Eds.), National Solar Obs., Sunspot, NM, p. 127

Albregtsen F., Maltby P., 1981c, *Solar Phys.* **74**, 147

Albregtsen F., Jorås P.B., Maltby P., 1984, *Solar Phys.* **90**, 17

Alfvén H., 1943, *Arkiv. Mat. Astron. Fysik* **29**, No. 11

Alissandrakis C.E., 1997, in *Advances in the Physics of Sunspots*, B. Schmieder, J.C. del Toro
    Iniesta, M. Vázquez (Eds.), ASP Conf. Ser. Vol. 118, p. 150

Alissandrakis C.E., Kundu M.R., 1982, *Astrophys. J.* **253**, L49

Alissandrakis C.E., Kundu M.R., 1984, *Astron. Astrophys.* **139**, 271

Alissandrakis C.E., Kundu M.R., Lantos P., 1980, *Astron. Astrophys.* **82**, 30

Alissandrakis C.E., Dialetis D., Mein P., Schmieder B., Simon G., 1988, *Astron. Astrophys.* **201**,
    339

Alissandrakis C.E., Georgakilas A.A., Dialetis D., 1992, *Solar Phys.* **138**, 93

Altrock R.C., Canfield R.C., 1974, *Astrophys. J.* **194**, 733

Antalová A., 1991, *Bull. Astron. Inst. Czechoslovakia* **42**, 319

Arena F., Landi Degl'Innocenti E., Noci G., 1990, *Solar Phys.* **129**, 259

Auer L.H., Heasley J.N., 1978, *Astron. Astrophys.* **64**, 67

Avrett E.H., 1981, in *The Physics of Sunspots*, L.E. Cram, J.H. Thomas (Eds.), National Solar
    Obs., Sunspot, NM, p. 235

Ayres T.R., 1996, in *Stellar Surface Structure*, K.G. Strassmeier (Ed.), Kluwer, Dordrecht, *IAU
    Symp.* **176**, 317

Babcock H.W., 1951, *Astrophys. J.* **114**, 1

Balasubramaniam K.S., Petry C.E., 1995, in *Infrared Tools for Solar Astrophysics: What's Next?*,
    J.R. Kuhn, M.J. Penn (Eds.), World Scientific, Singapore, p. 369

Balthasar H., 1999a, in *Magnetic Fields and Oscillations*, B. Schmider, A. Hofmann, J. Staude
    (Eds.), ASP Conf. Ser. Vol. 184, p. 141

Balthasar H. 1999b, *Solar Phys.* **187**, 389

Balthasar H., Schmidt W., 1993, *Astron. Astrophys.* **279**, 243

Balthasar H., Schmidt W., 1994, *Astron. Astrophys.* **290**, 649

Balthasar H, Wöhl H., 1983, *Solar Phys.* **88**, 65

Balthasar H., Vázquez M., Wöhl H., 1986, *Astron. Astrophys.* **155**, 87

Balthasar H., Schleicher H., Bendlin C., Volkmer R., 1996, *Astron. Astrophys.* **315**, 603

Balthasar H., Schmidt W., Wiehr E., 1997, *Solar Phys.* **171**, 331

Baranovsky E.A., 1974a, *Izv. Krimsk. Astron. Obs.* **49**, 25 (in russian)

Baranovsky E.A., 1974b, *Izv. Krimsk. Astron. Obs.* **51**, 56 (in russian)

Barnes G., Cally P.S., 2000, *Solar Phys.* **193**, 373

Beck J.G., Chapman G.A., 1993, *Solar Phys.* **146**, 49

Beckers J.M., 1962, *Australian J. Phys.* **15**, 327

Beckers J.M., 1968, *Solar Phys.* **3**, 258

Beckers J.M., 1969, *Solar Phys.* **9**, 372

Beckers J.M., 1976, *Astrophys. J.* **203**, 739

Beckers J.M., 1977, *Astrophys. J.* **213**, 900

Beckers J.M., Schneeberger T.J., 1977, *Astrophys. J.* **215**, 356

Beckers J.M., Schröter E.H., 1968, *Solar Phys.* **4**, 303

Beckers J.M., Schröter E.H., 1969a, *Solar Phys.* **7**, 22

Beckers J.M., Schröter E.H., 1969b, *Solar Phys.* **10**, 384

Beckers J.M., Tallant P.E., 1969, *Solar Phys.* **7**, 351

Beebe H.A., Baggett W.E., Yun H.S., 1982, *Solar Phys.* **79**, 31

Bellot Rubio L.R., Collados M., Ruiz Cobo B., Rodríguez Hidalgo I., 2000, *Astrophys. J.* **534**,
    989

Berdyugina S., Solanki S.K., Lagg A., 2002, in *Cool Stars, Stellar Systems and the Sun XII*, T.
    Ayres (Ed.), ASP Conf. Ser. in press.

Bernasconi P.A., Rust D.M., Georgoulis M.K., LaBonte B.J., 2002, *Solar Phys.* **209**, 119

Bewsher D., Loughhead R.E., 1959, *Australian J. Phys.*, **12**, 320

Bhatnagar A., 1967, *Kodaikanal Obs. Bull.* **180**, A13

Biermann L., 1941, *Vierteljahrsschrift Astron. Ges.* **76**, 194

Blanchflower S.M., Rucklidge A.M., Weiss N.O., 1998, *Monthly Notices Royal Astron. Soc.* **301**, 593

Bogdan T.J., 1992, in *Sunspots: Theory and Observations*, J.H. Thomas, N.O. Weiss (Eds.), Kluwer, Dordrecht, p. 345

Bogdan T.J., 1994, in *Solar Magnetic Fields*, M. Schüssler, W. Schmidt (Eds.), Cambridge Univ. Press, Cambridge, p. 229

Bogdan T.J., 1999, in *High Resolution Solar Physics: Theory, Observatins and Techniques*, T.R. Rimmele, K.S. Balasubramaniam, R.R. Radick (Eds.), ASP Conf. Ser. Vol. 183, p.78.

Bogdan T.J., 2000, *Solar Phys.* **192**, 373

Bogdan T.J., Braun D.C., 1995, in *Proc. 4th SOHO Workshop: Helioseismology*, V. Domingo et al. (Eds.), ESA SP-376, p. 31.

Bogdan T.J., Gilman P.A., Lerche I., Howard R., 1988, *Astrophys. J.* **327**, 451

Bogdan T.J., Brown T.M., Lites B.W., Thomas J.H., 1993, *Astrophys. J.* **406**, 723

Bogdan T.J., Brown D.C., Lites B.W., Thomas J.H., 1998, *Astrophys. J.* **492**, 379

Bogdan T.J., Rosenthal C.S., Carlsson M., et al., 2002, *Astron. Nachr.*, **323**, 196

Bogod V.M., Gel'freikh G.B., Willson R.F., Lang K.R., Opeikina L.V., Shatilov V., Tsvetkov S.V., 1992, , *Solar Phys.* **141** 303

Bones J., Maltby P., 1978, *Solar Phys.* **57**, 65

Bonet J.A., Ponz J.D., Vázquez M., 1982, *Solar Phys.* **77**, 69

Börner P., Kneer F., 1992, *Astron. Astrophys.* **259**, 307

Boyer R., 1980, *Astron. Astrophys. Suppl. Ser.* **40**, 277

Brahde R., 1972, *Solar Phys.* **26**, 318

Brajsa R., Wöhl H., Vrsnak B., et al. 2002, *Solar Phys.* **206**, 229

Brandt P.N., Stix M., Weinhardt H., 1994, *Solar Phys.* **152**, 119

Brandt P.N., Schmidt W., Steinegger M., 1991, *Solar Phys.* **129**, 191

Brants J.J., 1985, Observational Study of the Birth of a Solar Active Region. Ph.D. Thesis, University of Utrecht

Brants J.J., Zwaan C., 1982, *Solar Phys.* **80**,251

Braun D.C., 1995, *Astrophys. J.* **451**, 859

Braun D.C., Duvall T.J., Jr., LaBonte B.J., 1987, *Astrophys. J.* **319**, L27

Braun D.C., Duvall T.L., Jr., LaBonte B.J., 1988, *Astrophys. J.* **335**, 1015

Braun D.C., Duvall T.L., Jr., LaBonte B.J., Jefferies S.M., Harvey J.W., Pomerantz M.A., 1992, *Astrophys. J.* **391**, L113

Bray R.J., 1981, *Solar Phys.* **69**, 3

Bray R.J., Longhhead R.E., 1958, *Australian J. Phys.* **11**, 185

Bray R.J., Longhhead R.E., 1959, *Australian J. Phys.* **12**, 320

Bray R.J., Loughhead R.E., 1964, *Sunspots*, Chapman and Hall

Brekke K., Maltby P., 1963, *Ann. d'Astrophys.* 26, 383

Briand C., Solanki S.K., 1995, *Astron. Astrophys.* **299**, 596

Brickhouse N.S., LaBonte B.J., 1988, *Solar Phys.* **115**, 43

Brković A., Solanki S.K., Rüedi I., 2001, *Astron. Astrophys.* **373**, 1056

Brosius J.W., Holman G.D., 1989, *Astrophys. J.* **342**, 1172

Brosius J.W., Willson R.F., Holman G.D., Schmelz J.T., 1992, *Astrophys. J.* **386**, 347

Brown D.S., Nightingale R.W., Mefcalf T.R., Schrijver C.J., Shine R.A., Title A., Wolfson C.J., 2002, in *Magnetic Coupling of the Solar Atmosphere*, H. Sawaya-Lacoste (Ed.), ESA-SP 505, in press

Broxon J.W., 1942, *Phys. Rev.* **62**, 521

Brueckner G.E., Bartoe J.-D.F., Van Hoosier M.E., 1978, in *Proceedings OSO-8 Workshop*, E. Hansen, S. Schaffner (Eds.), University of Colorado Press, Boulder, CO, p. 380

Bruls J.H.M.J., Solanki S.K., Carlsson M., Rutten R.J., 1995, *Astron. Astrophys.* **293**, 225

Brunner W., 1930, *Astron. Mitt. Zürich* Nr. 124

Brynildsen N., Brekke P., Fredvik T., et al. 1998a, *Solar Phys.* **179**, 43

Brynildsen N., Brekke P., Fredvik T., et al. 1998b, *Solar Phys.* **179**, 279

Brynildsen N., Maltby P., Brekke P., et al. 1998c, *Astrophys. J.* **502**, L85

Brynildsen N., Maltby P., Brekke P., et al. 1999a, *Solar Phys.* **186**, 141

Brynildsen N., Leifsen T., Kjeldseth-Moe O., Maltby P., Wilhelm K., 1999b, *Astrophys. J.* **511**, L121

Brynildsen N., Maltby P., Fredvik T., et al. 2001a, *Solar Phys.* **198**, 89

Brynildsen N., Maltby P., Kjeldseth-Moe O., Wilhelm K., 2001b, *Astrophys. J.* **552**, L77

Bumba V., 1960, *Izv. Krymsk. Astrofiz. Observ.* **23**, 212

Bumba V., 1963a, *Bull. Astron. Inst. Czechoslovakia* **14**, 91

Bumba V., 1963b, *Bull. Astron. Inst. Czechoslovakia* **14**, 134

Bumba V., 1965, in *Stellar and Solar Magnetic Fields*, R. Lüst (Ed.), North-Holland Pub. Co., IAU Symp. 22, 305

Bumba V., Suda J., 1984, *Bull. Astron. Inst. Czechoslovakia* **35**, 28.

Bumba V., Klvaňa M., Kálman B., 1996, *Astron. Astrophys. Suppl. Ser.* **118**, 35

Bünte M., Solanki S.K., 1995, *Astron. Astrophys.* **297**, 861

Bünte M., Darconza G., Solanki S.K., 1993, *Astron. Astrophys.* **274**, 478

Buurman J., 1973, *Astron. Astrophys.* **29**, 329

Caccin B., Gomez M.T., Severino G., 1993, *Astron. Astrophys.* **276**, 219

Caligari P., Moreno-Insertis F., Schüssler M., 1995, *Astrophys. J.* **441**, 886

Cally P.S., Bogdan T.J., Zweibel E.G., 1994, *Astrophys. J.* **437**, 505

Carrington R.C., 1863, *Observations of the Spots on the Sun from November 9, 1853 to March 24, 1861 made at Redhill*, Williams and Norgate, London

Cattaneo F. 1999, *Astrophys. J.* **515**, L39

Chandrasekhar S., 1952, *Phil. Mag. (7th Ser.)* **43**, 501

Chandrasekhar S., 1961, *Hydrodynamic and Hydromagnetic Stability*, Clarendon Press, Oxford

Chandrasekhar S., Kendall P.C., 1957, *Astrophys. J.* **126**, 457

Chang H.-K., Chou D.-Y., La Bonte B., and the TON Team, 1997, *Nature* **389**, 825

Chapman G.A., Cookson A.M., Dobias J.J., 1994, *Astrophys. J.* **432**, 403

Chen H.-R., Chou D.-Y., and the TON Team, 1997, *Astrophys. J.* **490**, 452

Cheng C.C., Doschek G.A., Feldman U., 1976, *Astrophys. J.* **210**, 836

Chevalier S., 1907, *Astrophys. J.* **25**, 273

Chevalier S., 1914, *Ann. Obs. Zô–Sè (China)* **8**, C1

Chevalier S., 1916, *Ann. Obs. Zô–Sè (China)* **9**

Chevalier S., 1919, *Ann. Obs. Zô–Sè (China)* **11**, B10

Chistyakov V.F., 1962, *Soviet Astron.* **6**, 363

Chitre S.M., 1963, *Monthly Notices Royal Astron. Soc.* **126**, 431

Chitre S.M., 1992, in *Sunspots: Theory and Observations*, J.H. Thomas, N.O. Weiss (Eds.), Kluwer, Dordrecht, p. 333

Chitre S.M., Shaviv G., 1967, *Solar Phys.* **2**, 150

Chiuderi-Drago F., Bandiera R., Willson R.F., 1982, *Solar Phys.* **80**, 71

Chou D.-Y., 1987, *Astrophys. J.* **312**, 955

Chou D.-Y., Sun M.T., Huang T.Y., 1995, *Solar Phys.* **160**, 237

Choudhuri A.R., 1986, *Astrophys. J.* **302**, 809

Choudhuri A.R., 1992, in *Sunspots: Theory and Observations*, J.H. Thomas, N.O. Weiss (Eds.), Kluwer, Dordrecht, p. 243

Christopoulou E.B., Georgakilas A.A., Koutchmy S., 1999, in *Magnetic Fields and Oscillations*, B. Schmieder, A. Hofmann, J. Staude (Eds.), ASP Conf. Series, Vol. 184, p. 103

Christopoulou E.B., Georgakilas A.A., Koutchmy S., 2000, *Astron. Astrophys.* **354**, 305

Christopoulou E.B., Georgakilas A.A., Koutchmy S., 2001, *Astron. Astrophys.* **375**, 617

Clark A., Jr., 1979, *Solar Phys.* **62**, 305

Collados M., Del Toro Iniesta J.C., Vázquez M., 1987, *Solar Phys.* **112**, 281

Collados M., Martínez Pillet V., Ruiz Cobo B., del Toro Iniesta J.C., Vázquez M., 1994, *Astron. Astrophys.* **291**, 622

Covington A.E., 1947, *Nature* **159**, 405

Cowling T.G., 1934, *Monthly Notices Royal Astron. Soc.* **94**, 39

Cowling T.G., 1946, *Monthly Notices Royal Astron. Soc.* **106**, 218

Cowling T.G., 1953, in *The Solar System, Vol. 1, The Sun*, G.P. Kuipers (Ed.), Chicago University Press, p. 532

Cowling T.G., 1957, *Magnetohydrodynamics*, Interscience, New York

Cowling T.G., 1976, *Monthly Notices Royal Astron. Soc.* **177**, 409

Cram L.E., Thomas J.H., (Eds.) 1981, *The Physics of Sunspots*, National Solar Obs., Sunspot, NM

Danielson R.E., 1961a, *Astrophys. J.* **134**, 275

Danielson R.E., 1961b, *Astrophys. J.* **134**, 289

Danielson, R.E., 1964, *Astrophys. J.* **139**, 45

Danielson R.E., 1965, in *Stellar and Solar Magnetic Fields*, R. Lüst (Ed.), North Holland, Amsterdam, *IAU Symp.* **22**, 314

Dara H.C., Koutchmy S., Alissandrakis C.E., 1993, *Astron. Astrophys.* **277**, 648

Das A.K., Ramanathan A.S., 1953, *Z. Astrophys.* **32**, 91

David K.-H., Elste G., 1962, *Z. Astrophys.* **54**, 12

Degenhardt D., 1989, *Astron. Astrophys.* **222**, 297

Degenhardt D., 1991, *Astron. Astrophys.* **248**, 637

Degenhardt D., 1993, *Astron. Astrophys.* **277**, 235

Degenhardt D., Lites B.W., 1993a, *Astrophys. J.* **404**, 383

Degenhardt D., Lites B.W., 1993b, *Astrophys. J.* **416**, 875

Degenhardt D., Wiehr E., 1991, *Astron. Astrophys.* **252**, 821

Degenhardt D., Wiehr E., 1994, *Astron. Astrophys.* **287**, 620

Deinzer W., 1965, *Astrophys. J.* **141**, 548

Deinzer W., 1994, in *Solar Magnetic Fields*, M. Schüssler, W. Schmidt (Ed.), Cambridge Univ. Press, Cambridge, p.13

Deinzer W., Hensler G., Schüssler M., Weisshaar E., 1984a, *Astron. Astrophys.* **139**, 426

Deinzer W., Hensler G., Schüssler M., Weisshaar E., 1984b, *Astron. Astrophys.* **139**, 435

Del Toro Iniesta J.C., Martínez Pillet V., Vázquez M., 1991, in *Solar Polarimetry*, L. November (Ed.), National Solar Obs., Sunspot, NM, p. 224

Del Toro Iniesta J.C., Tarbell T.D., Ruiz Cobo B., 1994, *Astrophys. J.* **436**, 400

Del Toro Iniesta J.C., Bellot Rubio L.R., Collados M., 2001, *Astrophys. J.* **549**, L139

Deming D., Boyle R.J., Jennings D.E., Wiedemann G., 1988, *Astrophys. J.* **333**, 978

Deming D., Hewagama T., Jennings D.E., Wiedemann G., 1991, in *Solar Polarimetry*, L.J. November (Ed.), National Solar Obs., Sunspot, NM, p. 341

Denker C., 1998, *Solar Phys.* **180**, 81

Denker C., de Boer C.R., Volkmer R., Kneer F., 1995, *Astron. Astrophys.* **296**, 567

Dere K.P., Schmieder B., Alissandrakis C.E., 1990, *Astron. Astrophys.* **233**, 207

Deubner L., 1969, *Solar Phys.* **7**, 87

Deubner F.L., Göhring R., 1970, *Solar Phys.* **13**, 118

Dezsö L., Gerlei O., Kovács A., 1987, Debrecen Photoheliographic Results for the Year 1977, Publ. Debrecen Heliophys. Obs., Heliograph. Ser. No. 1, Debrecen.

Dezsö L., Gerlei O., Kovács A., 1997, Debrecen Photoheliographic Results for the Year 1978, Publ. Debrecen Heliophys. Obs., Heliograph. Ser. No. 2, Debrecen.

Dialetis D., Mein P., Alissandrakis C.E., 1985, *Astron. Astrophys.* **147**, 93

Dicke R.H., 1970, *Astrophys. J.* **159**, 25

Ding M.D., Fang C., 1989, *Astron. Astrophys.* **225**, 204

Doschek G.A., Feldman U., Bohlin J.D., 1976, *Astrophys. J.* **205**, L177

Doyle J.G., Raymond J.C., Noyes R.W., Kingston A.E., 1985, *Astrophys. J.* **297**, 816

D'Silva S., Choudhuri A.R., 1993, *Astron. Astrophys.* **272**, 621

D'Silva S., Howard R.F., 1994, *Solar Phys.* **151**, 213

D'Silva S., Duvall T.L., Jr., 1995, *Astrophys. J.* **438**, 454

Dubov E.E., 1965, *Soln. Dann.* **12**, 53

Dulk G.A., 1985, *Ann. Rev. Astron. Astrophys.* **23**, 169.

Duvall T.L., Gizon L., 2000, *Solar Phys.* **192**, 177

Duvall T.L. Jr., Jefferies S.M., Harvey J.W., Pomerantz M.A., 1993, *Nature*, **362**, 430

Duvall T.L., Jr., D'Silva S., Jefferies S.M., Harvey J.W., Schou J., 1996, *Nature* **379**, 235

Eddy J., Stephenson F.R., Yau K.K.C., 1989, *Quart. J. Roy. Astron. Soc.* **30**, 60

Efremov V.I., Parfimenko L.D., 1996, *Astron. Rep.* **40**, 89

Eibe M.T., Aulanier G., Faurobert M., Mein P., Malherbe J.M., 2002, *Astron. Astrophys.* **381**, 290

Ekmann G., 1974, *Solar Phys.* **38**, 73

Ekmann G., Maltby P., 1974, *Solar Phys.* **35**, 317

Emonet T., Cattaneo F., 2001, *Astrophys. J.* **560**, L197

Eriksen G., Maltby P., 1967, *Astrophys. J.* **148**, 833

Eschrich K.-O., Krause F., 1977, *Astron. Nachr.* **298**, 1

Evershed J., 1909, *Monthly Notices Royal Astron. Soc.* **69**, 454

Ewell M.W., 1992, *Solar Phys.* **137**, 215

Fang C., Tang Y.H., Ding M.D., Zhao J., Sakurai T., Hiei E., 1997, *Solar Phys.* **176**, 267

Feldman U., Cohen L., Doschek G.A.: 1982, *Astrophys. J.* **255**, 325

Finsterle W., 1995, *Diplomarbeit*, Institute of Astronomy, ETH Zürich

Flå T., Osherovich V.A., Skumanich A., 1982, *Astrophys. J.* **261**, 700

Flammarion C., 1880, *L'astronomie populaire*, Librairie Uranie, Paris

Fontenla J., White O.R., Fox P.A., Avrett E.H., Kurucz R.L., 1999, *Astrophys. J.* **518**, 480

Foukal P.V., 1976, *Astrophys. J.* **210**, 575

Foukal P.V., 1978, *Astrophys. J.* **223**, 1046

Foukal P.V., 1981, in *The Physics of Sunspots*, L.E. Cram, J.H. Thomas (Eds.), National Solar Obs., Sunspot, NM, p. 391

Foukal P.V., 1987, *in Theoretical Problems in High Resolution Solar Physics II* NASA-GSFC, p. 15

Foukal P.V., Duvall R., Jr., 1985, *Astrophys. J.* **296**, 739

Foukal P.V., Huber M.C.E., Noyes R.W. et al. 1974, *Astrophys. J.* **193**, L143

Foukal P.V., Fowler L.A., Livshits M., 1983, *Astrophys. J.* **267**, 863

Fowler L.A., Foukal P.V., Duvall T., Jr., 1983, *Solar Phys.* **8**4, 33

Fox P.A., Sofia S., Chan K.L., 1991, *Solar Phys.* **135**, 15

Fredrik R., Maltby P., 1998, *Solar Phys.* **184**,113

Fricke K., Elsässer H., 1965, *Z. Astrophys.* **63**, 35

Gadun A.S., Solanki S.K., Sheminova V.A., Ploner S.R.O., 2001, *Solar Phys.* **203**, 1

Galloway D.J., Proctor M.R.E., 1983, *Geophys. Astrophys. Fluid Dyn.* **24**, 109

García de la Rosa J.I., 1987a, in *The Role of Fine-Scale Magnetic Fields on the Structure of the Solar Atmosphere*, E.-H. Schröter, M. Vázquez, A.A. Wyller (Eds.), Cambridge University Press, Cambridge, pp. 140

García de la Rosa J.I., 1987b, in *Proc. 10th Europ. Regional Astron. Meeting of the IAU, Vol. 1: The Sun*, L. Hejna, M. Sobotka (Eds.), Astron. Inst. of Czech. Acad. Sci., Prague, p. 21

Gary D.E., Hurford G.J., 1987, *Astrophys. J.* **317**, 522

Gary D.E., Leblanc Y., Dulk G.A., Golub L., 1993, *Astrophys. J.* **412**, 421

Gelfreikh G.B., Lubyshev B.I., 1979, *Astron. Zh.* **56**, 562

Gilman P.A., Howard R., 1985, *Astrophys. J.* **295**, 233

Ginzburg V.L., Zheleznyakov V.V., 1961, *Sov. Astron. – AJ* **5**, 1

Giovanelli R.G., 1972, *Solar Phys.* **27**, 71

Giovanelli R.G., 1974, in *Chromospheric Fine Structure*, R.G. Athay (Ed.), Reidel, Dordrecht *IAU Symp.* **56**, 137

Giovanelli R.G., 1980, *Solar Phys.* **68**, 49

Giovanelli R.G., 1982, *Solar Phys.* **80**, 21

Giovanelli R.G., Jones H.P., 1982, *Solar Phys.* **79**, 267

Gizon L., Duvall T.L., Larsen R.M., 2000, *J. Astrophys. Astron.*, **21**, 339

Gnevyshev M.N., 1938, *Pulkovo Obs. Circ.* **24**, 37

Gokhale M.H., Zwaan C., 1972, *Solar Phys.* **26**, 52

Golovko A.A., 1974, *Solar Phys.* **37**, 113

Golub L., Herant M., Kalatka K., Lovas I., Nystrom G., Pardo F., Spiller E., Wilczynski J., 1990, *Nature*, **344**, 842

Golub L., Zirin H., Wang H., 1994, *Solar Phys.* **153**, 179

Goplaswamy N., Raulin J.P., Kundu M.R., Hildebrandt J., Krüger A., Hofmann A., 1996, *Astron. Astrophys.* **316**, L25

Gough D.O., Tayler R.J., 1966, *Monthly Notices Royal Astron. Soc.* **133**, 85

Grigorjev V.M., Katz J.M., 1972, *Solar Phys.* **22**, 119

Grigorjev V.M., Katz J.M., 1975, *Solar Phys.* **42**, 21

Grossmann-Doerth U., Schmidt W., 1981, *Astron. Astrophys.* **95**, 366

Grossmann-Doerth U., Schmidt W., Schröter E.H., 1986, *Astron. Astrophys.* **156**, 347

Grossmann-Doerth U., Pahlke K.-D., Schüssler M., 1987, *Astron. Astrophys.* **176**, 139

Grossmann-Doerth U, Schüssler M., Steiner O., 1998, *Astron. Astrophys.* **337**, 928

Gurman J.B., 1984, *Sol. Phys.*, **90**, 13

Gurman J.B., House L.L., 1981, *Solar Phys.* **71**, 5

Guseynov M.J., 1970, *Izv. Krymsk. Astrofiz. Observ.* **39**, 253

Hagyard M.J., West E.A., Cumings N.P., 1977, *Solar Phys.* **53**, 3

Hagyard M.J., Teuber D., West E.A., Tandberg-Hanssen E., Henze W., Beckers J.M., Bruner M., Hyder C.L., Woodgate B.E., 1983, *Solar Phys.* **84**, 13

Hagyard M.J., Smith Jr. J.B., Teuber D., West E.A., 1984, *Solar Phys.* **91**, 115

Hale G.E., 1892, *Astron. Astrophys.* **11**, 310

Hale G.E., 1908a, *Astrophys. J.* **28**, 100

Hale G.E., 1908b, *Astrophys. J.* **28**, 315

Hale G.E., Nicholson S.B., 1938, *Papers of the Mt. Wilson Obs. V, Part 1*, Carnegie Institution of Washington Publ. No. 489.

Harmon R., Rosner R., Zirin H., Spiller E., Golub L., 1993, *Astrophys. J.* **417**, L83

Harrison R.A., 1997, *Sol. Phys.*, **175**, 467

Harrison R.A., Lang J., Brooks D.H., Innes D.E., 1999, *Astron. Astrophys.* **351**, 1115

Harvey J.W., 1971, *Publ. Astron. Soc. Pacific* **83**, 539

Harvey J.W., 1985, in *Theoretical Problems in High Resolution Solar Physics*, H.U. Schmidt (Ed.), MPI f. Astrophysik, Garching, p. 183

Harvey K.L. (Ed.), 1992, The Solar Cycle, Astron Soc. Pacific Conf. Ser. Vol. **12**

Harvey K.L., 1993, *Magnetic Bipoles on the Sun*, Ph.D. Thesis, University of Utrecht

Harvey J.W., Breckinridge J.B., 1973, *Astrophys. J.* **182**, L137

Harvey J.W., Hall D.N.B., 1971, in *Solar Magnetic Fields*, R.F. Howard (Ed.), Reidel, Dordrecht, *IAU Symp.* **43**, 279

Harvey K.L., Harvey J.W., 1973, *Solar Phys.* **28**, 61

Harvey K.L., Harvey J.W., Martin S.F., 1975, *Solar Phys.* **40**, 87

Haugen E., 1967, *Solar Phys.* **2**, 227

Haugen E., 1969, *Solar Phys.* **9**, 88

Hénoux J.C., 1968, *Ann. Astrophys.* **31**, 511

Hénoux J.C., 1969, *Astron. Astrophys.* **2**, 288

Henson G.D., Kemp J.C., 1984, *Solar Phys.* **93**, 289

Henze W., Jr., 1991, in *Solar Polarimetry*, L.J. November (Ed.), National Solar Obs., Sunspot, NM, p. 16

Henze W., Jr., Tandberg-Hanssen E., Hagyard M.J., Woodgate B.E., Shine R.A., Beckers J.M., Bruner M., Gurman J.B., Hyder C.L., West E.A., 1982, *Solar Phys.* **81**, 231

Hewagama T., Deming D., Jennings D.E., Osherovich V., Wiedemann G., Zipoy D., Mickey D.L., Garcia H., 1993, *Astrophys. J. Suppl. Ser.* **86**, 313

Hiremath K.M., 2002, *Astron. Astrophys.* **386**, 674

Hirzberger J., Kneer F., 2001, *Astron. Astrophys.* **378**, 1078

Hofmann, A., Rendtel, J., 1989, *Astron. Nachr.*, **310**, 61

Hofmann A., Grigorjev V.M., Selivanov V.L., 1988, *Astron. Nachr.* **309**, 373

Hofmann J., Deubner F.-L., Fleck, B., 1993, in *The Magnetic and Velocity Fields of Solar Active Regions*, H. Zirin, G. Ai, H. Wang (Eds.), Astron. Soc. Pacific Conf. Series No. 46, *IAU Coll.* **141**, 44

Hofmann J., Deubner F.-L., Fleck B., Schmidt W., 1994, *Astron. Astrophys.* **284**, 269

Holmes J., 1961, *Monthly Notices Royal Astron. Soc.* **122**, 301

Holmes J., 1963, *Monthly Notices Royal Astron. Soc.* **126**, 155

Holzwarth V., Schüssler M., 2003, in preparation

Horn T., Staude J., Landgraf V., 1997, *Solar Phys.* **172**, 69

Houtgast J., van Sluiter A., 1948, *BAN* **10**, 325

Howard R.F., 1992, *Solar Phys.* **137**, 51

Hoyle F., 1949, *Some Recent Researches in Solar Physics*, Cambridge University Press, Cambridge

Hoyt D.V., Schatten K.H., 1998, *Solar Phys.* **179**, 189

Hudson H.S., Silva S., Woodard M., Willson R.C., 1982, *Solar Phys.* **76**, 211

Hughes D.W., Proctor M.R.E., 1988, *Ann. Rev. Fluid Mech.* **20**, 187

Hurlburt N.E., Matthews P.C., 1998, priv. communication

Hurlbert N.E., Rucklidge A.M., 2000, *Monthly Notices Royal Astron. Soc.* **314**, 793

Hurlburt N.E., Matthews P.C., Proctor M.R.E., 1996, *Astrophys. J.* **457**, 933

Hurlburt N.E., Matthews P.C., Rucklidge A.M., 2000, *Solar Phys.* **192**, 109

Ichimoto K., 1987, *Publ. Astron. Soc. Japan* **39**, 329

Ichimoto K., 1988a, *Publ. Astron. Soc. Japan* **40**, 103

Ichimoto K., 1988b, *Vistas Astron.* **31**, 113

Ikhsanov R.N., 1968, *Izv. Astron. Obs. Pulkovo* **184**, 94

Illing R.M.E., 1981, *Astrophys. J.* **248**, 358

Illing R.M.E., Landman D.A., Mickey D.L., 1974a, *Astron. Astrophys.* **35**, 327

Illing R.M.E., Landman D.A., Mickey D.L., 1974b, *Astron. Astrophys.* **37**, 97

Illing R.M.E., Landman D.A., Mickey D.L., 1975, *Astron. Astrophys.* **41**, 183

Ioshpa B.A., Obridko V.N., 1965, *Soln. Dannye* **3**, 54

Jahn K., 1989, *Astron. Astrophys.* **222**, 264

Jahn K., 1992, in *Theory of Sunspots*, J.H. Thomas, N. Weiss (Eds.), Cambridge University Press, p. 139

Jahn K., 1997, in *Advances in the Physics of Sunspots*, B. Schmieder, J.C. Del Toro Iniesta, M. Vázquez (Eds.), ASP Conf. Series No. 118, p. 122

Jahn K., Schmidt H.U., 1994, *Astron. Astrophys.* **290**, 295

Jakimiec J., 1965, *Acta Astron.* **15**, 145

Javaraiah J., 1999, *Solar Phys.* **189**, 289

Jensen E., Maltby P., 1965, *Astrophys. Norveg.* **10**, 17

Jensen E., Nordø J., Ringnes T.S., 1955, *Astrophysica Norwegica*, **5**, 167

Jensen J.M., Duvall T.L., Jr., Jacobsen B.H., Christensen-Dalsgaard J., 2001, *Astrophys. J.* **553**, L193

Johannesson A., 1993, *Astron. Astrophys.* **273**, 633

Jones H.P., Giovanelli R.G., 1982, *Solar Phys.* **79**, 247

Joy A.H., 1919, *Astrophys. J.* **49**, 167

Kakinuma T., Swarup G., 1962, *Astrophys. J.* **136**, 975

Kálmán B., 1979, *Izv. Krymsk. Astrofiz. Obs.* **60**, 114

Kálmán B., 1991, *Solar Phys.* **135**, 299.

Kambry M.A., Nishikawa J., Sakurai T., Ichimoto K., Hiei E., 1991, *Solar Phys.* **132**, 41

Kawakami H., 1983, *Publ. Astron. Soc. Japan* **35**, 459

Kawakami S., Makita M., Kurokawa H., 1989, *Publ. Astron. Soc. Japan* **41**, 175

Keller C.U., Stenflo J.O., Von der Lühe O., 1992, *Astron. Astrophys.* **254**, 355

Kemp J.C., Henson G.D., 1983, *Astrophys. J.* **266**, L69

Keppens R., 2000, in *Encyclopedia of Astronomy and Astrophysics*, Inst. of Physics Publishing, London, p. 3193

Keppens R., Martínez Pillet V., 1996, *Astron. Astrophys.* **316**, 229

Khomenko E., Collados M., Bellot Rubio L.R., 2002a, *Astrophys. J.* **i**n press

Khomenko E., Collados M., Bellot Rubio L.R., 2002b, *Il Nuovo Cimento C* **25** in press

Khutsishvili E.V., Gigolashvili M.Sh., Kvernadze T.M., 2002, *Solar Phys.* **206**, 219

Kingston A.E., Doyle J.G., Dufton P.L., Gurman J.B., 1982, *Solar Phys.* **81**, 47

Kitai R., 1986, *Solar Phys.* **104**, 287

Kjeldseth-Moe O., 1968a, in *Structure and Development of Solar Active Regions*, K.O. Kiepenheuer (Ed.), Reidel, Dordrecht, *IAU Symp.* **35**, 202

Kjeldseth-Moe O., 1968b, *Solar Phys.* **4**, 267

Kjeldseth Moe O., Maltby P., 1969, *Solar Phys.* **8**, 275

Kjeldseth Moe O., Maltby P., 1974a, *Solar Phys.* **36**, 101

Kjeldseth Moe O., Maltby P., 1974b, *Solar Phys.* **36**, 109

Kjeldseth-Moe O., Brynildsen N., Brekke P., Engvold O., Maltby P., Bartoe J.-D.F., Brueckner G.E., Cook J.W., Dere K.P., Soker D.G., 1988, *Astrophys. J.* **334**, 1066

Kjeldseth-Moe O., Brynildsen N., Brekke P., Maltby P., Brueckner G.E., 1993, *Solar Phys.* **145**, 257

Klvaňa M., Bumba V., Krivtsov A., 1998, in *Three-dimensional Structure of Solar Acive Regions*, C.E. Alissandrakis, B. Schmieder (Eds.), ASP Conf. Series Vol. 155, p. 79

Kneer F., 1972, *Astron. Astrophys.* **18**, 39 (in german)

Kneer F., 1973, *Solar Phys.* **28**, 361

Kneer F., Mattig W., 1978, *Astron. Astrophys.* **65**, 17

Kneer F., Mattig W., v. Uexküll M., 1981, *Astron. Astrophys.* **102**, 147

Knobloch E., Weiss N.O., 1984, *Monthly Notices Royal Astron. Soc.* **207**, 203

Knölker M., Schüssler M., 1988, *Astron. Astrophys.* **202**, 275

Knölker M., Schüssler M., Weisshaar E., 1988, *Astron. Astrophys.* **194**, 257

Kollatschny W., Stellmacher G., Wiehr E., Falipou M.A., 1980, *Astron. Astrophys.* **86**, 245

Kolmogorov A.N., 1941, *C.R. Acad. Sci. USSR* **31**, 99.

Kopp G., Rabin D., 1992, *Solar Phys.* **141**, 253

Köppen J., 1975, *Solar Phys.* **42**, 325

Kosovichev A.G., 1996, *Astrophys. J.* **461**, L55

Kosovichev A.G., 2002, *Astron. Nachr.*, **323**, 186

Kosovichev A.G., Duvall T.L., Jr., Scherrer P.H., 2000, *Solar Phys.* **192**, 159

Kosovichev A.G., Duvall T.L., Birch A.C., Gizon L., Scherrer P.H., Zhao J., 2002, *Adv. Space Res.* **29**, 1899

Kotov V.A., Koutchmy S., 1994, in *Infrared Solar Physics*, D. Rabin, J. Jefferies, C. Lindsey (Eds.), Kluwer, Dordrecht, *IAU Symp.* **154**, 265

Koutchmy S., Adjabshirazadeh A., 1981, *Astron. Astrophys.* **99**, 111

Krat V.A:, Karpinski V.N., Pravdjuk L.M., 1972, *Solar Phys.* **26**, 305

Krause F., Rüdiger G., 1975, *Solar Phys.* **42**, 107

Krivtsov A.M., Hofmann A., Staude J., Klvaňa M., Bumba V., 1998, *Astron. Astrophys.* **335**, 1077

Krüger A., Hildebrandt J., Bogod V.M., Korzhavin A.N., Akhmedov Sh.B., Gelfreikh G.B., 1986, *Solar Phys.* **105**, 111

Krüger A., Hildebrand J., Fürstenberg F., 1985, *Astron. Astrophys.* **143**, 72

Kundu M.R., Alissandrakis C.E., 1984, *Solar Phys.* **94**, 249

Kunzel H., 1960, *Astron. Nachr.* **285**, 271.

Kupka R., Labonte B.J., Mickey D.L., 2000, *Solar Phys.* **191**, 97

Kurokawa H., 1991, in *Flare Physics in Solar Activity Maximum 22*, Y. Uchida et al. (Eds.), Lecture Notes in Physics, Vol. 387, p. 39

Kurucz R.L., 1991, in *Stellar Atmospheres: Beyond Classical Models*, L. Crivellari, I. Hubeny, D.G. Hummer (Eds.), NATO ASI Series, Kluwer, Dordrecht, p. 440

Kurucz R.L., 1992, *Rev. Mexicana Astron. Astrof.* **23**, 187

Kurucz R.L., 1993, in *Preculiar vs. Normal Phenomena in A-Type and Related Stars*, M.M. Dworetsky, F. Castelli, R. Fraggina (Eds.), ASP Conf. Ser. Vol. 44, p. 87

Kusnezov D.A., 1968, *Soln. Dann.* **9**, 96

Kusoffsky V., Lundstedt H., 1986, *Astron. Astrophys.* **160**, 51

Küveler G., Wiehr E., 1985, *Astron. Astrophys.* **142**, 205

Lamb S.A., 1975, *Monthly Notices Royal Astron. Soc.* **172**, 205

Laming J.M., 1994, *Space Sci. Rev.* **70**, 107

Landgraf V., 1997, *Atron. Nachr.*, **318**, 129

Landi Degl'Innocenti E., 1979, *Solar Phys.* **63**, 237

Landman D.A., Finn G.D., 1979, *Solar Phys.* **63**, 221

Landolfi M., Landi Degl'Innocenti E., 1982, *Solar Phys.* **78**, 355

Landolfi M., Landi Degl'Innocenti E., Arena P., 1984, *Solar Phys.* **93**, 269

Lang K.R., Willson R.F., 1982, *Astrophys. J.* **255**, L111

Lang K.R., Willson R.F., Kile J.N. 1993, *Astrophys. J.* **419**, 398

Lean J., 1991, *Rev. Geophys.* **29**, 505

Lee J.W., 1992, *Solar Phys.* **139**, 267

Lee J.W., Hurford G.J., Gary D.E., 1993a, *Solar Phys.* **144**, 45

Lee J.W., Hurford G.J., Gary D.E., 1993b, *Solar Phys.* **144**, 349

Lee J.W., White S.M., Gopalswamy N., Kundu M.R., 1997, *Solar Phys.* **174**, 175

Leka K.D., 1995, *Are Solar Emerging Flux Regions Carrying Electric Current?* PhD Thesis, University of Hawaii

Leka K.D., 1997, *Astrophys. J.* **484**, 900

Leka K.D., Skumanich A., 1998, *Astrophys. J.* **507**, 454

Leka K.D., Van Driel-Gesztelyi L., Nitta N., Canfield R.C., Mickey D.L., Sakurai T., Ichimoto K., 1994, *Solar Phys.* **155**, 301

Leroy J.L., 1962, *Ann. Astrophys.* **25**, 127

Li W., Ai G., Zhang H., 1994, *Solar Phys.* **151**, 1

Lindsey C., Braun D.C., 1999, *Astrophys. J.* **510**, 494

Lindsey C., Kopp G., 1995, *Astrophys. J.* **453**, 517

Lindsey C., Braun D.C., Jefferies S.M., 1996, *Astrophys. J.* **470**, 636

Linsky J.L., Avrett E.H., 1970, *Publ. Astron. Soc. Pacific* **82**, 169

Lites B.W., 1980, *Solar Phys.* **68**, 327

Lites B.W., 1992, in *Sunspots: Theory and Observations*, J.H. Thomas, N.O. Weiss (Eds.), Kluwer, Dordrecht, p. 261

Lites B.W., Scharmer G.B., 1989, in *High Spatial Resolution Solar Observations*, O. von der Lühe (Ed.), National Solar Obs., Sunspot, NM, p. 286

Lites B.W., Skumanich A., 1981, in *Physics of Sunspots*, L.E. Cram, J.H. Thomas (Eds.), National Solar Obs., Sunspot, NM, p. 152

Lites B.W., Skumanich A., 1982, *Astrophys. J. Suppl. Ser.* **49**, 293

Lites B.W., Skumanich A., 1990, *Astrophys. J.* **348**, 747

Lites B.W., Skumanich A., Rees D.A., Murphy G.A., Carlsson M., 1987, *Astrophys. J.* **318**, 930

Lites B.W., Skumanich A., Rees D.E., Murphy G.A., 1988, *Astrophys. J.* **330**, 493

Lites B.W., Scharmer G.B, Skumanich A., 1990, *Astrophys. J.* **355**, 329

Lites B.W., Bida T.A., Johannesson A., Scharmer G.B., 1991, *Astrophys. J.* **373**, 683

Lites B.W., Elmore D.F., Seagraves P., Skumanich A., 1993, *Astrophys. J.* **418**, 928

Lites B.W., Low B.C., Martínez Pillet V., Seagraves P., Sskumanich A., Frank Z.A., Shine R.A., Tsuneta S., 1995, *Astrophys. J.* **446**, 887

Lites B.W., Thomas J.H., Bogdan T.J., Cally P.S., 1998, *Astrophys. J.* **497**, 464

Lites B.W., Socas-Navarro H., Skumanich A., Shimizu T., 2002, *Astrophys. J.* **575**, 1131

Liu Q., Song M., 1996, *Chin. Astron. Astrophys.* **20**, 291

Liu Y., Wang J., Yan Y., Guoxiang A., 1986, *Solar Phys.* **169**, 79

Livingston W.C., 1991, *Nature* **350**, 45

Livingston W., 2002, *Sol. Phys.*, **207**, 41

Livingston W., Wallace L., 1985, *Solar Phys.* **95**, 251

Loughhead R.E., Bray R.J., 1960, *Australian J. Phys.*, **13**, 139

Loughhead R.E., Bray R.J., Tappere E.J., 1979,, *Astron. Astrophys.* **79**, 69

Low B.C., 1975, *Astrophys. J.* **197**, 251

Low B.C., 1980, *Solar Phys.* **67**, 57

Low B.C., 1985, in *Measurements of Solar Vector Magnetic Fields*, M.J. Hagyard (Ed.), NASA CP-2374, p. 49

Lüst R., Schlüter A., 1954, *Z. Astrophys.* **34**, 263

Lustig G., Wöhl H., 1995, *Solar Phys.* **157**, 389

Makita M., 1963, *Publ. Astron. Soc. Japan* **15** 145

Makita M., 1986, *Solar Phys.* **106**, 269

Makita M., Kawakami H., 1986, *Publ. Astron. Soc. Japan* **38**, 257

Makita M., Morimoto M., 1960, *Publ. Astron Soc. Japan* **12**, 63

Makita M., Ohki Y., 1986, *Ann. Tokyo Astron. Obs.* **21**, 1

Makita M., Hamana S., Nishi K., Shimizu M., Koyano H., Sakurai T., Komatsu H., 1985, *Publ. Astron. Soc. Japan* **37**, 561

Maltby P., 1960, *Ann. Astrophys.*, **23**, 983

Maltby P., 1964, *Astrophys. Norvegica* **8**, 205

Maltby P., 1970, *Solar Phys.* **13**, 312

Maltby P., 1972, *Solar Phys.* **26**, 76

Maltby P., 1975a, *Solar Phys.* **43**, 91

Maltby P., 1975b, *Nature* **257**, 468

Maltby P., 1977, *Solar Phys.* **55**, 335

Maltby P., 1992a, in *Sunspots: Theory and Observations*, J.H. Thomas, N.O. Weiss (Eds.), Kluwer, Dordrecht, p. 103

Maltby P., 1992b, in *Surface Inhomogeneities on Late-Type Stars*, P.B. Byrne, D.J. Mullan (Eds.), Springer-Verlag, Berlin, p. 124

Maltby P., 1994, in *Infrared Solar Physics*, D.M. Rabin, J.T. Jefferies, C. Lindsey (Eds.), Kluwer, Dordrcht *IAU Symp.* **154**, 423

Maltby P., Eriksen G., 1967, *Solar Phys.* **2**, 249

Maltby P., Mykland N., 1969, *Solar Phys.* **8**, 23

Maltby P., Avrett E.H., Carlsson M., Kjeldseth-Moe O., Kurucz R.L., Loeser R., 1986, *Astrophys. J.* **306**, 284

Maltby P., Brynildsen N., Brekke P., et al. 1998, *Astrophys. J.* **496**, L117

Maltby P., Brynildsen N., Fredvik T., Kjeldseth-Moe O., Wilhelm K., 1999, *Solar Phys.* **190**, 437

Maltby P., Brynildsen N., Kjeldseth-Moe O., 2000, in *Recent Insights into the Physics of the Sun and Heliosphere: Highlights from SOHO and other Space Missions*, P. Brekke, B. Fleck, J.B. Gurman (Eds.), ASP, *IAU Symp.* **203**, 116

Martens P.C.H., Hurlburt N.E., Title A.M., Acton L.W., 1996, *Astrophys. J.* **463**, 372

Martin S.F., 1990, in *Solar Photosphere: Structure, Convection and Magnetic Fields*, J.O. Stenflo (Ed.), Kluwer, Dordrecht *IAU Symp.* **138**, 129

Martínez Pillet V., 1992, *Solar Phys.* **140**, 207

Martínez Pillet V., 1997, in *Advances in the Physics of Sunspots*, B. Schmieder, J.C. del Toro Iniesta, M. Vázquez (Eds.), Astron. Soc. Pacific Conf. Ser. Vol. 118, p. 212

Martínez Pillet V., 2000, *Astron. Astrophys.* **361**, 734

Martínez Pillet V., 2001, *Astron. Astrophys.* **369**, 644

Martínez Pillet V., 2002, *Astron. Nachr.*, **323**, 342

Martínez Pillet V., Vázquez M., 1990, *Astrophys. Space Sci.* **170**, 75

Martínez Pillet V., Vázquez M., 1993, *Astron. Astrophys.* **270**, 494

Martínez Pillet V., Moreno-Insertis F., Vázquez M., 1993, *Astron. Astrophys.* **274**, 521

Martínez Pillet V., Lites B.W., Skumanich A., Degenhardt D., 1994, *Astrophys. J.* **425**, L113

Mathew S.K., Solanki S.K., Lagg A., Collados M., Berdyugina S., Frutiger C., Krupp N., Woch J., 2002, , in *Poster Proc. 1st, Potsdam Thinkshop on Sunspots and Starspots*, K.G. Strassmeier, A. Washuettl (Eds.), AIP, p. 117

Matthews P.C., 1994, in *Solar Active Region Evolution: Comparing Models with Observations*, K.S. Balasubramaniam, G.W. Simon (Eds.), ASP Conf. Ser. Vol. 68, p. 56

Matthews P.C., Hurlburt N.W., Proctor M.R.E., Brownjohn D.P., 1992, *J. Fluid Mech.* **240**, 559

Matthews P.C., Proctor M.R.E., Weiss N.O., 1995 *J. Fluid Mech.*, **305**, 281

Mattig W., 1953, *Z. Astrophys.* **31**, 273

Mattig 1958, *Z. Astrophys.* **44**, 280

Mattig W., 1961, *Mitt. Astron. Gesell. Hamburg* **14**, 47

Mattig W., 1969, *Solar Phys.* **6**, 413

Mattig W., 1974, *Solar Phys.* **36**, 275

Mattig W., Mehltretter J.P., 1968, in *Structure and Development of Solar Active Regions*, K.O. Kiepenheuer (Ed.), Reidel, Dordrecht *IAU Symp.* **35**, p. 187

Mauas P., Avrett E.H., Loeser R., 1988, *Astrophys. J.* **330**, 1008

McIntosh P.S., 1981, in *The Physics of Sunspots*, L. Cram, J.H. Thomas (Eds.), NSO, Sunspot, N.M., p. 7

McIntosh P.S., 2000, *Encyclopedia of Astronomy and Astrophysics*, Institute of Physics Publishing, London, p. 3168

McPherson M.R., Lin H., Kuhn J.R., 1992, *Solar Phys.* **139**, 255

Metcalf T.R., Jiao L., McClymont N., Canfield R.C., Uitenbroek H., 1995, *Astrophys. J.* **439**, 474

Meyer F., Schmidt H.U., 1968, *Z. Ang. Math. Mech.*, **48**, T218

Meyer F., Schmidt H.U., Weiss N.O., Wilson P.R., 1974, *Monthly Notices Royal Astron. Soc.* **169**, 35

Meyer F., Schmidt H.U., Weiss N.O., 1977, *Monthly Notices Royal Astron. Soc.* **179**, 741

Michard R., 1953, *Ann. Astrophys.* **16**, 217

Mickey D.L., 1985a, in *Measurements of Solar Vector Magnetic Fields*, M.J. Hagyard (Ed.), NASA Conference Publ., CP-2374, p. 183

Mickey D.L., 1985b, *Solar Phys.* **97**, 223

Miles A.J., Roberts B., 1992, *Solar Phys.* **141**, 205

Miles A.J., Allen H.R., Roberts B., 1992, *Solar Phys.* **141**, 235

Miller R.A.S.J., 1960, *J. British Astron. Assoc.* **70**, 146

Milovanov A.V., Zelenyi L.M., 1992, *Geophys. Res. Lett.* **19**, 1419

Mogilevskij E.I., Demkina L.B., Ioshpa B.A., Obridko V.N., 1968, in *Structure and Development of Solar Active Regions*, K.O. Kiepenheuer (Ed.), Reidel, Dordrecht, *IAU Symp.* **235**, 315

Mogilevskij E.I., Obridko V.N., Shelting B.D., 1973, *Radiofizika* **16**, 1357

Molodenskii M.M., 1969, *Sov. Astron. – AJ* **12**, 585

Molodenskii M.M., 1974, *Solar Phys.* **39**, 393

Molowny-Horas R., 1994, *Solar Phys.* **154**, 29

Montavon C., 1992, *Diplomarbeit*, Institute of Astronomy, ETH Zürich

Montesinos B., Thomas J.H., 1993, *Astrophys. J.* **402**, 314

Montesinos B., Thomas J.H., 1997, *Nature* **390**, 485

Moon Y.-J., Yun H.-S., Park J.-S., 1998, *Astrophys. J.* **502**, 1027

Moore R.L., 1981a, *Astrophys. J.* **249**, 390

Moore R.L., 1981b, in *Physics of Sunspots*, L.E. Cram, J.H. Thomas (Eds.), National Solar Obs., Sunspot, NM, p. 259

Moore R.L., Rabin D., 1985, *Ann. Rev. Astron. Astrophys.* **23**, 239

Moreno Insertis F., 1997, in *Advances in the Physics of Sunspots*, B. Schmieder et al. (Eds.), ASP Conf. Ser. Vol. 118, p. 45

Moreno Insertis F., Vázquez M., 1988, *Astron. Astrophys.* **205**, 289

Moreno Insertis F., Schüssler M., Ferriz Mas A., 1992, *Astron. Astrophys.* **264**, 686

Moreno Insertis F., Caligari P., Schüssler M., 1994, *Solar Phys.* **153**, 449

Muglach K., Solanki S.K., Livingston W.C, 1994, in *Solar Surface Magnetism*, R.J. Rutten, C.J. Schrijver (Eds.), Kluwer Dordrecht, p. 127

Muller R., 1973a, *Solar Phys.* **29**, 55 (in french)

Muller R., 1973b, *Solar Phys.* **32**, 409 (in french)

Muller R., 1976, *Solar Phys.* **48**, 101

Muller R., 1987, in *The Sun, Proc. 10th European Regional Astron. Meeting of the IAU*, L. Hejna, M. Sobotka (Eds.), Astron. Inst. Czechoslovak Acad. Sci., Prag, p. 15

Muller R., 1992, in *Sunspots: Theory and Observations*, J.H. Thomas, N.O. Weiss (Eds.), Kluwer, Dordrecht, p. 175

Müller D.A.N., Schlichenmaier R., Steiner O., Stix M., 2002, *Astron. Astrophys.* **393**, 305

Murphy G.A., 1990, *The synthesis and inversion of Stokes spectral profiles*, NCAR Cooperative Thesis No. 124

Musman S., 1967, *Astrophys. J.* **149**, 201

Mykland N., 1973, *Solar Phys.* **28**, 49

Nakagawa Y., Raadu M.A., 1972, *Solar Phys.* **25**, 127

Nakagawa Y., Raadu M.A., Billings D.E., McNamara D., 1971, *Solar Phys.* **19**, 72

Nesme-Ribes E., Ferreira E.N., Mein P., 1993, *Astron. Astrophys.* **274**, 563

Neukirch T., Martens P.C.H., 1998, *Astron. Astrophys.* **332**, 1075

Neupert W.M., Brosius J.W., Thomas R.J., Thompson W.T., 1992, *Astrophys. J.* **392**, L95

Nicolas K.R., Kjeldseth-Moe O., Bartoe J.-D.F., Brueckner G.E., 1981, in *Physics of Sunspots*, L.E. Cram, J.H. Thomas (Eds.), National Solar Obs., Sunspot, NM, p. 167

Nicolas K.R., Bartoe J.-D.F., Brueckner G.E., Kjeldseth-Moe O., 1982, *Solar Phys.* **81**, 253

Nindos A., Kundu M.R., White S.M., Shibasaki K., Gopalswamy N., 2000, *Astrophys. J. Suppl.*, **130**, 485

Nishi K., 1962, *Publ. Astron. Soc. Japan* **14**, 325

Nordlund Å., Stein R.F., 1990, in *Solar Photosphere: Structure, Convection and Magnetic Fields*, J.O. Stenflo (Ed.), Kluwer, Dordrecht, *IAU Symp.* **138**, 191

Norton A.A., Ulrich R.K., 2000, *Solar Phys.* **192**, 403

November L.J., Simon G.W., Tarbell T.D., Title A.M., Ferguson S.H., 1986, in *Theoretical Problems in High Resolution Solar Physics II*, G. Athay, D.S. Spicer (Eds.), NASA Conf. Publ. 2483, p. 121

Noyes R.W., Raymond J.C., Doyle J.G., Kingston A.E., 1985, *Astrophys. J.* **297**, 805

Nye A., Bruning D., LaBonte B.J., 1988, *Solar Phys.* **115**, 251

Obridko V.N., 1968a, *Bull. Astron. Inst. Chechoslovakia* **19**, 183

Obridko V.N., 1968b, *Bull. Astron. Inst. Czechoslovakia* **19**, 186

Obridko V.N., 1985, *Sunspots and Complexes of Activity* (in Russian), Nauka, Moskva

Obridko V.N., Staude J., 1988, *Astron. Astrophys.* **189**, 232

Obridko V.N., Teplitskaya R.B., 1978, *Astronomiya* **14**, 7

Osherovich V.A., 1979, *Solar Phys.* **64**, 261

Osherovich V.A., 1980, *Solar Phys.* **68**, 297

Osherovich V.A., 1982, *Solar Phys.* **77**, 63

Osherovich V.A., Flå T., 1983, *Solar Phys.* **88**, 109

Osherovich V.A., Garcia H.A., 1989, *Astrophys. J.* **336**, 468

Osherovich V.A., Lawrence J.K., 1983, *Solar Phys.* **88**, 117

Pahlke K.-D., 1988, *Ph.D. Thesis*, University of Göttingen

Pahlke K.-D., Wiehr E., 1990, *Astron. Astrophys.* **228**, 246

Pallavicini R., Vaiana G.S., Jofani G., Felli M., 1979, *Astrophys. J.* **229**, 375

Pardon L., Worden S.P., Schneeberger T.J., 1979, *Solar Phys.* **63**, 247

Parker E.N., 1974, *Solar Phys.* **36**, 249

Parker E.N., 1975a, *Solar Phys.* **40**, 275

Parker E.N., 1975b, *Solar Phys.* **40**, 291

Parker E.N., 1978, *Astrophys. J.* **221**, 368

Parker E.N., 1979a, *Astrophys. J.* **230**, 905

Parker E.N., 1979b, *Astrophys. J.* **230**, 905

Parker E.N., 1979c, *Astrophys. J.* **234**, 333

Parker E.N., 1992, *Astrophys. J.* **390**, 290

Parnell C.E., Bewsher D., Harrison R.A., 2002, *Solar Phys.* **206**, 249

Penn M.J., Kuhn J.R., 1995, *Astrophys. J.* **441**, L51

Peter H., 1996, *Monthly Notices Royal Astron. Soc.* **278**, 821

Petrovay K., Moreno Insertis F., 1997, *Astrophys. J.* **485**, 398

Petrovay K., van Driel–Gesztelyi L., 1997, *Solar Phys.* **176**, 249

Petrovay K., Brown J.C., Van Driel-Gesztelyi L., Fletcher L., Marik M., Stewart G., 1990, *Solar Phys.* **127**, 51

Petrovay K., Martínez Pillet V., van Driel-Gesztelyi L., 1999, *Solar Phys.* **188**, 315

Pevtsov A.A., 1992, *Solar Phys.* **141**, 65

Piddington J.H., 1975, *Astrophys. Space Sci.* **34**, 347

Pizzo V.J., 1986, *Astrophys. J.* **302**, 785

Pizzo V.J., 1987, in *Theoretical Problems in High Resolution Solar Physics II*, G. Athay, D.S. Spicer (Eds.), NASA Conf. Publ. 2483, p. 1

Pizzo V.J., 1990, *Astrophys. J.* **365**, 764

Pizzo V.J., Mac Gregor K.B., Kunasz P.B., 1993, *Astrophys. J.* **413**, 764

Pneuman G.W., Solanki S.K., Stenflo J.O., 1986, *Astron. Astrophys.* **154**, 231

Proctor M.R.E., 1992, in *Sunspots: Theory and Observations*, J.H. Thomas, N.O. Weiss (Eds.), Kluwer, Dordrecht, p. 221

Proctor M.R.E., Weiss N.O., 1982, *Rep. Prog. Phys.* **45**, 1317

Prokakis T., 1974, *Solar Phys.* **35**, 105

Pulkkinen P., Tuominen I., 1998, *Astron. Astrophys.* **332**, 748

Rabin D., Moore R., Hagyard M.J., 1984, *Astrophys. J.* **287**, 404

Rast M.P., Fox P.A., Lin H., Lites B.W., Meisner R.W., White O.R., 1999, *Nature* **401**, 678

Rast M.P., Meisner R.W., Lites B.W., Fox P.A., White O.R., 2001, *Astrophys. J.* **557**, 864

Rayrole J., 1967, *Ann. Astrophys.* **30**, 257

Rayrole J., Semel M., 1968, in *Structure and Development of Solar Active Regions*, K.O. Kiepenheuer (Ed.), Reidel, Dordrecht, *IAU Symp.* **35**, 134

Rayrole J., Semel, M., 1970, *Astron. Astrophys.* **6**, 288

Richardson R.S., 1941, *Astrophys. J.* **93**, 24

Rimmele T.R., 1994, *Astron. Astrophys.* **290**, 972

Rimmele T.R., 1995a, *Astron. Astrophys.* **298**, 260

Rimmele T.R., 1995b, *Astrophys. J.* **445**, 511.

Rimmele T.R., 1997, *Astrophys. J.* **490**, 458

Ringnes T.S., 1964, *Astrophysica Norwegica* **8**, 303

Ringnes T.S., Jensen E., 1961, *Astrophysica Norvegica* **7**, 99

Roberts B., 1976, *Astrophys. J.* **204**, 268

Roberts, B., 1986, in *Small Scale Magnetic Flux Concentrations in the Solar Photosphere*, W. Deinzer, M. Knölker, H.H. Voigt (Eds.), Vandenhoeck & Ruprecht, Göttingen, p. 169

Roberts, B., 1992, in *Sunspot: Theory and Observations*, J.H. Thomas, N.O. Weiss (Eds.), Kluwer, Dordrecht, p. 303

Roberts B., Ulmschneider P., 1997, in *Solar and Heliospheric Plasma Physics*, G.M. Simnett, C.E. Alissandrakis, L. Vlahos (Eds.), Springer Verlag, Berlin, Lecture Notes in Physics Vol. 489, p. 75

Robinson R.D., Boice D.C., 1982, *Solar Phys.* **81**, 25

Rödberg H., 1966, *Nature* **211**, 394

Rodríguez Medina R., 1983, Masters Thesis, Universidad de La Laguna.

Rossbach M. Schröter E.H., 1970, *Solar Phys.* **12**, 95

Rouppe van der Voort L.H.M., 2002a, *Astron. Astrophys.* **389**, 1020

Rouppe van der Voort L., 2002b, in *Poster Proc 1st Potsdam Thinkshop on Sunspots and Starspots*, K. Strassmeier, A. Washuettl (Eds.), AIP, p. 27

Royal Greenwich Observers, 1925, *Monthly Notices Royal Astron. Soc.* **169**, 35

Rucklidge A.M., Schmidt H.U., Weiss N.O., 1995, *Monthly Notices Royal Astron. Soc.* **273**, 491

Rucklidge A.M., Weiss N.O., Brownjohn D.P., Matthews P.C., Prator M.R.E., 2000, *J. Fluid Mech.* **419**, 283

Rüedi I., Solanki S.K., Livingston W., 1995a, *Astron. Astrophys.* **293**, 252

Rüedi I., Solanki S.K., Livingston W., 1995b, *Astron. Astrophys.* **302**, 543

Rüedi I., Keller C.U., Solanki S.K., 1996, *Solar Phys.* **164**, 265

Rüedi I., Solanki S.K., Keller C.U., Frutiger C., 1998a, *Astron. Astrophys.* **338**, 1089

Rüedi I., Solanki S.K., Stenflo J.O., Tarbell T., Scherrer P.H., 1998b, *Astron. Astrophys.* **335**, L97

Rüedi I., Solanki S.K., Bogdan T., Cally P., 1999a, in *Solar Polarization*, K.N. Nagendra, J.O. Stenflo (Eds.), Kluwer, Dordrecht, p. 337

Rüedi I., Solanki S.K., Keller C.U., 1999b, *Astron. Astrophys.* **348**, L37

Ruzmaikin A., 1997, *Astron. Astrophys.* **319**, L13

Ryutova M., Shine R., Title A., Sakai J.I., 1998, *Astrophys. J.* **492**, 402

Sams B.J. III, Golub L., Weiss N.O., 1992, *Astrophys. J.* **399**, 313

Sánchez Almeida J., 1997, *Astron. Astrophys.* **324**, 763

Sánchez Almeida J., 1998, *Astrophys. J.* **497**, 967

Sánchez Almeida J., 2001, *Astron. Astrophys.* **369**, 643

Sánchez Almeida J., Bonet J.A., 1998, *Astrophys. J.* **505**, 1010

Sánchez Almeida J., Lites B.W., 1992, *Astrophys. J.* **398**, 359

Sánchez Almeida J., Landi Degl'Innocenti E., Martínez Pillet V., Lites B.W., 1996, *Astrophys. J.* **446**, 537

Savage B.D., 1969, *Astrophys. J.* **156**, 707

Scharmer G.B., Gudiksen B.V., Kiselman D., Löfdahl M.G., Rouppe van der Voort L.H.M., 2002, *Nature* **420**, 151

Schatten K.H., 1993, *J. Geophys. Res.* **98**, 18907

Schatzmann E., 1965, in *Stellar and Solar Magnetic Fields*, R. Lüst (Ed.), North-Holland Pub. Co., Amsterdam *IAU Symp.* **22**, 337

Schlichenmaier R., 1997, Ph.D. Thesis, Ludwig-Maximilians-Univ. München. *Die Dynamik magnetischer Flussröhren im Sonnenfleck: Ein Modell für den Evershed-Effekt und die penumbrale Feinstruktur* (in german)

Schlichenmaier R., 2002, *Astron. Nachr.* **323**, 303

Schlichenmaier R., Collados M., 2002, *Astron. Astrophys.* **381**, 668

Schlichenmaier R., Schmidt W., 1999, *Astron. Astrophys.* **349**, L37

Schlichenmaier R., Schmidt W. 2000, *Astron. Astrophys.* **358**, 1122

Schlichenmaier R., Solanki S.K., 2003, *Astron. Astrophys.* submitted

Schlichenmaier R., Jahn K., Schmidt H.U., 1998a, *Astrophys. J.* **493**, L121

Schlichenmaier R., Jahn K., Schmidt H.U., 1998b, *Astron. Astrophys.* **337**, 897

Schlichenmaier R., Bruls J.H.M.J., Schüssler M., 1999, *Astron. Astrophys.* **349**, 961

Schlichenmaier R., Müller D.A.N., Steiner O., Stix M., 2002, *Astron. Astrophys.* **381**, L77

Schlüter A., Temesvary S., 1958, in *Electromagnetic Phenomena in Cosmical Physics*, B. Lehnert (Ed.), Reidel, Dordrecht, *IAU Symp.* **6**, 263

Schmahl E.J., Kundu M.R., Strong K.T., Bentley R.D., Smith J.B., Krall J.R., 1982, *Solar Phys.* **80**, 233

Schmelz J.T., Holman G.D., Brosius J.W., Willson R.F., 1994, *Astrophys. J.* **434**, 786

Schmidt H.U., 1968, in *Structure and Development of Solar Active Regions*, K.O. Kiepenheuer (Ed.), Reidel, Dordrecht, *IAU Symp.* **35**, p. 95

Schmidt H.U., 1991, *Geophys. Astrophys. Fluid Dyn.*, 62, 249

Schmidt W., 2002, in *Magnetic Coupling of the Solar Atmosphere*, H. Sawaya-Lacoste (Ed.), EAS-SP 505, Proc. IAU colloq. No. 189, in press

Schmidt W., Balthasar H., 1994, *Astron. Astrophys.* **283**, 241

Schmidt W., Schlichenmaier R., 2000, *Astron. Astrophys.* **364**, 829

Schmidt H.U., Wegmann R., 1983, in *Dynamical Problems in Mathematical Physics*, B. Brosowski, E. Martensen (Eds.), Verlag P. Lang, Frankfurt, p. 137

Schmidt H.U., Simon G.W., Weiss N.O., 1985, *Astron. Astrophys.* **148**, 191

Schmidt H.U., Spruit H.C., Weiss N.O., 1986, *Astron. Astrophys.* **158**, 351

Schmidt W., Hofmann A., Balthasar H., Tarbell T.D., Frank Z.A., 1992, *Astron. Astrophys.* **264**, L27

Schmieder B., 1997, in *Solar and Heliospheric Plasma Physics*, G.M. Simnett, C.E., Alissandrakis, L. Vlahos (Eds.), Springer, Berlin, Lecture Notes in Phys. Vol. 489, p. 139

Schmieder B., Raadu M., Démoulin P., Dere K.P., 1989, *Astron. Astrophys.* **213**, 402

Schmieder B., del Toro Iniesta J.C., Vázquez M., (Eds.), 1997, *Advances in the Physics of Sunspots*, Astron. Soc. Pacific Conf. Ser. Vol. 118

Schrijver C.J., Cote J., Zwaan C., Saar S.H., 1989, *Astrophys. J.* **337**, 964

Schröter E.H., 1962, *Z. Astrophys.* **56**, 183

Schröter E.H., 1965a, *Z. Astrophys.* **62**, 228

Schröter E.H., 1965b, *Z. Astrophys.* **62**, 256

Schröter E.H., 1967, in *Solar Physics*, J.N. Xanthakis (Ed.), Interscience, London, p. 325

Schröter E.H., 1971, in *Solar Magnetic Fields*, R.F. Howard (Ed.), Reidel, Dordrecht, *IAU Symp.* **43**, 167

Schröter E.H., 1985, *Solar Phys.* **100**, 141

Schüssler M., 1980, *Nature* **288**, 150

Schüssler M., 1986, in *Small Scale Magnetic Flux Concentrations in the Solar Photosphere*, W. Deinzer, M. Knölker, H.H. Voigt (Eds.), Vandenhoeck & Ruprecht, Göttingen, p. 103

Schüssler M., 1990, in *Solar Photosphere: Structure, Convection and Magnetic Fields*, J.O. Stenflo (Ed.), Kluwer, Dordrecht, *IAU Symp.* **138**, 161

Schüssler M., 1992, in *The Sun – a Laboratory for Astrophysics*, J.T. Schmelz, J.C. Brown (Eds.), Kluwer, Dordrecht, p. 191

Schüssler M., 2002, *Astron. Nachr.* **323**, 377

Schüssler M., Caligari P., Ferriz-Mas A., Moreno Insertis F., 1994, *Astron. Astrophys.* **281**, L69

Schwabe S.H., 1843, *Astron. Nachr.* **20**, No. 495, 234

Secchi P.A., 1872, Die Sonne, Westermann Verlag, Braunschweig

Sengottuval M.P., Somasundaram K., 2001, *Solar Phys.* **198**, 79

Servajean R., 1961, *Ann. Astrophys.* **24**, 1

Settele A., Carroll T.A., Nickelt I., Norton A.A., 2002, *Astron. Astrophys.* **386**, 1123

Severino G., Gomez M.T., Caccin B., 1994, in *Solar Surface Magnetism*, R.J. Rutten, C.J. Schrijver (Eds.), Kluwer, Dordrecht, p. 169

Severny A.B., 1959, *Soviet Astron.*, **3**, 214 (*Astron. Zh.* **36**, 208)

Sheeley N.R., Jr., 1969, *Solar Phys.* **9**, 347

Sheeley N.R., Jr., 1972, *Solar Phys.* **25**, 98

Shibasaki K., 2001, *Astrophys. J.* **550**, 1113

Shine R.A., Title A.M., 2001, in *Encyclopedia of Astron. Astrophys.*, Inst. of Phys. Publishing, Bristol, Vol. 4, p. 3209

Shine R.A., Title A.M., Tarbell T.D., Topka K.P., 1987, *Science*, 238, 1264

Shine R.A., Title A.M., Tarbell T.D., Smith K., Frank Z.A., 1994, *Astrophys. J.* **430**, 413

Shinkawa T., Makita M., 1996, in *Magnetodynamic Phenomena in the Solar Atmosphere – Prototypes of Stellar Magnetic Activity*, Y. Uchida (Ed.), Kluwer, Dordrecht, p. 615

Siarkowski K., Sylwester J., Jakimiec J., Bentley R.D., 1989, *Solar Phys.* **119**, 65

Sigwarth M., Schmidt W., Schüssler M., 1998, *Astron. Astrophys.* **339**, L53

Simon G.W., Leighton R.B., 1964, *Astrophys. J.* **140**, 1120

Simon G.W., Weiss N.O., 1970, *Solar Phys.* **13**, 85

Simon G.W., Weiss N.O., Nye A.H., 1983, *Solar Phys.* **87**, 65

Simon G.W., Wilson P.R., 1985, *Astrophys. J.* **295**, 241

Skumanich A., 1992a, in *Surface Inhomogeneities on Late-Type Stars*, P.B. Byrne, D.J. Mullan (Eds.), Springer-Verlag, Berlin, p. 94

Skumanich A., 1992b, in *Sunspots: Theory and Observations*, J.H. Thomas, N.O. Weiss (Eds.), Kluwer, Dordrecht, p. 121

Skumanich A., 1999, *Astrophys. J.* **512**, 975

Skumanich A., Lites B.W., 1991, in *Solar Polarimetry*, L. November (Ed.), National Solar Observatory, Sunspot, NM, p. 307

Skumanich A., Osherovich V.A., 1981, in *Physics of Sunspots*, L.E. Cram, J.H. Thomas (Eds.), National Solar Obs., Sunspot, NM, p. 104

Skumanich A., Semel M., 1996, *Solar Phys.* **164**, 291

Skumanich A., Lites B.W., Martínez Pillet V., 1994, in *Solar Surface Magnetism*, R.J. Rutten, C.J. Schrijver (Eds.), Kluwer, Dordrecht, p. 99

Sobotka M., 1987, in *Proc. 10th European Regional Astronomy Meeting IAU, Vol. 1: The Sun*, L. Hejna, M. Sobotka (Eds.), Astron. Inst. of Czech. Acad. Sciences, Prague, p. 33

Sobotka M., 1988, *Solar Phys.* **124**, 37

Sobotka M., 1997, in *Advances in the Physics of Sunspots*, B. Schmieder et al. (Eds.), ASP Conf. Ser. Vol. 118, p. 155

Sobotka M., 2003, in *Solar Variability: From Core to Outer Frontier*, A. Wilson (Ed.), ESA SP-506, in press

Sobotka M., Sütterlin P., 2001, *Astron. Astrophys.* **380**, 714

Sobotka M., Bonet J.A., Vázquez M., 1992, *Astron. Astrophys.* **257**, 757

Sobotka M., Šimberová S., Bumba V., 1991, *Bull. Astron. Inst. Czechoslovakia* **42**, 250

Sobotka M., Bonet J.A., Vázquez M., 1993, *Astrophys. J.* **415**, 832

Sobotka M., Bonet J.A., Vázquez M., Hanslmeier A., 1995, *Astrophys. J.* **447**, L133

Sobotka M., Brandt P.N., Simon G.W., 1997a, *Astron. Astrophys.* **328**, 682

Sobotka M., Brandt P.N., Simon G.W., 1997b, *Astron. Astrophys.* **328**, 689

Sobotka M., Brandt P.N., Simon G.W., 1999, *Astron. Astrophys.* **348**, 621

Socas-Navarro H., 2002, in *Current Theoretical Models and Future High Resolution Solar Observations: Preparaing for ATST*, A.A. Peutsov, H. Vitenbroek (Eds.), ASP Conf. Ser., in press

Socas-Navarro H., Trujillo Bueno J., Ruiz Cobo B., 2000, *Science*, **288**, 1396

Solanki S.K., 1990, in *Solar Photosphere: Structure, Convection and Magnetic Fields*, J.O Stenflo (Ed.), Kluwer, Dordrecht, *IAU Symp*, **138**, 103

Solanki S.K., 1993, *Space Sci. Rev.* **61**, 1

Solanki S.K., 1995, in *Infrared Tools for Solar Astrophysics: What's Next?*, J.R. Kuhn, M.J. Penn (Eds.), World Scientific, p. 341

Solanki S.K., 1997a, in *Solar and Heliospheric Plasma Physics*, G.M. Simnett, C.E. Alissandrakis, L. Vlahos (Eds.), Springer Berlin, p. 49

Solanki S.K., 1997b, in *Advances in the Physics of Sunspots*, B. Schmieder, J.C. del Toro Iniesta, M. Vázquez (Eds.), Astron. Soc. Pacific Conf. Ser., Vol. 118, p. 178

Solanki S.K., 2000a, in *Encyclopedia of Astronomy and Astrophysics*, Institute of Physics Publishing, London, p. 3177

Solanki S.K., 2000b, in *Encyclopedia of Astronomy and Astrophysics*, Institute of Physics Publishing, London, p. 3180

Solanki, S.K., 2002, *Astron. Nachr.* **324**, 165

Solanki S.K., Montavon C.A.P., 1993, *Astron. Astrophys.* **275**, 283

Solanki S.K., Montavon C.A.P., 1994, in *Solar Surface Magnetism*, R.J. Rutten, C.J. Schrijver (Eds.), Kluwer, Dordrecht, p. 239

Solanki S.K., Rüedi I., 2003, *Astron. Astrophys.* submitted

Solanki S.K., Schmidt H.U., 1993, *Astron. Astrophys.* **267**, 287

Solanki S.K., Unruh Y.C., 1998, *Astron. Astrophys.* **329**, 747

Solanki S.K., Rüedi I., Livingston W., 1992, *Astron. Astrophys.* **263**, 339

Solanki S.K., Walther U., Livingston W., 1993, *Astron. Astrophys.* **277**, 639

Solanki S.K., Montavon C.A.P., Livingston W., 1994, *Astron. Astrophys.* **283**, 221

Solanki S.K., Finsterle W., Rüedi I., 1996a, *Solar Phys.* **164**, 253

Solanki S.K., Zufferey D., Lin H., Rüedi I., Kuhn J.R., 1996b, *Astron. Astrophys.* **310**, L33

Solanki S.K., Finsterle W., Rüedi I., Livingston W., 1999, *Astron. Astrophys.* **347**, L27

Solov'ev A.A., 1997, *Astron. Rep.* **41**, 121

Soltau D., 1994, in *Solar Magnetic Fields*, M. Schüssler, W. Schmidt (Eds.), Springer, Berlin, p. 155

Spruit H.C., 1976, *Solar Phys.* **50**, 269

Spruit H.C., 1977, *Solar Phys.* **55**, 3

Spruit H.C., 1979, *Solar Phys.* **61**, 363

Spruit H.C., 1981a, in *Physics of Sunspots*, L.E. Cram, J.H. Thomas (Eds.), National Solar Obs., Sunspot, NM, p. 98

Spruit H.C., 1981b, in *Physics of Sunspots*, L.E. Cram, J.H. Thomas (Eds.), National Solar Obs., Sunspot, NM, p. 359

Spruit H.C., 1982a, *Astron. Astrophys.* **108**, 348

Spruit H.C., 1982b, *Astron. Astrophys.* **108**, 356

Spruit H.C., 1987, in *The role of Fine-scale Magnetic Fields on the Structure of the Solar Atmosphere*, E.H. Schröter, M. Vázquez, A.A. Wyller (Eds.), Cambridge University Press, Cambridge, p. 199

Spruit H.C., 1991, in *The Sun in Time*, C.P. Sonett, M.S. Giampap, M.S. Mathews (Eds.), Univ. of Arizona Press, Tucson, p. 118

Spruit H.C., 2000, *Space Sci. Rev.* 94, 113

Spruit H.C., Bogdan T.J., 1992, *Astrophys. J.* **391**, L109

Spruit H.C., Van Ballegooigen A.A., Title A.M., 1987, *Solar Phys.* **110**, 115

Spruit H.C., Schüssler M., Solanki S.K., 1992, in *Solar Interior and Atmosphere*, A.N. Cox, W. Livingston, M.S. Matthews (Eds.), University of Arizona press, Tucson, AZ, p. 890

St. John C.E., 1913, *Astrophys. J.* **37**, 322

Stachnik R.V., Nisensen P., Ehn D.C., Hudgin R.H., Schirf V.E., 1977, *Nature*, **266**, 149

Stachnik R.V., Nisensen P., Noyes R.W., 1983, *Astron. Astrophys.* **271**, L37

Stanchfield D.C.H., II, Thomas J.H., Lites B.W., 1997, *Astrophys. J.* **477**, 485

Staude J., 1981, *Astron. Astrophys.* **100**, 284

Staude J., 1991, *Rev. Modern Astron.* **4**, 69

Staude J., 1994, in *Solar Surface Magnetism*, R.J. Rutter, C.J. Schrijver (Eds.), Kluwer, Dordrecht, p. 189

Staude J., 1999, in *Magnetic Fields and Oscillations*, B. Schmieder, A. Hofmann, J. Staude (Eds.), ASP Conf. Series Vol. 184, p. 113

Staude J., 2002, *Astron. Nachr.* **323**, 317

Staude J., Fürstenberg F., Hildebrandt J., Krüger A., Jakimiec J., Obridko V.N., Siarkowski M., Sylwester B., Sylwester J., 1983, *Acta Astron.* **33**, 441

Staude J., Fürstenberg F., Hildebrandt J., 1984, *Astron. Zh.* **61**, 956

Staude J., Zhugzhda Iu.D., Locans V., 1987, in *Proc. 10th European Regional Astronomy Meeting, Vol. 1: The Sun*, L. Hejna, M. Sobotka (Eds.), Astron. Inst. of Czech. Acad. Sci., Prag, p. 161

Stein R.F., Nordlund Å, 2002, in *Magnetic Coupling of the Solar Atmosphere, IAU Colloq. No. 189*, H. Sawaya-Lacoste (Ed.), ESA SP-505, in press

Steinegger M., Brandt P.N., Pap J., Schmidt W., 1990, *Astrophys. Space Sci.* **170**, 127

Steinegger M., Vázquez M., Bonet J.A., Brandt P.N., 1996, *Astrophys. J.* **461**, 478

Steinegger M., Bonet J.A., Vázquez M., 1997, *Solar Phys.* **171**, 303

Steiner O., Pneuman G.W., Stenflo J.O., 1986, *Astron. Astrophys.* **170**, 126

Steiner O., Grossmann-Doerth U., Knölker M., Schüssler M., 1996, *Solar Phys.* **164**, 223

Steiner O., Grossmann-Doerth U., Knölker M., Schüssler M., 1998, *Astrophys. J.* **495**, 468

Stellmacher G., Wiehr E., 1970, *Astron. Astrophys.* **7**, 432

Stellmacher G., Wiehr E., 1971, *Solar Phys.* **17**, 21

Stellmacher G., Wiehr E., 1975, *Astron. Astrophys.* **45**, 69

Stellmacher G., Wiehr E., 1980, *Astron. Astrophys.* **82**, 157

Stellmacher G., Wiehr E., 1981, *Astron. Astrophys.* **103**, 211

Stellmacher G., Wiehr E., 1985, in *High Resolution in Solar Physics*, R. Muller (Ed.), Springer Verlag Berlin, Lecture Notes in Physics, Vol. 233, p. 254

Stellmacher G., Wiehr E., 1988, *Astron. Astrophys.* **191**, 149

Stenflo J.O., 1984, *Adv. Space Res.* **4**, 5

Stenflo J.O., 1985, in *Measurements of Solar Vector Magnetic Fields*, M. Hagyard (Ed.), NASA CP, p. 263

Stenflo J.O., 1989, *Astron. Astrophys. Rev.* **1**, 3

Stenflo J.O., 1994, *Solar Magnetic Fields: Polarized Radiation Diagnostics*, Kluwer, Dordrecht

Stepanov V.E., 1965, in *Stellar and Solar Magnetic Fields*, R. Lüst (Ed.), *IAU Symp.* **22**, 267

Steshchenko N.V., 1967, *Izv. Krymsk. Astrofiz. Observ.* **37**, 21

Stix M., 2002, *Astron. Nachr.* **323**, 178

Strassmeier K. (Ed.), 2002, *Astron. Nachr.* **323** (special issue containing the proceedings of the 1st Potsdam Thinkshop on Sunspots and Starspots)

Strong K.T., Alissandrakis C.E., Kundu M.R., 1984, *Astrophys. J.* **277**, 865

Strous L.H., 1994, *Dynamics of Solar Active Regions: Patterns in Magnetic-Flux Emergence*, Ph.D. Thesis, Utrecht University

Stumpff P., 1961, *Z. Astrophys.* **52**, 73 (in german)

Stürenburg S., Holweger H., 1990, *Astron. Astrophys.* **237**, 125

Sun M.-T., Chou D.-Y., Lin C.-H. and the TON Team, 1997, *Solar Phys.* **176**, 59

Sütterlin P., 1998, *Astron. Astrophys.* **333**, 305

Sütterlin P., 2001, *Astron. Astrophys.* **374**, L21

Sütterlin P., Wiehr E., 1998, *Astron. Astrophys.* **336**, 367

Sweet P.A., 1955, *Vistas in Astronomy*, A. Beer (Ed.), Pergamon Press, London, Vol. 1, p. 675

Tagore S.G., Murali P., 1994, *Solar Phys.* **151**, 29

Tanaka K., 1991, *Solar Phys.* **136**, 133

Tandberg-Hanssen E., 1956, *Astrophysica Norwegica* **5**, 207

Tandberg-Hanssen E., Athay R.G., Beckers J.M., et al., 1981, *Astrophys. J.* **244**, L127

Tao L., Weiss N.O., Brownjohn D.P., Proctor M.R.E., 1998, *Astrophys. J.* **496**, L39

Teplitskaya R.B., Grigoryeva S.A., Skochilov B.G., 1978, *Solar Phys.* **56**, 293

Ternulo M., Zappala R.A., Zucarello F., 1981, *Solar Phys.* **74**, 111

Thiessen G., 1950, *Observatory* **70**, 234

Thomas J.H., 1981, in *The Physics of Sunspots*, L. Cram, J.H. Thomas (Eds.), National Solar Obs., Sunspot, N.M., p. 345

Thomas J.H., 1985, *Australian J. Phys*, **38**, 811

Thomas J.H., 1988, *Astrophys. J.* **333**, 407

Thomas J.H., 1996, in *Solar and Astrophysical Magnetohydrodynamic Flows*, K.C. Tsinganos (Ed.), Kluwer, Dordrecht, p. 39

Thomas J.H., Montesinos B., 1990, *Astrophys. J.* **359**, 550

Thomas J.H., Montesinos B., 1991, *Astrophys. J.* **375**, 404

Thomas J.H., Montesinos B., 1993, *Astrophys. J.* **407**, 398

Thomas J.H., Weiss N.O., 1992a, in *Sunspots: Theory and Observations*, J.H. Thomas, N. Weiss (Eds.), Kluwer, Dordrecht, p. 3

Thomas J.H., Weiss N.O., (Eds.), 1992b, *Sunspots: Theory and Observations*, Kluwer, Dordrecht

Thomas J.H., Cram L.E., Nye A.H., 1984, *Astron. Astrophys.* **285**, 368

Thomas J.H., Weiss N.O., Tobias S.M., Brummell N.H., 2002a, *Astron. Nachr.* **323**, 383

Thomas J.H., Weiss N.O., Tobias S.M., Brummell N.H., 2002b,, *Nature* **420**, 390

Title A.M., Frank Z.A., Shine R.A., Tarbell T.D., Topka K.P., Scharmer G., Schmidt W., 1992, in *Sunspots: Theory and Observations*, J.H. Thomas, N.O. Weiss (Eds.), Kluwer, Dordrecht, p. 195

Title A.M., Frank Z.A., Shine R.A., Tarbell T.D., Topka K.P., Scharmer G., Schmidt W., 1993, *Astrophys. J.* **403**, 780

Tönjes K., Wöhl H., 1982, *Solar Phys.* **75**, 63

Tousey R., Bartoe J.D.F., Bohlin J.D., 1973, *Solar Phys.* **33**, 265

Treanor P.J., 1960, *Monthly Notices Royal Astron. Soc.* **120**, 412

Tritschler A., Schmidt W., 1997, *Astron. Astrophys.* **321**, 643

Tritschler A., Schmidt W., 2002a, *Astron. Astrophys.* **382**, 1093

Tritschler A., Schmidt W., 2002b, *Astron. Astrophys.* **388**, 1048

Tsap T.T., 1965, *Izv. Krymsk. Astrofiz. Obs.* **33**, 92

Tsiropoula G., 2000, *Astron. Astrophys.* **357**, 735

Tsiropoula G., Dialetis D., Alissandrakis C.E., Mein P., Mein N., 1997, *Solar Phys.* **172**, 139

Tsiropoula G., Alissandrakis C.E., Main P., 2000, *Astron. Astrophys.* **355**, 375

Tuominen J., 1962, *Z. Astrophys.* **55**, 110

Unruh Y.C., Solanki S.K., Fligge M., 1999, *Astron. Astrophys.* **345**, 635

Unruh Y.C., Solanki S.K., Fligge M., 2000, *Space Sci. Rev.* **94**, 145

Vaiana G.S., Krieger A.S., Timothy A.F., Zombeck M., 1976, *Astrophys. Sp. Sci.* **39**, 75

Van Ballegooijen A.A., 1984, *Solar Phys.* **91**, 195

Van Driel-Gesztelyi L., Petrovay K., 1990, *Solar Phys.* **126**, 285

Van Driel-Gesztelyi L, Hofmann A., Schmieder B., Démoulin P., Csepura G., 1994, *Solar Phys.* **149**, 309

Van t'Weer, 1963, *Ann. Astrophys.* **26**, 185

Vögler A., Shelyag S., Schüssler M., Cattaneo F., Emonet T., Linde T., 2002, *Modelling of Stellar Atmsopheres*, Astron. Soc. Pacific, IAU Symp. 210, in press

Von Klüber H., 1947, *Z. Astrophys.* **24**, 121

Vourlidas A., Bastian T.S., Aschwanden M.J., Nitta N., 1996, *Solar Phys.* **163**, 99

Vourlidas A., Bastian T.S., Aschwanden M.J., 1997, *Astrophys. J.* **489**, 403

Vrabec D. 1971a, in *Solar Magnetic Fields*, R.F. Howard (Ed.), Reidel, Dordrecht, *IAU Symp.* **43**, 201

Vrabec D., 1971b, in *Solar Magnetic Fields*, R.F. Howard (Ed.), Reidel, Dordrecht, *IAU Symp.* **43**, 329

Vrabec D. 1974, in *Chromospheric Fine Structure*, R.G. Athay (Ed.), Reidel, Dordrecht, *IAU Symp.* **56**, 201

Waldmeier M., 1939, *Astron. Mitt. Zürich* No. 138, p. 439

Waldmeier M., 1955, Ergebnisse und Probleme der Sonnenforschung, 2. Aufl., Akad. Verlag, Leipzig.

Walker A.B.C., Barbee T.W., Jr., Hoover R.B., Lindblom J.F., 1988 *Science*, **238**, 61

Wallenhorst S.G., Howard R.F., 1982, *Solar Phys.* **76**, 203

Wallenhorst S.G., Topka K.P., 1982, *Solar Phys.* **81**, 33

Walther U., 1992, *Diplomarbeit*, Institute of Astronomy, ETH, Zürich

Wang H., 1992, in *The Solar Cycle*, K.L. Harvey (Ed.), ASP Conf. Ser. Vol. 27, p. 97

Wang J., 1994, *Solar Phys.* **155**, 285

Wang J., Shi Z., 1992, *Solar Phys.* **140**, 67

Wang H., Zirin H., 1992, *Solar Phys.* **140**, 41

Webb A.R., Roberts B., 1978, *Solar Phys.* **59**, 249

Webber J.C., 1971, *Solar Phys.* **16**, 340

Weber E.J., Davis L., Jr., 1967, *Astrophys. J.* **148**, 217

Wegmann R., 1981, in *Numerical Treatment of Free Boundary Value Problems*, J. Albrecht (Ed.), Birkhäuser, Stuttgart, p. 335

Weiss N.O., 1991, *Geophys. Astrophys. Fluid Dyn*, **62**, 229

Weiss N.O., 1997, in *Advances in the Physics of Sunspots*, B. Schmieder, J.C. Del Toro Iniesta, M. Vázquez (Eds.), ASP Conf. Series No. 118, p. 21

Weiss N.O., 2002, *Astron. Nachr.*, **323**, 371

Weiss N.O., Brownjohn D.P., Hurlburt N.E., Proctor M.R.E., 1990, *Monthly Notices Royal Astron. Soc.* **245**, 434

Weiss N.O., Brownjohn D.P., Matthews P.C., Proctor M.R.E., 1996, *Monthly Notices Royal Astron. Soc.* **283**, 1153

Wentzel D.G., 1992, *Astrophys. J.* **388**, 211

West E.A., Hagyard M.J., 1983, *Solar Phys.* **88**, 51

Westendorp Plaza C., del Toro Iniesta J.C., Ruiz Cobo B., Martínez Pillet V., Lites B.W., Skumanich A., 1997a, *Nature* **389**, 47

Westendorp Plaza C., del Toro Iniesta J.C., Ruiz Cobo B., Martínez Pillet V., Lites B.W., Skumanich A., 1997b, in *Advances in the Physics of Sunspots*, B. Schmieder et al. (Eds.), ASP Conf. Ser., Vol. 118, p. 202

Westendorp Plaza C., del Toro Iniesta J.C., Ruiz Cobo B., Martínez Pillet V., Lites B.W., Skumanich A., 1998, *Astrophys. J.* **494**, 453

Westendorp Plaza C., del Toro Iniesta J.C., Ruiz Cobo B., et al., 2001a, *Astrophys. J.* **547**, 1130

Westendorp Plaza C., del Toro Iniesta J.C., Ruiz Cobo B., et al., 2001b, *Astrophys. J.* **547**, 1148

White S.M., 2002, *Astron. Nachr.* **323**, 265

White S.M., Kundu M.R., 1997, *Solar Phys.* **174**, 31

White S.M., Kundu M.R., Gopalswamy N., 1991, *Astrophys. J.* **366**, L43

Wiehr E., 1969, *Ph.D. Thesis*, University of Göttingen

Wiehr E., 1994, *Astron. Astrophys.* **287**, L1

Wiehr E., 1995, *Astron. Astrophys.* **298**, L17

Wiehr E., 1996, *Astron. Astrophys.* **309**, L4

Wiehr E., 2000, *Solar Phys.* **197**, 227

Wiehr E., Balthasar H., 1989, *Astron. Astrophys.* **208**, 303

Wiehr E., Degenhardt D., 1992, *Astron. Astrophys.* **259**, 313

Wiehr E., Degenhardt D., 1993, *Astron. Astrophys.* **278**, 584

Wiehr E., Degenhardt D., 1994, *Astron. Astrophys.* **287**, 625

Wiehr E., Stellmacher G., 1985, in *High Resolution in Solar Physics*, R. Muller (Ed.), Lecture Notes in Physics Vol. 233, Springer Verlag, Berlin, p. 369

Wiehr E., Stellmacher, G., 1989, *Astron. Astrophys.* **225**, 528

Wiehr E., Koch A., Knölker M., Küveler G., Stellmacher G., 1984, *Astron. Astrophys.* **140**, 352

Wiehr E., Stellmacher G., Knölker M., Grosser H., 1986, *Astron. Astrophys.* **155**, 402

Wilson P.R., 1973, *Solar Phys.* **32**, 435

Wilson P.R., 1981, in *The Physics of Sunspots*, L.E. Cram, J.H. Thomas (Eds.), National Solar Obs., Sunspot, NM, p. 83

Wilson P.R., 1986, *Solar Phys.* **106**, 1

Wilson P.R., Cannon C.J., 1968, *Solar Phys.* **4**, 3

Wilson P.R., McIntosh P.S. 1969, *Solar Phys.* **10**, 370

Wilson P.R., Simon G.W. 1983, *Astrophys. J.* **273**, 805

Wittmann A.D., 1969, *Solar Phys.* **7**, 366

Wittmann A.D., 1971, *Solar Phys.* **20**, 365

Wittmann A.D., 1974, *Solar Phys.* **36**, 29

Wittmann A.D., Schröter E.H., 1969, *Solar Phys.* **10**, 357

Wittmann A.D., Wu Z.T., 1987, *Astron. Astrophys. Suppl. Ser.* **70**, 83

Wöhl H., Wittmann A., Schröter E.H., 1970, *Solar Phys.* **13**, 104

Yau K.K.C., Stephenson F.R., 1988, *Quart. J. Roy. Astron. Soc.* **146**, 49

Ye S.–H., Jin J.–H., 1993, *Solar Phys.* **146**, 229

Yoshimura H., 1983, *Solar Phys.* **87**, 251

Yun H.S., 1970, *Astrophys. J.* **162**, 975

Yun H.S., 1971a, *Solar Phys.* **16**, 379

Yun H.S., 1971b, *Solar Phys.* **16**, 398

Yun H.S., 1972, *Solar Phys.* **22**, 137

Yun H.S., Beebe H.A., Baggett W.E., 1981, in *Physics of Sunspots*, L.E. Cram, J.H. Thomas (Eds.),
   National Solar Obs., Sunspot, NM, p. 142

Yun H.S., Beebe H.A., Baggett W.E., 1984, *Solar Phys.* **92**, 145

Yurchyshyn V.B., Wang H., Goode P.R., 2001, *Astrophys. J.* **550**, 470

Zelenyi L.M., Milovanov A.V., 1991, *Sov. Astron. Lett.* **1**, 425

Zelenyi L.M., Milovanov A.V., 1992, *Sov. Astron. Lett.* **18**, 249

Zhang H., 1994, *Solar Phys.* **154**, 207

Zhang H., 1996, *Astron. Astrophys. Suppl. Ser.* **119**, 205

Zhang H., 1997, *Astrophys. J.* **479**, 1012

Zhang J., Solanki S.K., Wang J.-X., 2002, *Astron. Astrophys.* **i**n press

Zhao J., Kosovichev A.G., 2001, *Astrophys. J.* **557**, 384

Zheleznyakov V.V., 1962, *Soviet Astron.* **6**, 3

Zirin H., Liggett M.A., 1987, *Solar Phys.* **113**, 267.

Zirin H., Stein A., 1972, *Astrophys. J.* **178**, L85

Zirin H., Wang H., 1989, *Solar Phys.* **119**, 245

Zirin H., Wang H., 1993a, *Nature* **363**, 426

Zirin H., Wang H., 1993b, *Solar Phys.* **144**, 37

Zlotnik E.Ya., 1968, *Soviet Astron.* **12**, 245

Zwaan C., 1965, *Rech. Astr. Obs. Utrecht* **17**, part 4

Zwaan C., 1968, *Ann. Rev. Astron. Astrophys.* **6**, 135

Zwaan C., 1974a, *Solar Phys.* **37**, 99

Zwaan C., 1974b, in *Chromospheric Fine Structure*, R.G. Athay (Ed.), Reidel, Dordrecht, *IAU
   Symp.* **56**, 233

Zwaan C., 1975, *Solar Phys.* **45**, 115

Zwaan C., 1978, *Solar Phys.* **60**, 213

Zwaan C., 1981, *Space. Sci. Rev.* **28**, 385

Zwaan C., 1985, *Solar Phys.* **100**, 397

Zwaan C., 1987, *Ann. Rev. Astron. Astrophys.* **25**, 83

Zwaan C., 1992, in *Sunspots: Theory and Observations*, J.H. Thomas, N.O. Weiss (Ed.), Kluwer,
   Dordrecht, p. 75

Zwaan C., Buurman J., 1971, in *Solar Magnetic Fields*, R.W. Howard (Ed.), Reidel, Dordrecht,
   IAU Symp. **43**, 220

Zwaan C., Brants J.J., Cram L.E., 1985, *Solar Phys.* **95**, 3